


Spring 5-2008

Synthesis and Characterization of Polymeric Materials Derived From Multifunctional Alkyl α -Hydroxymethylacrylates

Jean-Francois Morizur
University of Southern Mississippi

Follow this and additional works at: <https://aquila.usm.edu/dissertations>

 Part of the [Materials Chemistry Commons](#), and the [Polymer Chemistry Commons](#)

Recommended Citation

Morizur, Jean-Francois, "Synthesis and Characterization of Polymeric Materials Derived From Multifunctional Alkyl α -Hydroxymethylacrylates" (2008). *Dissertations*. 1187.
<https://aquila.usm.edu/dissertations/1187>

This Dissertation is brought to you for free and open access by The Aquila Digital Community. It has been accepted for inclusion in Dissertations by an authorized administrator of The Aquila Digital Community. For more information, please contact aquilastaff@usm.edu.

NOTE TO USERS

Page(s) not included in the original manuscript and are unavailable from the author or university. The manuscript was scanned as received.

The University of Southern Mississippi

SYNTHESIS AND CHARACTERIZATION OF POLYMERIC MATERIALS

DERIVED FROM MULTIFUNCTIONAL

ALKYL α -HYDROXYMETHYLACRYLATES

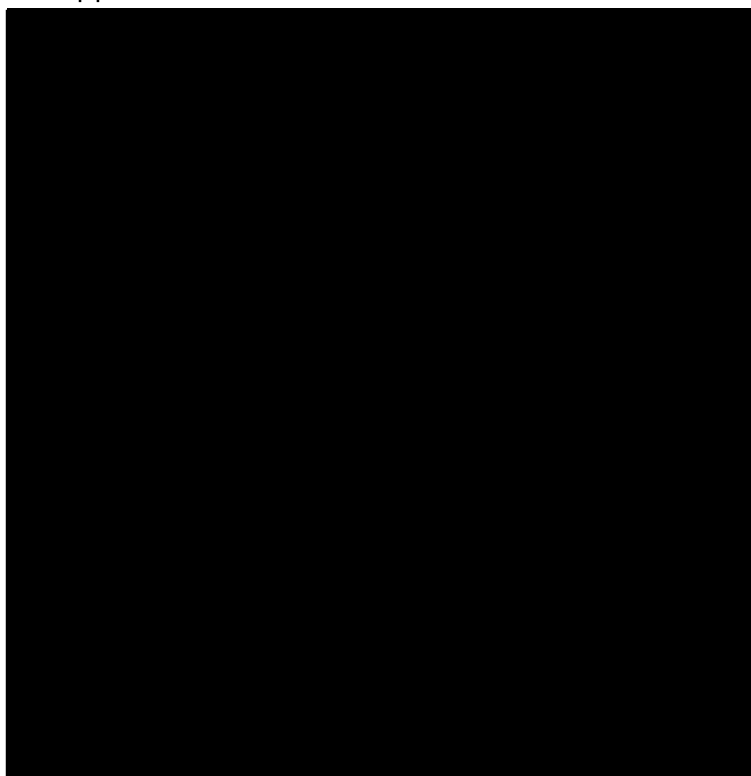
by

Jean-François Morizur

A Dissertation

Submitted to the Graduate Studies Office
of The University of Southern Mississippi
in Partial Fulfillment of the Requirements
for the Degree of Doctor of Philosophy

Approved:



May 2008

COPYRIGHT BY
JEAN-FRANÇOIS MORIZUR
2008

The University of Southern Mississippi

SYNTHESIS AND CHARACTERIZATION OF POLYMERIC MATERIALS

DERIVED FROM MULTIFUNCTIONAL

ALKYL α -HYDROXYMETHYLACRYLATES

by

Jean-François Morizur

A Dissertation

Submitted to the Graduate Studies Office
of The University of Southern Mississippi
in Partial Fulfillment of the Requirements
for the Degree of Doctor of Philosophy

May 2008

ABSTRACT

SYNTHESIS AND CHARACTERIZATION OF POLYMERIC MATERIALS DERIVED FROM MULTIFUNCTIONAL ALKYL α -HYDROXYMETHYLACRYLATES

by

Jean-François Morizur

May 2008

The research presented in this dissertation covers the investigation of new materials derived from alkyl α -hydroxymethylacrylates (RHMA).

The first project exposed in Chapter II involves the synthesis, characterization of RHMA-based reactive surfactants and their successful incorporation in acrylic latexes. The amphiphilic monomers testify of a good copolymerization behavior with other acrylic monomers such as methyl methacrylate and butyl acrylate although their extensive bulkiness. They led to the formation of well-defined polymeric particles via a seeded emulsion polymerization process and permitted decreasing significantly the water sensitivity of the resulting films as compared to film incorporating conventional emulsifier such as sodium dodecyl sulfate.

The research presented in Chapter III focuses of the use of such reactive surfactant as compatibilizer in polymer/TiO₂ nanocomposites. Their incorporation led to an increase in the overall UV-absorption properties of the resulting polymeric materials correlated by an enhancement of filler dispersion within the matrix.

The synthesis, characterization of RHMA-based cationic surfmers is discussed in Chapter IV. Their incorporation in poly(methyl methacrylate)/clay nanocomposites as compatibilizers is studied and the impact of the polymerization technique and of the film formation method used on the composite's properties investigated. Emulsion polymerization led to enhanced filler dispersion when a solvent-casting method was used to form the corresponding film.

Chapter V describes the synthesis and polymerization of alkyl 2-carboethoxyhydroxymethylacrylates. Such alkenes display interesting reactivity in radical polymerization compared to other hindered RHMA analogs however, the resulting homo- and copolymers still testify of low yields and molecular weights. This behavior is attributed to some degree of chain transfer to monomer that may involve the allylic proton.

Chapter VI presents the synthesis of polyfunctional 2-pyrrolidinone derivatives from a variety of new alkyl 2-carboethoxyhydroxymethylacrylates via a very efficient Michael addition/cyclization reaction sequence. Fast, clean, quantitative, and leading to compounds with no need for subsequent purification, this "click" reaction opens up a brand new synthetic window to the preparation of new optically active derivatives.

The preparation of new 2-pyrrolidinone acid derivatives is described in Chapter VII. The separation of the *cis* and *trans* isomers composing the resulting product were successfully separated by simple recrystallization technique. The

study of hydrogen bonding interactions intrinsic of such heterocycle allowed confirming the respective isomer structures.

The synthesis and photopolymerization kinetics of new pyrrolidinone methacrylate monomers are described in Chapter VIII as well as the characterization of the corresponding homopolymers. The importance of hydrogen-bonding interactions in the polymerization kinetics as well as on the final polymer properties are discussed. Responsible for enhancing the polymerization rate of the pyrrolidinone-containing monomers prepared, hydrogen-bonding interactions led to the apparition of a pseudo beta transition for the resulting homopolymers.

Chapter IX involves the synthesis of bis-pyrrolidinone acid derivatives. It was found that such derivatives display T_g s during thermal analysis. This polymer-like behavior is attributed to non-covalent supramolecular associations.

The final part of this dissertation involves the kinetics study of the Michael addition/cyclization reaction sequence and polymerization involving alkyl 2-carboethoxyhydroxymethylacrylates and primary amines. This new polymerization route led to the formation of a new class of poly(ester amide)s with potential applications as biodegradable coatings.

DEDICATION

To my parents and my brothers for their love
and constant support, and for always leading by example

ACKNOWLEDGEMENTS

There are a number of people to whom I must express my gratitude for helping me throughout my graduate career; without them, this work would not have been possible. First and foremost, I thank my graduate advisor, Professor Lon Jay Mathias, for his infinite support and enthusiasm for research. I want also to thank my advisor for all the great opportunities you offered me during these years, the challenges, the international exposure, and the independence in my projects. I want also to acknowledge my committee members for their advice, recommendations, and discussions over the past few years: Dr. William Jarrett, Dr. James Rawlins, Dr. Douglas Wicks, and Dr. Sergei Nazarenko. I am especially grateful to Dr. Jarrett for his assistance with Nuclear Magnetic Spectroscopy.

I would like at this point to mention several undergraduate students with whom I got the great opportunity to collaborate: Marc Pitrakian and Beryl Trentin from ECAM in Lyon, France, Marine Grehal from ITECH in Lyon, France, Laura Kubista and Tiffany Stedman. There are a number of other scientists with whom I have had the pleasure to collaborate with, and learn from. Dr. Derek J. Irvine, Professor at the University of Nottingham in England, who gave me the opportunity to realize an internship in the former Uniqema Research Center in Wilton, UK and to be part of his newly formed research group at Nottingham University, working on new reactive surfactants and supercritical fluids. Dr. Pierre Lourdin from ECAM in Lyon, France for the great collaboration that allowed

students from this engineering school to realize internships in the Department of Polymer Science at the University of Southern Mississippi. Dr. Charles E. Hoyle and Dr. Zhu Houi for the discussions, advice and great help in the pyrrolidinone methacrylates project. Sara Bayley, Maritza Abril, James Kopchick, and Dr. Kenneth Curry for assistance with TEM experiments and data interpretation; the Thames/Rawlins research group, for helping me with DLS and GPC experiments; and Kirt Page, for helping with X-ray analyses.

Many thanks go to the National Science Foundation IGERT program first cadre students with whom I enjoyed taking part of this challenging entrepreneurship program and traveling the world for the sake of a great educational experience: Paul Wheeler, Lisa K. Kemp, Stacy Trey, Micah Black, Alicyn Rhoades, Nicholas Hammond, Ericka Johnson, Jessica Adkins, Misty Rowe, Stephen Slauson, and Dave Weldon. I want to thank my advisor Dr. Lon Jay Mathias for allowing me to participate to this great educational adventure and the other faculty members for their support: Dr. Douglas Wicks, Dr. Judith Giordan and Dr. Ken Malone.

I would also like to express special thanks to the members of the Mathias Research Group, past and present, for the great working atmosphere. Without their support, all this work would not have been possible. Carl Bennett, Tara Smith, Greg Brust, Paul Wheeler, Bekir Dizman, Heidi Assumption, Bianca Shemper, Dr. Junzuo Wang, Dr. Bishua Nayak, Ethem Kaya, Eylem Tas, Hussein Tas, Smita Gosh, Shailesh Goswami, Ted Novistsky and Christopher Lange. I could not forget to mention some people in the Department of Polymer

Science who made things a lot easier. Machell Haynes, Anita Bishop, Silke Branch, Lisa Gill, Rick Durden, Helen Rassier, and Beverly McNeese were always there for me and have solved a number of administrative difficulties. I would like to thank also Steve Selph for his great assistance in repairing equipment in record time. Finally, very special thanks to all my classmates, and in particular Gilles Divoux, Alp Alidedeoglu and Renato Granzoti that were always there to help during the whole graduate program with comments and criticisms and became great friends.

TABLE OF CONTENTS

DEDICATION.....	v
ACKNOWLEDGMENTS.....	vi
LIST OF ILLUSTRATIONS.....	xii
LIST OF TABLES.....	xviii
CHAPTER	
I. INTRODUCTION.....	1
RHMA chemistry	
Reactive surfactants in heterophase polymerization	
Catalytic chain transfer polymerization (CCTP)	
Polymer nanocomposites	
Polyfunctional 2-pyrrolidinones	
Supramolecular assemblies	
Biodegradable poly(ester amide)s	
References	
II. SYNTHESIS OF NEW ACRYLATE-BASED NONIONIC SURFMERS AND THEIR USE IN HETEROPHASE POLYMERIZATION.....	28
Abstract	
Introduction	
Results and Discussion	
Conclusions	
Experimental	
References	
III. NEW POLYMERIC SURFACTANTS SYNTHESIZED VIA CATALYTIC CHAIN TRANSFER POLYMERIZATION: PMMA/TiO ₂ NANOCOMPOSITES.....	69
Abstract	
Introduction	
Results and Discussion	
Conclusions	
Experimental	
References	

IV.	NEW ACRYLATE-BASED CATIONIC REACTIVE SURFACTANTS AND THEIR USE IN THE FORMATION OF PMMA/CLAY NANOCOMPOSITES VIA EMULSION POLYMERIZATION.....	89
	Abstract	
	Introduction	
	Results and Discussion	
	Conclusions	
	Experimental	
	References	
V.	SYNTHESIS AND POLYMERIZATION OF ETHYL 2-CARBO-ETHOXYHYDROXYMETHYLACRYLATE.....	122
	Abstract	
	Introduction	
	Results and Discussion	
	Conclusions	
	Experimental	
	References	
VI.	SYNTHESIS OF NEW POLYFUNCTIONAL 2-PYRROLIDINONE FROM ALKYL 2-CARBOETHOXYHYDROXYMETHYL-ACRYLATES.....	137
	Abstract	
	Introduction	
	Results and Discussion	
	Conclusions	
	Experimental	
	References	
VII.	SYNTHESIS OF POLYFUNCTIONAL 2-PYRROLIDINONE ACID DERIVATIVES FROM ETHYL 2-CARBOETHOXYHYDROXY-METHYLACRYLATE.....	163
	Abstract	
	Introduction	
	Results and Discussion	
	Conclusions	
	Experimental	
	References	
VIII.	SYNTHESIS AND POLYMERIZATION OF NEW MULTIFUNCTIONAL PYRROLIDINONE METHACRYLATE MONOMERS.....	182

Abstract
Introduction
Results and Discussion
Conclusions
Experimental
References

IX. SUPRAMOLECULAR MATERIALS FROM NEW POLY-FUNCTIONAL 2-PYRROLIDINONE ACID DERIVATIVES.....205

Abstract
Introduction
Results and Discussion
Conclusions
Experimental
References

X. NEW BIODEGRADABLE POLY(ESTER AMIDE)S FROM ALKYL 2-CARBOETHOXYHYDROXYMETHYLACRYLATES.....216

Abstract
Introduction
Results and Discussion
Conclusions
Experimental
References

LIST OF ILLUSTRATIONS

Figure	
1.1.	Alkyl α -hydroxymethylacrylates.....2
1.2.	DABCO (left) and 3-quinuclidinol (right).....3
1.3.	Stabilization of the zwitterionic intermediate by the creation of a intramolecular hydrogen bond.....4
1.4.	Cobalt porphyrins (left) and cobaloximes (right).....8
1.5.	Catalytic chain transfer polymerization mechanism.....9
1.6.	Nanocomposite morphologies.....11
1.7.	Polymer architectures made using covalent and non-covalent links between building blocks.....16
1.8.	Hydrogen bonds between two ureidopyrimidinone units.....17
2.1.	RHMA-based monomer.....32
2.2.	^1H and ^{13}C NMR spectra of surfmer S1.....36
2.3.	FT-IR spectrum of surfmer S1 (NaCl).....37
2.4.	^{13}C NMR spectra of S1-co-MMA copolymer (CDCl_3).....40
2.5.	^1H NMR spectra of latex L1 and surfmer S1 (CDCl_3).....42
2.6.	Particle size evolution of latexes.....45
2.7.	Particle size distributions of the final latexes determined by laser light scattering.....45
2.8.	SEM Micrographs of latex L5.....47
2.9.	AFM pictures of film made from latex L5 (height on left and phase on right).....48
2.10.	Neat film (from L5).....50
2.11.	Washed film (from L5).....50
2.12.	AFM topographical images of film from L0 (SDS surfactant), neat (A) and washed with dionized water (B).....51
3.1.	Formation of amphiphilic oligomers via CCTP (CoBF catalyst).....72
3.2.	^{13}C NMR spectra of surfmer S1 and MMA-co-S1 copolymer incorporating 10 mol-% of surfmer (CDCl_3).....75

3.3.	^1H NMR spectrum of MMA-co-surfmer copolymer C (CDCl_3).....	76
3.4.	UV-VIS spectra for the nanocomposites 1 (A), 2 (B), 3 (C) and 4 (D).....	79
3.5.	TEM image of PMMA/ TiO_2 nanocomposite (5 wt-% TiO_2 , no surfactant).....	80
3.6.	TEM image of PMMA/ TiO_2 nanocomposite (5 wt-% TiO_2 , 2.5 wt-% surfactant C). The inset is at higher magnification (scale bar=20 nm).....	81
4.1.	Surfactants investigated.....	93
4.2.	^{13}C NMR spectra of intermediates 1, 3 and gemini surfmer 4 (CDCl_3).....	96
4.3.	SEM images of latex L1 (A) and latex L1 with 5 wt-% of sodium Laponite (B) (scale bar: 500 nm).....	98
4.4.	DSC curves for melt-pressed films obtained from latex L1 containing 0 wt-% (■), 2.5 wt-% (●), 5 wt-% (▲) and 10 wt-% (▼) of Laponite respectively.....	100
4.5.	Tan(δ) diagram for melt-pressed films obtained from latex L1 containing 0 wt-% (■), 2.5 wt-% (●), 5 wt-% (▲) and 10 wt-% (▼) of Laponite respectively.....	101
4.6.	TGA diagrams for PMMA/clay nanocomposites incorporating surfmer 2a (neat (a); 2.5 wt-% (b); 5 wt-% (c); 10 wt-% (d)).....	102
4.7.	XRD patterns for nanocomposite melt-pressed films obtained from Latex L1 (0 wt-% (A), 2.5 wt-% (B), 5 wt-% (C), 10 wt-% (D) of sodium Laponite).....	103
4.8.	XRD patterns for neat Laponite clay (A), OML1 (B), OML2 (C), OML3 (D).....	104
4.9.	FT-IR spectra for OML1 (A), OML2 (B), OML3 (C) and neat Laponite RD (D).....	105
4.10.	Storage modulus of nanocomposite film obtained from latex L3 as function of the film formation method.....	107
4.11.	TEM micrographs of films incorporating gemini surfmer 4 obtained by melt press method.....	109
4.12.	TEM micrographs of films incorporating gemini surfmer 4 obtained by solvent cast method.....	110

4.13.	XRD patterns of nanocomposite films incorporating 10 wt-% of Laponite clay obtained from Latex L3 (solvent-casted (A), melt-pressed (B)).....	111
5.1.	RHMA monomer.....	123
5.2.	^{13}C NMR spectrum of ECHMA (CDCl_3).....	126
5.3.	^{13}C NMR spectrum of 3-hydroxyitaconic acid (CDCl_3 -DMSO- d_6).....	127
5.4.	^1H NMR spectra of ECHMA (A), PMMA (B) and the corresponding copolymer 2 (C) (CDCl_3).....	129
5.5.	GPC trace of the copolymers prepared in DMSO as function of comonomer feed (a: 40%, b: 30%, c: 20%, d: 10%, e: 5%).....	130
6.1.	Polyfunctional pyrrolidinones.....	139
6.2.	^{13}C NMR spectra of compounds 1-4 (CDCl_3).....	142
6.3.	Peak evolution at 3200, 1695 and 1643 cm^{-1}	143
6.4.	Reaction between dimethyl itaconate, ethyl 2-carboethoxyhydroxymethylacrylate and hexylamine. ^1H NMR of reaction batch before (left) and after addition of hexylamine (right) (vinyl peaks region, CDCl_3).....	145
6.5.	Peak area percentage at 1643 cm^{-1} (C=C stretching) as function of reaction conversion observed by real-time FT-IR for dimethyl itaconate (a), ethyl 2-carboethoxyhydroxymethylacrylate (b), n-butyl 2-carboethoxyhydroxymethylacrylate (c) and methyl 2-carboethoxyhydroxymethylacrylate (d).....	146
6.6.	^{13}C NMR of pyrrolidinone 6 (CDCl_3).....	148
6.7.	FT-IR spectra of ethyl 2-carboethoxyhydroxymethylacrylate 2 and pyrrolidinone 6.....	149
6.8.	^{13}C NMR of cyclic hydroxamic acid 14 (D_2O).....	149
7.1.	Polyfunctional 2-pyrrolidinone acid derivatives.....	164
7.2.	NOE correlations.....	165
7.3.	NOESY spectrum for isomer isomer 4b (DMSO- d_6).....	166
7.4.	^{13}C NMR spectra of 2-pyrrolidinones 4a and 4b (DMSO- d_6).....	167
7.5.	^{13}C NMR spectrum of monomer 6 (CDCl_3).....	169
7.6.	FT-IR spectra of intermediate 4 and monomer 6 (NaCl).....	169
7.7.	Polarized microscope photographs of crystals of 5a and 5b.....	170

7.8.	^{13}C NMR spectrum of 4-hydroxy-1-methyl-5-oxopyrrolidine-3-carboxylic acid (DMSO-d6).....	171
7.9.	^{13}C NMR spectra of 2-pyrrolidinone 5 at different temperatures (DMSO-d6).....	172
7.10.	2-pyrrolidinone 5 carbonyl chemical shifts as function of temperature...	173
7.11.	Minimized energies for <i>cis</i> and <i>trans</i> isomers 5a and 5b.....	173
8.1.	Structures of 2-pyrrolidinone containing monomers.....	184
8.2.	^{13}C NMR spectra of 2-pyrrolidinone monomer 3 (CDCl_3) and the corresponding homopolymer PyP1 (DMSO-d6).....	186
8.3.	APT spectrum of 2-pyrrolidinone monomer 3 (CDCl_3).....	186
8.4.	^{13}C NMR spectra of 2-pyrrolidinone monomer 4 (CDCl_3) and the corresponding homopolymer PyP2 (DMSO-d6).....	188
8.5.	Photopolymerization conversion values for a series of methacrylate monomers.....	189
8.6.	Hydrogen bonding interactions for the pyrrolidinone methacrylates investigated.....	191
8.7.	Conversion profiles for methacrylates in NMP (50/50).....	192
8.8.	Photocopolymerization conversion values for HEMA/Monomer 1, 4:1 mixture (A) and 1:1 mixture (B).....	193
8.9.	DSC traces of polymers PyP2 (A) and PyP1 (B) (second scans).....	194
9.1.	^{13}C NMR spectrum of bis-pyrrolidinone intermediate (CDCl_3).....	208
9.2.	^{13}C NMR carbonyl regions of diester intermediates (CDCl_3).....	209
9.3.	^{13}C NMR spectrum of BP2 (DMSO-d6).....	210
9.4.	Bis-2-pyrrolidinone acids (BP2) before exposition (left) and after exposition (right) to air.....	210
9.5.	2 nd scan DCS traces for BP1 (A), BP2 (B) and BP3 (C).....	211
9.6.	Proposed supramolecular association (BP1).....	212
10.1.	Alkyl 2-carboethoxyhydroxymethylacrylates.....	218
10.2.	^{13}C NMR spectrum of hexane bis-2-carboethoxyhydroxymethylacrylate 3 (CDCl_3).....	220

10.3.	Real-time ^{13}C NMR monitoring of the Michael addition/cyclization reaction ($\text{R}_1=\text{CH}_2\text{CH}_3$, $\text{R}_2=(\text{CH}_2)_5\text{CH}_3$, in CDCl_3).....	221
10.4.	Real-time ^{13}C NMR profiles of carbon C_1 , C_2 and C_3 for the reaction between ethyl 2-carboethoxyhydroxymethyl acrylate 1 and hexylamine.....	222
10.5.	Real-time ^{13}C NMR profiles of carbon C_1 , C_2 and C_3 for the reaction between 3 and hexylamine (left) and comparison of profiles for 2 and 3 (right).....	223
10.6.	^{13}C NMR spectra of butyl 1-hexyl-4-hydroxy-5-oxopyrrolidine-3-carboxylate 2' (top, CDCl_3) and poly(ester amide) A (bottom, solid state CP/MAS).....	226
10.7.	^{13}C NMR spectrum of poly(ester amide) B (solid state CP/MAS).....	227
10.8.	^{13}C NMR spectrum of monomer 4 (CDCl_3).....	229
10.9.	^1H NMR spectrum of poly(ester amide) C (CHCl_3).....	230

Scheme

1.1.	The Baylis-Hillman reaction.....	3
1.2.	Synthesis of 5-alkyl-4-carboethoxy-3-hydroxy-pyrrolidinones.....	14
1.3.	Synthesis of 1-alkyl-5-oxo-3-pyrrolidinecarboxylic acid methyl esters.....	15
1.4.	Synthesis of 1-phenylethyl-5-oxo-3-pyrrolidinecarboxylic acid.....	15
2.1.	Synthesis of α -chloromethylacryloyl chloride (CMAC).....	33
2.2.	Synthesis of surfmers 1-5.....	34
3.1.	Surfmer synthesis.....	73
4.1.	Synthesis of reactive surfactants 2a and 2b.....	94
4.2.	Synthesis of gemini reactive surfactant 4.....	94
5.1.	Synthesis of ECHMA.....	125
5.2.	Synthesis scheme for 2-hydroxy-3-methylenesuccinic acid.....	126
7.1.	Synthesis of 2-pyrrolidinone acid derivatives.....	167
7.2.	Synthesis of 2-pyrrolidinone-containing monomer 6.....	168
8.1.	Synthesis of 2-pyrrolidinone monomer 3.....	185
8.2.	Synthesis of 2-pyrrolidinone monomer 4.....	

10.1. Synthesis of alkyl 2-carboethoxyhydroxymethylacrylates 1, 2 and 3.....	219
10.2. Synthesis of poly(ester amide)s A and B.....	225
10.3. Synthesis of poly(ester amide) C.....	229

Equation

1.1. Mayo equation.....	9
-------------------------	---

LIST OF TABLES

Table	
2.1.	Structures of the acrylate-based reactive surfactants investigated.....35
2.2.	Homopolymerization characteristics of surfmer 1-5.....38
2.3.	Copolymerization characteristics of surfmers 1-5.....39
2.4.	Characteristics of the final latexes.....43
2.5.	Molecular weights of latexes.....44
2.6.	Particle size and roughness of the films obtained from latexes determined by Atomic Force Microscopy.....51
2.7.	Freeze/thaw test and stability in different electrolyte solutions (+++: immediate flocculation; ++:partly flocculated after 1 day; +: complete flocculation after 1 month).....52
2.8.	Recipe used to obtain the seed (30% solids).....61
2.9.	Recipe used in the semi-continuous emulsion polymerizations (50% solids).....61
3.1.	MMA-surfmer copolymers obtained by CCTP.....74
3.2.	Nanocomposites preparation.....78
4.1.	Characteristics of the final latexes.....97
4.2.	Storage modulus and glass transition temperature of PMMA/clay nanocomposites obtained by the emulsion method.....103
4.3.	Treated clays characteristics.....104
4.4.	Storage modulus and glass transition temperature of PMMA/clay nanocomposites obtained by in-situ polymerization.....106
4.5.	Impact of the film formation method onto the storage modulus and glass transition temperature for nanocomposites obtained by the emulsion process.....107
5.1.	Apparent molecular weights of ECHMA homopolymers.....128
5.2.	Apparent molecular weights of ECHMA-MMA copolymers.....128
5.3.	Effect of ECHMA comonomer concentration on molecular weight of copolymer.....130

6.1.	Effect of base on the alkyl 2-carboethoxyhydroxymethylacrylates formation.....	140
6.2.	Synthesis of alkyl 2-carboethoxyhydroxymethylacrylates 1-4.....	141
6.3.	Polyfunctional 2-pyrrolidinone derivatives.....	147
8.1.	Performance analysis of methacrylate monomers at 25°C.....	190
9.1.	Bis-pyrrolidinone acid derivatives characteristics.....	207
10.1.	Michael addition/cyclization reaction characteristics.....	224
10.2.	Poly(ester amide)s characteristics.....	228

CHAPTER I

INTRODUCTION

The research presented in this dissertation covers the investigation of new materials derived from alkyl α -hydroxymethylacrylates (RHMA). Each chapter is a self-contained project that includes an abstract, introduction, results and discussion, experimental, conclusions and references section. Chapter II deals with the synthesis of new acrylate-based reactive surfactants and their incorporation in acrylic latexes. Chapter III concentrates on the copolymerization of such reactive surfactant with methyl methacrylate via catalytic chain transfer polymerization to form well-defined amphiphilic macromonomers that are evaluated as polymeric surfactant in TiO₂/PMMA nanocomposites. The synthesis of new cationic reactive surfactants and a gemini analog is presented in Chapter IV and their incorporation in polymer/clay nanocomposite evaluated. Chapter V describes the synthesis and polymerization study of alkyl 2-carboethoxyhydroxyethylacrylates. Chapter VI presents the synthesis of new multifunctional 2-pyrrolidinones from alkyl 2-carboethoxyhydroxymethylacrylates via a very efficient Michael addition/cyclization sequence. The following chapter (VII) describes the synthesis of new 2-pyrrolidinone acid derivatives and the efficient separation of the corresponding *cis* and *trans* isomers. The synthesis and photopolymerization kinetics of new pyrrolidinone methacrylate monomers are described in Chapter VIII as well as the characterization of the corresponding homopolymers. The synthesis of 2-pyrrolidinone acid derivatives led to the subsequent discovery of pyrrolidinone acid-based supramolecular associations

(Chapter IX). Finally, the kinetic study of the Michael addition/cyclization reaction sequence and polymerization involving alkyl 2-carboethoxyhydroxymethylacrylates and primary amines is described in Chapter X as well as the formation of new poly(ester amide)s derived from these newly formed alkenes. This introductory chapter briefly summarizes RHMA chemistry and current research in the domains of reactive surfactant synthesis, polymeric surfactants, polymer nanocomposites, multifunctional 2-pyrrolidinone derivatives, supramolecular assemblies and poly(ester amide)s.

RHMA Chemistry

The majority of acrylate and methacrylate monomers and crosslinkers are built on simple syntheses and contain a single pendent group. Alkyl hydroxymethylacrylate esters, derived from alkyl α -hydroxymethylacrylates (RHMA), shown in Figure 1.1 are vinyl monomers which present a very high radical polymerizability when $R=H$. This high reactivity can be retained (or caused) by the large number of functional groups present in the molecule.

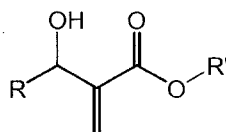
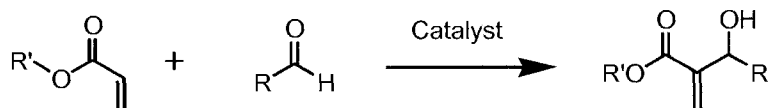


Figure 1.1. Alkyl α -hydroxymethylacrylates.

RHMA monomers allow the manipulation of at least two different functional groups. Specifically, the presence of the hydroxyl group and the carboxylic acid ester group permit further reactions to modify or substitute the basic functionalities.

RHMA monomers can be readily synthesized via the Baylis-Hillman reaction involving commercial acrylates. Other reactions have been reported by Villieras,¹ Rosenthal² and Ferris.³ The Baylis-Hillman reaction involves conjugated compounds such as esters that add to aldehydes via the α -carbon in the presence of a catalyst to give allylic alcohols as shown in Scheme 1.1.^{4,5}



Scheme 1.1. The Baylis-Hillman reaction.

This type of reaction has great synthetic utility as it converts simple starting materials into densely functionalized products, although it sometimes suffers from low reaction rates and low yields, especially for acrylates. The rate and conversion of the Baylis-Hillman reaction can be significantly improved by the use of nucleophilic non-hindered bases such as 1,4-diaza[2.2.2]bicyclooctane (DABCO, Figure 1.2) rather than simple tertiary amines.



Figure 1.2. DABCO (left) and 3-quinuclidinol (right).

Further improvement has been achieved using 3-quinuclidinol (Figure 1.2). This is apparently due to the stabilization of the zwitterionic intermediate by the formation of an intramolecular hydrogen bond (Figure 1.3).⁶ It has also been reported that an increase in the reaction rate is obtained by adding acetic acid⁷ or methanol⁸ to the reaction mixture, thus inducing the formation of intermolecular

hydrogen bonds. The presence of a hydroxyl group within the acrylate showed similar same effects on the reaction rate and conversion.⁹

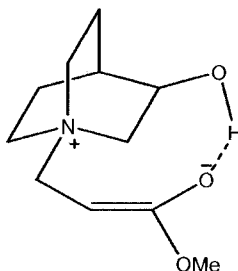


Figure 1.3. Stabilization of the zwitterionic intermediate by the creation of a intramolecular hydrogen bond.

The use of non-nucleophilic bases such as 1,8-diazabicyclo[5.4.0]undec-7-ene (DBU) may also improve both reaction rate and chemical yield.¹⁰ Several non-amine catalysts/systems such as dimethyl sulfide/ TiCl_4 ,^{11,12} TiCl_4 ,^{13,14} trialkylphosphines and metal complexes such as $\text{RhH}(\text{PPh}_3)_4$ and $\text{RuH}_2(\text{PPh}_3)_4$ have also been successfully utilized for coupling activated alkenes and carbon electrophiles.¹⁵

It has also been demonstrated that the use of formaldehyde ($\text{R}=\text{H}$, Scheme 1.1) results in monomers that polymerize radically as fast as, or faster than, typical methacrylates.¹⁶ This formulation allows having functional monomers that are readily available from commercial acrylates with a wide array of R groups.

The polar, resonance, and steric effects of the substituents play an important role in the reactivity of RHMA monomers. For instance, acrylate monomers having α -alkyl substituents greater than methyl show poor or no polymerizability under free radical polymerization conditions due to steric

effects.^{17,18} In contrast, the substitution of an oxygen atom β atom to the double bond increases the reactivity of the monomer by overcoming steric effects.¹⁹ RHMA monomers show excellent polymerizability, giving very high molecular weight polymers, due to a combination of hydrogen bonding and electronic effects of the ester group that increases propagation while decreasing chain transfer.²⁰

Reactive Surfactants in Heterophase Polymerization

Polymeric dispersions are used in a wide range of applications such as synthetic rubber, paints, adhesives, binders for non-woven fabrics, impact modifiers for plastic matrices, additives for construction materials, flocculants, and rheological modifiers. Environmental concerns and government regulations are making it necessary to substitute solvent-borne systems with water-borne systems, leading to important developments in the field of aqueous polymeric dispersion. This interest grows also due to the fact that polymeric dispersions have some unique properties that meet a wide range of application requirements and compared with other polymerization processes, polymerization in dispersed media presents substantial advantages concerning the controllability of the processes used. Dispersed polymers can be produced via different processes such as emulsion polymerization, inverse emulsion polymerization, dispersion polymerization, miniemulsion polymerization, microemulsion polymerization, and by emulsification of preformed polymers.²¹⁻²⁴

Emulsion polymerization is the most common process for the production of dispersed polymers, also called latexes. This process requires the use of

amphiphilic molecules or surfactants that have great importance in the production and applications of the dispersed polymers. Surfactants play an important role in the the nucleation of the latex particles, the emulsification of monomer droplets and/or preformed polymer, and the stabilization of the polymer particles during the polymerization and the shelf life of the product. They can, however, have adverse effects such as inducing foam²⁵ or migration through the aqueous phase, causing destabilization of the latex particles in certain latex-based formulations for example.²⁶ This can induce further problems during processing of the latexes, for example when the latex is coated the surfactant can desorb under the influence of the intensity of the shear and cause destabilization. This migration phenomenon can lead to segregation²⁷ and concentration of the surfactant molecules in pockets, which increases percolation by water and water sensitivity. The surfactant can also migrate to the film-air surface of the film²⁶ and affect gloss, or to the film-substrate interface, affecting adhesion. Mechanical properties such as hardness²⁸ can then be greatly affected by the segregation of these small molecules. A common way to reduce the amount of surfactant is to replace it partially with functionalized monomers such as methacrylic acid, methacrylamide and sulfonated monomers derivatives such as 2-sulfoethyl methacrylate. However, relatively large amounts of these comonomers are needed to obtain sufficient stabilization effects, and this can impact the overall properties of the polymer.

A more promising way to reduce the negative effects of surfactants comes from the use of reactive surfactants, also called polymerizable surfactants. In this

case, the surfactant is covalently bound to the polymer matrix, which leads to a decrease of the migration phenomenon in the polymer film. These reactive surfactants can be a combination of a surfactant and an initiator (inisurf),²⁹⁻³¹ a surfactant and a transfer agent (transurf),³²⁻³⁵ or a surfactant and a monomer, referred to as a surfmer or polymerizable surfactant.³⁶ Another advantage coming from the use of reactive surfactants resides in the potential reduction of the amount of surface-active matter used in the reaction process.²⁵

It should be pointed out that the stability of the system cannot be adjusted independently by varying the reactive surfactant concentration, as can be done with conventional non-reactive surfactants, without strongly affecting the polymerization rate and the molecular weight distribution.³⁰

Catalytic Chain Transfer Polymerization (CCTP)

It was Enikolopyan, et al. that discovered in the early 1980's that certain cobalt complexes were able to catalyze the chain transfer to monomer reaction in methacrylate polymerizations.^{37,38} This polymerization modification allowed decreasing the molecular weight of the product with little effect on the yield while requiring only ppm quantities of the corresponding catalyst. Further developments in the use of these catalysts have led to a polymerization technique that is now widely used for the production of low molecular-weight polymers and macromonomers.³⁹ The complexes that show catalytic chain transfer activity are primarily cobaloximes and porphyrins (see Figure 1.4 below).

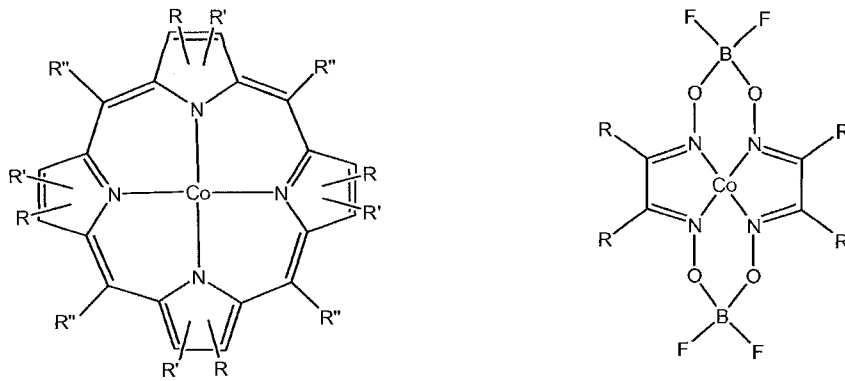


Figure 1.4. Cobalt porphyrins (left) and cobaloximes (right).

Other compounds such as molybdenum and chromium complexes have also been studied, but cobalt-based species have remained the most popular and effective. The mechanism was for some time a matter of conjecture, but is now generally assumed to involve the cobalt hydride⁴⁰ as shown in Figure 1.5.

Polymerization starts by the addition of an initiating species, which produces propagating radicals. Chain transfer occurs when one of these radicals encounters the catalyst (Co(II)). The catalyst abstracts a hydrogen atom from the growing chain end, producing a dead polymer with an unsaturated terminal bond and the cobalt hydride (Co(III)-H). The reinitiation/regeneration step occurs when the hydrogen atom is transferred to a monomer, thereby regenerating the catalyst and forming a new propagating species.

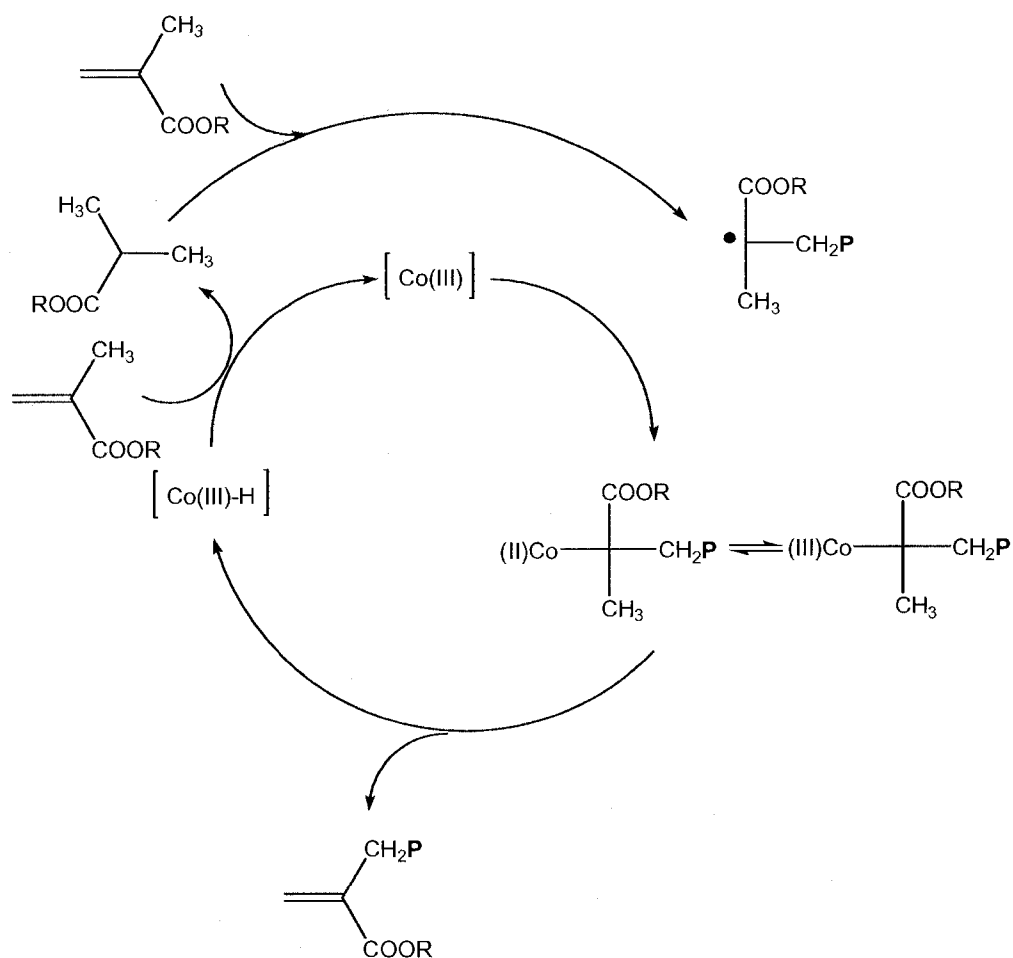


Figure 1.5. Catalytic chain transfer polymerization mechanism.

The chain-transfer catalysts are very sensitive to the presence of oxygen, so that degassing of reaction solutions is required and peroxide initiators cannot generally be used. Catalysts are usually sensitive to the solvent used during the reaction and the pH. Prediction of molecular weights in chain-transfer reactions generally make use of the Mayo equation:^{40,41}

Equation 1.1. Mayo equation.

$$\frac{1}{DP_n} = \frac{1}{DP_{n_0}} + \frac{C_{tr} \cdot [\text{Co(II)}]}{[M]}$$

where DP_n and DP_{n_0} are the number-average degree of polymerization with and without the addition of chain-transfer agent.

One of the largest areas of application for catalytic chain transfer (CCT) is in the production of macromonomers. The terminal double bond in CCT products makes them particularly useful for applications like paints requiring low-viscosity materials that can be further reacted.^{42,43} Further end-group functionalization of the macromonomer formed can be realized by reaction of the terminal double bond.^{39,43,44}

Polymer Nanocomposites

Polymer-layered silicate nanocomposites. Polymer nanocomposites have recently attracted intense industrial and academic interest due to their remarkably enhanced properties compared to unfilled resins or to more conventional composite materials. Such materials incorporate inorganic fillers usually composed of sheets, with a thickness of one to a few nanometers and a length of 30 nm to several micrometers. Among these materials, clays have been widely used in the formation of nanocomposites. Clay minerals contain active sites such as hydroxyl groups located at the edge and are also characterized by the presence of exchangeable metal cations such as sodium, lithium, and calcium located in the interlayer spacing. Consequently, cationic surfactants can be electrostatically attached onto clay surfaces by a cation exchange process. The preparation of polymer/clay nanocomposite materials was first reported in 1961 by Blumstein, demonstrating the polymerization of vinyl monomers intercalated into Montmorillonite (MMT).⁴⁵ However, it was the work of

researchers at the Toyota Central Research laboratories that opened great perspective for the development of nanocomposites. They reported that incorporation of small amounts of MMT into nylon-6 resulted in a remarkable enhancement of the thermal and mechanical properties of the nanocomposite material.^{46,47} Since then, a huge number of works have been published in this field.⁴⁸⁻⁵⁰

The physical properties of polymer nanocomposites mainly depend on the degree of dispersion of the filler and on the ability to produce intercalation or exfoliation of the clay layers within the polymer matrix (Figure 1.6).

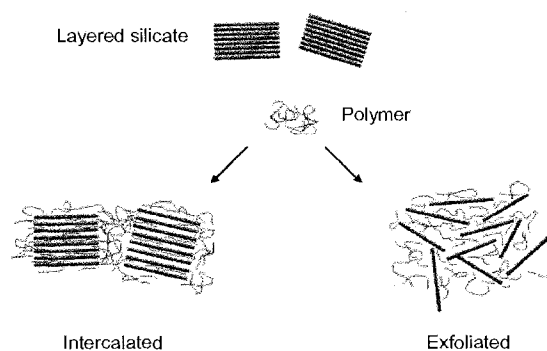


Figure 1.6. Nanocomposite morphologies.

Different methods to prepare polymer/clay nanocomposites are reported: exfoliation/adsorption, in situ polymerization, and melt intercalation. Typical clay modifiers for melt intercalation processes are quaternary alkyl ammonium salts, which are incorporated onto the clay surface through cation exchange to impart hydrophobicity to the clay layers. In situ polymerization mostly involves the incorporation of organic groups capable of reacting with polymers or initiating polymerization of monomers in order to create a chemical link between the inorganic phase and the polymeric matrix. Amongst the pioneering works in this

field are those of Giesenking,⁵¹ Hendricks,⁵² and Grim and Allaway⁵³ who showed that the structural inorganic cations of bentonite could be successfully replaced by organic cations. Henry and Dekking^{54,55} reported in a series of papers the modification of bentonite and kaolinite by adsorption of 2,20-azobisiso-butyramidine hydrochloride (AIBA) by means of an ion exchange reaction and the subsequent polymerization of methyl methacrylate, styrene, styrene-butadiene, vinyl acetate, chloroprene, acrylamide, and acrylonitrile. More recently, Fu and Qutubuddin⁵⁶ intercalated vinylbenzyl dimethyl dodecylammonium chloride (VDAC) into MMT through cation exchange, dispersed the organoclay in styrene, and performed polymerization in bulk. Fan et al.⁵⁷ reported the synthesis of mono- and bicationic free radical initiators and their intercalation into the MMT galleries to initiate the free radical polymerization of styrene from the clay surface. In a related strategy, Weimer, et al., synthesized delaminated PS/silicate nanocomposites by anchoring a living free radical polymerization initiator into the silicate layers followed by bulk polymerization.⁵⁸ Velten, et al. recently reported the intercalation of various tert-butylammonium peroxides, and their use as polymerization initiators to produce exfoliated nanocomposites.⁵⁹

Another promising method to enhance the degree of dispersion of the filler in the polymer matrix was described first by Bougeat-lami and coworkers.⁶⁰ They reported the formation of colloidal nanocomposite particles by in situ emulsion polymerization, leading to enhanced dispersion of the inorganic filler within the polymeric matrix.

Polymer-TiO₂ nanocomposites. TiO₂ nanoparticles are widely used in paint, paper making, plastic, cosmetic, and pharmaceutical industries due to its outstanding physicochemical properties. Pigments in paint serve to provide color, hide the substrate, and modify application and/or performance properties. The paint industry was reported in 1999 to be the most important titania pigment consumer of the global pigment consumption.⁶¹

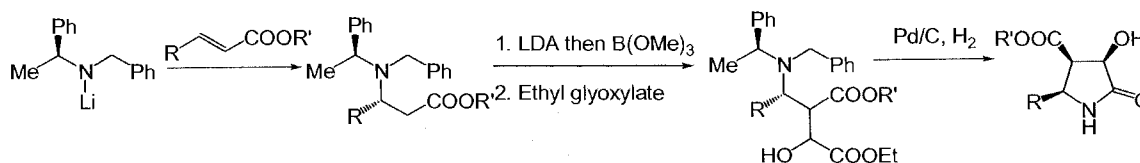
Recent regulations in paint formulations restricting the use of organic solvents have seen the rapid development of water-based formulations. This is in spite of the fact that achieving high levels of gloss with aqueous paint systems remains a complex task. Complete dispersion of pigments in water-based paints is fraught with difficulty; if aggregates are present, the end-use properties including gloss, opacity, tint strength, color distribution and storage stability will be highly affected. Incomplete dispersion of pigment particles causes uneven coloring and the optimum effect of the pigments is not fully utilized.

Polymeric dispersants are generally used to disperse titania pigment particles.⁶² Ionic dispersants can stabilize titania pigment particles in the aqueous phase, with the stabilization performance being pH and ionic strength dependent. For example, the ionized state of ionic dispersants cannot be maintained during the drying process of water-based paint film, leading to pigment aggregation in the resultant dry films.⁶³ Non-ionic dispersants reduce pigment particle interactions through steric stabilization and are generally not sensitive to pH or ionic strength changes.

Polyfunctional 2-Pyrrolidinones

Polyfunctional pyrrolidinones are optically active molecules that have received a great amount of attention in the past two decades. They have been principally examined as intermediates for synthesizing more complex biologically important molecules.^{64,68} 2-Pyrrolidinone moieties have been used in the past and are still used extensively as psychotropic, anti-hypertensive agents, inhibitors of proteolytic catalysis, and antimuscarinic agents.^{66–68} More specifically, hydroxyl-substituted 2-pyrrolidinones have been used for the treatment of brain insufficiencies, as cognition activators and as valuable building blocks for medicinally important compounds.

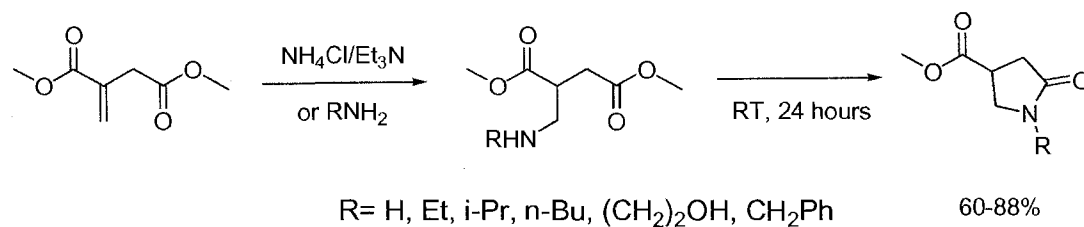
Much interest resides in developing new routes that can lead to chiral pyrrolidinones with multiple functional groups. Among these routes are three important synthetic schemes that lead to the formation of multifunctional pyrrolidinone derivatives. First, Jiang and Ma reported the chemical routes shown in Scheme 1.2 that lead to the formation of 5-alkyl-4-carboethoxy-3-hydroxy-pyrrolidinones via coupling of N,N-disubstituted amino esters with ethyl glyoxylate.⁶⁹



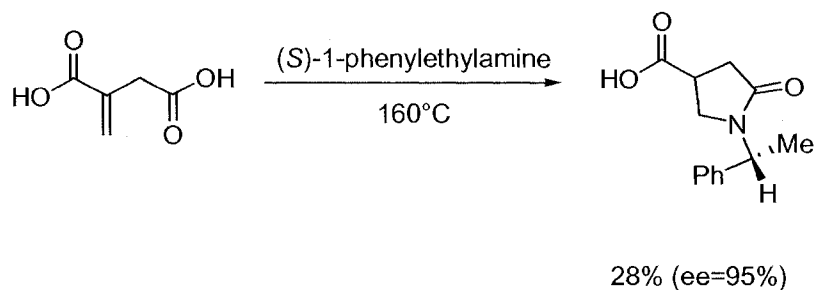
Scheme 1.2. Synthesis of 5-alkyl-4-carboethoxy-3-hydroxy-pyrrolidinones.

Another efficient route was reported by Valentin, et al., in which methyl esters of 1-alkyl-5-oxo-3-pyrrolidinecarboxylic acids were obtained by reaction of dimethyl itaconate with primary amines (Scheme 1.3).⁷⁰ Finally, multifunctional 2-

pyrrolidinone derivatives were also synthesised by Wyatt et al. starting from itaconic acid and (*S*)-1-phenylethylamine, with high enantiomeric excess (95%) (Scheme 1.4).⁷¹



Scheme 1.3. Synthesis of 1-alkyl-5-oxo-3-pyrrolidinecarboxylic acid methyl esters.



Scheme 1.4. Synthesis of 1-phenylethyl-5-oxo-3-pyrrolidinecarboxylic acid.

Supramolecular Assemblies

Synthesis of polymers by linking the monomers via non-covalent interactions, or of polymer networks by using non-covalent interactions of functionalized side chains, represent attractive approaches that have been of great interest for the scientific community over the past decades (Figure 1.7). Highly directional hydrogen bonds may result in strong binding when used in concert. When built into an array, the strength and selectivity of interaction can be tuned as a function of the number of functionalities and their respective positioning as donor and acceptor. There has been much interest in studying

arrays of hydrogen bonds since the strength and selectivity of interaction are critical in determining the properties of the resulting polymer-like material.

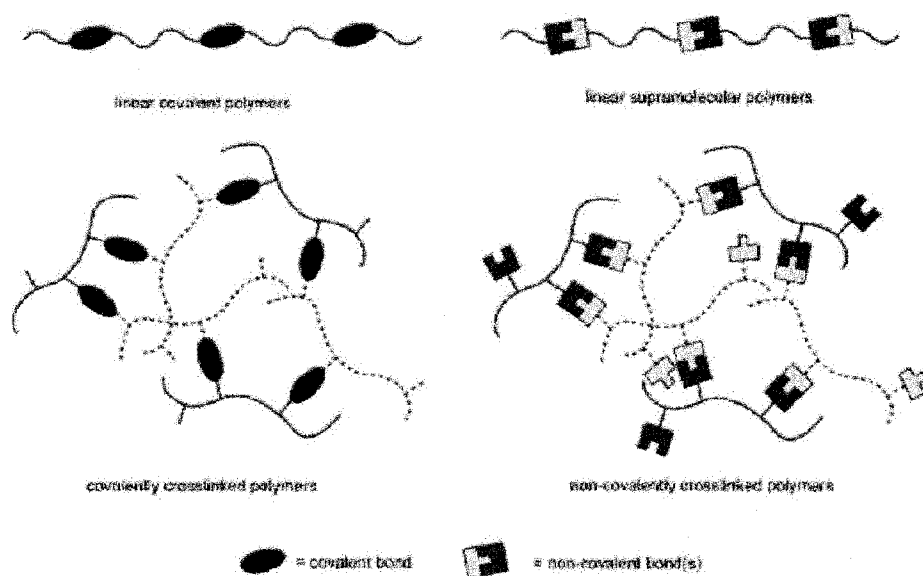


Figure 1.7. Polymer architectures made using covalent and non-covalent links between building blocks.

Early work on the synthesis of polymeric species via self-assembly was described by Kato and Frechet^{72,73} then later by Griffin,⁷⁴ who used multiple single hydrogen bonding functional groups to obtain supramolecular associations behaving like polymers. Despite the success of this approach, an inherent limitation is that single hydrogen bonds allow different hydrogen bonding motifs. This problem was later remedied by pre-organizing hydrogen bonds on a rigid scaffold to form well defined arrays.^{75–82} Linear arrays can offer the advantage of constraining the hydrogen bonding to limited possibilities for interaction with other functional motifs. The first use of arrays of hydrogen bonds in the assembly of supramolecular polymers was reported by Lehn and co-workers in 1993, for assembly of polymeric liquid crystalline and lyotropic mesophases using 2,6-

diamidopyridine- and thymine-functionalized building blocks.^{83,84} However, it was not until 1997, when the ureidopyrimidinone unit was discovered, that it became possible to assemble supramolecular polymers in dilute solution (Figure 1.8).⁸⁵ This work highlighted how linear polymers could be constructed using hydrogen-bonds in the same way and obeying the same principles as traditional condensation polymers.

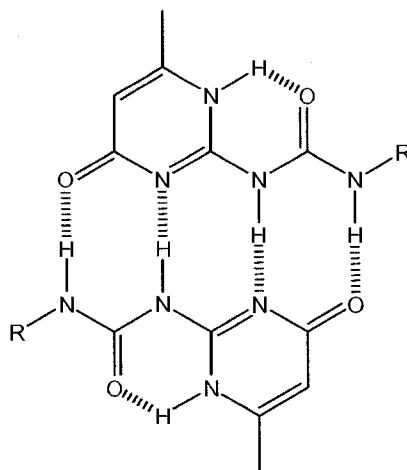


Figure 1.8. Hydrogen bonds between two ureidopyrimidinone units.

Supramolecular assembly via hydrogen-bonding interactions can find application in crystallization on various scales, robotics and manufacturing,^{86,87} porous network materials, helical superstructures,⁸⁸ nanotubes and wires, microelectronics and microdevices based on two- and three-dimensional systems, and in computers and biosensors.

Biodegradable Poly(ester amide)s

Over the past decade, great concern has been raised for the preservation of the environment. Biodegradable and recyclable materials became more and more attractive leading to growth in their respective markets. This has resulted in both academic science and industry to try to develop biodegradable polymers

and implement more effective and extensive recycling of waste to prevent the increasing contamination of the global environment. It is well known that aliphatic polyesters are biodegradable and hydrolyzable synthetic polymers, and some are already being commercialized. However, they possess insufficient thermal and/or mechanical properties that limit their broader use. For instance, a series of α -hydroxypolyesters, such as poly(glycolic acid) (PGA), poly(lactic acid) (PLA), and their copolymers, have been widely used as bioabsorbable sutures and surgical implants.⁸⁹ Other types of polyesters, such as poly(caprolactone), poly(β -propiolactone), and poly(butyrolactone), have also been successfully used as biodegradable polymers in drug delivery and agricultural uses.^{90,91}

Aliphatic polyamides are generally not biodegradable, although there are a few reports demonstrating their biodegradability.^{92,93} However, compared to polyesters, aliphatic polyamides display higher thermal stability, higher modulus, and higher tensile strength. A combination of both aliphatic polyesters and polyamides is of great interest in order to prepare biodegradable materials with improved mechanical and processing properties.^{94,95} Such polymers are called poly(ester amide)s.

A wide range of poly(ester amide)s have already been prepared by either polycondensation or ring-opening polymerization techniques. There are two basic types of aliphatic poly(ester amide)s (PEAs): those derived from non-amino acids like aliphatic diamines and those derived from amino acids like L-phenylalanine, L-leucine, and/or L-lysine.⁹⁶⁻⁹⁹ Both types of PEAs have been studied for their

potential biomedical applications, but the amino acid derived PEAs appear to have better biocompatibility than those from aliphatic diamines.¹⁰⁰

REFERENCES

- 1 Villiéras, J.; Rambaud, M. *Synthesis* **1982**, *11*, 924-926.
- 2 Rosenthal, R.W.; Schwartzman, L.H.; Greco, N.P. *Journal of Organic Chemistry* **1963**, *28*, 2835-2838.
- 3 Ferris, A.F. *Journal of Organic Chemistry* **1955**, *20*, 780-787.
- 4 Baylis, A.B.; Hillman, M.E.D. *Chem. Abstr.* **1972**, *77*, 34174.
- 5 Morita, K.; Suzuki, Z.; Hirose, H. *Bull. Chem. Soc. Jpn.* **1968**, *41*, 2815.
- 6 Drewes, S.E.; Freese, S.D.; Emslie, N.D.; Roos, G.H.P. *Synth. Commun.* **1988**, *18*, 1565-1668.
- 7 Ameer, F.; Drewes, S.E.; Freese, S.D.; Kaye, P.T. *Synth. Commun.* **1990**, *20*, 1611-1614.
- 8 Hoffman, H.M.R. *J. Org. Chem.* **1988**, *53*, 3701-3712.
- 9 Basavaiah, D.; Sarma, P.K.S. *Chem. Commun.* **1990**, *20*, 1611-1614.
- 10 Aggarwal, V.K.; Mereu, A. *Chem. Commun.* **1990**, 2311-2312.
- 11 Kataoka, T.; Kinoshita, H.; Kinoshita, S.; Iwamura, T.; Watanabe, S. *Angew. Chem. Int. Ed.* **2000**, *39*, 2358.
- 12 Basavaiah, D.; Muthukumaran, K.; Sreenivasulu, B. *Synlett* **1999**, 1249.
- 13 Li, G.; Wei, H.X.; Gao, J.J.; Caputo, T.D. *Tetrahedron Lett.* **2000**, *41*, 1.
- 14 Basavaiah, D.; Sreenivasulu, B.; Mallikarjuna, R.R.; Muthukumaran, K. *Synth. Commun.* **2001**, *31*, 2987.
- 15 Drewes, S.E.; Roos, G.H.P. *Tetrahedron* **1988**, *44*, 4653.
- 16 Nippon Shokubai, www.shokubai.co.jp, accessed Aug, **2004**.
- 17 Chikanishi, K.; Tsuruta, T. *Makromol. Chem.* **1965**, *81*, 198.

- 18 Cheng, J.; Yamada, B.; T. Otsu, T. *J. Polym. Sci., Part A: Polym. Chem.* **1991**, 29, 1837.
- 19 Reed, S.F.; Baldwin, M.G. *J. Polym. Sci., Part A: Polym. Chem.* **1963**, 1, 1919.
- 20 Avci, D.; Kusefoglu, S.H.; Thomson, R.D.; Mathias, L.J. *J. Polym. Sci., Part A: Polym. Chem.* **1994**, 32, 2937.
- 21 Lovell, P.A.; El-Aasser, M.S. *Emulsion Polymerization and Emulsion Polymers: Chistester*, John Wiley **1997**.
- 22 Fitch, R.M. *Polymer Colloids. A Comprehensive Introduction*, Academic Press, London **1997**.
- 23 Daniels, E.S.; Sudol, E.D.; El-Aasser, M.S. *Polymer Latexes: Preparation, Characterization, and Applications*, ACS Symposium Series, Vol. 492, Washington, DC **1992**.
- 24 Candau, F.; Ottewill, R.H. *Scientific Methods for the Study of Polymer Colloids and Their Applications*, Kluwer Academic Publishers, Dordrecht **1990**.
- 25 Malyukova, Y.B.; Naumova, S.V.; Gristkova, I.A.; Bondarev, A.N.; Zubov, V.P. *Polym. Sci.* **1991**, 33, 1361.
- 26 Lam, S.; Hellgren, A.C.; Sjoberg, M.; Holmberg, K.; Schoonbrood, H.A.S.; Unzué, M.J.; Asua, J.M.; Tauer, K.; Sherrington, D.C.; Montoya-Goni, A. *J. Appl. Polym. Sci.* **1997**, 66, 187.
- 27 Duchesne, B.; Gerharz, G. *Polym. Int.* **1997**, 43, 187.
- 28 Holmberg, K. *Prog. Org. Coat.* **1992**, 20, 235.

- 29 Ivanchev, S.S.; Pavljuchenko, V.N.; Byrdina, N.A. *J. Polym. Sci., Part A: Polym. Chem.* **1987**, *25*, 47.
- 30 Tauer, K.; Goebel, K.H.; Kosmella, S.; Neelsen, J.; Stahler, K. *Plaste Kautsch.* **1988**, *35*, 373.
- 31 Tauer, K.; Goebel, K.H.; Kosmella, S.; Stähler, K. J. Neelsen, *Makromol. Chem., Macromol. Symp.* **1990**, *31*, 107.
- 32 Hamaide, T.; Revillon, A.; Guyot, A. *Eur. Polym. J.* **1987**, *23*, 787.
- 33 Vidal, F.; Hamaide, T. *Polym. Bull.* **1995**, *35*, 1.
- 34 Guyot, A.; Vidal, F. *Polym. Bull.* **1995**, *34*, 569.
- 35 Vidal, F.; Guyot, A. *Polym. Adv. Technol.* **1995**, *6*, 473.
- 36 Vidal, F.; Guillot, J.; Guyot, A. *Polym. Adv. Technol.* **1994**, *6*, 473.
- 37 Enikolopyan, N.S.; Smirnov, B.R.; Ponomarev, G.V.; Belgovskii, I.M. *J. Polym. Sci., Polym. Chem. Edn.* **1981**, *19*, 879–889.
- 38 Karmilova, L.V.; Ponomarev, G.V.; Smirnov, B.R.; Belgovskii, I.M. *Russ. Chem. Rev.* **1984**, *53*, 132.
- 39 Gridnev, A.; Ittel, S.D. *Chem. Rev.* **2001**, *101*, 3611–3659.
- 40 Heuts, J.P.A.; Muratore, L.M.; Davis, T.P. *Macromol. Chem. Phys.* **2000**, *201*, 2780–2788.
- 41 Odian, G. *Principles of Polymerization New York: Wiley-Interscience*, 3rd ed. **1991**.
- 42 Mayo, F.R. *J. Am. Chem. Soc.* **1943**, *65*, 2324–2329.
- 43 Heuts, J.P.A.; Roberts, G.E.; Biasutti, J.D. *Aust. J. Chem.* **2002**, *55*, 381–398.

- 44 Mulhaupt, R. *Macromol. Chem. Phys.* **2003**, *204*, 289–327.
- 45 Blumstein A. *J. Polym. Sci., Part A: Polym. Chem.* **1965**, *3*, 2665.
- 46 Okada, A.; Kawasumi, M.; Suki, A.; Kurauchi, T.O. *Mater. Res. Soc. Symp. Proc.* **1990**, *171*, 45.
- 47 Yano, K.; Usuki, A.; Kurauchi, T.; Kamigaito, O. *J. Polym. Sci., Part A: Polym. Chem.* **1993**, *31*, 2493.
- 48 Lee, J.; Takekoshi, T.; Giannelis, E.P. *Mater. Res. Soc. Symp.* **1997**, *457*, 513.
- 49 Noh, M.W.; Jang, L.W.; Lee, D.C. *J. Appl. Polym. Sci.* **1999**, *74*, 179.
- 50 Lee, J.; Giannelis, E. *Macromolecules* **2001**, *34*, 4098.
- 51 Giesecking, J.E. *Soil. Sci.* **1939**, *47*, 1.
- 52 Hendricks, S.B. *Phys. Chem. Ithaca* **1941**, *45*, 65.
- 53 Grim, R.E.; Allaway, W.H.J. *J. Am. Ceram. Soc.* **1947**, *30*, 137.
- 54 Henry, G.; Dekking, G. *J. Appl. Polym. Sci.* **1965**, *9*, 1641.
- 55 Henry, G.; Dekking, G. *J. Appl. Polym. Sci.* **1967**, *11*, 23.
- 56 Fu, X.; Qutubuddin, S. *Polym. Compos.* **2001**, *42*, 807.
- 57 Fan X, Xia C, Advincula R. *Langmuir* **2003**, *19*, 4381.
- 58 Weimer, M.W.; Chen, H.; Giannelis, E.P.; Sogah, D.Y. *J. Am. Chem. Soc.* **1999**, *121*, 1615.
- 59 Velten, R.A.; Shelden, W.R.; Caseri, U.W.; Suter, Y.L. *Macromolecules* **1999**, *32*, 3590.
- 60 Negrete-Herrera, N.; Putaux, J.-L.; Bourgeat-Lami, L. *Progress in Solid State Chemistry* **2006**, *34*, 121-137.

- 61 Adam, R. *Paint & Ink International* **1999**, 12, 24-27.
- 62 Patton, T. *Paint Flow and Pigment Dispersion*, New York: John Wiley & Sons, 2nd ed. **1979**.
- 63 Clayton, J. *Surface Coatings International* **1997**, 9, 414-420.
- 64 Harrison, T. *Contemp. Org. Synth.*, **1995**, 2, 209
- 65 (a) Moody, C. M.; Young, D. W. *Tetrahedron Lett.* **1994**, 35, 7277-7280;
(b) Meyers, A. I.; Snyder, L. *J. Org. Chem.* **1993**, 58, 36-42; (c) Rigo, B.; Fasseur, D.; Cherepy, N.; Couturier, D. *Tetrahedron Lett.* **1989**, 30, 7057-7060.
- 66 (a) Hanessian, S.; Reinhold, U.; Ninkovic, S. *Tetrahedron Lett.* **1996**, 37, 8967-8970; (b) Galeazzi, R.; Eremia, S.; Mobbili, G.; Orena, M. *Tetrahedron: Asymmetry* **1996**, 7, 79-88; (c) Hanessian, S.; Atovelomanana, V. *Synlett.* **1990**, 501-503.
- 67 (a) Ghelfi, F.; Bellesia, F.; Forti, L.; Ghirardini, G.; Grandi, R.; Libertini, E.; Montemaggi, M. C.; Pagnoni, U. M.; Pinetti, A.; De Buyck, L.; Parsons, A. F. *Tetrahedron* **1999**, 55, 5839-5852; (b) Cossy, J.; Cases, M.; Pardo, D. G. *Synlett* **1998**, 507-509; (c) Murakami, S.; Takemoto, T.; Shimizu, Z. *J. Pharm. Soc. Jpn.* **1953**, 73, 1026-1028.
- 68 Galeazzi, R.; Mobbili, G.; Orena, M. *Tetrahedron* **1996**, 52, 1069-1084.
- 69 Ma, D.; Jiang, J. *Tetrahedron: Asymmetry* **1998**, 9, 575-579.
- 70 Felluga, F.; Pitacco, G.; Prodan, M.; Pricl, S.; Visintin, M.; Valentin, E. *Tetrahedron: Asymmetry* **2001**, 12, 3241-3249.

- 71 Arvanitis, E.; Motevalli, M.; Wyatt, P. B. *Tetrahedron Lett.* **1996**, *37*, 4277–4280.
- 72 Kihara, H.; Kato, T.; Uryu, T.; Frechet, J.M.J. *Chem. Mater.* **1996**, *8*, 961–968.
- 73 Kumar, U.; Kato, T.; Frechet, J.M.J. *J. Am. Chem. Soc.* **1992**, *114*, 6630–6639.
- 74 St. Pourcain, C.B.; Griffin, A.C. *Macromolecules* **1995**, 4116–4121.
- 75 Castellano, R.K.; Clark, R.; Craig, S.L.; Nuckolls, C.; Rebek, J. *Proc. Natl. Acad. Sci.* **2000**, *97*, 12418–12421.
- 76 Castellano, R.K.; Nuckolls, C.; Eichhorn, S.H.; Wood, M.R.; Lovinger, A.J.; Rebek, J. *Angew. Chem., Int. Ed.* **1999**, *38*, 2603–2606.
- 77 Castellano, R.K.; Rebek, J. *J. Am. Chem. Soc.* **1998**, *120*, 3657–3663.
- 78 Castellano, R.K.; Rudkevich, D.M.; Rebek, J. *Proc. Natl. Acad. Sci.* **1997**, *94*, 7132–7137.
- 79 Xu, H.; Rudkevich, D.M. *Chem. Eur. J.* **2004**, *10*, 5432–5442.
- 80 Whitesides, G.M.; Simanek, E.E.; Mathias, J.P.; Seto, C.T.; Chin, D.; Mammen, M.; Gordon, D.M. *Acc. Chem. Res.* **1995**, *28*, 37–44.
- 81 Choi, S.; Li, X.; Simanek, E.E.; Akaba, R.; Whitesides, G.M. *Chem. Mater.* **1999**, *11*, 684–690.
- 82 Klok, H.A.; Joliffe, K.A.; Chauer, C.L.; Prins, L.J.; Spatz, J.P.; Moller, M.; Timmerman, P.; Reinhoudt, D.N. *J. Am. Chem. Soc.* **1999**, 7154–7155.
- 83 Gulick-Krymicki, T.; Fouquey, A.M.; Lehn, J.-M. *Proc. Natl. Acad. Sci.* **1993**, *90*, 163–167.

- 84 Kotera, M.; Lehn, J.M.; Vigneron, J.P. *J. Chem. Soc., Chem. Commun.* **1994**, 197–199.
- 85 Sijbesma, R.P.; Beijer, F.H.; Brunsveld, L.; Folmer, B.J.B.; Hirschberg, J.; Lange, R.F.M.; Lowe, J.K.L.; Meijer, E.W. *Science* **1997**, 278, 1601–1604.
- 86 Goodsell, D.S. *Bionanotechnology: Lessons from Nature* New York: John Wiley & Sons **2003**.
- 87 Goodsell, D.S. *The Machinery of Life*, Heidelberg: Springer **1993**.
- 88 Li, S.; Hill, C.P.; Sundquist, W.I.; Finch, J. *Nature* **2000**, 407, 409–413.
- 89 Holland, S.J.; Tighe, B.J.; Gould, P.I.J. *Controlled Release* **1986**, 4, 155.
- 90 Field, R. D.; Rodriguez, F.; Finn, R. K. *J. Appl. Polym. Sci.* **1974**, 18, 3571.
- 91 Athisen. T.; Lewis. M.; Albertsson. A.C. *J. Appl. Polym. Sci.* **1991**, 42, 2365.
- 92 Hashimoto, K.; Hamano, T.; Okada, M. *J Appl Polym Sci* **1994**, 54, 1579.
- 93 Aikawa, T.; Ohtsuka, T.; Sanui, K.; Kurusu, Y.; Sato, A. *Chem. Abstr.* **1988**, 109, 5538.
- 94 Barrows, T.H.; Grussing, D.M.; Hegdahl, D.W. *Trans. Soc. Biomater.* **1983**, 109.
- 95 Veld, P.J.A.I.; Dijkstra, P.J.; Feijen, J. *Macromol. Chem. Phys.* **1992**, 193, 2713-2730.
- 96 Grigat, E.; Koch, R.; Timmermann, R. *Polym. Degrad. Stab.* **1998**, 59, 223-226.
- 97 Paredes, N.; Rodriguez-Galan, A.; Puiggali, J. *J. Polym. Sci., Part A: Polym. Chem* **1998**, 36, 1271-1282.

- 98 Helder, J.; Dijkstra, D. J.; Feijen, J. J. *Biomed. Mater. Res.* **1990**, *24*, 1005.
- 99 Tokiwa, Y.; Suzuki, T.J. *Appl. Polym. Sci.* **1979**, *24*, 1701.
- 100 Lips, P.; Dijkstra, P.J. Biodegradable Polyesteramides. In *Biodegradable Polymers for Industrial Applications*. **2005**, 107-139.

CHAPTER II
SYNTHESIS OF NEW ACRYLATE-BASED NONIONIC SURFMERS AND
THEIR USE IN HETEROPHASE POLYMERIZATION

Abstract

New acrylate-based non-ionic reactive surfactants have been successfully designed, synthesized, and polymerized. Their homo- and copolymerization properties were studied and while a low degree of homopolymerization was achieved, good copolymerization behavior with methyl methacrylate was observed. High solid content acrylic latexes were prepared using these new amphiphilic reactive molecules, which were shown to have covalently incorporated these reactive surfactants. Well-defined latex particles with narrow particle size distributions were produced. Both scanning electron microscopy and atomic force microscopy (AFM) techniques were used to confirm the size and size distribution of the particles formed. AFM measurements conducted on the films formed from these latexes allowed demonstration of their low degree of water sensitivity. This indicates a low level of surfactant migration during the film formation and that the surfmers have been successfully incorporated into the final copolymers produced via heterophase polymerizations.

Introduction

Emulsion polymerization is one of the most important techniques for preparing polymers from an industrial point of view. Emulsion polymerization is carried out to obtain film-forming latexes useful in water-borne coatings. It is necessary to introduce surfactants into the polymerization recipe in order to

control both the size of the particles and the stability of latexes. However, the presence of these species, which are generally low molecular weight compounds, and mainly associated with the polymeric particle through adsorption, which involves weak associative bonds such as hydrogen or π -bonding, may result in adverse effects on the latex and final polymer properties. For instance, lack of stability under specific conditions, such as high shear, freezing, or high ionic strength, may arise from the use of conventional surfactants. Furthermore, these amphiphilic molecules may migrate through the matrix upon film formation¹⁻³ and affect the overall properties of the final polymeric material such as adhesion, water sensitivity, and gloss.⁴⁻⁷ Migration of these molecules may also induce their association and agglomeration leading to phase separation and an increase in the anisotropy in the final polymer that may affect its mechanical properties.

The use of polymerizable surfactants can avoid these issues as they can deliver the amphiphilic properties of standard surfactants but can also chemically interact (e.g., covalently bind) with the growing polymer chains. In so doing, the secondary effects on the final polymer are reduced as they are chemically bound to the matrix and the surfactants cannot migrate in the same way as conventional surfactants. Thus, the risk of desorption is dramatically reduced. Reactive surfactants can participate in the polymerization process, as an initiating moiety (*inisurf*), a moiety capable of chain transfer (*transurf*), or a group capable of copolymerization during the free radical polymerization (*surfmer*).⁸⁻¹⁶ Most of the work to date that deals with reactive surfactants involved surfmers as these

molecules give the greatest potential molecular diversity. Anionic, cationic, and non-ionic surfmers have been synthesized and applied in emulsion polymerizations.¹⁷ The use of surfmers has been shown to improve the water resistance and surface adhesion in comparison to conventional emulsifiers.¹⁸⁻¹⁹ Water and vapor permeability were also shown to be reduced when surfmers were used.²⁰

The reactivity of the polymerizable surfactant and its adsorption characteristics are critical factors in defining its performance. To be effective, the surfmer must react such that, during the main part of the polymerization, its incorporation into the polymer being produced is low. This avoids surfmer being buried into the bulk of the polymeric particle and maximizes the amount of surfmer present at the surface. Thus, the surfactant activity is maximized and the quantities required are kept to a minimum. However, toward the end of the reaction, high surfmer incorporation should be achieved to avoid the presence of unreacted species in the final polymer, which may eventually migrate through the film during final film formation.²¹

A wide range of surfmers have already been developed based on acrylates, methacrylates, styrenics and maleates. The main limitation on surfmer use at the moment is related to the reactivity of the polymerizable unit. Traditionally, the reactivity of the functional groups has been restricted to prevent the “burying” phenomenon, resulting in surfmers that are applied only to niche opportunities.²²⁻⁴⁰

Here we report the synthesis of new amphiphilic alkyl α -methylacrylate-based molecules and their incorporation as reactive surfactants in heterophase polymerizations. Hydroxymethylacrylate esters (RHMA) are vinyl monomers, which have a very high susceptibility to undergo radical polymerization. This high reactivity can be tailored by the nature of the functional groups present in the molecule. The polarity, resonance and steric effects of the substituents all play an important role in defining the reactivity of RHMA monomers. For instance, conventional acrylate monomers having α -alkyl double bond substituents larger than a methyl group exhibit poor or no ability to polymerize under free radical polymerization conditions due to steric effects.^{41,42} In contrast, the substitution of an oxygen atom β to the double bond increases the reactivity of the monomer by (a) helping to overcome these steric effects and (b) due to a combination of hydrogen bonding and electronic effects that promote propagation while decreasing chain transfer.^{43,44} As a result, RHMA-based monomers as shown in Figure 2.1 possess excellent capability for polymerization, giving rise to very high molecular weight polymers. More importantly, when copolymerized with other acrylates or methacrylates, these monomers lead essentially to random copolymers and good control of final polymer composition can be achieved.

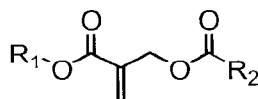
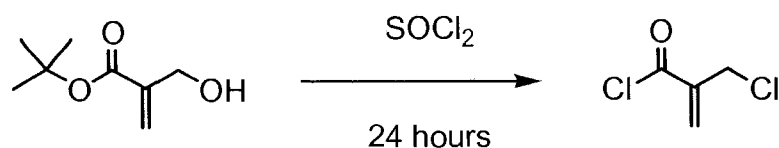


Figure 2.1. RHMA-based monomer.

In this chapter, we report the synthesis of new RHMA-based reactive surfactants and their incorporation into high solid content acrylic latexes. The study of the surface of latex films incorporating these reactive surfactants by atomic force microscopy (AFM) is also reported where the surfactant's influence on the topographical features, roughness and surface defects of the film were probed using this technique.

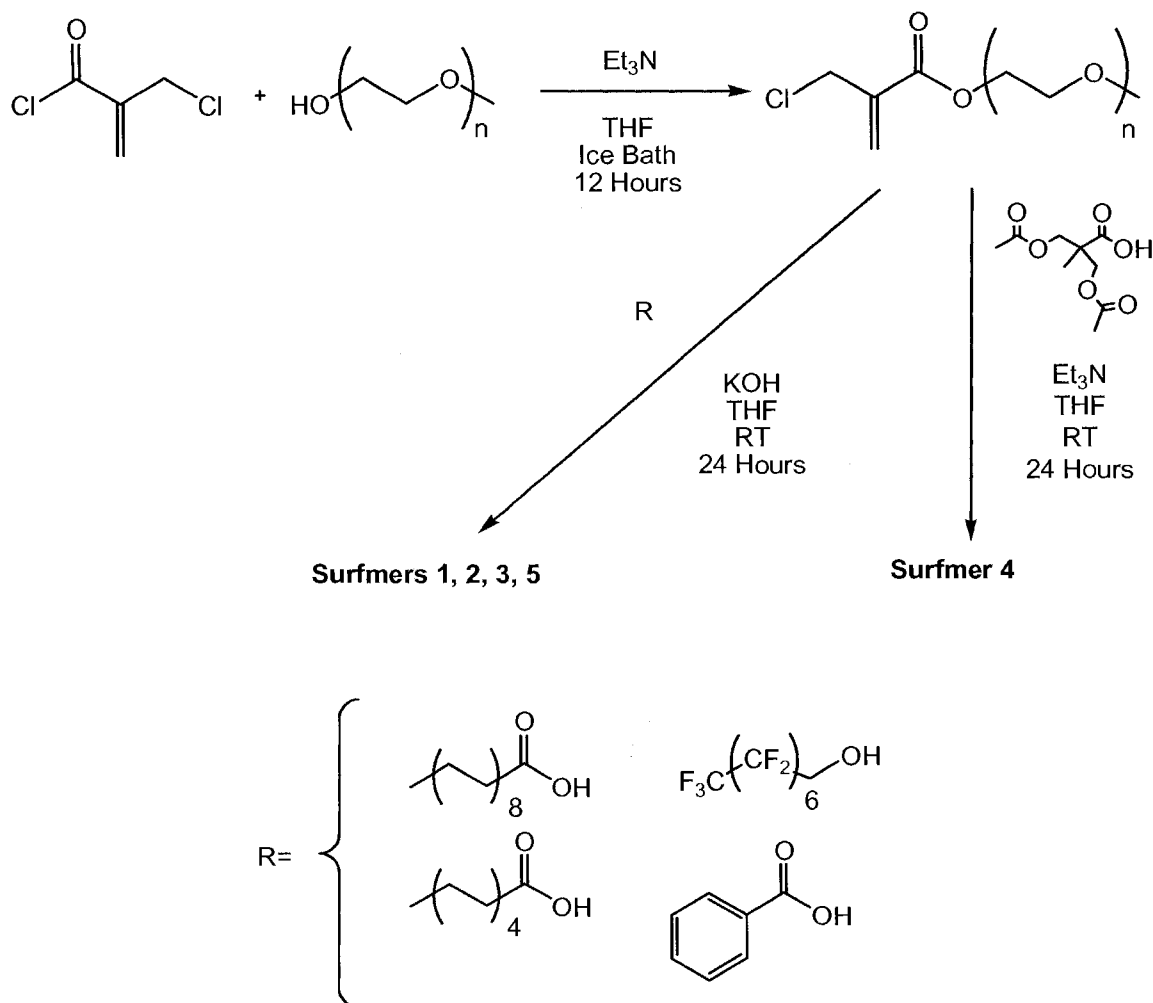
Results and Discussion

Synthesis and characterization of the surfmers. All the reactive surfactants synthesized are composed of a hydrophobic part, a polymerizable double bond, and a hydrophilic part. In this study, the hydrophobic part is either an aliphatic, aromatic, or perfluorinated moiety, while the hydrophilic part in all cases is a poly(ethylene glycol) methyl ether moiety. Different hydrophobic moieties were incorporated in order to determine the effect on particle stability during the emulsion polymerization as well as final polymer characteristics. A methacrylate group links the hydrophobic and hydrophilic moieties and constitutes the reactive site. This group will become involved in the emulsion copolymerization reactions with methyl methacrylate (MMA), n-butyl acrylate (BuA), and acrylic acid (AA). The macromonomers were all synthesized by functionalization of the α -(chloromethyl)acryloyl chloride (CMAC) intermediate which was synthesized according to the synthetic scheme presented in Scheme 2.1. This compound allows two different functional groups to be incorporated on either side of the polymerizable double bond.



Scheme 2.1. Synthesis of α -chloromethylacryloyl chloride (CMAC).

The reactive surfactants shown in Table 2.1 were synthesized following the general synthetic routes presented in Scheme 2.2. They were all obtained in good yields and purities (as determined by High Pressure Liquid Chromatography (HPLC)). Poly(ethylene glycol) methyl ether (MPEG) of a molecular weight of 350 g/mol, chosen to constitute the hydrophilic part of these molecules, was first reacted with CMAC to form the intermediate MPCMA (Scheme 2.2) that was subsequently reacted with different carboxylic acids or alcohols in the presence of base. To form surfmers S1, S2, and S3, MPCMA was reacted at room temperature with different aliphatic and aromatic carboxylic acid potassium salts. This mild procedure gave high purity products in high yields after filtration of the reaction mixture and evaporation of the solvent. ^1H NMR was used to follow the formation of the desired products by monitoring the appearance of the proton peaks at 4.78, 4.77 and 5.04 ppm, corresponding to the allylic-methylene protons of the ester form of the respective monomers.



Scheme 2.2. Synthesis of surfmers 1-5.

Surfmer **4** was synthesized following the same procedure by reaction of MPCMA with the potassium salt of 2,2-bis(acetoxymethyl)-propionic acid; the acid was obtained from the reaction of 2,2-bis(hydroxymethyl)-propionic acid and an excess of acetic anhydride at room temperature. The fluorinated surfmer (S5) was obtained by reaction of MPCMA and pentadecafluoro-1-octanol in the presence of potassium hydroxide. The structures of the different intermediates and macromonomers were confirmed by ^1H , ^{13}C NMR and FT-IR while their

purity was evaluated by HPLC (Table 2.1). As an example, ^{13}C NMR and FT-IR spectra of S1 are shown in Figures 2.2 and 2.3.

Table 2.1. Structures of the acrylate-based reactive surfactants investigated.

surfmr	Structure	MW (g/mol)	purity (%) ^(a)
S1		700.55	98
S2		588.35	97
S3		538.2	96
S4		634.28	98
S5		816.17	97

(a) – Evaluated by HPLC.

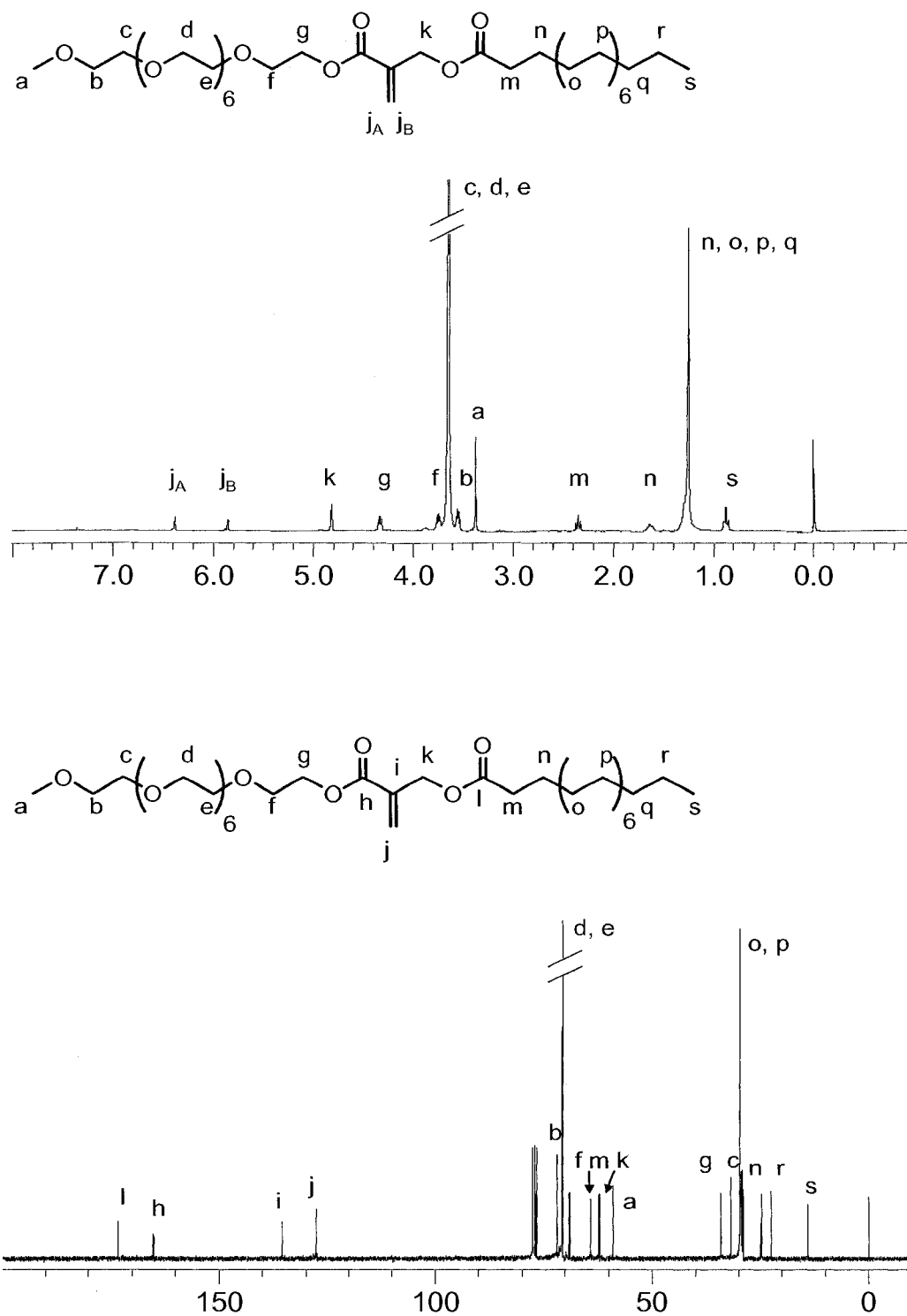


Figure 2.2. ^1H and ^{13}C NMR spectra of surfmer S1.

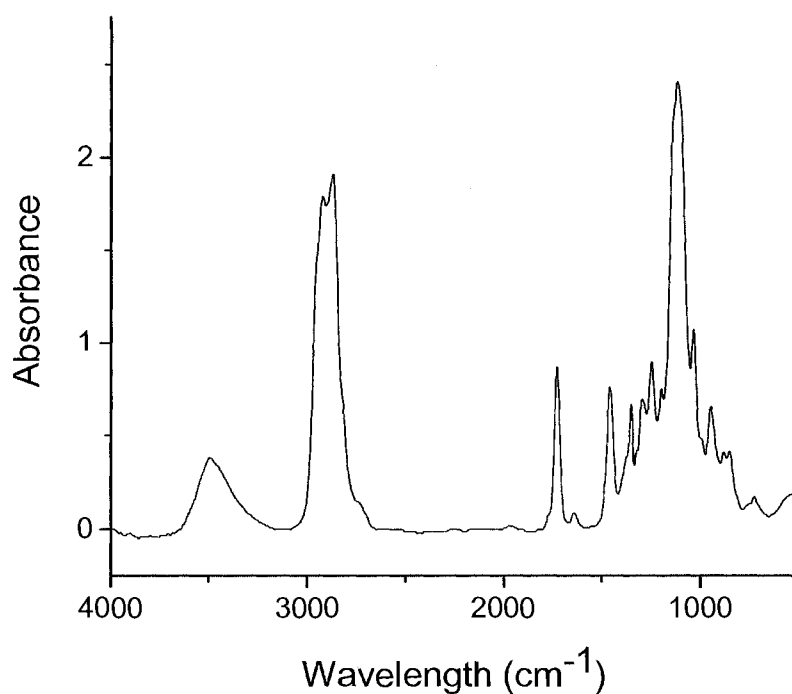


Figure 2.3. FT-IR spectrum of surfmer S1 (NaCl).

Homopolymerization of the reactive surfactants. In a first series of experiments, the homopolymerization of the reactive surfactants S1 - S5 in water was investigated in order to determine their capacity to homopolymerize in an aqueous medium. The results of these experiments are given in Table 2.2. The monomers were all homopolymerized in deionized water at 80 °C using ammonium persulfate as the water soluble initiator. Polymerizations were carried out over 24 hours to ensure maximum conversions.

Table 2.2. Homopolymerization characteristics of surfmer 1-5.

sample	surfmer	Solvent	Mn/1000 (g/mol)	PDI	conversion (%) ^(a)
H1	S1	Water	3.9	1.23	62.3
H2	S2	Water	6.7	1.4	54.2
H3	S3	Water	5.3	1.32	40.3
H4	S4	Water	-	-	(b)
H5	S5	Water	6.8	1.5	70.1

(a) – Determined by gravimetry.

(b) – No polymer was formed.

As shown in Table 2.2, low yields and low molecular weights were obtained for all systems. All these polymers precipitated from solution during polymerization due to agglomeration of the growing chains. Attempts to polymerize these monomers in organic solvents (for example, tetrahydrofuran) gave even lower molecular weight polymers. This suggests that pre-organization of the amphiphilic molecules in water by the formation of micelles leads to higher degrees of polymerization in aqueous medium than in organic solvent. It is well known that polymeric surfactants show generally lower values of critical micelle concentration (CMC) than small molecules. Thus, in the aqueous medium, the amphiphilic molecules will be above their CMC and arranged into micelles. During the homopolymerization, however, the critical concentration is continually decreasing as the polymeric chain is growing. At the same time, the homopolymers have vastly reduced degrees of freedom in which to orientate themselves due to the steric restrictions placed on them by their neighboring monomers. Both of these factors restrict the surfmers ability to organize themselves into micelles and their influence on the system continues to increase until the point that agglomeration occurs, ending by the precipitation of the polymer in water. It should be noticed that surfmer polymerization in the aqueous

phase should be minimized because it can promote flocculation and loss of the surfmer.

Copolymerization of the reactive surfactants. During the course of an emulsion polymerization, the surfmer may be incorporated into the polymer backbone by both copolymerization and chain transfer to the surfmer. The extent of surfmer copolymerization depends on the reactivity ratios of the surfmer and the monomers. In a second series of experiments, copolymerization of the reactive surfactants S1 - S5 in THF has been investigated in order to determine their capacity to copolymerize with a less bulky monomer, methyl methacrylate. As an example, the ¹³C NMR spectrum of the S1-co-MMA copolymer is shown in Figure 2.4.

Table 2.3. Copolymerization characteristics of surfmers 1-5.

sample	surfmer-MMA feed ratio	solvent	temp. (°C)	Mn/1000 (g/mol)	PDI	yield (%)	surfmer incorporation (%) ^(a)
P0	1	THF	65	20.52	1.22	98.0	-
P1	1:4	THF	65	17.0	1.48	97.3	93
P2	1:4	THF	65	17.5	1.32	88.7	76
P3	1:4	THF	65	19.4	1.35	91.2	98
P4	1:4	THF	65	18.5	1.41	92.4	78
P5	1:4	THF	65	17.2	1.25	82.0	83

(a) – Determined by analysis of ¹H NMR spectra of copolymers.

The disappearance of the resonances corresponding to the vinyl carbons of the monomers and the appearance of backbone peaks is consistent with the surfmer having undergone vinyl polymerization. The copolymerization results shown in Table 2.3 suggest that these monomers copolymerized well with this comonomer, with surfmer incorporation being fairly close to the monomer feed ratio.

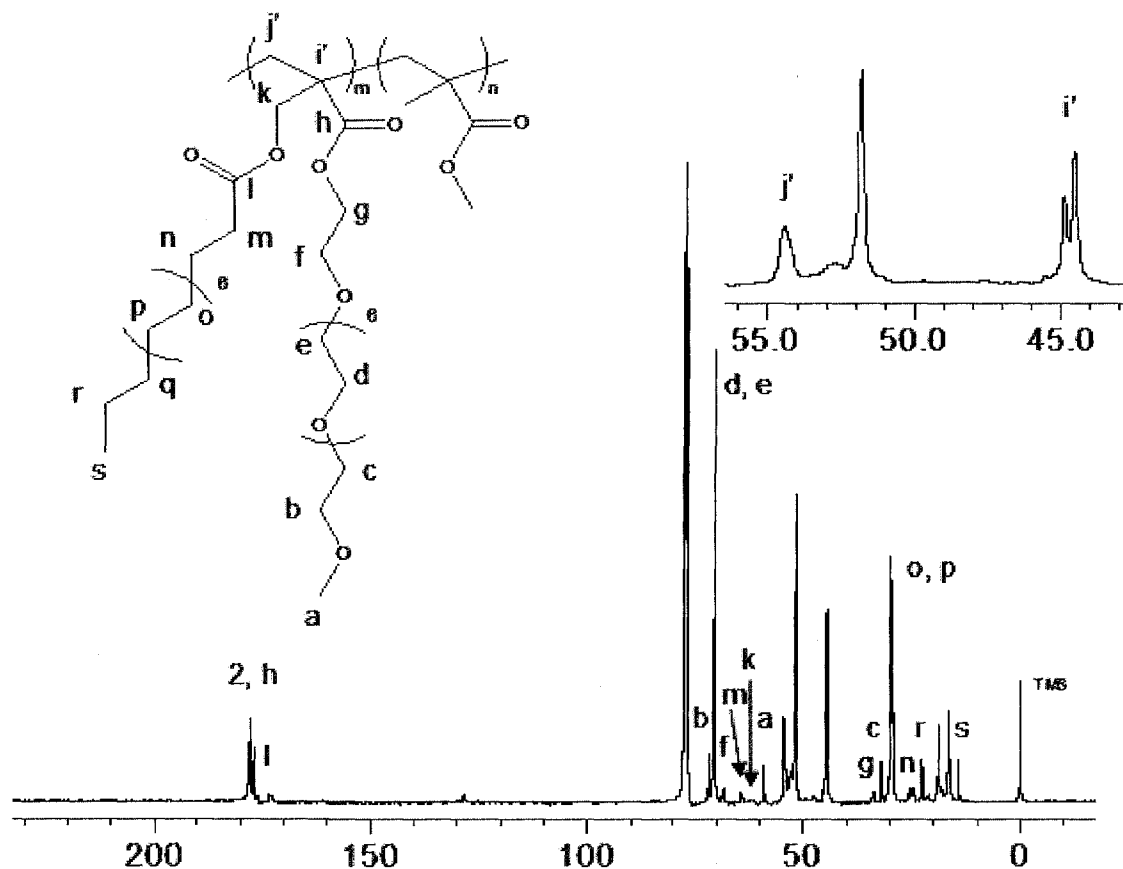


Figure 2.4. ^{13}C NMR spectrum of S1-co-MMA copolymer (CDCl_3).

Earlier studies showed that RHMA-based monomers lead essentially to random copolymer when copolymerized with MMA. Similar copolymerizations were carried out with n-butyl acrylate also showing high incorporation of the amphiphilic comonomer in the final copolymer. As mentioned earlier, the reactivity of the surfmer and its adsorption characteristics are critical in surfmer performance. The surfmer should not be able to homopolymerize too efficiently in order to avoid destabilization of the latex particles as they are forming. Furthermore, to minimize negative effects on the final material performance (a) the reactive surfactant conversion should be high at the end of the polymerization to ensure that there is little or no free surfactant in the final polymer and (b) large

amounts of surfmer homopolymerization should be avoided to minimize the presence of surface-active, amphiphilic polymeric coproducts. It is believed that a competition between homopolymerization and copolymerization will take place during the emulsion polymerization and that the observed balance between the homo- and copolymerization behavior of the surfmers reported in this study suggest that they have great potential for use in heterophase polymerization techniques. This is because their molecular structure has been demonstrated to lead to a preference toward efficient copolymerization with monomers such as MMA and BuA. Thus, during the course of the emulsion polymerization, they will not produce significant amounts of homopolymer due to their relative bulkiness nor will they leave unreacted surfmer due to their high potential toward copolymerization.

Emulsion polymerizations. High solids content MMA/BuA/AA (29/69/2) latexes were prepared via seeded semi-continuous emulsion polymerizations. Table 2.4 lists the percentage of coagulum and the particle size of the latexes investigated. These data show that a high conversion of monomers was achieved as determined by gravimetry. No vinyl peak from the surfmer reactive double bonds could be seen in ^1H NMR spectra (D_2O) of the latexes suggesting high incorporation of the surfmer into the polymer. Further characterization of the centrifuged latexes was attempted using NMR spectroscopy. NMR analysis of the final serum after centrifugation systematically showed that no surfmer was remaining in the liquid phase. This result indicates that either complete incorporation occurred or that centrifugation was unable to eliminate the

physically adsorbed species. Finally, for all latexes, the recovered polymer was washed with hot methanol in order to remove any adsorbed species and the methanol-soluble fraction was analyzed by proton NMR spectroscopy in CDCl_3 solution. ^1H NMR allowed determination of incorporation of surfmer in the final copolymers produced by heterophase polymerization. As an example, Figure 2.5 shows ^1H NMR spectra of both surfmer S1 and the corresponding polymer recovered from latex L1. Proton peaks at 3.64 ppm and 1.25 ppm were observed in the polymer spectrum, corresponding to the MPEG and hydrocarbon units, respectively, of S1. This attests to efficient incorporation of the surfmer in the final polymeric matrix.

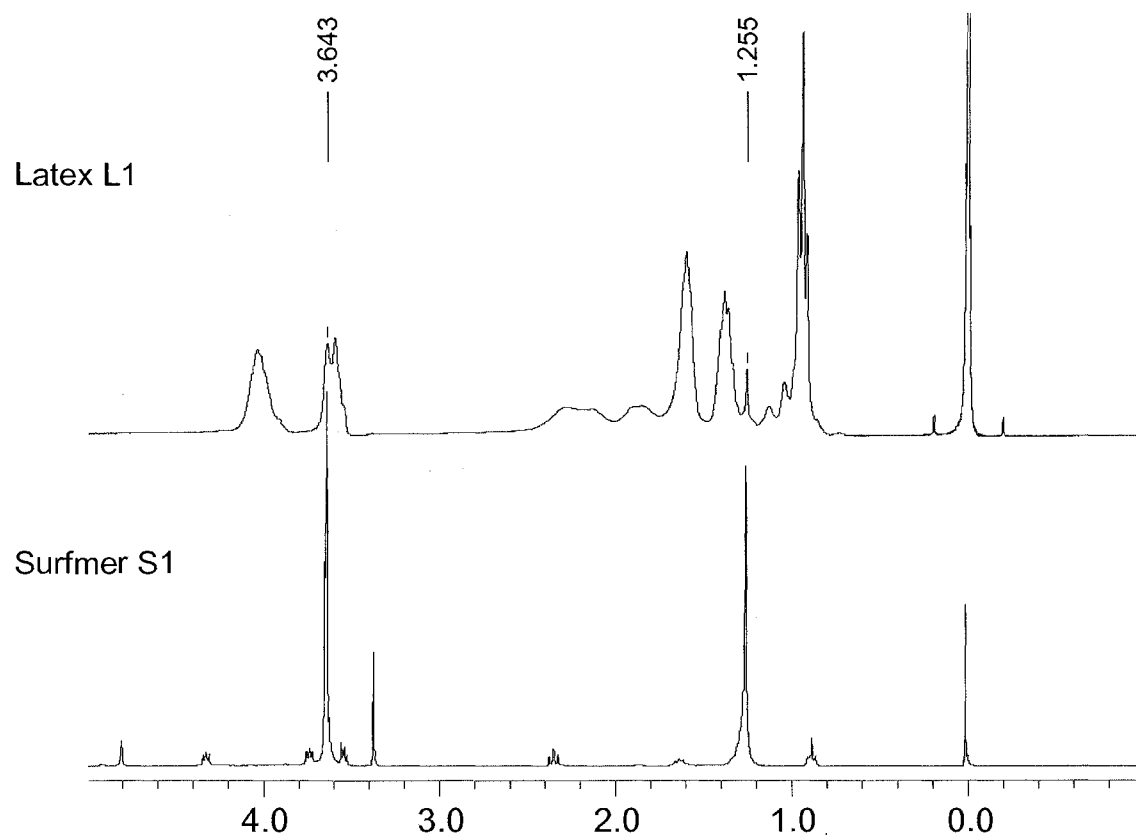


Figure 2.5. ^1H NMR spectra of latex L1 and surfmer S1 (CDCl_3).

Although surfmers S1, S2, S3 and S5 did lead to stable polymeric emulsions, coagulation occurred during the emulsion polymerization involving S4 and no stable latex could be formed. It is believed that the higher degree of hydrophilicity of surfmer S4 compared to the other surfactants resulted in an inability to efficiently stabilize the growing particles during the polymerization process because too much surfmer was located in the aqueous phase. In all the reported emulsion polymerizations in this paper, the amount of surfmer added to form the latex was approximately 1 mol-% as reported in Table 2.4. This value could be lowered as the critical micelle concentration of the surfactants was much lower than the fixed surfactant concentration. For instance, the CMC for surfmer S1 was evaluated to be 0.095 g/L.

Table 2.4. Characteristics of the final latexes.

latex	surfactant	feed time (h)	Dp seed (nm)	surfactant concentration (wt-%/mol-%)	initiator/(g)	coagulum (%)	Dp (nm)	appearance of latex
L0	SDS	2	89	1 mol-%	APS/ 0.30	<1	151.3	(a)
L1	S1	2	89	4.16/1.00	APS/ 0.32	2.5	163.4	(a)
L2	S2	2	89	4.03/1.15	APS/ 0.34	1.5	171.5	(a)
L3	S3	2	89	4.04/1.26	APS/ 0.30	<1	190.3	(b)
L4	S4	2	89	4.10/1.08	APS/ 0.30	-	-	(c)
L5	S5	2	89	4.14/0.85	APS/ 0.31	1.7	164.5	(b)

(a) – Typical latex appearance.

(b) – Very thick latex.

(c) – Emulsion polymerization was not successfully achieved.

Apparent molecular weights obtained for the corresponding latexes formed are summarized in Table 2.5. We observed a large range of molecular weights for the latexes obtained. These differences may be attributed to some degree of secondary nucleation arising during the polymerization. For instance, the low molecular weight observed for latex L3 maybe due to the higher degree

of hydrophilicity of this compound as compared to the other reactive surfactants investigated. It should be noticed that these data are based on polystyrene standards and that some degree of uncertainty should be taken in account considering these results. Nevertheless, we should expect some impact on final molecular weight as the hydrophilicity of the corresponding surfactant is increased.

Table 2.5. Molecular weights of latexes.

Latex	Surfactant	Mn/1000 (g/mol)	Mw/1000 (g/mol)	PDI	conversion (%) ^(a)
L0	SDS	220.3	386.4	1.75	95
L1	S1	158.3	350.7	2.22	98
L2	S2	183.1	384.9	2.10	96
L3	S3	84.9	204.4	2.40	99
L5	S5	284.4	358.6	1.26	94

(a) – Determined by gravimetry (equation 1).

Evolution of the particle size during the polymerization reaction was followed for each system by withdrawing aliquots of latex at different times and carrying out dynamic light scattering measurements. The particle size evolution for each system is shown in Figure 2.6. It was found that the final particle size was obtained after 4 hours by analysis of the data collected over a 24 hour period. DLS measurements also showed that low particle size polydispersity indexes were obtained for all latexes investigated (Table 2.4). DLS distribution profiles corresponding to latex L1-L5 are shown in Figure 2.7. Scanning electron microscopy allowed confirming this data as shown in Figure 2.8 (Latex L5). The SEM pictures were taken in the high vacuum mode and the particle size and particle size distribution could be seen to be in good agreement with the dynamic light scattering measurements.

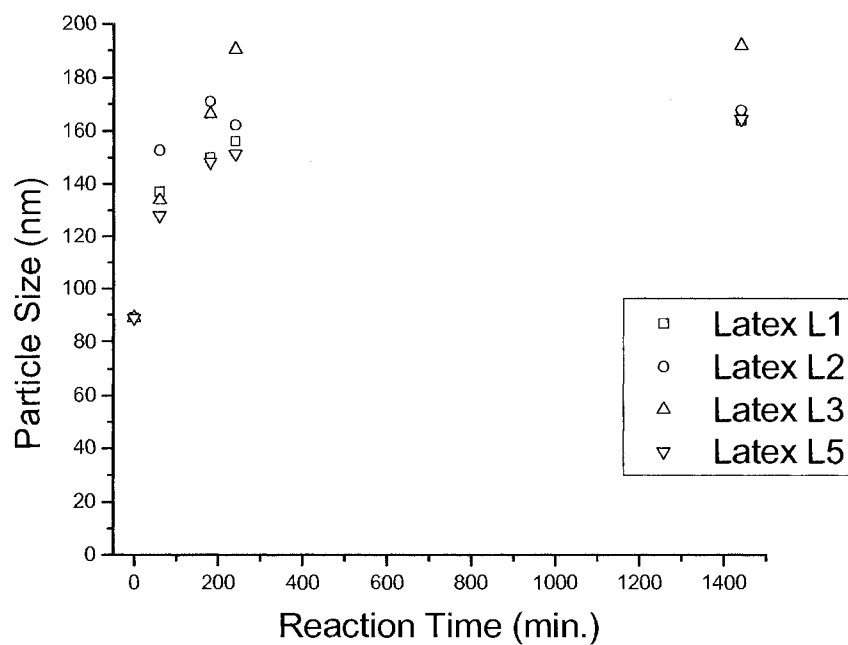


Figure 2.6. Particle size evolution of latexes.

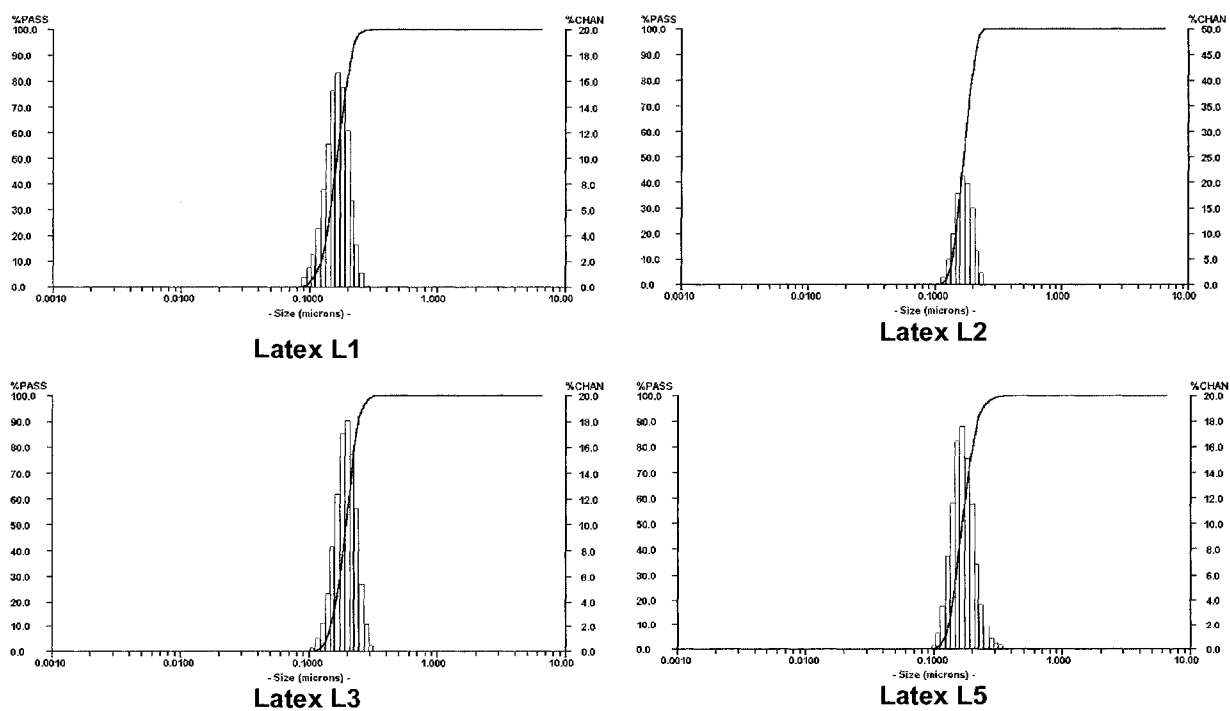


Figure 2.7. Particle size distributions of the final latexes determined by laser light scattering.

As reported in Table 2.4, a low amount of coagulum was noted, suggesting a low amount of destabilization during the heterophase polymerization. Unzué et al. reported that, in a similar reaction at 50% solids with 1 mol-% of non-ionic methacrylate-based reactive surfactant, a large amount of coagulum was obtained.²² It was suggested that this behaviour was a consequence of homopolymerization of methacrylate surfmer in the aqueous phase, leading to the formation of a type of water-soluble polymer capable of causing bridging flocculation. By comparison, while homopolymerization of the surfmers S1 – S5 is certainly possible, as shown in the homopolymerizations reported earlier in this section, the low amount of coagulum that has been observed in the emulsion polymerizations detailed in this study suggest that these materials exhibit low amounts of homopolymerization and are more able to copolymerize efficiently during the heterophase polymerization. Thus, it is concluded that the molecular design of the surfmers in this work has successfully influenced the balance between aqueous phase homopolymerization and heterophase copolymerization such that their performance is better tuned toward achieving a successful emulsion polymerization which produces a high quality final polymer than other reactive surfactants used in the past.

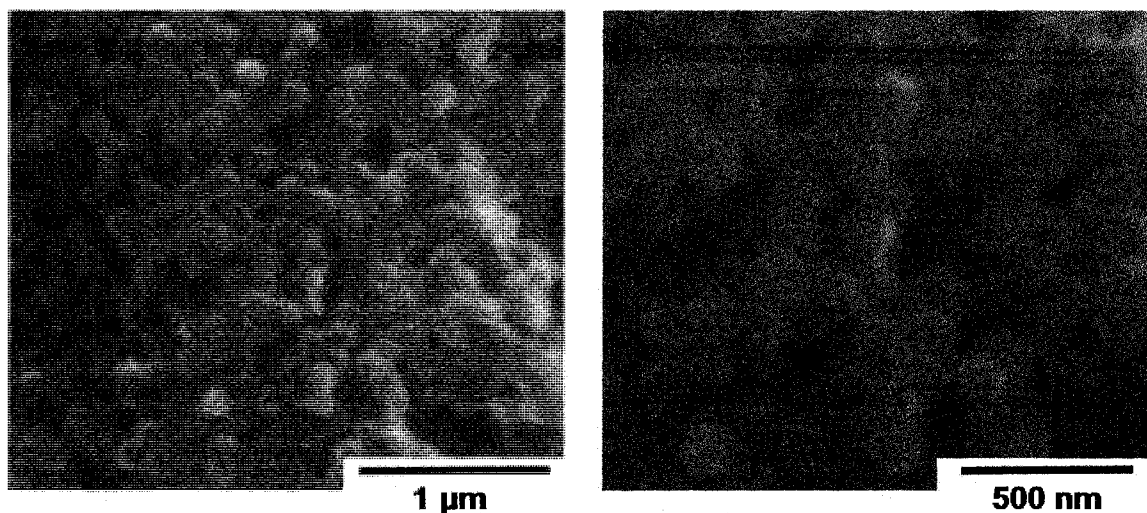


Figure 2.8. SEM Micrographs of latex L5.

Film surface morphology. During setting and drying of a latex film, any surfactant that is only physically adsorbed and not chemically bound to the resulting polymer may either remain at the particle surface or phase separate from the polymer. If the surfactant undergoes phase separation, the water flux may carry it to the film surface. Alternatively, it may accumulate in the interstices between the particles. From there it will migrate to the film–air or film–substrate interface through a long-term exudation process. The surfactant may also segregate from the matrix and form aggregates and pockets that could affect the overall polymer properties.

The mobility of surfactants during film formation has been widely studied using a wide range of different techniques such as fourier transform infra-red spectroscopy (FT-IR), attenuated total reflectance (ATR), transmission electron microscopy (TEM), and AFM.⁴⁶⁻⁵⁰ AFM is an attractive technique due to the fact that it is non-destructive.⁴⁸ In this study AFM was used to observe the surface morphology of the films directly and also to evaluate the roughness of the tested

film before and after exposing to water. This technique allowed the particle sizes, previously determined via dynamic light scattering (DLS) to be confirmed, as the AFM measurements of the particle sizes and particle size distributions for all latexes were in good agreement with DLS measurements. Figure 2.9 shows typical AFM pictures (height and phase) obtained under tapping mode conditions for the films studied where individual latex particles could be observed.

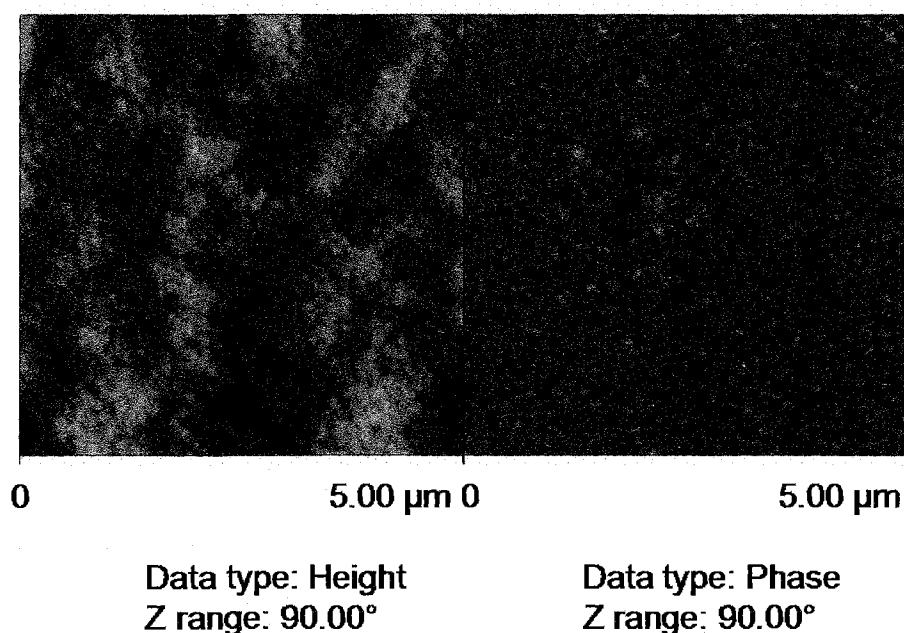


Figure 2.9. AFM pictures of film made from latex L5 (height on left and phase on right).

Asua and co-workers showed that the surface of a film incorporating conventional non-reactive surfactants such as sodium lauryl sulfate (SLS) is totally covered with the surfactant, obscuring the individual particle identities. In our study, this behaviour could be confirmed as no particle could be identified by

AFM characterization of the film incorporating SDS. However, the particles appeared well defined for all the other films by AFM measurements, attesting to low migration of surfactant upon film formation. Furthermore, the narrow polydispersities previously reported by DLS measurements were also found to be in good agreement with the AFM results for all films formed. Topographical images were obtained for both the neat film and the film washed extensively with deionized water as shown in Figures 2.10 and 2.11. Difference in the root mean square (rms) surface roughness between the two films was then determined by AFM for each system as reported in Table 2.6. Upon rinsing with deionised water, the non-bonded and highly water soluble reactive surfactant should be washed away. The roughness of the remaining film is caused by disruption of the particle packing by the migrating surfactant phase, as described by Juhué, et al..⁴⁹ Very little difference could be observed in roughness measurements for these systems as compared to the film incorporating SDS as surfactant (Figure 2.12), consistent with the conclusion that surfactant migration has been minimized in these systems.

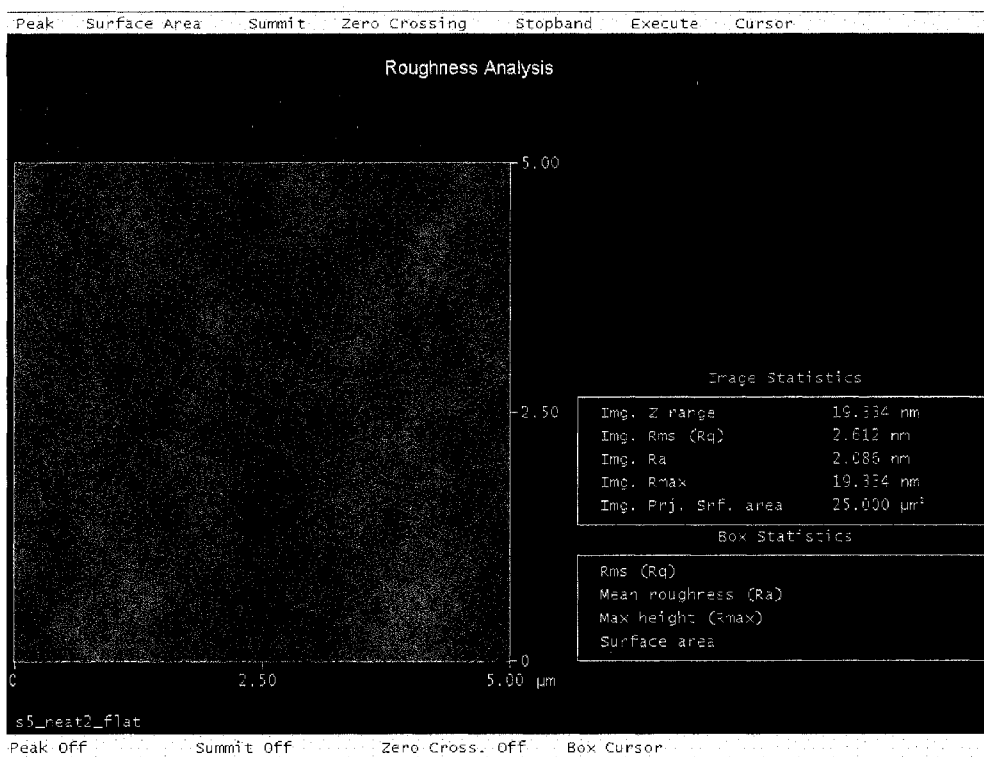


Figure 2.10. Neat film (from L5).

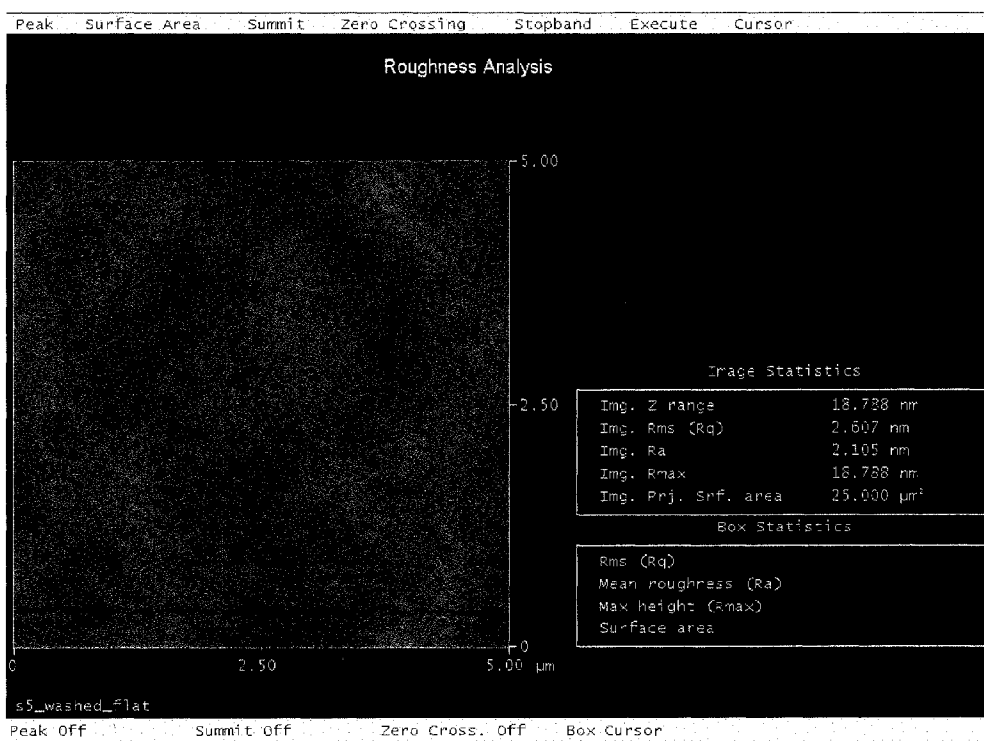


Figure 2.11. Washed film (from L5).

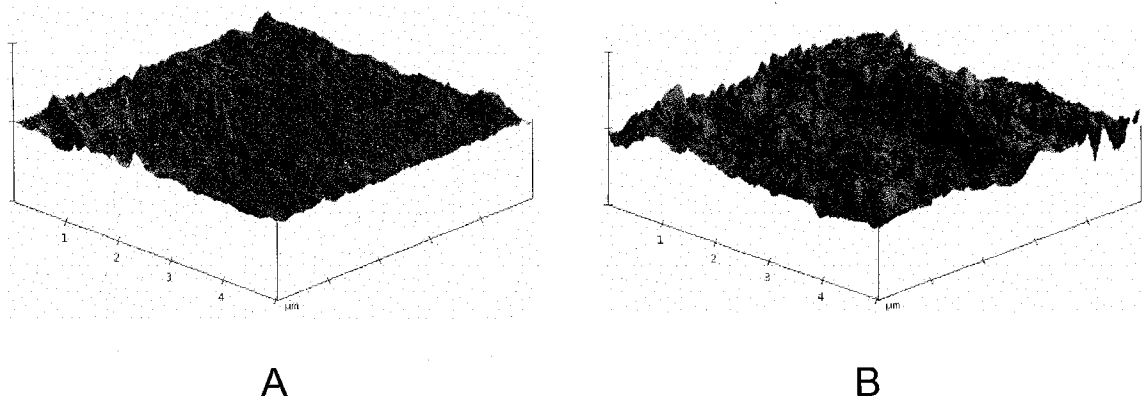


Figure 2.12. AFM topographical images of film from L0 (SDS surfactant), neat (A) and washed with dionized water (B).

Table 2.6. Particle size and roughness of the films obtained from latexes determined by Atomic Force Microscopy.

latex	Roughness (nm)	Dp (nm)
L0 (neat)	5.14	N/A
L0 (washed)	14.32	N/A
L1 (neat)	3.04	173.5
L1 (washed)	3.23	173.5
L2 (neat)	3.44	162.5
L2 (washed)	3.23	162.5
L3 (neat)	2.87	194.5
L3 (washed)	3.56	194.5
L5 (neat)	2.08	166.7
L5 (washed)	2.10	166.7

Latex stability. The stability of the polymeric emulsions produced was assessed by addition of electrolyte solution to the corresponding latexes. The results are summarized in Table 2.7. All latexes showed complete flocculation after 24 hours at -20°C . However, the latexes showed differences in flocculation behaviour dependant on the electrolyte solution used in the test. Latexes that incorporated surfmers S3 and S5 were found to be the most stable latexes. Structure-property

relationship determination of the surfmers is currently in progress to better understand this behavior.

Table 2.7. Freeze/thaw test and stability in different electrolyte solutions (+++ : immediate flocculation; ++: partly flocculated after 1 day; +: complete flocculation after 1 month).

latex	0.1M NaCl	0.5M NaCl	1.0M NaCl	0.1M MgSO ₄	freezing -20°C
L1	++	+++	+++	+++	+++
L2	+++	+++	++	+++	+++
L3	++	+	+	+	+++
L5	++	++	++	+	+++

Conclusions

New acrylate-based, non-ionic reactive surfactants were specifically designed to optimize the reactivity of the surfmer by balancing the bulkiness of the macromeric surfmers with the reactivity of the polymerizable double bond they contained. The aim of the design was to create species which had a more reactive double bond that is usually found in non-migratory surfactants to maximize the incorporation into the emulsion polymer, thus reducing any secondary interfacial effects and leaching of the surfmer during the course of the polymerization. These target molecules were synthesized successfully and used in high solid content emulsion polymerization of butyl acrylate, methyl methacrylate and acrylic acid. Analysis of the final polymers from these emulsion reactions via NMR support the conclusion that high levels of surfmer incorporation into the emulsion polymer were achieved. Additionally, low levels of coagulum were observed in these reactions, suggesting a high stability of the

emulsions during the reaction. Well defined particles and narrow particle size distributions were observed by dynamic light scattering which was confirmed by microscopy measurements (SEM and AFM).

Homogeneous and transparent films were formed from the latexes which exhibited little difference in surface roughness values between the neat films and the films washed extensively with deionised water. This latter result suggests a very low degree of surfactant migration through the polymeric matrix during the film formation. Additionally, the AFM images clearly showed the presence of individual latex particles which again supports the conclusion that the macromeric surfmer is highly incorporated into the polymeric film. Thus, it is concluded that these surfmers impart very interesting and beneficial properties to the emulsion polymerizations conducted in this study. This strategy of attempting to optimize the balance between the reactivity of the double bond and the bulkiness of the molecules has delivered real benefit to the heterophase polymerization systems investigated. This balance of surfmer reactivity allows the amphiphilic surfmers to stabilize the growing polymer particles and be incorporated within the final copolymer. These factors lead to the production of films which present reduced water sensitivity compared to those made using conventional surfactants. These new acrylate-based reactive surfactants are the first of a new library of amphiphilic monomers able to efficiently stabilize the growing polymeric particles in acrylic emulsion polymerizations and confer higher stability on the final polymeric material.

Experimental

Materials. The following reagents were used as received without further purification with the exception of methyl methacrylate (Aldrich Chemical Company), which was redistilled over calcium hydride (Aldrich Chemical Company) and 2,2'-azobis(2-methylpropionitrile) (AIBN) which was recrystallized from methanol (Fisher Scientific). Poly(ethylene glycol) methyl ether ($M_n=350$ g/mol) and thionyl chloride were purchased from Acros Organics. t-Butyl acrylate, paraformaldehyde, 2,2-bis-(hydroxymethyl)propionic acid, benzoic acid, stearic acid, decanoic acid, pentadecafluoro-1-octanol, triethylamine, 1,4-diaza[2.2.2]bicyclooctane (DABCO) and sodium dodecyl sulfate (SDS) were purchased from Aldrich. Acetic anhydride, butyl acrylate (BuA, technical grade), potassium hydroxide, and acrylic acid (AA) were purchased from Fluka. Ammonium persulfate (APS, ACS reagent) was purchased from Acros Chemical Company. Toluene, tetrahydrofuran and any other solvents were obtained from Aldrich or Fisher. t-Butyl α -hydroxymethylacrylate (t-BHMA) was prepared using a previously published procedure.⁴⁵

Instrumentation and characterization. Molecular weights and molecular weight distributions of the polymers obtained by solution polymerization were measured using size exclusion chromatography (SEC) on a system equipped with four styrene gel mixed bed columns (American Polymer Standard Corporation, Mentor, OH) using THF as eluent. Polystyrene standards (MWs ranging from 4630 to 400,000 g/mol) were used for calibration. Molecular weights and molecular weight distributions of the final latexes were determined by gel

permeation chromatography (GPC) with THF as eluent. Solution ^1H and ^{13}C NMR spectra were collected on a Varian Mercury 300 MHz spectrometer operating at a frequency of 75.47 MHz for carbon. NMR spectra were recorded at room temperature using CDCl_3 with TMS as an internal reference. FT-IR spectra were obtained using a Bio-Rad DIGILAB FTS 6000 FTIR spectrometer equipped with a Ge MIRacle™ single reflection ATR cell using 32 co-added scans. The particle sizes and particle size distributions of latexes were measured by dynamic light scattering (Microtrac UPA 150).

Synthesis of α -chloromethylacryloyl chloride (CMAC) A. t-BHMA (20 g, 0.126 mol) and excess of thionyl chloride were added to a 100 ml round bottom flask and stirred at ambient temperature for 24 hours. Most of the thionyl chloride was removed under vacuum. Vacuum distillation of the residue gave α -(chloromethyl)acryloyl chloride as a clear liquid in ca. 60% yield.

FTIR (cm^{-1} , NaCl): 3107, 2966, 1742, 1637, 1407, 1284, 967, 896; ^1H NMR (CDCl_3) δ 4.26 (s, 2H, CH_2Cl), 6.41 and 6.74 (s, 2H, $\text{CH}_2=\text{C}$); ^{13}C NMR (CDCl_3) δ 41.53 (CH_2Cl), 136.14 ($\text{CH}_2=\text{C}$), 141.14 ($\text{C}=\text{CH}_2$), 166.78 ($\text{C}=\text{O}$).

Synthesis of MPEG α -chloromethylmethacrylate (MPCMA) B. In a 250 ml round-bottom flask, poly(ethylene glycol) methyl ether (20g, 57.1 mmol) was added to 100 ml of dried THF. The solution was stirred at -10°C for 30 min. CMAC (10.32 g, 74.3mmol) diluted in 50 ml of dried THF was then added dropwise to the stirring mixture. The resulting mixture was stirred overnight at room temperature. The precipitate was filtered off and the solvent removed under

reduced pressure. Excess CMAC was removed by washing the crude oil with aliquots (3 X 60 ml) of hexane to give MPCMA as light brown oil in ca. 94% yield.

FTIR (cm^{-1} , NaCl): 3407, 1742, 1641, 1407, 1118, 812; ^1H NMR (CDCl_3) δ 4.30 (s, 2H, CH_2Cl), 6.01 and 6.41 (s, 2H, $\text{CH}_2=\text{C}$), 4.35 (t, 2H, $\text{CH}_2\text{C}=\text{CH}_2$), 3.38 (s, 1H, CH_2OCH_3), 3.61 (s, 2H, $\text{CH}_2\text{CH}_2\text{O}$); ^{13}C NMR (CDCl_3) δ 41.53 (CH_2Cl), 128.96 ($\text{CH}_2=\text{C}$), 136.74 ($\text{C}=\text{CH}_2$), 164.85 ($\text{C}=\text{O}$), 64.32 ($\text{CH}_2\text{C}=\text{O}$), 70.54 (CH_2O), 58.99 (CH_2OCH_3).

Synthesis of the surfmers S1-S3. First, stearic acid, decanoic acid and benzoic acid potassium salts were obtained by mixing at room temperature, in THF, the corresponding acid (1 mol) with of potassium hydroxide in slight excess (1.05 mol). The salts were then collected by filtration of the crude mixture and dried overnight at 60°C in a vacuum oven. Then, in a 250 ml round-bottom flask, the corresponding acid potassium salt (26.1 mmol) was dispersed in THF. MPEG α -chloromethylmethacrylate was then added to the salt solution dropwise at room temperature. The resulting mixture was allowed to stir at room temperature for 24 hours. The precipitate was filtered off and the solvent removed under reduced pressure to give the corresponding monomers in quantitative yields.

Surfmer S1 - FTIR (cm^{-1} , NaCl): 3492, 2871, 1730, 1641, 1118; ^1H NMR (CDCl_3) δ 4.77 (s, 2H, CH_2O), 5.81 and 6.34 (s, 2H, $\text{CH}_2=\text{C}$), 4.30 (t, 2H, $\text{CH}_2\text{C}=\text{CH}_2$), 3.34 (s, 1H, CH_2OCH_3), 3.61 (s, 2H, $\text{CH}_2\text{CH}_2\text{O}$); ^{13}C NMR (CDCl_3) δ 62.13 ($\text{CH}_2\text{C}=\text{CH}_2$), 127.42 ($\text{CH}_2=\text{C}$), 135.30 ($\text{C}=\text{CH}_2$), 165.09 ($\text{C}=\text{O}$), 173.13 ($\text{C}=\text{O}$),

64.09 ($\text{CH}_2\text{C}=\text{O}$), 70.56 (CH_2O), 59.01 (CH_2OCH_3), 14.13 (CH_3CH_2), 22.68 (CH_2CH_3), 24.91 ($\text{CH}_2\text{CH}_2\text{C}=\text{O}$), 29.68 (CH_2), 31.92 ($\text{CH}_2\text{CH}_2\text{CH}_3$), 34.19 ($\text{CH}_2\text{C}=\text{O}$).

Surfmer S2 - FTIR (cm^{-1} , NaCl): 3490, 2872, 1731, 1641, 1118; ^1H NMR (CDCl_3) δ 4.78 (s, 2H, CH_2O), 5.82 and 6.32 (s, 2H, $\text{CH}_2=\text{C}$), 4.31 (t, 2H, $\text{CH}_2\text{C}=\text{CH}_2$), 3.32 (s, 1H, CH_2OCH_3), 3.61 (s, 2H, $\text{CH}_2\text{CH}_2\text{O}$); ^{13}C NMR (CDCl_3) δ 62.10 ($\text{CH}_2\text{C}=\text{CH}_2$), 127.38 ($\text{CH}_2=\text{C}$), 135.28 ($\text{C}=\text{CH}_2$), 165.04 ($\text{C}=\text{O}$), 173.06 ($\text{C}=\text{O}$), 64.07 ($\text{CH}_2\text{C}=\text{O}$), 70.54 (CH_2O), 58.98 (CH_2OCH_3), 14.12 (CH_3CH_2), 22.66 (CH_2CH_3), 24.88 ($\text{CH}_2\text{CH}_2\text{C}=\text{O}$), 29.65 (CH_2), 31.89 ($\text{CH}_2\text{CH}_2\text{CH}_3$), 34.16 ($\text{CH}_2\text{C}=\text{O}$).

Surfmer S3 - FTIR (cm^{-1} , NaCl): 3492, 1740, 1641, 1622, 1118; ^1H NMR (CDCl_3) δ 5.04 (s, 2H, CH_2O), 5.93 and 6.42 (s, 2H, $\text{CH}_2=\text{C}$), 4.33 (t, 2H, $\text{CH}_2\text{C}=\text{CH}_2$), 3.34 (s, 1H, CH_2OCH_3), 3.61 (s, 2H, $\text{CH}_2\text{CH}_2\text{O}$), 8.04 (t, 1H, $\text{CH}=\text{C}$), 7.44 (t, 1H, $\text{CH}=\text{CH}$), 7.54 (t, 1H, $\text{CH}=\text{CHCH}$); ^{13}C NMR (CDCl_3) δ 62.77 ($\text{CH}_2\text{C}=\text{CH}_2$), 127.73 ($\text{CH}_2=\text{C}$), 135.18 ($\text{C}=\text{CH}_2$), 165.07 ($\text{C}=\text{O}$), 165.84 ($\text{C}=\text{O}$), 64.14 ($\text{CH}_2\text{C}=\text{O}$), 70.49 (CH_2O), 58.96 (CH_2OCH_3), 129.77 ($\text{C}=\text{CO}$), 129.62 ($\text{CH}=\text{C}$), 128.42 ($\text{CH}=\text{CH}$), 133.17 ($\text{CH}=\text{CHCH}$).

Synthesis of 2,2-bis(acetoxymethyl)propionic acid. In a 250ml Erlenmeyer, 2,2-bis(hydroxymethyl)propionic acid (15 g, 0.11 mol) and acetic anhydride in slight excess (23.79 g, 0.233 mol) were mixed overnight. The excess of acetic

anhydride was removed by vacuum distillation of the crude residue to give 2,2-bis(acetoxymethyl)-propionic acid in as a white solid in ca. 99% yield.

FTIR (cm^{-1} , KBr): 2929, 1745, 1376, 1234; ^1H NMR (CDCl_3) δ 2.08 (s, 3H, $\text{CH}_3\text{C}=\text{O}$), 1.29 (s, 3H, CH_3C), 4.25 (s, 2H, $\text{CH}_2\text{C}=\text{O}$), 11.58 (OH); ^{13}C NMR (CDCl_3) δ 17.77 (CH_3C), 20.76 ($\text{CH}_3\text{C}=\text{O}$), 46.0 (CCH_3), 65.29 ($\text{CH}_2\text{C}=\text{O}$), 170.95 ($\text{C}=\text{O}$), 178.44 ($\text{C}=\text{O}$).

Synthesis of surfmer S4. In a 250 ml round bottom flask, MPCMA (15 g, 33.1 mmol) and triethylamine (4.7ml, 33.1 mmol) were added to 75 ml of dry THF. To the stirring solution, 2,2-bis(acetoxymethyl)-propionic acid was added dropwise. The resulting mixture was allowed to stir overnight at room temperature. The precipitate was filtered of and the solvent removed under reduced pressure to give surfmer S4 as light brown oil in ca. 95% yield.

FTIR (cm^{-1} , NaCl): 2871, 2930, 1730, 1641, 1119; ^1H NMR (CDCl_3) δ 1.27 (s, 3H, CH_3C), 2.06 (s, 3H, $\text{CH}_3\text{C}=\text{O}$), 3.38 (s, 3H, CH_3O), 4.24 (s, 2H, CH_2C), 4.34 (t, 2H, $\text{CH}_2\text{OC}=\text{O}$), 4.87 (s, 2H, $\text{CH}_2\text{C}=\text{O}$), 5.86 and 6.41 (s, 2H, $\text{CH}_2=\text{C}$); ^{13}C NMR (CDCl_3) δ 17.80 (CH_3C), 20.71 ($\text{CH}_3\text{C}=\text{O}$), 46.27 (CCH_3), 63.03 ($\text{CH}_2\text{C}=\text{CH}_2$), 58.99 (CH_2OCH_3), 64.14 ($\text{CH}_2\text{C}=\text{O}$), 65.35 ($\text{CH}_2\text{C}=\text{O}$), 70.49 (CH_2O), 127.73 ($\text{CH}_2=\text{C}$), 134.83 ($\text{C}=\text{CH}_2$), 164.82 and 170.50 and 172.15 ($\text{C}=\text{O}$).

Synthesis of surfmer S5. In a 250 ml round-bottom flask, pentadecafluoro-1-octanol (10.42g, 26.1 mmol) was mixed with potassium hydroxide (1.46g, 26.1 mmol) in THF (100 ml) for 5 hours. MPCMA (13 g, 19.9 mmol), diluted in 30 ml of

dried THF, was then added dropwise. The resulting mixture was allowed to stir at 60 °C for 24 hours. The precipitate was filtered off and the solvent removed under reduced pressure to give surfmer S5 as light brown oil in ca. 89% yield.

FTIR (cm^{-1} , NaCl): 3490, 1730, 1641, 1118, 936, 813; ^1H NMR (CDCl_3) δ 3.32 (s, 3H, CH_3O), 3.99 (m, 2H, CH_2CF_2), 4.28 (t, 2H, $\text{CH}_2\text{OC=O}$), 4.31 (s, 2H, CH_2O), 5.86 and 6.33 (s, 2H, $\text{CH}_2=\text{C}$); ^{13}C NMR (CDCl_3) δ 58.85 (CH_3O), 61.43 ($\text{CH}_2\text{C}=\text{CH}_2$), 63.93 ($\text{CH}_2\text{C}=\text{O}$), 67.64 (CH_2CF_2), 72.54 (CH_2O), 127.14 ($\text{CH}_2=\text{C}$), 135.75 ($\text{C}=\text{CH}_2$), 165.27 ($\text{C}=\text{O}$).

Solution free radical homopolymerization of surfmers S1-S5. In a typical polymerization procedure, the surfmer (2 mmol) was dissolved in deionised water (20 ml) and stirred under nitrogen for 30 minutes in a 100-ml round bottom flask. The temperature was gradually increased and stabilized at 70 °C. Ammonium persulfate (0.045 g, 0.2 mmol) was dissolved in water (1 ml) and added to the stirring solution in one portion. The solution was allowed to stir for four hours under nitrogen atmosphere. The resulting product was filtered and dried overnight in vacuum oven to give the corresponding homopolymer.

Solution free radical copolymerization of surfmers S1-S5 and MMA. In a typical copolymerization procedure, the surfmer (1.97 mmol) and MMA (0.79 g, 7.91 mmol) were mixed in 10 ml of THF, under nitrogen, in a 50 ml 3-necked round bottom flask equipped with a condenser. The solution temperature was gradually brought to 60 °C. The resulting solution was allowed to stir for 30 minutes prior to addition of AIBN (0.031 g, 0.188 mmol) in one portion, which had

been pre-dissolved in THF. The flask was sealed and the solution was stirred for 24 hours under a nitrogen atmosphere. The final polymeric solution was finally precipitated into hexane giving the corresponding copolymer which was filtered and dried.

Latex preparation. MMA/BA/AA copolymer latexes were prepared by means of seeded semi-continuous emulsion polymerization. This polymerization technique was chosen because it allows good control of reaction batch temperature, particle nucleation, final particle size and size distribution. The recipe for the seed is given in Table 2.8, and the recipe for the seeded reaction is in Table 2.9. The reactions were carried out in a 500 ml glass reactor equipped with a reflux condenser, a stainless steel stirrer at 200 rpm, a nitrogen inlet, and a water bath for temperature control. The seed was prepared by means of batch emulsion polymerization using the following procedure. The monomers, water and the surfactant were mixed together and the resulting mixture poured into the reactor, placed into a water bath temperature controlled at 65°C, and allowed to stir for 30 minutes under nitrogen blanket. The initiator (APS) was dissolved in 2.5 ml of water and injected into the reactor. The reaction was carried out overnight to ensure complete monomer conversion. The final seed latex had a solid content of 30 wt-% and a final average particle size of 89 nm determined by DLS measurements.

Table 2.8. Recipe Used to Obtain the Seed (30% solids).

compound	seed (g)
water	300
MMA	33.75
BuA	82.5
AA	4
surfactant (SDS)	2.3
initiator (APS)	1.15
total	323.7

Table 2.9. Recipe Used in the Semi-continuous Emulsion Polymerizations (50% solids).

compound	initial charge (g)	feed 1 (g)	feed 2 (g)
seed	52		
H ₂ O	100		50
MMA	1.88	20	
BuA	4.10	44	
AA		2	
surfactant			3
APS	0.02		0.30
NaHCO ₃			0.70
Total	158	66	53

Reaction conditions: T, 65°C; stirring rate, 200 rpm; reaction time in semi batch, 2 h; reaction time in batch, 2 h; flow rate 1: 0.55 g/min; flow rate 2: 0.45 g/min.

Two separate streams were used in the preparation of the final latex: one with the neat monomers, and another which contained the surfactant, initiator and buffer. Feeding of the streams was achieved by use of two Masterflex diastolic pumps (Cole-Parmer Instrument Company) for the monomer feed and for the aqueous stream. The addition of monomer and aqueous solutions were both controlled by a Camille 2000 Data Acquisition System (Dow, Camille Products, LLC) coupled to the Camille TG (v4.0.5) acquisition software. In these reactions, the initial charge was purged with nitrogen for 30 minutes before

starting the feeding. After the feeding period the system was left to react overnight to ensure high monomer conversion.

Latex characterizations. At the end of the reaction, samples were taken to determine the particle size via dynamic light scattering measurements. The mean particle size was measured by light scattering (Microtrack UPA 150). The amount of coagulum was measured by collecting the coagulum on the reactor wall and stirrer, and by filtering the latex using a Mesh Filter from Gardco, Inc. The result is presented as weight of coagulum per total weight of monomer added.

Gravimetric analysis was performed to determine the percentage of solids in the final latex product and then the percentage conversion for the corresponding emulsion polymerization: 1 g of latex was poured into a preweighed vial; the polymer was precipitated out of the water by the addition of methanol which was decanted off, and the polymer washed several times with aliquots of methanol to remove unreacted monomer, surfmer or initiator. The vial was then placed into vacuum oven to remove residual methanol and the resulting polymer weight was then compared to the original emulsion solid content to determine the overall monomer conversion. The latexes were centrifuged and analysis via NMR spectroscopy of both the final serum after centrifugation and recovered polymer allowed evaluating the final reactive surfactant incorporation.

Film formation. Latexes were drawn down on a glass microslide substrate (carefully washed with acetone and deionized water prior to latex deposition) using a 3-mil drawdown bar and allowed to dry at room temperature overnight. The films formed were then used in the AFM measurements.

Latex stability. Stability of the latexes synthesized was assessed by the following method. To 1 g of latex in four vials, the same amount of the following electrolyte test solutions were added, 0.1 M MgSO_4 , 0.1 M NaCl, 0.5 M NaCl, 1.0 M NaCl. The time for flocculation to occur was assessed visually. For the freeze/thaw test, a small amount of latex (2 ml) was kept at -20°C for 24 hours. After 24 hours at room temperature, the flocculation was assessed by visual observation.

Scanning electron microscopy (SEM). Particle morphology and particle distribution were visualized using scanning electron microscopy. In a typical sample preparation, the specimen was prepared by depositing dilute latex onto a carbon adhesive tab and then coating the dried residue with gold (5 nm) using a sputter coater Emitech K550X. The images were obtained with a FEI Quanta 200 scanning electron microscope under high vacuum conditions.

Atomic force microscopy (AFM). Surface topographies were investigated of the films formed by spreading the corresponding latex onto glass microslide. The topography of the air-film surface was characterized using a Dimension 3000 scanning probe microscope (Digital Instruments, Santa Barbara, CA). The probe for surface topography was purchased from Veeco Probes, CA, and was an etched silicon probe, 125 μm long with a resonant frequency of 275 kHz, nominal force constant of 40 N/m, and a nominal tip radius of 10 nm. Height and phase images were collected simultaneously on 5 μm x 5 μm scan size with an image resolution of 256x256 pixels at a scan rate of 1 Hz. Surface roughness and

section analysis were performed on a 5 μm x 5 μm scan area for all the samples using Nanoscope v5.30 r2 image analysis software.

REFERENCES

- 1 Roulstone, B. J.; Wilkinson, M. J.; Hearn, J. *Polym. Int.* **1992**, 27, 43.
- 2 Zhao, C. I.; Holl, Y.; Pith, T.; Lambla, M. *Colloid Polym. Sci.* **1987**, 265, 823.
- 3 Evanson, K. W.; Urban, M. W. *J. Appl. Polym. Sci.* **1991**, 42, 2287.
- 4 Bradford, E.B.; Vanderhoff, J.W. *J. Macromol. Chem.* **1996**, 1, 335.
- 5 Piirma, I. *Makromol. Chem. Macromol. Symp.* **1990**, 35, 467.
- 6 Holmberg, K. *Prog. Org. Coat.* **1992**, 20, 325.
- 7 Guyot, A.; Tauer, K. *Adv. Polym. Sci.* **1994**, 111, 43.
- 8 Schoonbrood, H. A. S.; Asua, J. M. *Acta Polym.* **1998**, 49, 671.
- 9 Tauer, K.; Asua, J. M., Ed.; Kluwer Academic Publishers: Dordrecht, **1997**, 463.
- 10 Guyot, A. *Curr. Opin. Colloid Interface Sci.* **1996**, 1, 580.
- 11 Holmberg, K. *Prog. Org. Coat.* **1992**, 20, 235.
- 12 Urquiola, M. B.; Dimonie, V. L.; Sudol, E. D.; El-Aasser, M. S. *J. Polym. Sci., Part A: Polym. Chem. Ed.* **1992**, 30, 2619.
- 13 Urquiola, M. B.; Dimonie, V. L.; Sudol, E. D.; El-Aasser, M. S. *J. Polym. Sci., Part A: Polym. Chem. Ed.* **1992**, 30, 2631.
- 14 Urquiola, M. B. Ph.D. Dissertation, Lehigh University, **1992**.
- 15 Schoonbrood, H. A. S.; Unzue, M. J.; Beck, O. J.; Asua, J. M. *Macromolecules* **1997**, 30, 6024.
- 16 Urretabizkaia, A.; Asua, J. M. *J. Polym. Sci., Part A: Polym. Chem.* **1994**, 32, 1761.

- 17 Guyot, A.; Tauer, K. *Adv. Polym. Sci.* **1994**, *111*, 43.
- 18 Unzue, M.J.; Schoonbrood, H.A.S.; Asua, J.M.; Montoya, A.; Sherrington, D.C.; Stahler, K.; Goebel, K.H.; Tauer, K.; Sjoberg, M.; Holmberg, K. *J. Appl. Polym. Sci.* **1997**, *66*, 1803.
- 19 Yokota, K.; Ichihara, A.; Shinike, H. U.S. Patent 5,324,862, **1994**.
- 20 Aramendia, E.; Barandiaran, M.J.; de la Cal, J.C.; Grade, J.; Blease, T.; Asua, J.M. *J. Poly. Sci., Part A: Poly. Chem.* **2002**, *40*, 1552-1559.
- 21 Schoonbrood, H.A.S.; Asua, J.M. *Macromolecules* **1997**, *30*, 6034.
- 22 Schoonbrood, H.A.S.; Unzue, M.J.; Beck, O.J.; Asua, J.M.; Montoya A.; Sherrington, D.C. *Macromolecules* **1997**, *30*, 6024.
- 23 Goux, A. ; Guyot, A. *J. Appl. Polym. Sci.* **1997**, *65*, 2289.
- 24 Green, B.W.; Sheetz, D.P. *J. Colloid Interface Sci.* **1970**, *32*, 96.
- 25 Green, B.W.; Saunders, F.L. *J. Colloid Interface Sci.* **1970**, *33*, 393.
- 26 Tsaur, S.L.; Fitch, R.B. *J. Colloid Interface Sci.* **1987**, *115*, 450.
- 27 Chen, S.A.; Chang, H.S. *J. Polym. Sci., Part A: Polym. Chem.* **1985**, *23*, 2615.
- 28 Sherrington, D.C.; Joynes, D. *Polymer* **1997**, *38* (6), 1427.
- 29 Montoya, A.; Sherrington, D.C.; Schoonbrood, H.A.S.; Asua, J. M. *Polymer* **1999**, *40*, 1359.
- 30 Favresse, P.; Laschewsky, A. *Colloid Polym. Sci.* **1999**, *277*, 792.
- 31 Nkansah, A.; Solomon, R. D.; Williams, S. O. U.S. Patent 5 962 580, **1995**.
- 32 Nobel, J.W. U.S. Patent 4 455 263, **1983**.

- 33 Nobel, J.W. U.S. Patent 4 511 691, **1984**.
- 34 Schmitt, K.D. U.S. Patent 4 582 137, **1984**.
- 35 Kanegafuchi K. Patent 1 427 789, **1976**.
- 36 Flach, H.N.; Grassert, I.; Oehme, G. *Macromol. Chem. Phys.* **1994**, 195, 3289.
- 37 Nagai, K.; Satoh, H.; Kuramoto, N. *Polymer* **1992**, 33 (24), 5303.
- 38 Peiffer, D.G. *Polymer* **1990**, 31, 2353.
- 39 Chern, C.S.; Chen, Y. C. *Polym. J.* **1996**, 28 (7), 627.
- 40 Malyukova, Y. B.; Navmava, S. V.; Gritskova, I. A.; Bondarev, A. N.; Zubov, V. P. *Russian Polym. Sci.* **1991**, 33, 1361.
- 41 Chikanishi, K.; Tsuruta, T. *Makromol. Chem.* **1965**, 81, 198.
- 42 Cheng, J.; Yamada, B.; Otsu, T. *J. Polym. Sci., Part A: Polym. Chem.* **1991**, 29, 1837.
- 43 Reed, S.F.; Baldwin, M.G. *J. Polym. Sci., Part A: Polym. Chem.* **1963**, 1, 1919.
- 44 Avci, D.; Kusefoglu, S.H.; Thomson, R.D.; Mathias, L.J. *J. Polym. Sci., Part A: Polym. Chem.* **1994**, 32, 2937.
- 45 Mathias, L.J.; Warren, R.M.; Huang, S. *Macromolecules* **1991**, 24, 2036.
- 46 Tebelius, L.K.; Urban, M.W. *J. Appl. Polym. Sci.* **1995**, 56, 387.
- 47 Vijayendran, B.R.; Bone, T. *J. Disp. Sci. Technol.* **1982**, 3, 81.
- 48 Zhao, C.L.; Dobler, F.; Pith, T.; Holl, Y.; Lambla, M. *J. Colloid Interf. Sci.* **1989**, 128, 437.

- 49 Juhu , D.; Wang, Y.; Lang, J.; Leung, O.; Goh, M.C.; Winnik, M. *J. Polym. Sci., Part B: Polym. Phys.* **1995**, 33, 1123.
- 50 Rynders, R.M.; Hegedus, C.R.; Gilicinski, A.G. *J. Coat. Technol.* **1995**, 67, 59.

CHAPTER III

NEW POLYMERIC SURFACTANTS SYNTHESIZED VIA CATALYTIC CHAIN TRANSFER POLYMERIZATION: PMMA/TiO₂ NANOCOMPOSITES

Abstract

New acrylate-based polymeric surfactants were synthesized using catalytic chain transfer polymerization to produce graft copolymer macromonomers with molecular weights of approximately 4,000 g/mol. These macromonomers were characterized via NMR spectroscopy and their unique terminal vinyl groups were successfully observed. These polymeric surfactants, which contain both multiple anchoring functional groups and stearic stabilizing grafts, were subsequently introduced into the preparation of PMMA/TiO₂ nanocomposites. The UV-absorption characteristics of the composite materials were determined by UV-Vis spectroscopy and the nature of the corresponding TiO₂ dispersions were evaluated by transmission electron microscopy. An increased absorption in the UV region was observed for the nanocomposite films that incorporated the surfactants when compared to the “neat” PMMA/TiO₂ equivalents. An increase in the UV-absorption was also noticed when the amphiphilic character of the macromonomer was increased. Furthermore TEM images of the nanocomposites revealed a decrease in aggregate average size when the surfactant was used.

Introduction

In recent decades, the synthesis of polymer nanocomposite materials has been intensely studied due to their extraordinary properties and widespread

potential applications. As examples, construction materials from automotive to aerospace,^{1,2} biomaterials from tissue engineering to dental/orthopedic implants,^{3,4} and semiconductor to photocatalytic materials have been investigated.⁵ A diversity of crystalline materials, i.e., three-dimensional nano metal oxides, two-dimensional layered silicates, and one-dimensional carbon nanotubes, have been used for reinforcing the polymer matrixes.⁶ In addition to nanoclay and carbon nanotubes, oxide nanoparticles are emerging fillers for many applications. For instance, titanium dioxide (TiO_2) was used as a radiopacifier in dental composites and bone cements,^{7,8} as a solid plasticizer of poly(ethylene oxide) for lithium batteries,^{9,10} as a dye in a conjugated polymer for photoelectrochemical¹¹ or photoconductive¹² agents, and as a photocatalyst in a photodegradable TiO_2 -polystyrene nanocomposite film.¹³

Titanium dioxide is an inexpensive, nontoxic, and photostable material, which has good optical and photocatalytic properties for many applications. TiO_2 photocatalysts have been applied in the purification of water and air, in degradation processes of organic pollutants, in medical treatment, and in microorganism photolysis. Such nanoparticle has been used as a white pigment for many years, because it has a high refractive index and possesses the ability to reflect and refract light more effectively than any other pigment. In addition, it can be used in a wide variety of applications, where ultraviolet protection is required because of its ability to absorb ultraviolet light.¹⁴

The main problem encountered in the formation of polymer nanocomposites in general and polymer/ TiO_2 materials in particular is the

prevention of particle aggregation that may greatly affect the overall properties of the materials generated. This problem can be overcome by modification of the surface of the particles¹⁵⁻¹⁷ or incorporation of polymeric dispersants possessing anchoring group capable of strongly adsorbing onto the particle in order to confer high compatibilization. Many studies have been undertaken to find appropriate polymeric molecules for this purpose.¹⁸⁻²² Examples of functional groups that can be used to anchor polymeric chains to mineral oxide particles are amines, ammonium and quaternary ammonium groups, carboxylic, sulphonic, and phosphoric acid groups and their salts, acid sulphate and phosphate ester groups.²³ Block copolymers of ethylene oxide (EO) and propylene oxide (PO) have been used for many years to disperse TiO₂ in water-based paints.²⁴

Different polymerization techniques have been extensively used to produce well-defined polymeric surfactants. These include atom transfer radical polymerization (ATRP)²⁵, reversible addition-fragmentation chain transfer (RAFT)²⁶ and catalytic chain transfer polymerization (CCTP). Catalytic chain transfer polymerization is a free radical polymerization technique in which specific cobalt complexes act as chain transfer agents (CTAs) and catalyze the transfer of hydrogen from a growing free radical chain to an olefin. The cobalt complex is not consumed, and the rate constant of catalytic chain transfer (CCT) is believed to be diffusion controlled²⁷, thus low molecular weight polymers can be prepared with CTA on a ppm level. The overall process allows the synthesis of oligomers from methacrylates with an unsaturated end group. Oligomers with

a terminal double bond behave as macromonomers and can be used to prepare graft, block, and telechelic polymers.^{28,29}

In this chapter, amphiphilic oligomers were synthesized via catalytic chain transfer polymerization employing the low spin bis(difluoroboryl)dimethylglyoximate cobalt (II) (CoBF) complex (Figure 3.1). The structures of the generated macromonomers were characterized via NMR spectroscopy. A variety of low molecular weight ($M_n \sim 4,000$ g/mol) macromonomers were created (by varying the reaction conditions) and subsequently incorporated as compatibilizer in PMMA/TiO₂ nanocomposites.

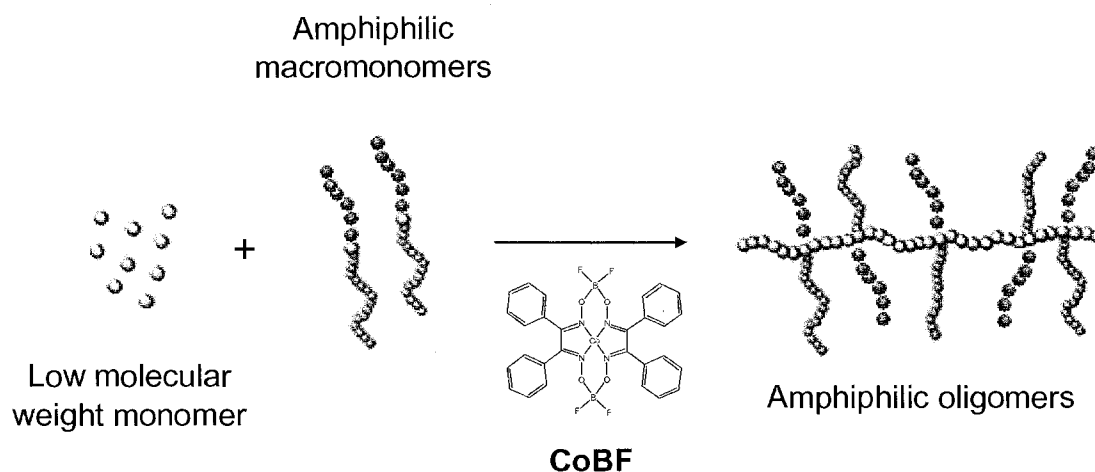
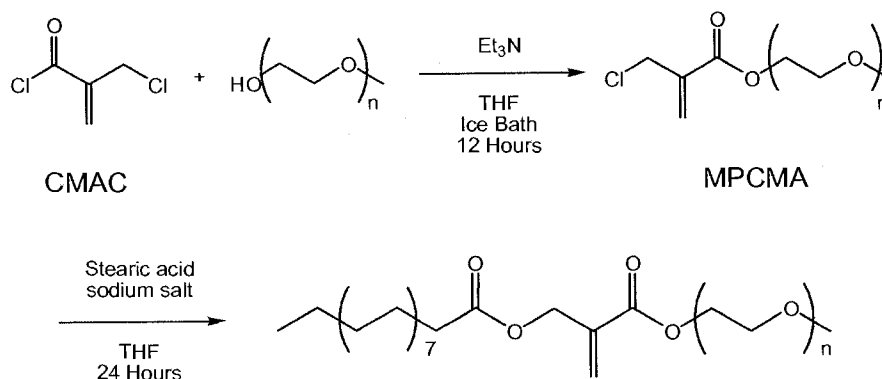


Figure 3.1. Formation of amphiphilic oligomers via CCTP (CoBF catalyst).

Results and Discussion

Monomer synthesis. The reactive surfactant investigated in this study is composed of a hydrophobic part, a polymerizable double bond, and a hydrophilic part. In this study the hydrophobic part is an alkane moiety, while the hydrophilic part is a poly(ethylene glycol) methyl ether moiety which is readily water soluble. A methacrylate group links both hydrophobic and hydrophilic moiety and

constitutes the reactive site. This reactive amphiphilic molecule was synthesized as described in Chapter II, by functionalization of the α -chloromethylacryloyl chloride (CMAC) intermediate, which was synthesized according to a previously published procedure (Scheme 3.1).



Scheme 3.1. Surfmer synthesis.

CMAC allows two different functional groups to be incorporated on either side of the polymerizable double bond. For instance, different combinations of hydrophobic and hydrophilic groups can be added in order to form reactive amphiphilic molecules. Here, MPEG was first reacted with CMAC to form the intermediate MPCMA (Scheme 3.1) to form the hydrophilic moiety, which was then reacted with stearic acid in the presence of potassium hydroxide to form the corresponding surfmer. This mild procedure gave clean, high purity product after filtration of the reaction mixture and evaporation of the solvent, $^1\text{H NMR}$ was used to follow the formation of the desired product by monitoring the appearance of the proton peaks at 4.78 ppm, corresponding to the α -methylene protons. The structure of the intermediate and the resulting reactive surfactant were confirmed

by NMR and FT-IR spectroscopy, while their high purity was confirmed by HPLC.

¹H, ¹³C NMR, and FT-IR spectra are displayed in Chapter II, Figures 2.2 and 2.3.

Catalytic chain transfer polymerizations. Copolymerization of the reactive surfactant with methyl methacrylate was investigated in Chapter II. This monomer possesses of a good copolymerization behavior with such comonomers. For instance, high incorporation of the monomer in the final copolymer was observed. Here, additional copolymerizations of the monomer with methyl methacrylate were carried out in the presence of cobalt catalyst. The copolymerization results are shown in Table 3.1. The monomer copolymerizes well with the corresponding comonomer even in the presence of cobalt catalyst, with the surfmer incorporation being very close to monomer feed.

Table 3.1. MMA-surfmer copolymers obtained by CCTP.

name	surfmer (mol-%)	CoBF (mg)	temp. (°C)	AIBN (mol-%)	Mn (g/mol)	Mw (g/mol)	PDI	surfmer incorporation (%)
A	2	1.01	85	4 (1x4)	3227	8652	2.66	N/A
B	5	1.03	85	4	4063	9264	2.28	94
C	10	1.06	85	4	4373	7630	1.74	97
D	0	0	85	0.2	42400	56800	1.34	-
E	0	1.01	85	4	3316	10237	3.08	-
F	10	0	85	4	19832	31898	1.61	96

Monomer incorporation was determined by ¹H NMR spectroscopy. The incorporation value for copolymer A, obtained by CCT polymerization, could not be obtained due to an excessive signal to noise. Table 3.1 presents also the monomer conversion, polydispersity, and apparent molecular weights. Number

average molecular weights of about 4,000 g/mol were obtained. It should be taken into consideration that these GPC results are based on polystyrene standards. The ^{13}C NMR spectra of the surfmer and the corresponding copolymer with methyl methacrylate (10 wt-% surfmer) are shown in Figures 3.2. These results confirm that the reactive surfactant investigated copolymerizes well with MMA even in the presence of cobalt catalyst, leading to the desired amphiphilic oligomers.

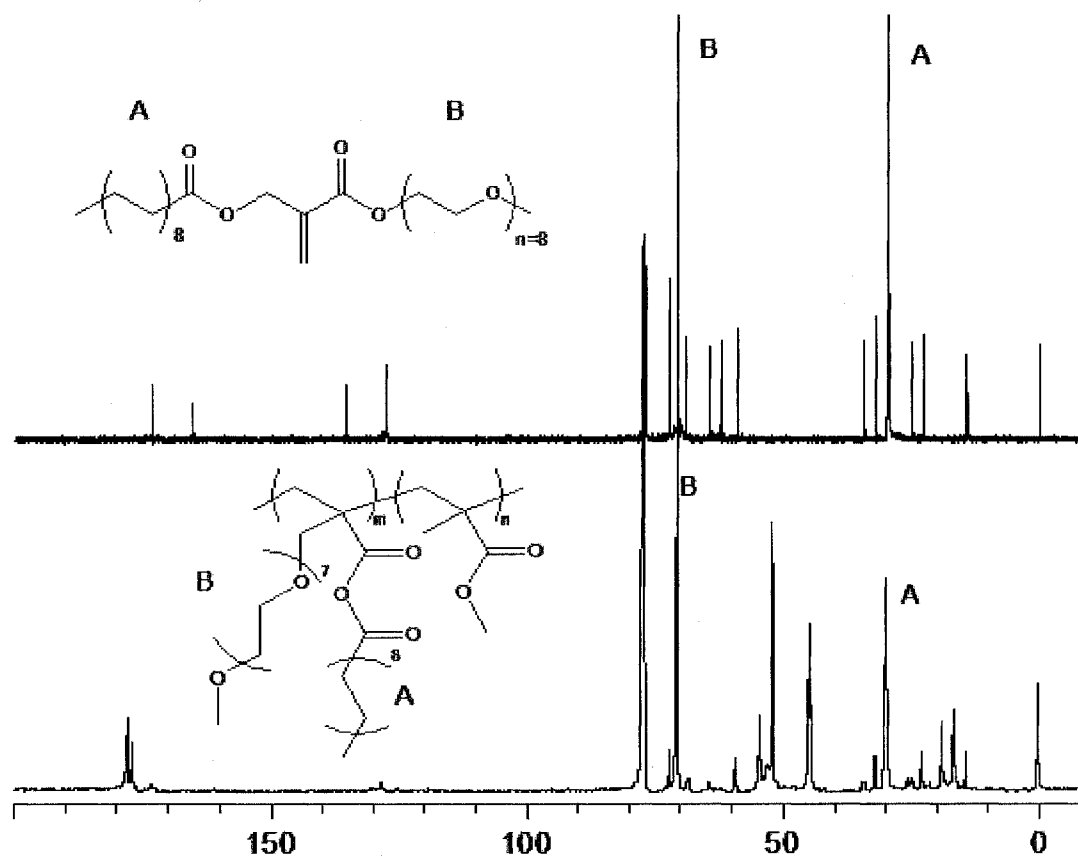


Figure 3.2. ^{13}C NMR spectra of surfmer S1 and MMA-co-S1 copolymer incorporating 10 mol-% of surfmer (CDCl_3).

The disappearance of the resonances corresponding to the vinyl carbons of the monomers and their appearance as backbone peaks is consistent with the

surfmer having undergone vinyl polymerization. Vinyl group proton peaks at 5.58 and 6.20 ppm were observed via ^1H NMR as shown in Figure 3.3. These resonance peaks relate to the terminal unsaturated vinyl functional group that is introduced to the polymer chain as a result of the CCTP catalytic cycle and thus confirms that the CoBF catalyst used is active in this polymerization.

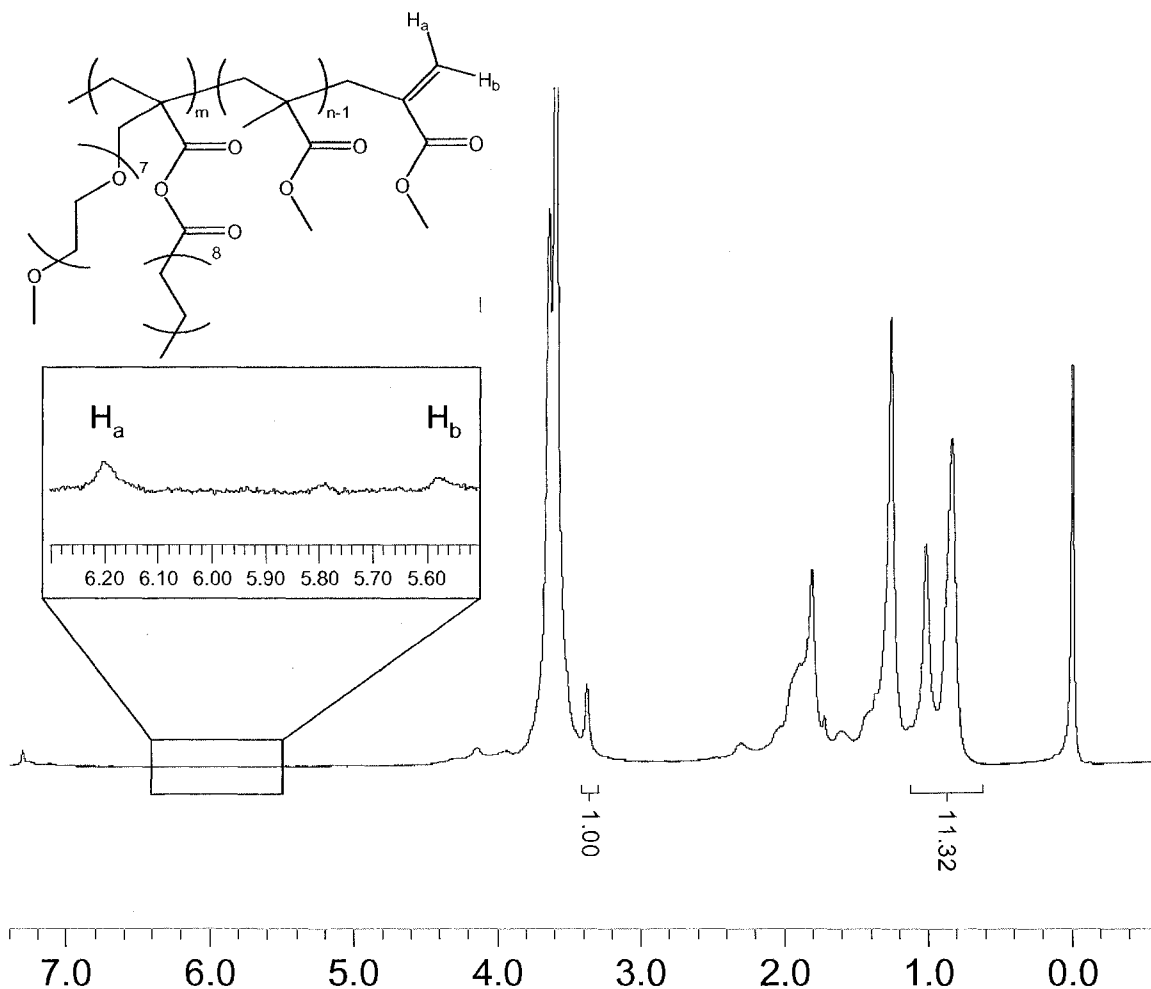


Figure 3.3. ^1H NMR spectrum of MMA-co-surfmer copolymer C (CDCl_3).

Due to the presence of this terminal functionality, the oligomers produced have the potential to be further functionalized, incorporated in polymer as pendant groups via free radical polymerization technique or used chain transfer

agents. It should be noted that the macromonomers prepared with CCTP can be copolymerized in a sequential polymerization. The macromonomer reactivity in these copolymerizations depends strongly on the choice of monomers used in the second stage polymerization. Acrylates are reported to yield efficient copolymerization with such macromonomers, while methacrylates react poorly.³⁰ In the latter, the macromonomer does not copolymerize, but acts as a chain transfer agent via β -scission.³¹ Vinyl acetate was reported not to give any copolymerization at all. In the copolymerization of macromonomers with acrylic monomers, polymer chains are formed with a comb-like structure, with the macromonomer chains as side chains from the main polymer backbone.

In the work presented in this chapter, the amphiphilic macromonomers were incorporated in PMMA/TiO₂ nanocomposites to act as compatibilizers between the inorganic filler and the polymeric matrix. Their incorporation as monomer in the final polymer is not discussed and could be subject to further consideration. For the reasons just discussed, we do not expect in this particular case high degree of copolymerization with MMA and believe that compatibilization will be determined by the degree of non-bonded association of the macromonomers with the PMMA matrix.

Nanocomposite preparation and characterization. Nanocomposites were prepared by means of *in situ* polymerization. The corresponding TiO₂ amount was dispersed in MMA, mixed overnight and sonicated for 30 minutes before polymerization. Approximately 0.1 wt-% initiator (AIBN) was added to the sample. A freeze thaw technique allowed degassing the mixture prior to polymerization.

The flask was then purged with argon and placed in an oil bath at 65 °C for 24 hours to ensure high monomer conversion. The resulting polymer was isolated by successive reprecipitations into methanol from THF and drying under reduced pressure. All nanocomposites incorporated the same amount of TiO₂ nanoparticles (5 wt-%) and the concentration of macromonomeric surfactant was also kept constant to 2.5 wt-%. The three polymer/TiO₂ nanocomposites **1**, **2** and **3** incorporate macromonomers **A**, **B** and **C** respectively (Table 3.2).

Table 3.2. Nanocomposites preparation.

entry	macromonomer name/wt-%	TiO ₂ (wt-%)	temp. (°C)	AIBN (mol-%)
1	A/2.5	5	65	0.2
2	B/2.5	5	65	0.2
3	C/2.5	5	65	0.2
4	0	5	65	0.2

Each polymeric material was subsequently dissolved in tetrahydrofuran at the same concentration (g/L). Nanocomposites films were then formed by spin coating each polymeric solution onto a NaCl disk. The absorbance of each film was then characterized using a UV-VIS spectrometer. Figure 3.4 illustrates the ultraviolet-visible absorbance spectra obtained for the nanocomposite acrylic polymers prepared by in situ polymerization. The UV-VIS spectrum of neat PMMA was also recorded and is shown in Figure 3.4 as well. The results show that the polymers with nano-TiO₂ particles embedded have absorbance in the UV range (290-400 nm) in comparison with PMMA. The results also show variation in the UV absorbance as a function of the nature of the polymeric surfactant introduced. Indeed, nanocomposites incorporating macromonomer **C** show

higher absorbance in this region than the polymers incorporating macromonomers **A** and **B**. A correlation between the amount of amphiphilic unit within the copolymer backbone and the total absorbance can be drawn as the amount of nanoparticles was kept the same in all films. The optical change observed is caused by the quantum size effect of the nanoparticles. This means that when the particle size is reduced and aggregation avoided, the higher surface area makes the atoms and electrons at the surface have different behavior from atoms and electrons within the bulk of the particles. The increase in UV absorbance as a function of the polymeric surfactant used to disperse the particles indicates that a better dispersion of the TiO_2 filler is reached when macromonomer **C** is used. The difference in molecular weight is believed to be negligible in this case.

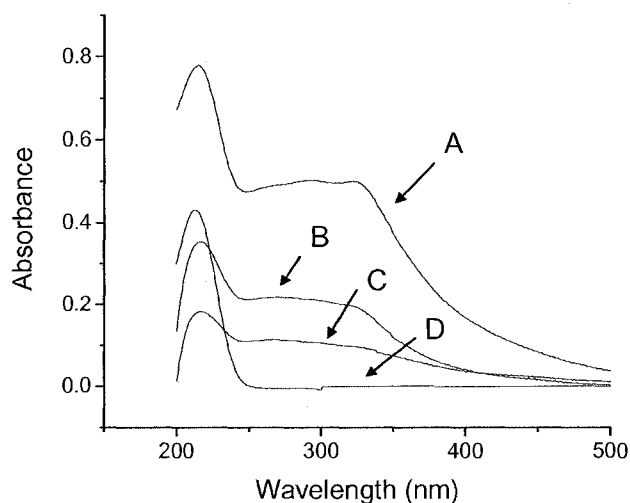


Figure 3.4. UV-VIS spectra for the nanocomposites **1 (A)**, **2 (B)**, **3 (C)** and **4 (D)**.

Transmission electron microscopy allowed investigating the morphology of each nanocomposite formed. Figures 3.5 and 3.6 illustrate the dispersion of 5 wt-% TiO_2 nanoparticles in PMMA film with no surfactant and with 2.5 wt-% of

oligomeric surfactant **C**, respectively. It can be observed that the corresponding macromonomer leads to enhanced filler dispersion as smaller aggregates can be detected compared to neat PMMA/TiO₂ with no surfactant. These data tend to confirm the absorbance results discussed above: a higher degree of filler dispersion arises when the oligomeric reactive surfactant is introduced, increasing the overall absorbance properties of the resulting nanocomposites.

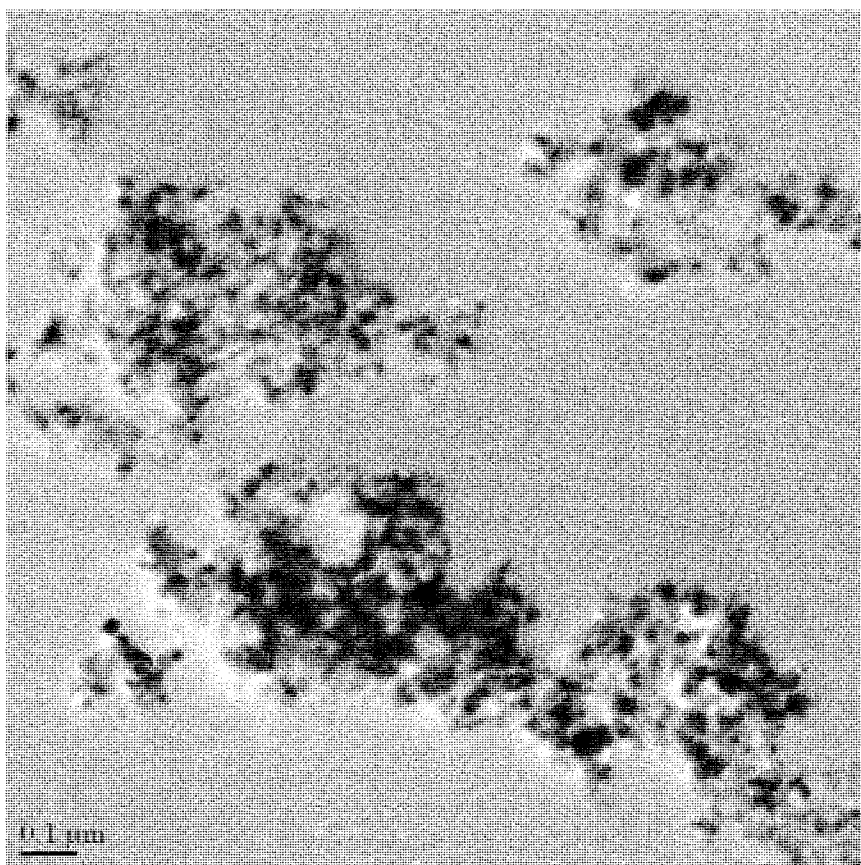


Figure 3.5. TEM image of a section of PMMA/TiO₂ nanocomposite (5 wt-% TiO₂, no surfactant).

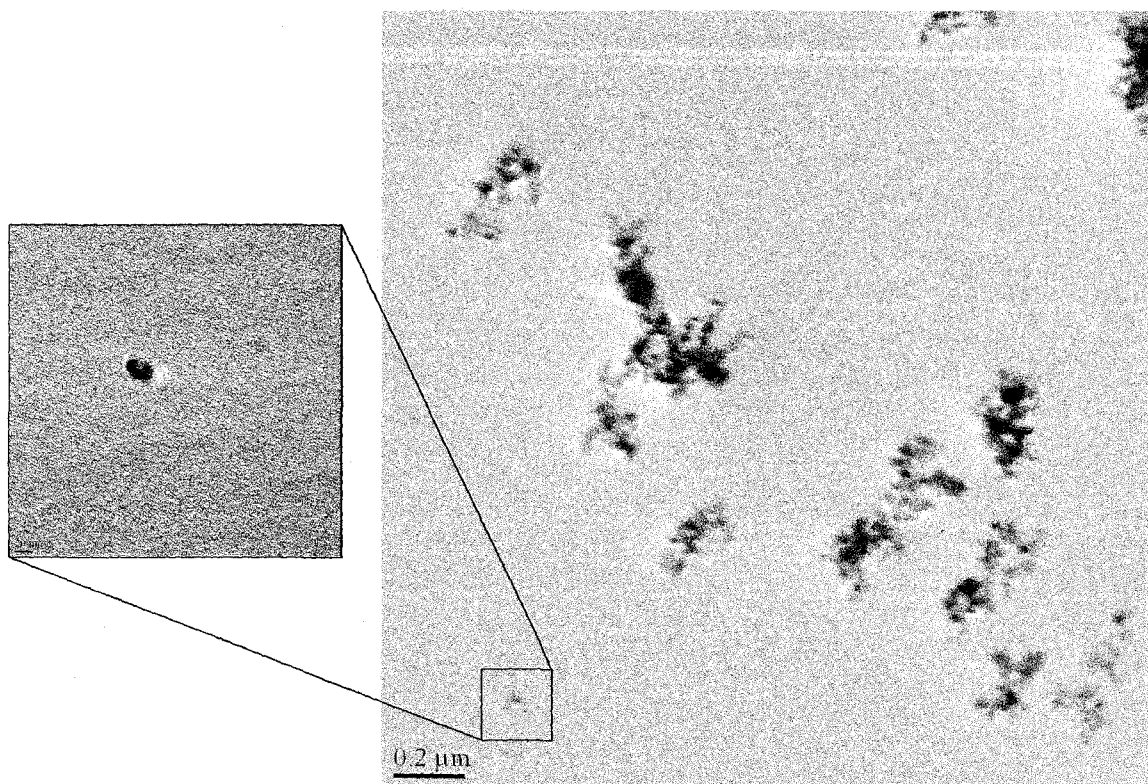


Figure 3.6. TEM image of a section of PMMA/TiO₂ nanocomposite (5 wt-% TiO₂, 2.5 wt-% surfactant C). The inset is at higher magnification (scale bar=20 nm).

Even if an enhancement in both UV-absorption and filler dispersion was observed, it is believed that the low copolymerization efficiency of the monomer with MMA may lead to segregation of the surfactant within the matrix, which affects the overall material's properties. Higher degrees of dispersion could be obtained by increasing the reactivity of both comonomers during polymerization.

Conclusions

An acrylate-based non-ionic reactive surfactant that has been incorporated successfully in acrylic latex in the previous chapter was here copolymerized with methyl methacrylate via catalytic chain transfer polymerization in order to prepare well-defined amphiphilic reactive oligomers.

Macromonomers were synthesized successfully with apparent molecular weights of about 4,000 g/mol. These surfactants were then subsequently evaluated as compatibilizers in PMMA/TiO₂ nanocomposites. An increase in the overall UV-absorption as a function of the concentration of amphiphilic unit introduced in the systems was observed, causing a higher degree of dispersion of the nanoparticles within the polymeric matrix. Transmission electron microscopy allowed determining morphologies of the nanocomposites. A decrease of the average aggregate size was observed when the oligomeric surfactants were introduced, testifying to a better compatibilization of the nanoparticles with the PMMA matrix.

Experimental

Materials. The following reagents were used as received with the exception of methyl methacrylate (Aldrich Chemical Company), which was distilled over calcium hydride (Aldrich Chemical Company) and 2,2'-azobis(2-methylpropionitrile) (AIBN, Fisher Scientific) which was recrystallized from methanol. Poly(ethylene glycol) methyl ether (Mn=350 g/mol) was purchased from Acros Organics. t-Butyl acrylate, paraformaldehyde, and 1,4-diaza[2.2.2]bicyclooctane (DABCO) were purchased from Aldrich. Toluene, tetrahydrofuran and all other solvents were obtained from Aldrich or Fisher. t-Butyl α -hydroxymethylacrylate (t-BHMA) was prepared using a previously published procedure.³⁰ Bis(boron difluorodiphenylglyoximate) cobalt(II) (cobaloxime tetra-phenyl) was purchased from DuPont and used as received without further purification. Nano-TiO₂ was purchased from Degussa.

Instrumentation and characterization. Molecular weights and molecular weight distributions of the polymers obtained by solution polymerization were measured using size exclusion chromatography (SEC) on a system equipped with four styrene gel mixed bed columns (American Polymer Standard Corporation, Mentor, OH) using THF as eluent. Polystyrene standards (MWs ranging from 4630 to 400,000 g/mol) were used for calibration. Solution ^1H and ^{13}C NMR spectra were collected on a Varian Mercury 300 MHz spectrometer operating at a frequency of 75.47 MHz for carbon. NMR spectra were recorded at room temperature using CDCl_3 solvent with TMS as internal reference. FT-IR spectra were obtained using a Bio-Rad FTS 5000 FT-IR spectrometer.

Synthesis of α -chloromethylacryloyl chloride (CMAC). In a 250 ml one neck round bottom flask, t-BHMA (50g, 0.316 mol) and a large excess thionyl chloride were added and stirred at ambient temperature overnight. Most of the thionyl chloride was removed under vacuum and vacuum distillation gave α -chloromethylacryloyl chloride as a clear liquid in 65% yield. FT-IR (cm^{-1}): 3107, 2966, 1742, 1637, 1407, 1284, 967, 896; ^1H NMR (CDCl_3) δ 4.26 (s, 2H, CH_2Cl), 6.41 and 6.74 (s, 2H, $\text{CH}_2=\text{C}$); ^{13}C NMR (CDCl_3) δ 41.53 (CH_2Cl), 136.14 ($\text{CH}_2=\text{C}$), 141.14 ($\text{C}=\text{CH}_2$), 166.78 ($\text{C}=\text{O}$).

Synthesis of MPEG α -chloromethylmethacrylate (MPCMA). In a 250 ml round bottom flask, poly(ethylene glycol) methyl ether (20 g, 57.1 mmol) was added to 100 ml of dried THF. The solution was stirred at -10°C for 30 minutes. CMAC (10.32 g, 74.3 mmol) diluted in 50 ml of dried THF was then added dropwise to the stirring mixture. The resulting mixture was stirred overnight at room

temperature. The precipitate was filtered and the solvent removed under reduced pressure. Excess CMAC was removed by washing the crude oil with three aliquots of hexane to give MPCMA as light brown oil in ca. 94% yield.

$^1\text{H NMR}$ (CDCl_3) δ 4.30 (s, 2H, CH_2Cl), 6.01 and 6.41 (s, 2H, $\text{CH}_2=\text{C}$), 4.35 (t, 2H, $\text{CH}_2\text{C}=\text{CH}_2$), 3.38 (s, 1H, CH_2OCH_3), 3.61 (s, 2H, $\text{CH}_2\text{CH}_2\text{O}$); $^{13}\text{C NMR}$ (CDCl_3) δ 41.53 (CH_2Cl), 128.96 ($\text{CH}_2=\text{C}$), 136.74 ($\text{C}=\text{CH}_2$), 164.85 ($\text{C}=\text{O}$), 64.32 ($\text{CH}_2\text{C}=\text{O}$), 70.54 (CH_2O), 58.99 (CH_2OCH_3).

Surfmer synthesis. First, stearic acid potassium salt was obtained by mixing at room temperature, in THF, the corresponding acid (1 mol) with potassium hydroxide in slight excess (1.05 mol). The salt was then collected by filtration of the crude mixture and dried overnight at 60 °C in a vacuum oven. Then, in a 250 ml round-bottom flask, the corresponding acid potassium salt (26.1 mmol) was dispersed into THF. MPEG α -chloromethylmethacrylate was then added to the salt solution dropwise at room temperature. The resulting mixture was allowed to stir at room temperature for 24 hours. The precipitate was filtered off and the solvent removed under reduced pressure to give the corresponding monomers in quantitative yields.

$^1\text{H NMR}$ (CDCl_3) δ 4.77 (s, 2H, CH_2O), 5.81 and 6.34 (s, 2H, $\text{CH}_2=\text{C}$), 4.30 (t, 2H, $\text{CH}_2\text{C}=\text{CH}_2$), 3.34 (s, 1H, CH_2OCH_3), 3.61 (s, 2H, $\text{CH}_2\text{CH}_2\text{O}$); $^{13}\text{C NMR}$ (CDCl_3) δ 62.13 ($\text{CH}_2\text{C}=\text{CH}_2$), 127.42 ($\text{CH}_2=\text{C}$), 135.30 ($\text{C}=\text{CH}_2$), 165.09 ($\text{C}=\text{O}$), 173.13 ($\text{C}=\text{O}$), 64.09 ($\text{CH}_2\text{C}=\text{O}$), 70.56 (CH_2O), 59.01 (CH_2OCH_3), 14.13 (CH_3CH_2),

22.68 (CH_2CH_3), 24.91 ($\text{CH}_2\text{CH}_2\text{C}=\text{O}$), 29.68 (CH_2), 31.92 ($\text{CH}_2\text{CH}_2\text{CH}_3$), 34.19 ($\text{CH}_2\text{C}=\text{O}$).

Catalytic chain transfer polymerizations. All reactions were carried out using 100 ml test tubes equipped with In a typical polymerization procedure 50 ppm of cobaloximes methyl (0.00234g) was dissolved under nitrogen in dried toluene (30ml) in a 100 ml 3 necked round bottom flask equipped with a condenser. The corresponding monomer and methyl methacrylate were added to the complex solution. The resulting mixture was stirred for 30 minutes under a nitrogen blanket. The solution temperature was then gradually raised to 95 °C. In a separate 100 ml, round bottom flask was dissolved AIBN (0.201 g, 1.21 mmol) in dried toluene (20 ml). The initiator solution was allowed to stir for 30 minutes under Nitrogen blanket. Once the temperature was stabilized, a single portion of initiator solution was poured into the reaction flask every hour for four hours, corresponding to four aliquots of initiator solution. The flask was then removed from the oil bath one hour after the last initiator shot. The final product was washed with heptane to give the polymer as a soft yellow solid in 83% yield.

Polymerizations and nanocomposites preparation by *in situ*

polymerization. TiO_2 (0.1 g, 5 wt-%) was dispersed in MMA (2 g), mixed overnight, and sonicated for 30 minutes before polymerization. Approximately 0.1 wt-% of initiator (AIBN) was added to the sample. A freeze thaw technique allowed degassing the mixture prior to polymerization. The flask was then purged with argon and placed in an oil bath at 65 °C for 24 hours to ensure high monomer conversion.

Film preparation. Films were formed by dissolving a given amount of polymer/clay nanocomposite in THF. The resulting polymer solution was then poured into an aluminum cup and allowed to dry under air flow for 5 days to give films with thicknesses of approximately 100 μm . All the films were then characterized without further treatment.

UV-VIS characterization. The absorbance spectra of the acrylic films in the range of 200-500 nm wavelength of light were determined using a UV-VIS spectrometer (Hitachi UV-3000, Japan) with a scan speed of 300 nm/min.

Nanocomposite morphology. Specimens for transmission electron microscopy were prepared by microtoming the samples at an angle of 6° to the diamond knife and at a speed of 1.5–3.5 mm/s on a Reichard-Jung Ultracut E microtome. Ultrathin sections (70 nm thick) were placed on copper TEM grids. The sections were viewed using a Zeiss EM 109-T electron microscope (Carl Zeiss, Jena, Germany) operating at 200 kV.

REFERENCES

- 1 Kawasumi, M. *J. Polym. Sci., Part A: Polym. Chem.* **2004**, *42*, 819.
- 2 Njuguna, J.; Pielichowski, K. *Adv. Eng. Mater.* **2004**, *6*, 204.
- 3 Shi, X.; Hudson, J.L.; Spicer, P.P.; Tour, J. M.; Krishnamoorti, R.; Mikos, G. *Biomacromolecules* **2006**, *7*, 2237.
- 4 Li, H.; Chen, Y.; Xie, Y. *Mater. Lett.* **2003**, *57*, 2848.
- 5 Caseri, W. *Macromol. Rapid Commun.* **2000**, *21*, 705.
- 6 Wypych, F.; Satyanarayana, K.G. *J. Colloid Interface Sci.* **2005**, *285*, 532.
- 7 Ramires, P.A.; Giuffrida, A.; Milella, E. *Biomaterials* **2002**, *23*, 397.
- 8 Yoshida, K.; Taira, Y.; Atsuta, M. *J. Dent. Res.* **2001**, *80*, 864.
- 9 Croce, F.; Appetecchi, G.B.; Persi, L.; Scrosati, B. *Nature* **1998**, *394*, 456.
- 10 Ahn, J.H.; Wang, G.X.; Liu, H.K.; Dou, S.X. *J. Power Sources* **2003**, *119*–*121*, 422.
- 11 Petrella, A.; Tamborra, M.; Curri, M. L.; Cosma, P.; Striccoli, M.; Cozzoli, P.D.; Agostiano, A. *J. Phys. Chem. B* **2005**, *109*, 1554.
- 12 Kocher, M.; Daubler, T.K.; Harth, E.; Scherf, U.; Gugel, A.; Neher, D. *Appl. Phys. Lett.* **1998**, *72*, 650.
- 13 Zan, L.; Tian, L.; Liu, Z.; Peng, Z. *Appl. Catal., A* **2004**, *264*, 237
- 14 Kickelbick G. *Prog. Polym. Sci.* **2003**, *28*, 83–114.
- 15 Marutani, E.; Yamamoto, S.; Ninjagar, T.; Tsujii, Y.; Fukuda, T.; Takano, M. *Polymer* **2004**, *45*, 2231–2235.
- 16 Zhang, S.W.; Zhou, S.X.; Weng, Y.M.; Wu, L.M. *Langmuir* **2005**, *21*, 2124–8.

- 17 Erdem, B.; Hunisicker, R.A.; Simmons, G.W.; Sudol, E.D.; Dimonie, V.L.; El-Aasser, M.S. *Langmuir* **2001**, *17*, 2664–2669.
- 18 Craft, R. *Mod. Paint and Coatings* **1991**, *81*, 38-43.
- 19 Van den Haak, H.J.W. *J. Coatings Tech.* **1997**, 137-142.
- 20 Pattanaik, M.; Rout, T.K.; Sengupta, D.K. *Surf. Coatings Int.* **2000**, *12*, 592-596.
- 21 Kostelnik, R.J.; Wen, F.C. **2001**, USA Patent 6,197,104.
- 22 Chen, H.T.; Ravishankar, S.A.; Farinato, R.S. *Inter. J. Min. Process.* **2003**, *72*, 75-86.
- 23 Creutz, S.; Jerome, R.; Kaptijn, G.M.P.; van der Werf, A.W.; Akkerman, J.M. *J. Coatings Tech.* **1998**, *70*, 41-46.
- 24 Bouvy, A. *Europ. Coating J.* **1996**, *11*, 822-826.
- 25 Pattern, T.E.; Matyjaszewski, K.; *Adv. Mater.* **1998**, *10*, 901.
- 26 Moad, G.; Chiefari, J.; Chong, Y.K. *Polym. Int.* **2000**, *49*, 993.
- 27 Kukulj, D.; Davis, T.P. *Macromol. Chem. Phys.* **1998**, *199*, 1697.
- 28 Gridnev, W.J.; Simonsick Jr., S.D.; Ittel, J. *Polym. Sci. A: Polym. Chem.* **2000**, *38*, 1911.
- 29 Gridnev, J. *Polym. Sci. A: Polym. Chem.* **2000**, *38*, 1753.
- 30 Cacioli, P.; Hawthorne, D.G.; Laslett, R.L.; Rizzardo, E.; Solomon, D.H.; *J. Macromol. Sci. Chem. A* **1986**, *23*, 839.
- 31 Haddleton, D.M.; Maloney, D.R.; Suddaby, K.G.; Clarke, A.; Richards, S.N. *Polymer* **1997**, *38*, 6207.

CHAPTER IV
NEW ACRYLATE-BASED CATIONIC REACTIVE SURFACTANTS AND THEIR
USE IN THE FORMATION OF PMMA/CLAY NANOCOMPOSITES VIA
EMULSION POLYMERIZATION

Abstract

The synthesis of new acrylate-based cationic macromeric surfactants is described and their incorporation in methyl methacrylate latexes investigated. Well-defined latex particles with narrow particle distributions were produced and scanning electron microscopy was used to confirm the size and size distribution of the particles formed. Nanocomposites were formed from these latexes and their mechanical properties were investigated. The glass transition of the film formed increased with clay loading. The film formation method was shown to have a great impact onto the dispersion of the particles and final material properties. For instance, it has been found that solvent casting leads to a better dispersion of the filler in the polymer matrix as compared to a melt-pressing method.

Introduction

For many years, attention has been paid to the incorporation of inorganic fillers in polymeric matrix in order to improve numerous material's properties such as stiffness, strength, thermal stability, flame retardancy, solvent and UV resistance, and gas barrier properties.^{1,2} Several procedures have been used to produce polymer/silicate nanocomposites such as melt blending, solvent casting, sol-gel methods, and *in situ* polymerization.^{3,4} Two different nanocomposite

morphologies are generally obtained and can usually be classified as either exfoliated or intercalated with some degree of aggregation.⁵ Melt processing consists of blending a molten thermoplastic polymer with clay at high temperature and high shear, which can sometimes lead to thermodegradation during processing.⁶ Sol-gel processes have been used in the past by Muh et al.⁷ and by Moszner and coworkers⁸ to prepare organic-inorganic hybrid materials through hydrolysis and condensation of organically modified silanes containing free radically polymerizable methacrylate groups. In the past, the *in situ* polymerization technique has been also extensively used. In this particular case, the clay is swollen in the monomer and polymerization is carried out between and around the layers of clay.

The main concerns in the design of polymer-clay nanocomposites are the degree of dispersion of the nanoparticles into the matrix and the level of affinity of the filler with the organic phase. The common methods discussed above lead to a dispersing degree and interfacial adhesion of the filler with the polymer insufficient in order to reach desirable materials properties. Recently, emulsion polymerization has attracted a great amount of interest in order to achieve a high degree of dispersion of the clay particles into the polymeric matrix. Galembeck and coworkers have reported the synthesis of poly(styrene-co-butyl acrylate-co-acrylic acid)/MMT nanocomposites utilizing an aqueous colloidal polymer dispersion technique. In this method, the surfactant is used as stabiliser during the emulsion polymerization and as compatibilizer between the polymeric particle and the filler. The high degree of dispersion of clays in water makes the

approach very attractive. Many surfactants, reactive or not, have been used in the past to form polymer/clay nanocomposites via heterophase polymerization technique. The use of polymerizable surfactants (surfmers) is attractive because of the direct chemical link between the surfactant and the polymer. To achieve high conversion and good distribution of the stabiliser around the polymeric particle, the reactivity of the polymerizable surfactant and its adsorption characteristics are critical factors. To be effective the surfmers must react such that, during the main part of the polymerization, surfmer incorporation into the polymer being produced is low. This avoids surfmer being dragged into the bulk of the polymeric particle and maximizes the amount of surfmer present at the surface. Thus, the surfmers activity is maximized and the quantities required kept to a minimum. However, toward the end of the reaction, high surfmer incorporation should be achieved to avoid leaving quantities of free surfmer in the polymer, which may eventually migrate to surfaces and interfaces during final product use; e.g., film formation.⁹ This may decrease also the affinity between the polymer and the inorganic filler.

A wide range of surfmers have already been developed incorporating reactive groups such as acrylates, methacrylates, styrenics and maleates. The main limitation on surfmer use at the moment is related to the reactivity of the polymerizable unit within them. Traditionally, the reactivity of the functional groups has been restricted to prevent the “burying” phenomenon and thus, the situation that they are applied to are niche opportunities.¹⁰⁻¹⁶ As illustrated in Chapter II, hydroxymethylacrylate esters are vinyl monomers which have a very

high susceptibility to undergo radical polymerization and their reactivity can be tailored by the nature of the functional groups present in the molecule. They show high potential in heterophase polymerization. Here we are interested in investigating amphiphilic α -hydroxymethylacrylate derivatives and their incorporation as reactive surfactants in emulsion polymerizations in order to lead to the formation of PMMA/clay nanocomposites with enhanced performances.

Generally, the inorganic particles typically used in the formation of nanocomposites are layered silicates such as synthetic Laponite.¹⁷ Laponite clay consists of particles of about 25 nm in diameter and 0.92 nm in thickness.¹⁸ It has a layer structure composed of repeats of six octahedral magnesium ions sandwiched between two layers of four tetrahedral silicon atoms and an overall empirical formula $\text{Na}^{0.7}\text{[(Si}_8\text{Mg}_{5.5}\text{Li}_{0.3}\text{)O}_{20}\text{(OH)}_4\text{]}^{-0.7}$.¹⁹ Laponite has the advantages over natural clay like Montmorillonite of being chemically pure, synthetic, and free from crystalline silica impurities.

In the present chapter, we report the synthesis of new RHMA-based reactive surfactants, their incorporation into PMMA acrylic latexes, and the subsequent formation of PMMA/Laponite clay nanocomposites. The study of the resulting nanocomposites mechanical properties and morphologies was conducted as function of the nature of the surfactant, the polymerization process, and the film formation method.

Results and Discussion

Surfmers synthesis and characterization. All the reactive surfactants synthesized are composed of a hydrophobic part spacing a polymerizable double

bond and an imidazolium moiety. The imidazolium group acts as electrostatic linkage between the polymeric particle and the clay platelets dispersed into the aqueous phase. The imidazolium moiety was chosen for its enhanced thermal stability compared to ammonium surfactants.²⁰ The reactive surfactants synthesized are presented in Figure 4.1.

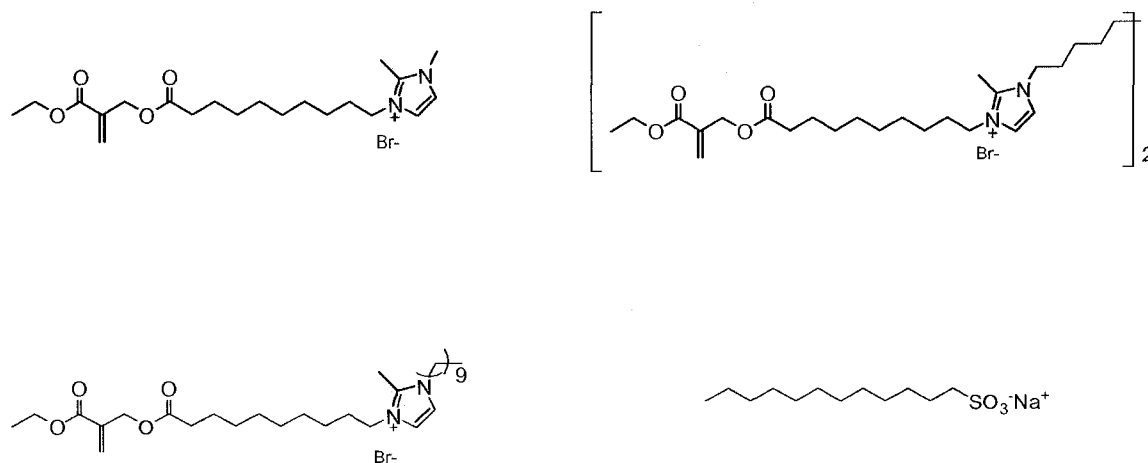
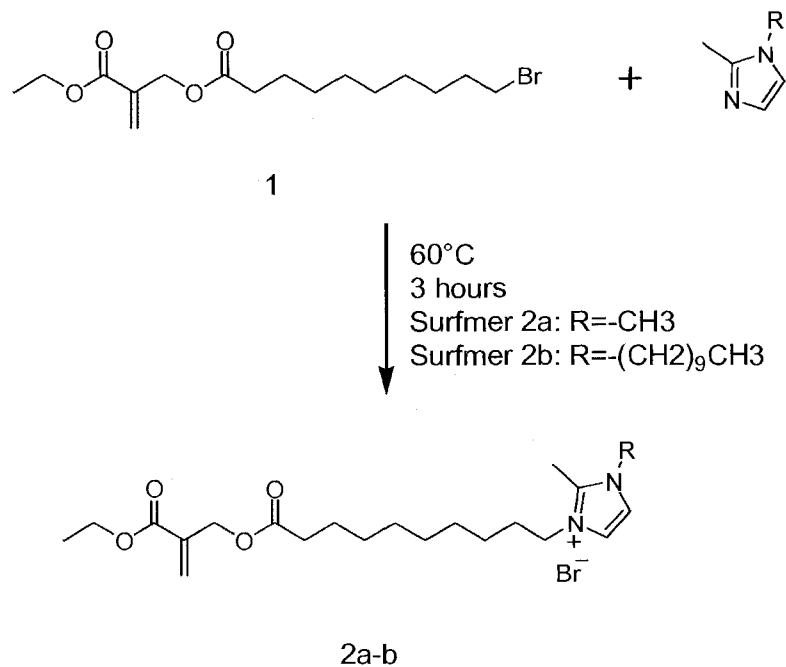
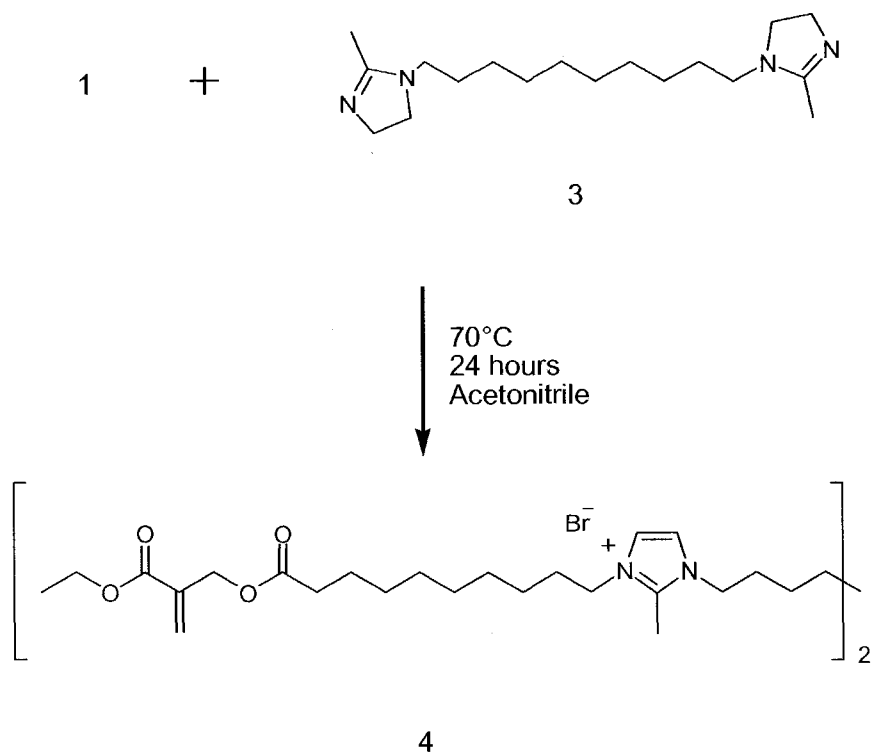


Figure 4.1. Surfactants investigated.

These surface active compounds are interesting candidates to compatibilize the clay with the polymeric matrix. The surfmers incorporate a methacrylate group located at one end of the hydrophobic part, allowing the reactive site to be buried into the particle in order to maximize incorporation of the surfmer during emulsion copolymerization with MMA. These macromonomers were all synthesized in two steps as shown in Schemes 4.1 and 4.2.



Scheme 4.1. Synthesis of reactive surfactants **2a** and **2b**.



Scheme 4.2. Synthesis of gemini reactive surfactant **4**.

First, ethyl α -chloromethylacrylate (ECMA), which was synthesized according to previously reported literature,²¹ was reacted with 11-bromoundecanoic acid in the presence of triethylamine to give the intermediate **1**. ¹³C NMR allowed monitoring the reaction by following the disappearance of the peak at 42.4 ppm corresponding to chlorine methylene. This intermediate allows different imidazolium hydrophilic groups to be incorporated. Surfmers **2a** and **2b** were subsequently obtained by reaction of this latter intermediate with 1,2-dimethylimidazole and 1-methyl-2-decylimidazole respectively. This mild procedure gave clean, high purity products after precipitation into cold diethyl ether and subsequent evaporation of the solvent under reduced pressure. ¹H NMR was used to follow the formation of the desired products and to monitoring the disappearance of the proton triplet peak at 3.38 ppm, corresponding to the elimination of bromide, which confirmed product formation.

Next, we were interested in synthesizing a gemini surfmer analog to the reactive surfactants **2a** and **2b** because this molecule would allow incorporating statistically twice as more cationic sites onto the polymeric particle with the same degree of surfmer conversion. The gemini reactive surfactant **4** was synthesized following the procedure illustrated in Scheme 4.2. 1,10-Bis(2-methylimidazole)-decane **3** was first obtained by reacting 2-methylimidazole and 1,10-dibromodecane in THF under reflux conditions in the presence of triethylamine as acid scavenger. The diimidazole compound was isolated by filtration of triethylamine white salt and removal of the solvent under reduced pressure. Washing several times with dionized water led to compound **3** in quantitative

yield. Compound **3** was then reacted with 2 eq. of intermediate **1**, in dried tetrahydrofuran and in reflux conditions. The structures of the different intermediates and macromonomers were confirmed by NMR and FT-IR. As an example, ^{13}C NMR spectra of the intermediates **1** and **3**, and gemini surfactant **4** are shown in Figure 4.2. These spectra show the disappearance of the peak belonging to the carbon next to the bromine, indicating the formation of the expected product.

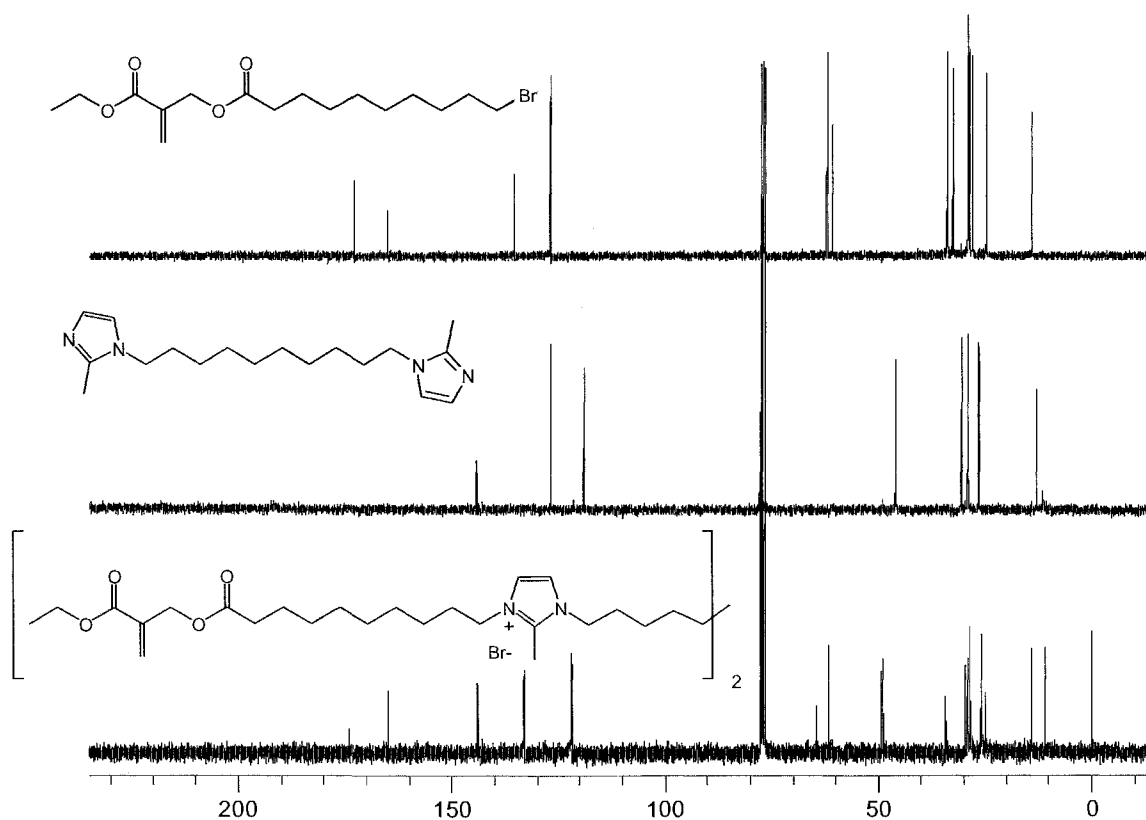


Figure 4.2. ^{13}C NMR spectra of intermediates **1**, **3** and gemini surfmer **4** (CDCl_3).

Emulsion polymerizations. Methyl methacrylate latexes were prepared by batch emulsion polymerization incorporating the different reactive surfactants discussed above. Table 4.1 lists monomer conversion, number average

molecular weight, molecular weight dispersity, particle size, and particle size distribution for each latex formed.

Table 4.1. Characteristics of the final latexes.

latex	surfactant	amount surfactant (mol-%)	Mn (g/mol) ^(a)	PDI	conv. (%) ^(b)	D (μm) ^(c)	width (μm)
L0	SDS	2.24	386,000	1.35	97	0.048	0.021
L1	2a	1.06	110,000	3.45	98	0.106	0.046
L2	2b	1.11	98,000	3.56	97	0.132	0.052
L3	4	0.54	107,000	2.65	97	0.124	0.034

(a) – Determined using size exclusion chromatography.

(b) – Determined by gravimetry.

(c) – Evaluated using dynamic light scattering.

These data show that high conversion of monomers was achieved as determined by gravimetry. No vinyl peak from the surfmer reactive double bonds could be seen in the ¹H NMR spectra (D₂O) of the latexes, suggesting high incorporation of the surfmer into the polymer. All the surfmers gave stable emulsions and insignificant amounts of coagulum, suggesting little destabilization during the heterophase polymerization. In all the reported emulsion polymerizations in this chapter, the amount of surfmer added to form the latex was approximately 1 mol-%.

Average particle sizes of 106, 128, and 132 nm were measured by dynamic light scattering for the latexes incorporating surfactant **2a**, **2b**, and **4**, respectively. Narrow particle size distributions were also measured for all latexes. Both sizes and size distributions of polymeric particles were confirmed by scanning electron microscopy (Figure 4.3).

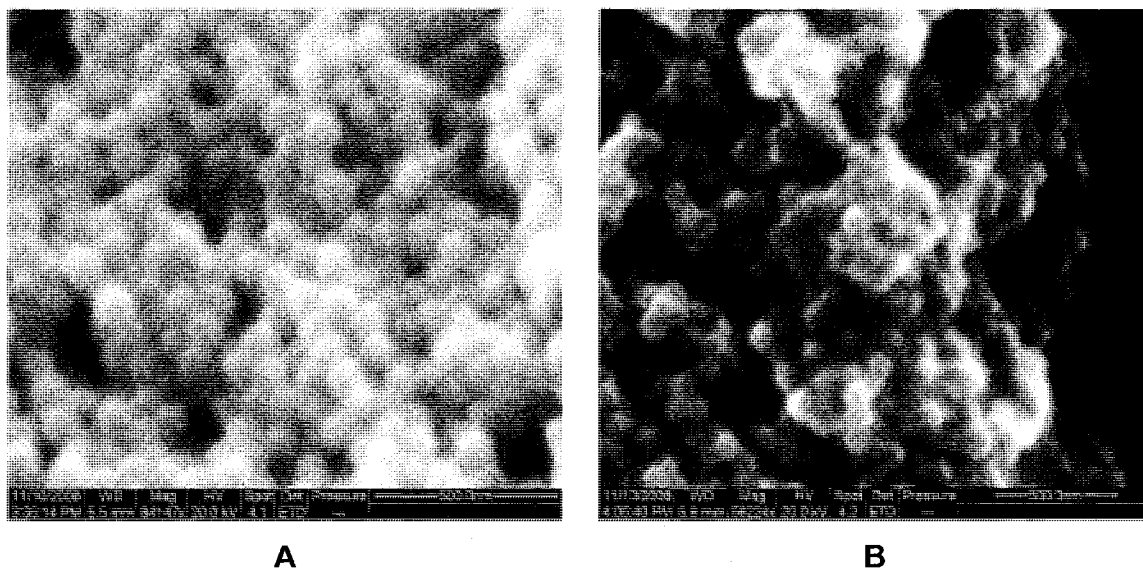


Figure 4.3. SEM images of latex L1 (A) and latex L1 with 5 wt-% of sodium Laponite (B) (scale bar: 500 nm).

The low amount of coagulum that could be detected in the emulsion polymerisations detailed in this study suggest that these materials exhibit little homopolymerization and good copolymerization behavior during the heterophase polymerization. Thus, it is concluded that the molecular design of the surfmers in this work has successfully influenced the balance between aqueous phase homopolymerization and heterophase copolymerisation.

Preparation of nanocomposites from PMMA latexes. A first series of nanocomposites were formed by addition of different amounts of untreated sodium Laponite clay (2.5, 5, 10 wt-%) to the latexes formed above. In the emulsion preparation method, the cationic reactive surfactants act as stabilizer and compatibilizer with the clay platelets dispersed into the aqueous phase while in the in situ polymerization the same surfactants act essentially as an intercalating agent allowing the polymerization of MMA within the clay interlayer spacing. It is believed that the in situ copolymerization behavior between MMA

and the reactive surfactant is greatly affected by the close proximity of each surfactant on the clay surface. Indeed, the close proximity of the reactive groups can induce homopolymerization of the cationic monomers via a pseudo intramolecular polymerization reaction, leading to poor comonomer incorporation in the final nanocomposite polymer matrix. This behavior cannot be controlled and would have a large effect on the final nanocomposite properties.

To avoid this uncertainty of linkage of the clay to the polymeric matrix, an emulsion-based method is proposed in this study. In the emulsion polymerization process, the reactive surfactants are incorporated first into the polymeric matrix and the polar group left available for further cationic exchange reaction on the surface of the sodium clay platelets. In order to maximize the interaction between the particle surface and the clay platelets, one must ensure high dispersion of the filler into the aqueous phase. For instance, sodium Laponite clay readily dissolves in deionized water for the concentrations targeted. The concentration considered in this study allows monodispersity of the clay dispersion in the aqueous phase and maximizes the surface area of the filler.

Scanning electron microscopy (SEM) was used to determine changes in particle morphology upon addition of the filler. We could notice an increase in viscosity upon clay addition, behavior illustrated by the appearance of aggregates as shown in Figure 4.3. The nanocomposites were prepared by drying the corresponding clay/latex mixture in air for 2 days and forming films by a melt-press method. Dynamic scanning calorimetry (DSC) performed on the resulting films revealed an increase in the glass transition temperature (T_g) of the

nanocomposites prepared with the emulsion technique as compared to pure polymer (Figure 4.4). The T_g evolution was verified by DMA through $\tan \delta$ (Figure 4.5) showing similar increases as seen by DSC. These data show that T_g increased by 14 °C, 9 °C, and 6 °C for the nanocomposites incorporating the surfactants **2a**, **2b**, and **4**, respectively.

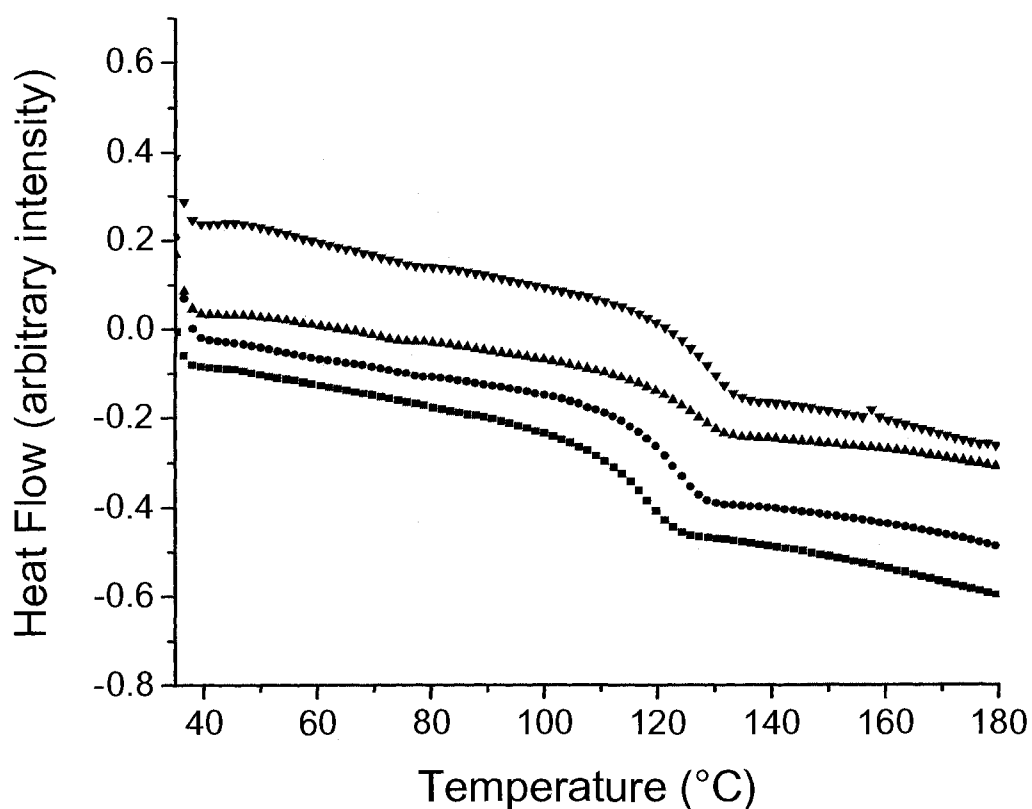


Figure 4.4. DSC curves for melt-pressed films obtained from Latex L1 containing 0 wt-% (■), 2.5 wt-% (●), 5 wt-% (▲) and 10 wt-% (▼) of Laponite respectively.

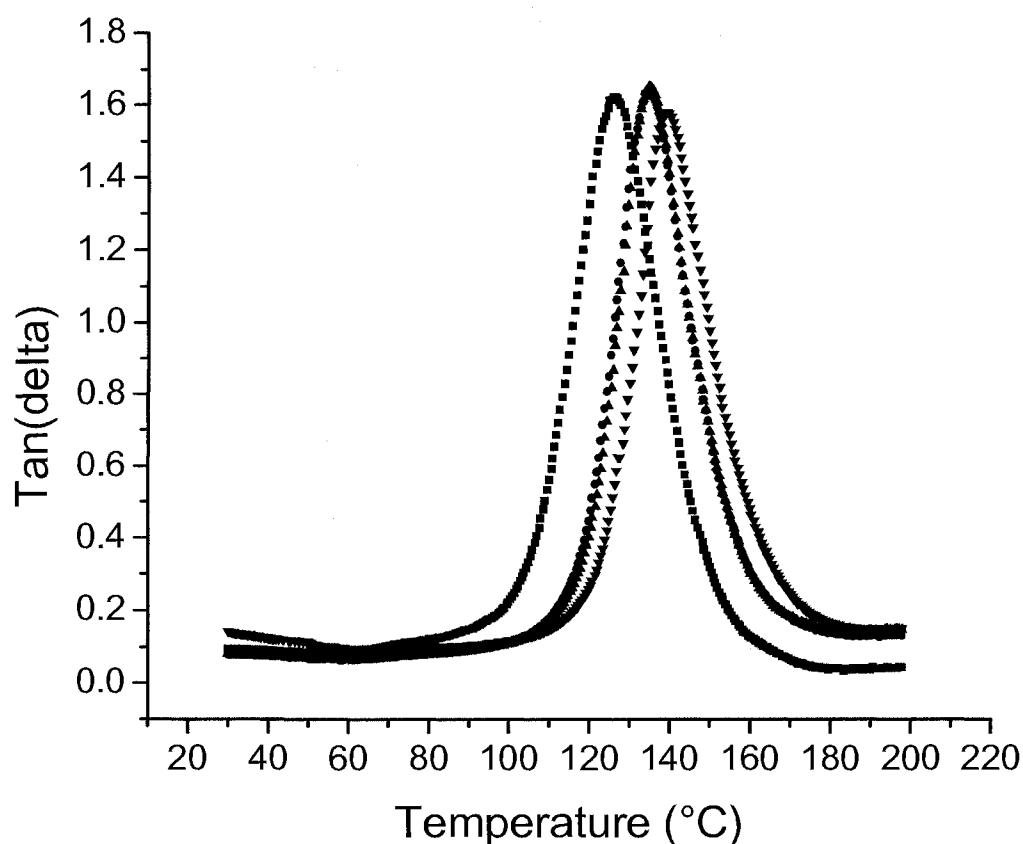


Figure 4.5. Tan(δ) diagram for melt-pressed films obtained from Latex L1 containing 0 wt-% (■), 2.5 wt-% (●), 5 wt-% (▲) and 10 wt-% (▼) of Laponite respectively.

A decrease in T_g for the neat polymers obtained from the latexes was also noted. This is attributed to a plasticizing effect of the surfactant incorporated into the matrix. Thermal degradation was monitored by thermal gravimetry analysis, and the behavior is shown in Figure 4.6 for pure PMMA and the nanocomposites. Hirata, et al., reported that two main reaction stages take place during degradation of PMMA in nitrogen atmosphere. The first stage, which can be divided into two steps, represents decomposition of weak head-to-head linkages

and impurities in the range between 160°C and 240°C, while decomposition of PMMA chain-ends occurs around 290°C. The second stage, between 300 and 400°C, represents random scission of the polymer chains. In Figure 4.8, pure PMMA displays these two reaction stages, while the nanocomposites display only the second stage associated with random scission decomposition.

PMMA/clay nanocomposites also showed an increase in the 10 wt-% decomposition temperature for the nanocomposites prepared here due to the decrease in the rate of evolution of degradation products through the polymeric matrix.

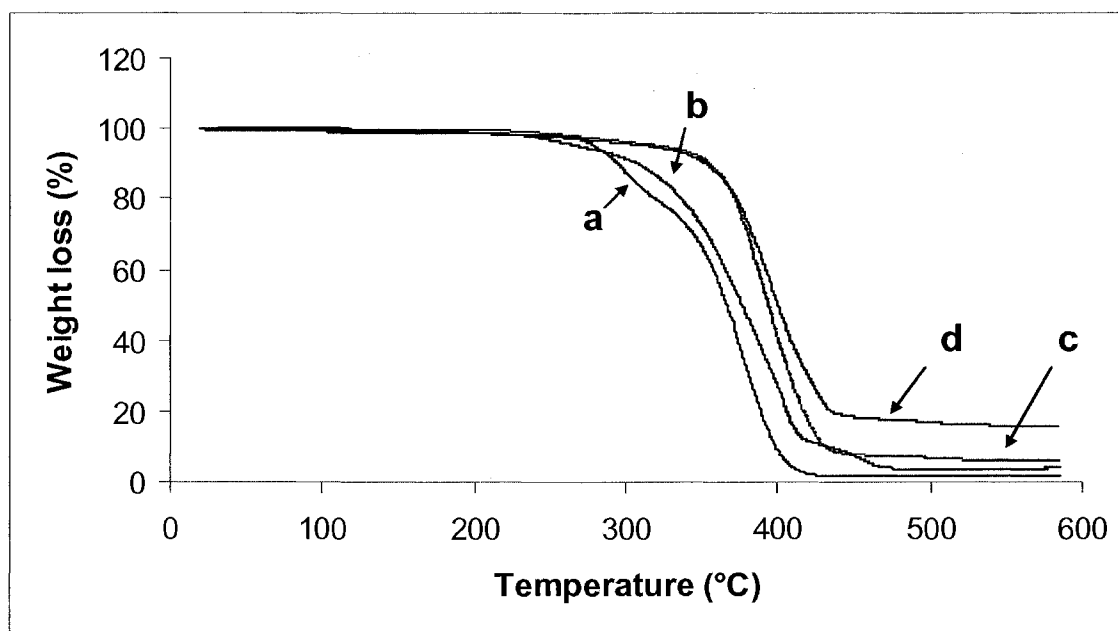


Figure 4.6. TGA diagrams for PMMA/clay nanocomposites incorporating surfmer **2a** (neat (a); 2.5 wt-% (b); 5 wt-% (c); 10 wt-% (d)).

Dynamic mechanical analysis was used to measure the viscoelastic properties of the polymer nanocomposite melt-pressed films as a function of temperature (Table 4.2). The modulus slightly increased with addition of clay as

function of the clay loading, but the high standard deviation does not permit any definitive interpretation. XRD patterns of the films obtained by melt-pressing techniques revealed some degree of intercalation as shown in Figure 4.7.

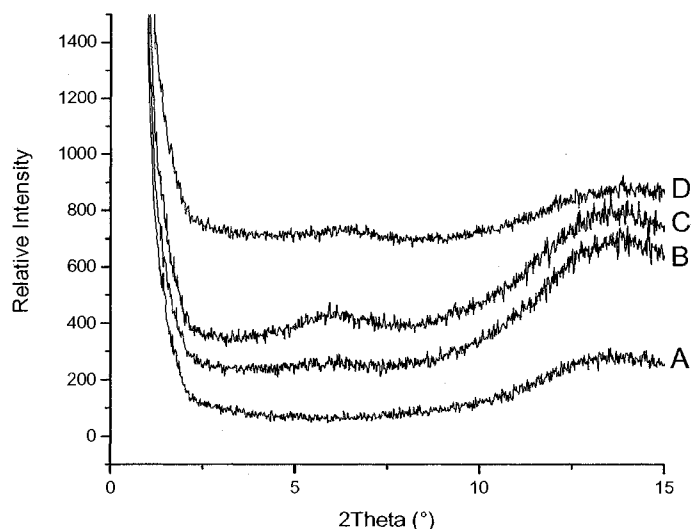


Figure 4.7. XRD patterns for nanocomposite melt-pressed films obtained from Latex L1 (0 wt-% (A), 2.5 wt-% (B), 5 wt-% (C), 10 wt-% (D) of sodium Laponite).

Table 4.2. Storage modulus and glass transition temperature of PMMA/clay nanocomposites obtained by the emulsion method.

Entry	surfactant	clay amount (wt-%)	Tg (°C/std. dev.)	storage modulus (MPa/std. dev.)
0	SDS	0	130/0.5	2573/213
1	2a	0	125/0.5	2020/352
2	-	2.5	134/0.8	2617/301
3	-	5	135/0.7	3266/316
4	-	10	139/0.8	2650/385
5	2b	0	130/0.3	2235/315
6	-	2.5	132/0.5	2454/285
7	-	5	135/0.6	2755/186
8	-	10	139/0.4	2985/254
9	4	0	126/0.3	2132/245
10	-	2.5	132/0.6	2254/243
11	-	5	133/0.7	2654/321
12	-	10	133/0.6	2556/213

Preparation of nanocomposites via *in situ* polymerization. *In situ*

polymerization was carried out in the presence of different clays treated with the reactive surfactant **2a**, **2b**, and **4**. Evidence of the surfmer incorporation was revealed by X-ray, TGA, and FT-IR analysis as shown in Figures 4.8 and 4.9, and Table 4.3.

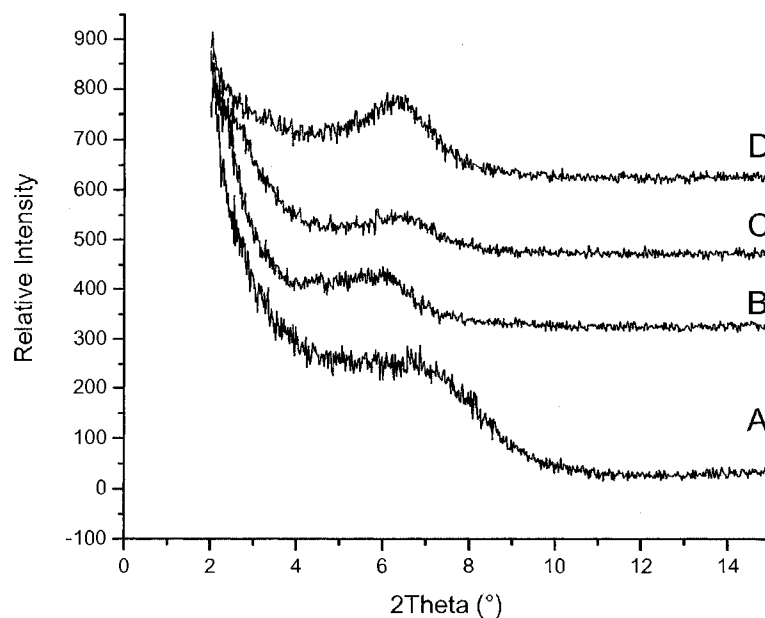


Figure 4.8. XRD patterns for neat Laponite clay (A), OML1 (B), OML2 (C), OML3 (D).

Table 4.3. Treated clays characteristics.

clay	surfactant	MW surfactant (g/mol)	CEC clay (meq/100g)	clay organic content (wt-%) ^(a)	ion exchange (meq/100g)
OML1	2a	459.41	60	15.7	34.2
OML2	2b	585.65	60	20.9	35.7
OML3	4	856.92	60	13.7	15.9

(a) – Determined by thermal gravimetry analysis of the corresponding treated clay.

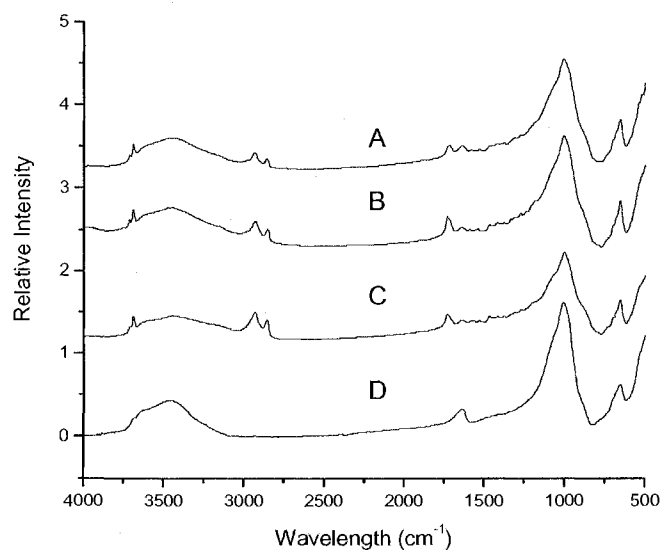


Figure 4.9. FT-IR spectra for OML1 (A), OML2 (B), OML3 (C) and neat Laponite RD (D).

PMMA/clay nanocomposites incorporating 10 wt-% of different organically modified clays (OMLx) were formed and the polymer characteristics are summarized in Table 4.4. Films were formed by a melt-pressing technique. Here also, dynamic mechanical analysis was used to measure the viscoelastic properties of the polymer nanocomposite formed as function of temperature (Table 4.4). No change in T_g and no significant increase of the storage modulus could be noticed as compared to the nanocomposites formed by means of the emulsion technique, using the same amount of clay in each material. XRD patterns revealed high degrees of intercalation for all nanocomposites synthesized by the in situ polymerization technique.

Table 4.4. Storage modulus and glass transition temperature of PMMA/clay nanocomposites obtained by in-situ polymerization.

entry	surfmer	clay amount (wt-%)	Mn (g/mol)	PDI	Tg (°C)	storage modulus (MPa/std. dev.)
0	-	0	41,200	2.53	120	2571/215
1	2a	5	100,644	1.46	125	2440/320
2	2b	5	42,876	2.31	121	2670/254
3	4	5	89,232	1.58	125	2767/276

Effect of film formation method on nanocomposite morphology. We decided to investigate the impact of the film formation technique on the overall nanocomposite mechanical properties. In addition to the films obtained with the melt-pressing method, another series of films was prepared via solvent-casting with toluene as solvent. Dynamic mechanical analysis was then used to measure their viscoelastic properties as a function of temperature. It was found that the PMMA/clay nanocomposites formed via emulsion polymerization showed an increase in their storage modulus below the glass transition temperature as compared to the same nanocomposite for which the film was obtained by melt press method. Above Tg, the rubbery plateau modulus for the nanocomposites produced via emulsion polymerization was higher when the film was obtained via the solvent-casting method as compared to the melt-pressed films as shown in Figure 4.10 and Table 4.4. This is attributed to a better distribution of the clay platelets when this film formation method is used. When the film is formed via a melt-press process, high shear is induced leading to orientation and reaggregation of the clay platelets within the polymeric matrix. The isotropy of the system

conferred by the emulsion technique is lost, affecting greatly mechanical properties below and above T_g .

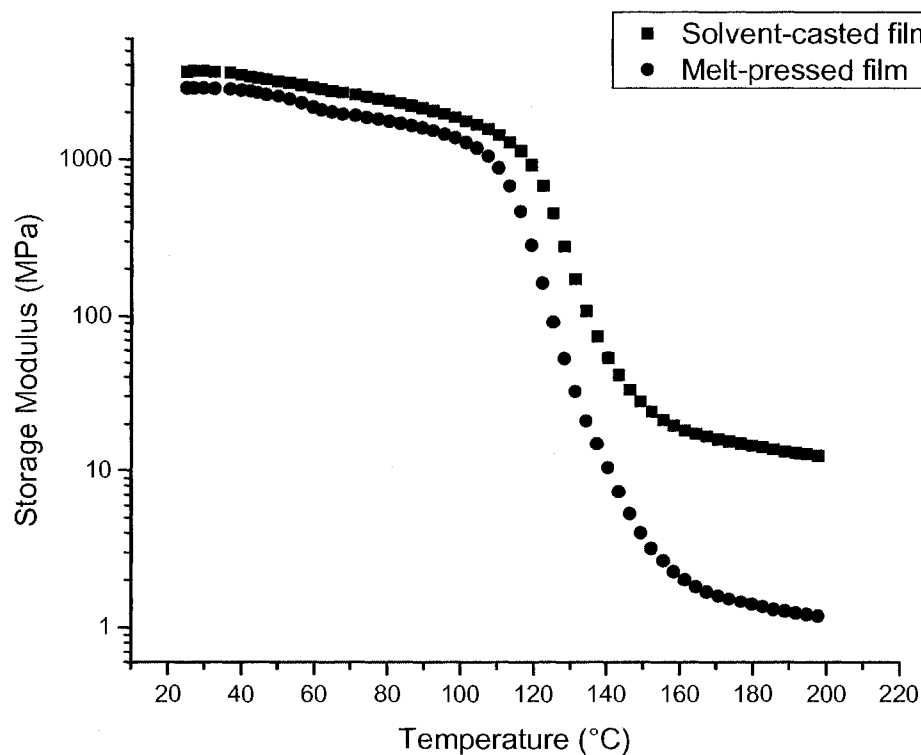


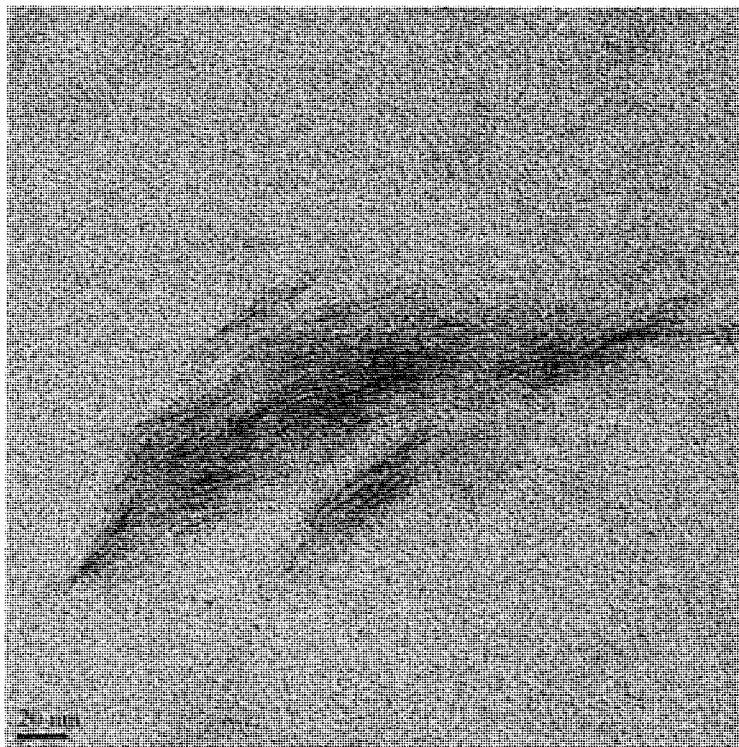
Figure 4.10. Storage modulus of nanocomposite film obtained from Latex L3 as function of the film formation method.

Table 4.4. Impact of the film formation method onto the storage modulus and glass transition temperature for nanocomposites obtained by the emulsion process.

Entry	surfmer	clay amount (wt-%)	T _g melt/solvent (°C)	storage modulus melt/solvent (Mpa)
1	2a	10	136/139	2650/3698
2	2b	10	138/139	2985/3878
3	4	10	133/133	2556/3393

Transmission electron microscopy was used to analyse the dispersion as a function of the method employed to form the nanocomposites and also of the film formation method. Figures 4.11 and 4.12 show TEM images of the nanocomposites obtained via different polymerization processes and film formation methods. These images show that the film formation technique has little effect on the morphology of the nanocomposites obtained by in-situ polymerization. However, this effect is more pronounced for the nanocomposites obtained from the PMMA latex where less aggregation and better filler dispersion was observed.

A
In situ polymerization
Melt press method



B
Emulsion polymerization
Melt press method

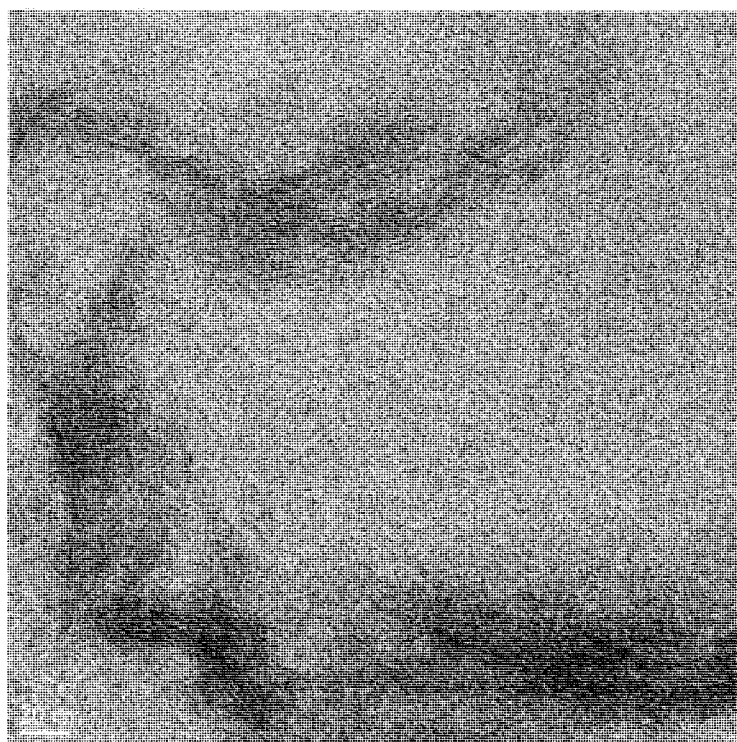
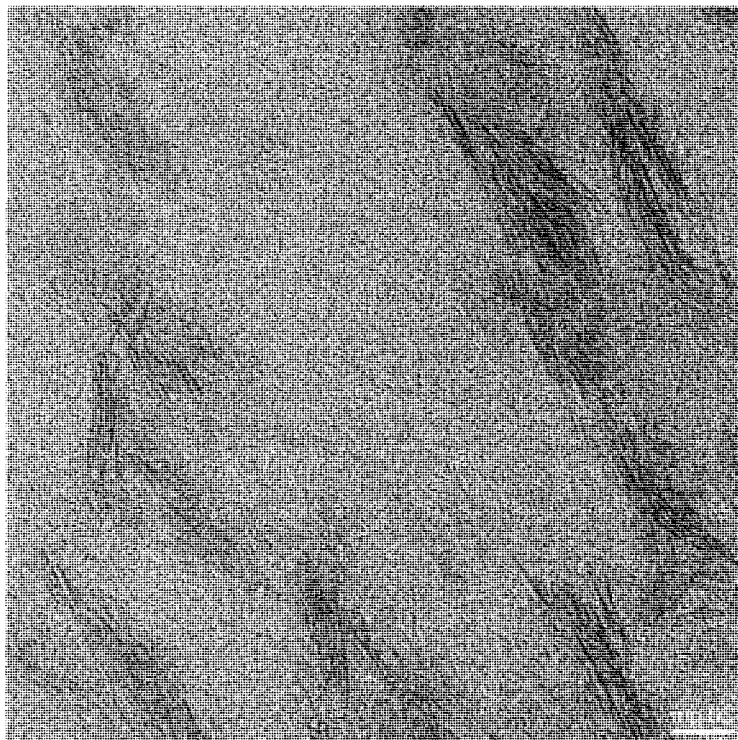


Figure 4.11. TEM micrographs of films incorporating gemini surfmer **4** obtained by melt press method.

C

In situ polymerization
Solvent cast method

**D**

Emulsion polymerization
Solvent cast method

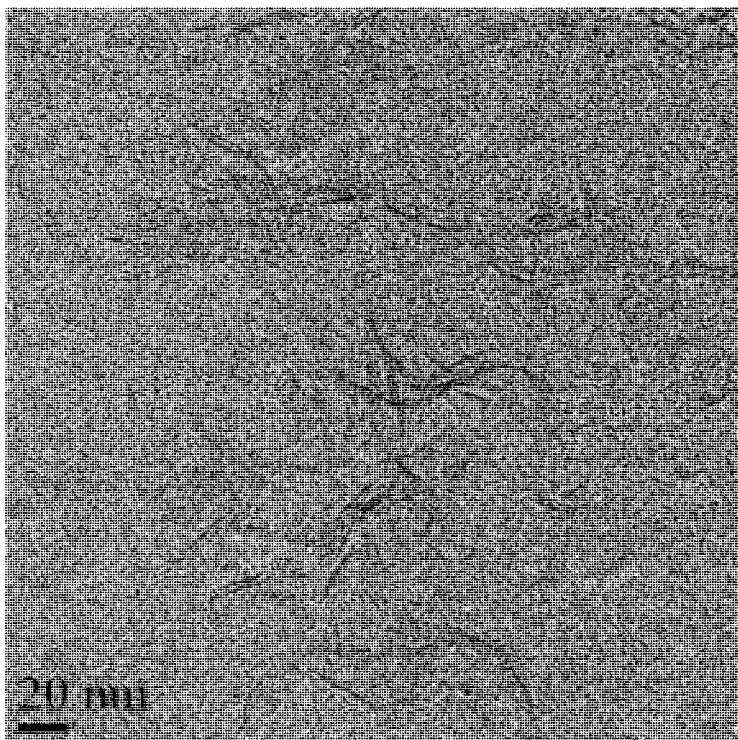


Figure 4.12. TEM micrographs of films incorporating gemini surfmer **4** obtained by solvent cast method.

XRD patterns confirmed the TEM observations as illustrated in Figure 4.13. Indeed, these patterns revealed some degree of intercalation for the film formed via melt-pressing while the other method leads to film for which the XRD pattern does not present any diffraction peak using the same amount of inorganic filler. The lack of XRD peak in the latter case confirms thus a lower degree of intercalation and correlates with a better dispersion of the filler within the matrix.

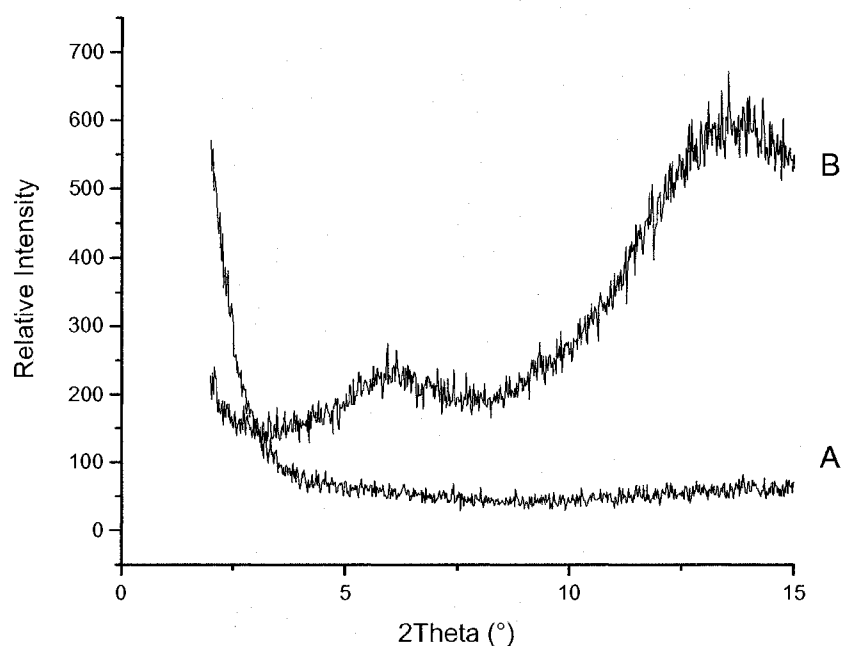


Figure 4.13. XRD patterns of nanocomposite films incorporating 10 wt-% of Laponite clay obtained from latex L3 (solvent-casted (A), melt-pressed (B)).

Conclusions

New RHMA-based reactive cationic surfactants were successfully synthesized. Stable poly(methyl methacrylate) latexes were formed via a batch polymerization method incorporating each of the reactive surfactants. PMMA/clay nanocomposites incorporating 2.5, 5, and 10 wt-% Laponite RD clay were formed

via incorporation of the filler into latexes. An increase in both thermal transitions and storage modulus changes was observed for all systems. The film formation method seems to have a great impact on the inorganic filler dispersion and overall material performance. For instance, we observed a high degree of intercalation when the melt-pressing method was used to form the film. WADX and TEM characterization techniques confirmed agglomeration in the films. We found that the solvent-casting method increases the overall dispersion of the filler in the matrix, leading to an increase of the storage modulus in both glassy and rubbery regions. We believe that strong interactions between the clay platelets and the polymer can be maximized using this latter method. This increase in clay affinity to polymer resulted in an increase in the mechanical performance of the nanocomposites formed.

Experimental

Materials. Laponite RD (CEC; 55mmol/100 g) was purchased from Southern Clay Products, Inc. (Gonzales, TX) and used as received. Ethyl- α -hydroxymethylacrylate was purchased from Shokubai Chemical Company and 2-ethylhexyl acrylate was purchased from Aldrich Chemical Company, both were used without any further purification. 11-Bromoundecanoic acid was purchased from Aldrich and used as received. Thionyl chloride was purchased from Acros Organics and used as received. 1-Methyl-2-decylimidazole and 1,10-decanediol were purchased from Aldrich chemical company and used as received. 2,2'-Azobis(2-methylpropionitrile) (AIBN) was purchased from Aldrich and recrystallized from methanol. Methyl methacrylate (MMA) was purchased also from Aldrich and

redistilled over CaH_2 (also from Aldrich). Acrylic acid (AA, Fluka) was used as supplied. 2,2-Azobis(2-methylpropionamine dihydro-chloride) (V50) was purchased from Wako Chemicals and used as received. Sodium dodecyl sulfate (SDS) was purchased from Aldrich Chemical Company and used as received. Ethanol (95%; AAPER Alcohol, Shelbyville, KY) and tetrahydrofuran (THF, HPLC grade; Fisher Scientific, Pittsburgh, PA) were also used as received. All other solvents were purchased from Aldrich Chemical Company.

Instrumentation and characterization. Solution NMR spectra were collected on a Varian Mercury 300 MHz spectrometer operating at a frequency of 75.47 MHz for carbon. Molecular weights and molecular weight distributions of the polymers were measured by gel permeation chromatography (GPC) using THF as eluent (1 ml/min). Polystyrene standards (molecular weights ranging from 162 to 6,035,000 g/mol) were used for calibration. Particle size and particle size distribution of latexes were measured by dynamic light scattering (Microtrac UPA 150). Thermal gravimetry analysis (TGA) experiments were performed on a TA 2960, controlled by a Thermal Analyst 2100. The temperature was ramped at a heating rate of $10^\circ\text{C}/\text{min}$ under nitrogen atmosphere to a temperature well above the degradation temperature (600°C).

Dynamic scanning calorimetry (DSC) experiments were performed on a TA Instrument 2920, controlled by a Thermal Analyst 2100. All scans were taken at a heat rate of $10^\circ\text{C}/\text{min}$ under nitrogen atmosphere to a maximum of 180°C , than cooled to room temperature and re-scanned at the same heating rate. The T_g values were recorded from the second scan data for the samples. Dynamic

mechanical analysis (DMA) tests were carried out using a DMA Q800 at a heating rate of 2 °C/min from 30 to 200°C at a frequency of 1 Hz. Mid-angle X-ray diffraction (XRD) measurements were performed on a Rigaku Ultima III diffractometer using Cu K α radiation ($\lambda = 1.5405 \text{ \AA}$) in the 2θ range of 2-15°. Specimens for scanning electron microscopy were prepared by depositing dilute latex onto carbon adhesive tabs and then coating with gold (5 nm). Images were obtained with a FEI Quanta 200 scanning electron microscope under high vacuum conditions. Specimens for transmission electron microscopy were prepared by microtoming the samples at an angle of 6° to the diamond knife and at a speed of 1.5–3.5 mm/s on a Reichard-Jung Ultracut E microtome. Ultrathin sections (70 nm thick) were placed on copper TEM grids. The sections were viewed using a Zeiss EM 109-T electron microscope (Carl Zeiss, Jena, Germany) operating at 200 kV.

Synthesis of ethyl α -(11-bromoundecanoate) methylacrylate 1. Ethyl α -chloromethacrylate (ECMA) was synthesized from EHMA following literature procedure.²¹ In a typical procedure, 11-bromoundecanoic acid (38.2 g, 144 mmol) along with 150 ppm of hydroquinone were first dissolved in 100 ml of dried THF in a 250 ml round bottom flask. Triethylamine (14.6 g, 144 mmol) was then added in one portion. The corresponding α -chloromethylacrylate (144 mmol) was finally added dropwise and the resulting mixture was allowed to stir at room temperature for 24 hours. The salt was filtered off and the solvent removed under reduced pressure. The crude product was washed with three aliquots of brine

solution to give ethyl α -(11-bromoundecanoate) methylacrylate **1** as brown oil in c.a. 92% yield (isolated).

^1H NMR (CDCl_3) δ 2.30 (t, 2H, $\text{CH}_2\text{-CO}$), 3.35 (t, 2H, $\text{CH}_2\text{-Br}$), 4.21 (q, 2H, $\text{CH}_2\text{-CH}_3$), 4.77 (s, 2H, $\text{CH}_2\text{-O}$), 5.78 and 6.31 (s, 1H, $\text{CH}_2=\text{C}$); ^{13}C NMR (CDCl_3) δ 14.13 (CH_3CH_2), 33.98 ($\text{CH}_2\text{-Br}$), 34.15 ($\text{CH}_2\text{-C=O}$), 60.92 ($\text{CH}_2\text{-CH}_3$), 62.21 ($\text{CH}_2\text{-O}$), 126.99 ($\text{CH}_2=\text{C}$), 135.55 ($\text{C}=\text{CH}_2$), 165.15 and 173.13 ($\text{C}=\text{O}$).

Surfmers 2a and 2b. In a 250 ml round bottom flask equipped with a condenser, the intermediate **1** (10 g, 27.2 mmol) was added to 100 ml of THF. The corresponding imidazole derivative (30 mmol) was added in one portion to the stirring mixture. The solution was allowed to stir at 60 °C for 3 hours. Upon reaction completion, the precipitate was filtered off, washed with diethyl ether and dried under reduced pressure to give the corresponding surfmers **2a** and **2b**, which show the following data:

Surfmer 2a: c.a. 95% isolated yield; ^1H NMR (CDCl_3) δ 2.22 (t, 2H, $\text{CH}_2\text{-CO}$), 2.77 (s, 3H, N- CH_3), 3.91 (s, 3H, $\text{CH}_3\text{-C}$), 3.98 (t, 2H, $\text{CH}_2\text{-N}$), 4.13 (q, 2H, $\text{CH}_2\text{-O}$), 6.34 and 6.48 (s, 2H, $\text{CH}_2=\text{C}$), 7.44 and 7.60 (s, 2H, $\text{CH}=\text{CH}$); ^{13}C NMR (CDCl_3) δ 10.89 ($\text{CH}_3\text{-C}$), 14.06 ($\text{CH}_3\text{-CH}_2$), 34.32 ($\text{CH}_2\text{-CO}$), 36.08 ($\text{CH}_3\text{-N}$), 49.19 ($\text{CH}_2\text{-N}$), 61.65 (CH_2CH_3), 64.35 ($\text{CH}_2\text{-O}$), 121.48 and 132.80 ($\text{CH}=\text{CH}$), 122.86 ($\text{CH}_2=\text{C}$), 133.05 ($\text{C}=\text{CH}_2$), 164.82 and 173.98 ($\text{C}=\text{O}$).

Surfmer 2b: c.a. 92% isolated yield; ^1H NMR (CDCl_3) δ 2.23 (t, 2H, $\text{CH}_2\text{-CO}$), 3.79 (s, 3H, $\text{CH}_3\text{-C}$), 3.98 and 4.07 (t, 2H, $\text{CH}_2\text{-N}$), 4.13 (q, 2H, $\text{CH}_2\text{-O}$), 6.34 and 6.48 (s, 2H, $\text{CH}_2=\text{C}$), 7.44 and 7.60 (s, 2H, $\text{CH}=\text{CH}$); ^{13}C NMR (CDCl_3) δ 10.87 ($\text{CH}_3\text{-C}$), 14.02 ($\text{CH}_3\text{-CH}_2$), 34.32 ($\text{CH}_2\text{-CO}$), 48.94 and 49.14 ($\text{CH}_2\text{-N}$),

61.54 (CH₂CH₃), 64.29 (CH₂-O), 121.41 and 132.89 (CH=CH), 121.97 (CH₂=C), 133.33 (C=CH₂), 164.80 and 173.93 (C=O).

1,10-Bis(2-methylimidazol)decane 3. In a 250 ml one neck round bottom flask equipped with a condenser, 1,10-dibromodecane (10 g, 33.3 mmol), 2-methylimidazole (2.79 g, 33.9 mmol) and triethylamine (3.44 g, 33.9 mmol) were added to 60 ml of dried THF. The reaction batch temperature was gradually increased to 65 °C and the mixture allowed to stir for 24 hours. Upon completion of the reaction, as monitored by ¹H NMR, the triethyl ammonium salt was filtered off and the crude mixture concentrated under reduced pressure. The resulting product was diluted in 30 ml of dichloromethane and washed with 3 aliquots of brine solution to remove the remaining 2-methylimidazole. The organic phase was then concentrated under reduced pressure to afford **3** in c.a. 92% yield.

¹H NMR (CDCl₃) δ 2.23 (t, 2H, CH₂-CO), 3.79 (s, 3H, CH₃-C), 3.98 and 4.07 (t, 2H, CH₂-N), 4.13 (q, 2H, CH₂-O), 6.34 and 6.48 (s, 2H, CH₂=C), 7.44 and 7.60 (s, 2H, CH=CH); ¹³C NMR (CDCl₃) δ 10.87 (CH₃-C), 14.02 (CH₃-CH₂), 34.32 (CH₂-CO), 48.94 and 49.14 (CH₂-N), 61.54 (CH₂CH₃), 64.29 (CH₂-O), 121.41 and 132.89 (CH=CH), 121.97 (CH₂=C), 133.33 (C=CH₂), 164.80 and 173.93 (C=O).

Gemini surfmer 4. In a 250 ml one neck round bottom flask equipped with a condenser, **3** (5 g, 16.5 mmol) and **1** (6.41 g, 17 mmol) were added to 50 ml of acetonitrile. The reaction batch temperature was gradually increased to 70 °C and the mixture allowed to stir for 24 hours. Upon completion of the reaction, as monitored by ¹H NMR, the salt was filtered off and washed with three aliquots of

cold diethyl ether. Subsequent reprecipitations in diethyl ether gave gemini surfactant **4** in c.a. 86% yield.

^1H NMR (CDCl_3) δ 2.23 (t, 2H, CH_2CO), 3.79 (s, 3H, CH_3C), 3.98 and 4.07 (t, 2H, CH_2N), 4.13 (q, 2H, CH_2O), 6.34 and 6.48 (s, 2H, $\text{CH}_2=\text{C}$), 7.44 and 7.60 (s, 2H, $\text{CH}=\text{CH}$); ^{13}C NMR (CDCl_3) δ 10.87 (CH_3C), 14.02 (CH_3CH_2), 34.32 (CH_2CO), 48.94 and 49.14 (CH_2N), 61.54 (CH_2CH_3), 64.29 (CH_2O), 121.41 and 132.89 ($\text{CH}=\text{CH}$), 121.97 ($\text{CH}_2=\text{C}$), 133.33 ($\text{C}=\text{CH}_2$), 164.80 and 173.93 ($\text{C}=\text{O}$).

Clay Treatment. Three different organically modified clays were prepared by incorporation of each of the cationic surfmers described above. Organically Modified Laponite (OML) was obtained by ion exchange using Laponite and the cationic surfactant according to the procedure described below. Clay (10 g), water (1 L), and 1.5 equivalents of surfactant were stirred at 70 °C overnight on a magnetic stir plate. The mixture was then hot-filtered using a Buchner filter with Whatman #2 filter paper. The slurry was then washed with two liters of hot water (70 °C) followed by drying under vacuum for two hours. The dry clay was then ground into a powder using a mortar and pestle. The clay was next Soxhlet extracted with ethanol overnight under a nitrogen blanket; this extraction was repeated using tetrahydrofuran (THF). The final product (organically modified clay) was vacuum dried and ground using a mortar and pestle.

Polymerizations and nanocomposite preparation. *Batch emulsion*

polymerization. All emulsion polymerizations were carried out in a 250 ml three neck round bottom flask using the same concentration of water (80 g), MMA (20 g) and initiator (0.24 g). MMA and water were bubbled with nitrogen for 30

minutes before use. Surfactant concentration was varied from 12 to 72 mmol. Experiments were carried out at 65 °C under nitrogen atmosphere using mechanical stirring (300 rpm) for 24 hours to ensure high monomer conversion. In all experiments, materials were introduced into the reactor in the following sequence: water, surfactant, monomer, and initiator. Two polymerizations were carried out for each concentration of surfactant in order to check the reproducibility of the reaction. Upon reaction completion, Laponite clay (2.5, 5 or 10 wt-%) was dispersed in deionized water and introduced dropwise into a given amount of latex; the resulting mixture was allowed to stir for one day. The mixed clay-latex dispersions were then dried under reduced pressure at room temperature for 24 hours.

In situ polymerization. The corresponding organophilic clay (0.1 g, 5 wt-%) was dispersed in MMA (2 g), mixed overnight, and sonicated for 30 minutes before polymerization. Approximately 0.1 wt-% of initiator (AIBN) was added to the sample. A freeze thaw technique degassed the mixture prior to polymerization. The flask was then purged with argon and placed in an oil bath at 65 °C for 24 hours to ensure high monomer conversion. The resulting polymer was isolated by successive reprecipitations in methanol from THF and dried under reduced pressure.

Film preparation. *Melt-pressing method.* Films were formed using a Carver press (Carver Inc., Indiana) at 160 °C, leading to film for which the thickness was approximately 150 μm .

Solvent cast method. Films were formed by dissolving a given amount of polymer/clay nanocomposite in toluene. The resulting polymer solution was then poured into an aluminum cup and allowed to dry in air for five days to give films for which the thickness was approximately 100 μm . All the films were then characterized without any further treatment.

REFERENCES

- 1 Bharadwaj, R.K.; Mehrabi, A.R.; Hamilton, C.; Trujillo, C.; Murga, M.; Fan, R.; Chavira, A.; Thompson, A.K. *Polymer* **2002**, *43*, 3699.
- 2 Tong, X.; Zhao, H.; Tang, T.; Feng, Z.; Huang, B. *J. Polym. Sci. Part A: Polym. Chem.* **2002**, *40*, 1706.
- 3 Lim, S.K.; Kim, J.W.; Chin, I.; Kwon, Y.K.; Choi, H.J. *Chem. Mater.* **1989** *2002*, *14*.
- 4 Jun, J.; Suh, K. *J. Appl. Polym. Sci.* **2003**, *90*, 458.
- 5 Zerda, A.S.; Caskey, T.C.; Lesser, A.J. *Macromolecules* **2003**, *36*, 1603.
- 6 Decker, C.; Zahouily, K.; Keller, L.; Benfarhi, S.; Bendaikha, T.; Baron, J. *J. Mater. Sci.* **2002**, *37*, 4831.
- 7 Muh, E.; Marquardt, J.; Klee, J.E.; Frey, H.; Mulhaupt, R. *Macromolecules* **2001**, *34*, 5778.
- 8 Moszner, N.; Volkel, T.; von Clausbruch, S.C.; Geiter, E.; Batliner, N.; Rheinberger, V. *Macromol. Mater. Eng.* **2002**, *287*, 339.
- 9 Schoonbrood, H.A.S.; Asua, J.M. *Macromolecules* **1997**, *30*, 6034.
- 10 Schoonbrood, H.A.S.; Unzue, M.J.; Beck, O.J.; Asua, J.M.; Montoya Goni, A.; Sherrington, D.C. *Macromolecules* **1997**, *30*, 6024.
- 11 Goux, A.; Guyot, A. *J. Appl. Polym. Sci.* **1997**, *65*, 2289.
- 12 Green, B.W.; Sheetz, D.P. *J. Colloid Interface Sci.* **1970**, *32*, 96.
- 13 Green, B.W.; Saunders, F.L. *J. Colloid Interface Sci.* **1970**, *33*, 393.
- 14 Tsaur, S.L.; Fitch, R.B. *J. Colloid Interface Sci.* **1987**, *115*, 450.
- 15 Chen, S.A.; Chang, H.S. *J. Polym. Sci., Part A: Polym. Chem.* **1985**, *23*, 2615.

- 16 Sherrington, D.C.; Joynes, D. *Polymer* **1997**, *38*, 1427.
- 17 Velde, B. *Introduction to Clay Minerals: Chemistry, Origins, Uses, and Environmental Significance*, Chapman & Hall: London, **1992**.
- 18 Product information available at <http://www.laponite.com/>
- 19 Edwards, G.; Halley, P.; Martin, D.; Le, T. *The Production of Novel Organo-Clay for Use in the Production of Nanocomposite Materials*, A University of Queensland Chemical Engineering undergraduate thesis available online at <http://www.cheque.uq.edu.au/ugrad/theses> (last updated on 06/15/**2007**).
- 20 Awad, W.H.; Gilman, J.W.; Nyden, M.; Harris, R.H.; Sutto, T.E.; Callahan, J.; Trulove, P.C.; DeLong, H.C.; Fox, D.M. *Thermochimica Acta* **2004**, *409*, 3-11.
- 21 Mathias, L.J.; Warren, M.R.; Huang, S. *Macromolecules* **1991**, *24*, 2036-2042.

CHAPTER V
SYNTHESIS AND POLYMERIZATION OF
ETHYL 2-CARBOETHOXYHYDROXYMETHYLACRYLATE

Abstract

The synthesis and polymerization study of ethyl 2-carboethoxyhydroxy methylacrylate is described. These RHMA-based monomers display interesting polymerization properties compared to other RHMA analogs previously investigated.

Introduction

Monoesters and diesters derived from itaconic acid have attracted a lot of attention not only because itaconic acid is obtained by a fermentation process, but also due to the great variety of polymers that can be prepared possessing two lateral ester and/or acid groups.^{1, 2, 3} Homopolymerization and copolymerization of dialkyl itaconate esters (DRIs) with other monomers, like styrene or methyl methacrylate, have been extensively studied. It was reported that DRI are radically polymerized at moderate rates to yield high molecular weight polymer in spite of bulky substituents.^{4, 5}

Aside from DRIs, the majority of acrylate and methacrylate monomers and crosslinkers are built on simple syntheses and contain a single pendent group. We have extensively investigated hydroxymethylacrylate esters (RHMA) shown in Figure 5.1, as multifunctional monomers which have very high radical polymerizability.^{6, 7} RHMA monomers allow the manipulation of at least two different functional groups. Both the hydroxyl group and the carboxylic acid ester

group permit a variety of derivatization reactions in order to modify or substitute the basic structure. Most important, RHMA monomers can be readily synthesized via the Baylis-Hillman reaction involving commercial acrylates reacting with aldehydes (e.g., paraformaldehyde) via the α -carbon in the presence of a base catalyst such as DABCO to give allylic alcohols. It has been demonstrated that the use of formaldehyde results in monomers such as methyl α -hydroxymethylacrylate (MHMA) and higher alkyl ester analogs that polymerize radically as fast as, or faster than, typical methacrylate and itaconate derivatives⁸ and give an order of magnitude higher molecular weight.⁹

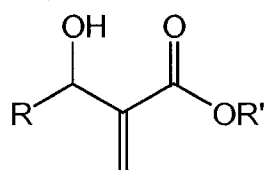


Figure 5.1. RHMA monomer.

The combined polar, resonance and steric effects of the substituents play an important role in the reactivity of RHMA monomers. For instance, RHMA monomers having α -alkyl substituents greater than hydrogen (e.g., from reaction of acrylates with acetaldehyde or other aldehydes) show poor or no polymerizability under free radical conditions due to steric effects.^{10, 11} Both homopolymerization and copolymerization of such monomers with either methyl methacrylate or styrene were found to be sluggish, giving very low yield polymer and insignificant incorporation of the corresponding comonomer into the final product. In contrast, substitution at the RHMA oxygen atom β to the double bond with electron withdrawing groups (e.g., converting the alcohol to an ester)

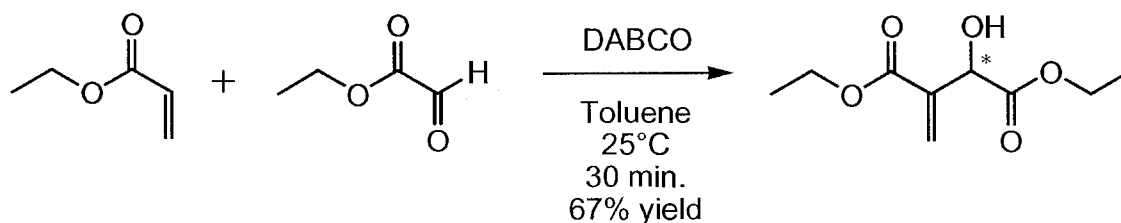
increases the reactivity of the monomer.¹² A wide range of ether and esters derivatives have been synthesized and successfully polymerized showing higher reactivity than itaconate derivatives.^{13, 14} Thus, RHMA monomers show excellent polymerizability, allow formation of a variety of multifunctional derivatives, and give high molecular weight polymers, due to a combination of hydrogen bonding and/or electronic effects that increase propagation while decreasing chain transfer.¹⁵

We were interested in the synthesis of a new RHMA derivative, ethyl 2-carboethoxyhydroxymethylacrylate, and of its diacid analog, 3-hydroxyitaconanic acid, to evaluate the combined features of RHMA monomers and itaconate diesters derivatives. This report describes the initial evaluation of their synthesis and radical polymerizability.

Results and Discussion

Monomer synthesis. Ethyl 2-carboethoxyhydroxymethylacrylate (ECHMA) was synthesized via the Baylis-Hillmann which has been extensively used in the production of monomers like RHMAs. This reaction involves conjugated compounds such as acrylic acid esters that add to aldehydes via the α -carbon in the presence of a catalyst to give allylic alcohols.^{16, 17} This type of reaction has great synthetic utility as it converts simple starting materials into densely functionalized products, although it sometimes suffers from low reaction rates and low yields. The rate and conversion of the Baylis-Hillman reaction can be significantly improved by the use of nucleophilic non-hindered bases such as 1,4-diaza[2.2.2]bicyclooctane (DABCO) rather than simple tertiary amines. Here we

report a very rapid reaction to give ethyl 2-carboethoxyhydroxymethylacrylate in quantitative yield. Ethyl glyoxylate was reacted with ethyl acrylate in the presence of DABCO in toluene (Scheme 5.1). The reaction was slightly exothermic. The disappearance of the ^{13}C NMR resonance peaks for the acrylate and the appearance of a new peak corresponding to the new carbon substituent allowed monitoring the course of the reaction. It should be noted that the formation of a small amount of a side-product occurred during the reaction. This compound has not been isolated and is still under investigation. High vacuum distillations permitted purification of the main product as a clear liquid.



Scheme 5.1. Synthesis of ECHMA.

Figure 5.2 shows the ^{13}C NMR spectrum for the isolated monomer. The appearance of the two peaks at 128.9 and 138.2 ppm correspond to the new double bond carbons, while the appearance of the unique new peak at 71.3 ppm (hydroxymethylene carbon) confirms formation of the expected product.

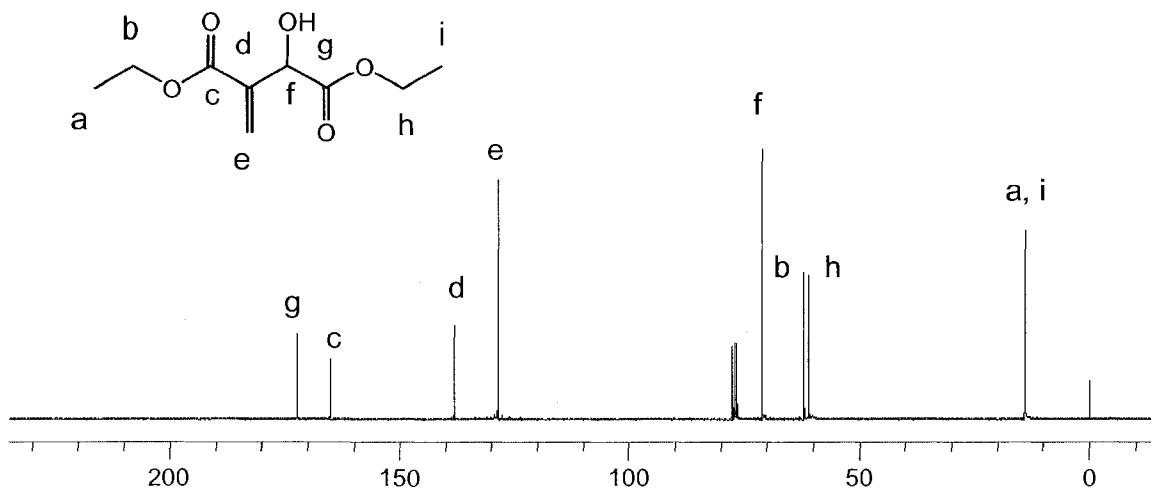
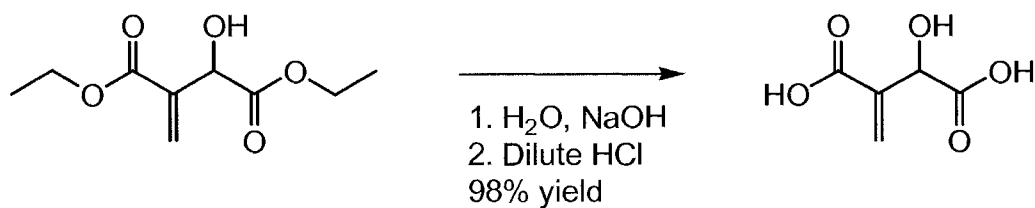


Figure 5.2. ^{13}C NMR spectrum of ECHMA (CDCl_3).

The corresponding diacid was synthesized by hydrolysis of the ethyl ester groups under basic conditions. Using a 1:1 molar ratio of sodium hydroxide in water relative to the monomer ester groups, the reaction was highly exothermic and the formation of the disodium salt was completed in just a few minutes as monitored by ^1H NMR (D_2O). Treatment of the product salt with dilute hydrochloric acid (Scheme 5.2) gave the diacid compound for which the ^{13}C NMR spectrum is shown in Figure 5.3. Disappearance of the peaks corresponding to the ethyl groups and the shift downfield of the carbonyl peaks confirmed hydrolysis.



Scheme 5.2. Synthesis scheme for 2-hydroxy-3-methylenesuccinic acid.

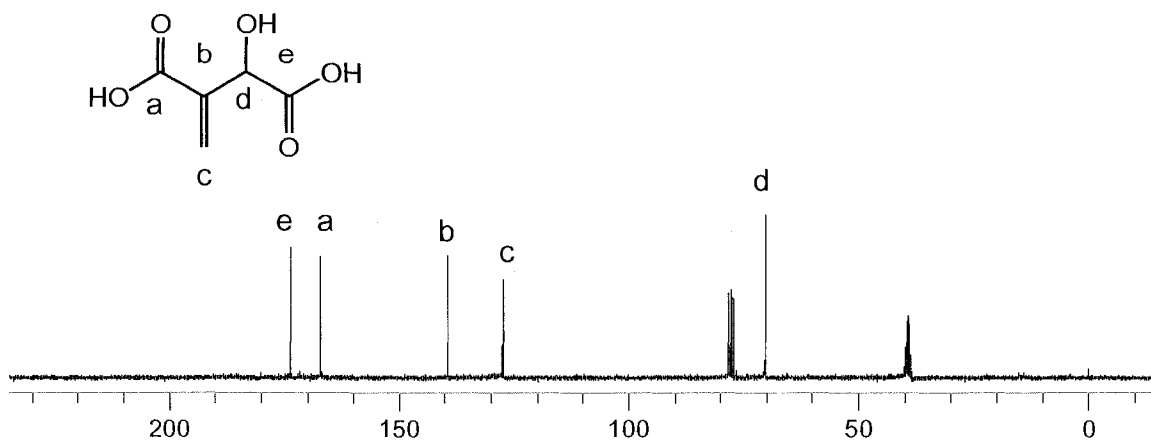


Figure 5.3. ^{13}C NMR spectrum of 2-hydroxy-3-methylenesuccinic acid (CDCl_3 -DMSO- d_6).

Polymerization study. Homopolymerizations of ethyl 2-carboethoxyhydroxymethylacrylate and the diacid were attempted as was copolymerization with methyl methacrylate in order to qualitatively determine the polymerizability of these new compounds. Figure 5.4 shows the ^1H NMR spectrum of the copolymer of ethyl 2-carboethoxyhydroxymethylacrylate with MMA. Incorporation of the comonomer is confirmed by the presence of broad peaks at 1.23 and 4.18 ppm corresponding to the ethyl ester protons of the itaconate. Tables 5.1 and 5.2 show the results for the homopolymerization of both compounds. While homopolymerization was confirmed with GPC and NMR for the diester, no polymer formation was observed for the diacid. Changes in the initiator concentration did not promote polymerization nor did modification of the reaction conditions. The diester homopolymer shows a low degree of polymerization and a low conversion, characteristics that could be attributed to some degree of chain transfer occurring during the polymerization. Indeed, the allylic proton is activated by the presence of the ester group next to it, leading to a resonance stabilized

allylic radical after hydrogen abstraction. It is not clear why the diacid species would be more susceptible to chain transfer than the diester, if indeed this is the reason for no polymer formation for the diacid. Finally, solubility of the monomer in specific solvents might also affect the degree of polymerization (propagation versus chain transfer).

Table 5.1. Apparent molecular weights of ECHMA homopolymers.

entry	initiator (wt-%)	solvent	temp. (°C)	Mn (g/mol)	Mw (g/mol)	PDI	conversion (%) ^a
1	1	-	65	4673	7096	1.51	39.9
2	1	methanol	65	4965	9074	1.82	55.1
3	1	THF	65	5308	7750	1.46	54.1
4	1	toluene	65	4430	6865	1.54	67.0
5	1	DMSO	65	878	2624	2.98	31.2

a: Determined via ¹H NMR analysis.

Table 5.2. Apparent molecular weights of ECHMA-MMA copolymers.

entry	ECHMA (mol-%)	initiator (mol-%)	solvent	temp. (°C)	Mn (g/mol)	PDI	yield (%)	ECHMA incorporation (%) ^a
0	-	1	toluene	65	20500	1.22	95	-
1	20	1	-	65	11853	2.42	34	12
2	20	1	methanol	65	11056	2.40	52	13
3	20	1	THF	65	7695	2.44	55	11
4	20	1	toluene	65	6556	2.71	56	14
5	20	1	DMSO	65	15319	2.43	51	6
6	20	(BP) ^b 1	toluene	100	5280	1.95	41	-
7	20	(BP) 2	toluene	100	4695	1.84	37	-

a: Determined via ¹H NMR analysis.

b: Benzoyl peroxide

Copolymerization of both the diester and the diacid with methyl methacrylate were attempted under various conditions. With 3-hydroxyitaconic acid, no incorporation was observed in the final copolymer with MMA in comparison with the diester corresponding that showed significant degree of incorporation (Table 5.2). The incorporation amounts were determined by NMR

spectroscopy (Figure 5.4); the appearance of peaks belonging to the diester and disappearance of the peaks in the double region confirmed incorporation of the comonomer in the final copolymer.

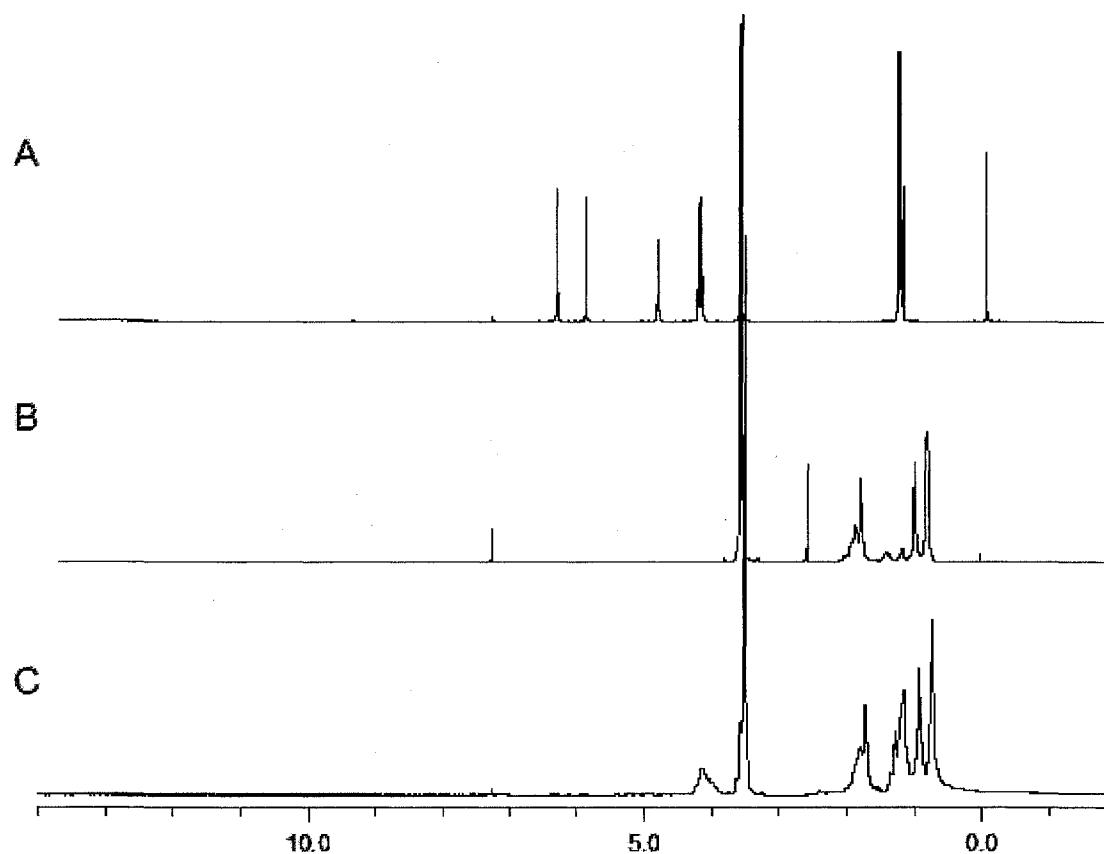


Figure 5.4. ¹H NMR spectra of ECHMA (A), PMMA (B) and the corresponding copolymer **2** (C) (CDCl₃).

Solvent seemed to have a strong effect on monomer conversion and on the apparent molecular weight. Indeed, the highest molecular weight was reported for the copolymer produced in DMSO although incorporation was low in comparison with the copolymer synthesized in toluene that gave lower molecular weight but higher comonomer incorporation. The use of benzoyl peroxide as initiator did not seem to have any effect on the apparent molecular weight or on

the overall isolated yield (Table 5.2). The concentration of comonomer in the feed also had an effect on the final copolymer composition and molecular weight. It was found that, as the concentration of comonomer increases, the final copolymer molecular weight decreases significantly (Table 5.3 and Figure 5.5). This behavior probably involves competitive chain transfer occurring during polymerization.

Table 5.3. Effect of ECHMA comonomer concentration on molecular weight of copolymer.

entry	comonomer (mol-%)	initiator (mol-%)	solvent	temp. (°C)	Mn (g/mol)	PDI	yield (%)
0	0	1	DMSO	65	20500	1.8	91
1	5	1	DMSO	65	14959	3.1	69
2	10	1	DMSO	65	14338	2.9	68
3	20	1	DMSO	65	12113	2.6	47
4	30	1	DMSO	65	10441	2.6	37
5	40	1	DMSO	65	9619	2.3	20

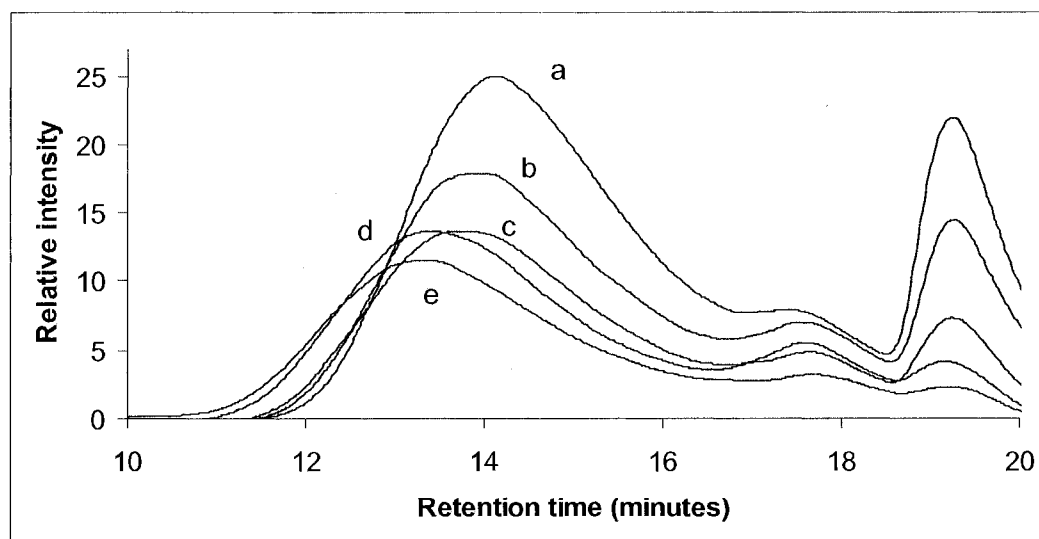


Figure 5.5. GPC trace of the copolymers prepared in DMSO as function of comonomer feed (a: 40%, b: 30%, c: 20%, d: 10%, e: 5%).

Conclusions

Ethyl 2-carboethoxyhydroxymethylacrylate and diacid derivative were synthesized successfully via the Baylis-Hillmann pathway. ECHMA as homopolymerized and copolymerized with MMA but attempts to polymerize the diacid failed. The apparent molecular weights of the former suggest some degree of chain transfer involving this new monomer. To date, this monomer corresponds to the first RHMA derivative with a second allylic substituent different than a proton that yields significant polymer. Kinetic studies and further study of the polymerizability of the present monomer are needed to more completely understand this behavior.

Experimental

Materials. Ethyl glyoxylate, 50% in toluene, was purchased from Alfa Aesar and used as received. 4-Diaza[2.2.2]bicyclooctane (DABCO) and ethyl acrylate were purchased from Aldrich Chemical Company and used as received. Methyl methacrylate (MMA) was purchased from Aldrich and was redistilled with CaH_2 (also from Aldrich). All solvents were purchased from Acros Chemical Company, Fisher, or Aldrich Chemical Company. AIBN was purchased from Aldrich and recrystallized from methanol before use. Benzoyl peroxide was purchased from Aldrich and used as received.

Analyses. Solution ^1H and ^{13}C NMR spectra were collected on a Varian Mercury 300 MHz spectrometer operating at a frequency of 75.47 MHz for carbon. Molecular weights and molecular weight distributions of the polymers were measured with gel permeation chromatography (GPC) on a system equipped

with PLgel Individual Pore Size columns from Polymer Laboratories Ltd. using THF as eluent (1 ml/min). Polystyrene standards (molecular weights ranging from 162 to 6,035,000 g/mol) were used for calibration.

Synthesis of ethyl 2-carboethoxyhydroxymethylacrylate (ECHMA). This monomer was synthesized according to literature procedure.¹⁸ Ethyl glyoxylate, 50% in toluene (20.39 g, 199.7 mmol), DABCO (3.64 g, 32.4 mmol) and ethyl acrylate (20 g, 199.7 mmol) were added to a 250 ml round bottom flask. The mixture was stirred at room temperature for 24 hours. The crude solution was then concentrated under reduced pressure. The resulting mixture was washed with three aliquots of brine solution followed by three aliquots of deionized water. The organic phase was dried over a bed of sodium sulfate. Two successive vacuum distillations of the residue gave ECHMA as a clear liquid in 67% yield (27.1 g).

FT-IR (cm^{-1}) 3492 (O-H), 1739 to 1729 (C=O, multiple peaks), 1639 (C=C).

^1H NMR (CDCl_3) δ 1.23 (t, 3H, -CH₃), 1.26 (t, 3H, -CH₃), 4.18 (t, 2H, -CH₂CH₃), 4.22 (t, 2H, -CH₂CH₃), 4.81 (s, H, -CHOH), 5.89 and 6.33 (s, 2H, CH₂=C); ^{13}C NMR (CDCl_3) δ 14.0 (-CH₃), 61.13 (-CH₂CH₃), 62.19 (-CH₂CH₃), 71.26 (-CHOH), 128.85 (CH₂=C), 138.13 (C=CH₂), 165.13 and 172.34 (C=O).

Synthesis of 3-hydroxyitaconic acid. First, sodium hydroxide (1.98 g, 49.5 mmol) was dissolved in 20 ml of deionized water in a 250 ml Erlenmeyer. ECHMA (10 g, 49.5 mmol) was then added dropwise to this stirring aqueous solution. The reaction was exothermic and release of ethanol was observed, refluxing up on the wall of the flask. The resulting mixture was allowed to stir for

one hour and then cooled to room temperature. The crude solution was then precipitated into cold acetone to give the sodium salt as a white solid in ca 98% yield (9.8 g). Then, in a 250 ml round bottom flask, the 3-hydroxyitaconic acid disodium salt (5 g, 26.6 mmol) was added to 100 ml of acetone and stirred vigorously. A dilute solution of hydrochloric acid was then added dropwise to the stirring solution. The solution was filtered and the solvent removed under reduced pressure. The resulting oil was then precipitated into diethyl ether twice and dried in a vacuum oven overnight to give 3-hydroxyitaconic acid as a yellow solid in ca. 98% yield; m.p. 156 °C (observed by DSC).

^1H NMR (CDCl_3) δ 5.01 (s, 1H, -CHOH), 6.09 and 6.43 (s, 2H, $\text{CH}_2=\text{C}$); ^{13}C NMR (CDCl_3) δ 73.36 (-CHOH), 123.20 ($\text{CH}_2=\text{C}$), 144.94 ($\text{C}=\text{CH}_2$), 173.94 and 179.22 ($\text{C}=\text{O}$).

Free radical homopolymerization of ethyl 2-carboethoxyhydroxyacrylate. In a typical polymerization procedure, ECHMA (2.01 g, 9.94 mmol) was added to 10 ml of dried toluene in a 50 ml round bottom flask and stirred under nitrogen for 30 minutes. The temperature was gradually increased to 65 °C and stabilized. Then, AIBN (0.02 g, 0.12 mmol), dissolved separately in 1 ml of dried toluene was added to the stirring solution in one portion. The solution was allowed to stir for 24 hours under a nitrogen blanket. Solvent was then removed under reduced pressure and the polymer characterized without further purification.

Free radical copolymerization of ethyl 2-carboethoxyhydroxyacrylate and MMA. In a typical copolymerization procedure, ECHMA (0.04 g, 0.199 mmol) and MMA (2 g, 1.99 mmol) were added to 20 ml of dried THF in a 50 ml three-necked

round bottom flask equipped with a condenser. The solution temperature was gradually increased to 65 °C and the mixture allowed stirring for 30 minutes under a nitrogen atmosphere. AIBN (0.02 g, 0.124 mmol), dissolved separately in dried THF, was then added to the stirring solution in one portion. The flask was sealed and the solution was stirred for 24 hours under a nitrogen blanket. The resulting viscous mixture was precipitated into methanol to give the corresponding copolymer.

REFERENCES

- 1 Tate, B.E. *Vinyl and Diene Monomers*, Wiley Interscience, New York **1970**, 205.
- 2 Otsu, T.; Watanabe, H.; Yang, J.Z., Yoshioka, M.; Matsumoto, A. *Makromol. Chem. Macromol. Symp.* **1992**, 63, 87.
- 3 Cowie, J.M.G. *Pure Appl. Chem.* **1979**, 51, 2331.
- 4 Nagai, S.; Uno, T.; Yoshida, K. *Kobunshi Kagaku* **1968**, 15, 550.
- 5 Marvel, C. S.; Shepherd, T. H. *J. Org. Chem.* **1969**, 24, 599.
- 6 Mathias, L.J.; Kusefoglu H.S.; Kress A.O. *Macromolecules* **1987**, 20, 2326.
- 7 Mathias, L.J.; Warren, R.M.; Huang, S. *Macromolecules* **1991**, 24, 2036.
- 8 Reed, S.F.; Baldwin, M.G. *J. Polym. Sci., Part A: Polym. Chem.*, **1963**, 1, 1919.
- 9 Coltrain, B.K.; Ferrar, W.T.; Salva, J.M. *J. Polym. Sci., Part A: Polym. Chem.* **1993**, 31, 2261.
- 10 Chikanishi, K.; Tsuruta, T. *Makromol. Chem.* **1965**, 81, 198.
- 11 Cheng, J.; Yamada, B.; Otsu, T. *J. Polym. Sci., Part A: Polym. Chem.* **1991**, 29, 1837.
- 12 B. Yamada, M. Satake, and T. Otsu, *Makromol. Chem.* **1991**, 192, 2713.
- 13 Thomson, R.D.; Barclay, T.B.; Basu, K.R.; Mathias, L.J. *Polym. J.* **1995**, 27, 325.
- 14 Yamada, B.; Tagashira, S.; Otsu, T. *Polym. Bull.*, **1993**, 30, 235.

15 Avci, D.; Kusefoglu, S.H.; Thomson, R.D.; Mathias, L.J. *J. Polym. Sci., Part A: Polym. Chem.* **1994**, 32, 2937.

CHAPTER VI

SYNTHESIS OF NEW POLYFUNCTIONAL 2-PYRROLIDINONE FROM ALKYL
2-CARBOETHOXYHYDROXYMETHYLACRYLATES**Abstract**

The synthesis of alkyl 2-carboethoxyhydroxymethylacrylates via the Baylis-Hillman reaction pathway is described. These activated alkenes possess an extremely high reactivity to Michael addition with primary amines leading to a simple, mild, and efficient route to the preparation of new polyfunctional pyrrolidinones.

Introduction

The synthesis of multifunctional 2-pyrrolidinones or γ -lactams has attracted a great amount of interest over the last decade. Optically active, these compounds have found a lot of applications in domains ranging from biology to biochemistry and pharmaceuticals. Among these applications, they have been widely used as psychotropic¹ and anti-hypertensive agents,² inhibitors of proteolytic catalysis,³ and antimuscarinic agents,⁴ with these moieties exhibiting interesting biological and pharmacological activities. γ -Lactams have also been used as key intermediates in the total synthesis of more complex biological molecules.⁵ The pyrrolidinone scaffold appears in diverse naturally occurring molecules. For example, as a pyrroglutamyl group, it caps the amino terminus of peptide hormones such as gonadotropin releasing hormone.⁶ The function of this pyrrolidinone group is to stabilize the peptide's N-terminus against aminoprotease-mediated degradation. In other cases, it serves as a

conformationally rigid scaffold. More highly substituted pyrrolidinones have also shown a wide range of activities. Examples include antagonist of the integrins ($\alpha\beta3$, $\alpha\beta5$, and $\alpha\beta6$)⁷ and antagonist of the chemokine receptor CCR5.⁸ Other γ -lactams have been used to inhibit fatty acid and cholesterol biosynthesis for the treatment of lipoprotein disorders⁹ and to inhibit phosphodiesterase IV, which is an enzyme linked to allergic and inflammatory diseases.¹⁰ Finally, 4-substituted γ -lactams exhibit improved antiepileptic activity, as compared to levetiracetam.¹¹

The formation of the functionalized γ -lactams from itaconic acid derivatives is an interesting and viable approach that has been widely used in the past. For example racemic 1-benzyl-3-alkyl-4-methoxycarbonyl-2-pyrrolidinones were prepared from β -alkylated itaconates and benzylamine through a conjugate addition–lactamization sequence.¹² (*S*)-(-)-4-methoxycarbonyl-2-pyrrolidinone was also synthesized by Wyatt et al. starting from itaconic acid and (*S*)-(-)-1-phenylethylamine, with high enantiomeric excess (95%).¹³

Our interest in such compounds derives from the fact that their naturally occurring oxygen analogues, which belong to a small class of compound generally known as paraconic acids, possess important biological properties.¹⁴ Among them, (-)-methylenolactocin,¹⁵ isolated from the culture filtrate of *Penicillium sp.*, shows antitumor and antibiotic activity; protolichesterinic acid,¹⁶ isolated from several species of moss *Cetraria*, is an antitumor, antibacterial and growth regulating compound; while (-)-phaseolinic acid¹⁷ is a metabolite of a fungus, *Macrophomina phaseolina*. Many asymmetric syntheses of paraconic

acid derivatives are reported,¹⁸ and also a few chemoenzymatic syntheses.¹⁹ In that work, we directed our attention to the synthesis of their aza analogues, which, in view of their potential biological activity, could be of interest due to the lower toxicity of the lactam ring when compared to that of the lactone ring.²⁰ Jiang and al. reported the synthesis of functionalized pyrrolidinones via the coupling of N,N-disubstituted β -amino esters with ethyl glyoxylate. In this work, pyrrolidinones derivatives were obtained via a conjugate addition/aldol condensation/ deprotection/cyclization approach. Herein we were interested in designing new polyfunctional pyrrolidinones derivatives (Figure 6.1) via a Michael addition/cyclization reaction involving alkyl 2-carboethoxyhydroxymethylacrylates and primary amines.

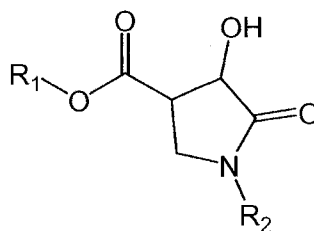


Figure 6.1. Polyfunctional pyrrolidinones.

Results and Discussion

Synthesis of alkyl 2-carboethoxyhydroxymethylacrylates 1-4. Alkyl 2-carboethoxyhydroxymethylacrylates that incorporate different groups such as methyl, ethyl, n-butyl, and t-butyl were synthesized via the Baylis-Hillman pathway following previously reported literature.²¹ This reaction involves conjugated compounds such as esters that react with aldehydes via the α -carbon in the presence of a catalyst to give allylic alcohols.^{22,23} This type of reaction has

great synthetic utility as it converts simple starting materials into densely functionalized products, although it sometimes suffers from low reaction rates and low yields. Nucleophilic bases such as triethylamine, N,N-dimethylaminopyridine (DMAP) and 1,4-diaza[2.2.2]bicyclooctane (DABCO) were tested in the formation of ethyl 2-carboethoxyhydroxymethylacrylates **1** in order to determine the most suitable base. Table 6.1 shows that the reaction that involved DABCO as catalyst gave the highest product yield after 24 hours. We noticed that the nature of the base has also a great effect on the reaction time as shown in Table 6.1. Reaction conversions were followed by ^1H NMR by monitoring of vinyl peaks disappearance over time. It was noticed that the reaction, slightly exothermic, was completed after 30 minutes when DABCO was used as catalyst. A change in color was noticed also during the extension of the reaction, although this color disappeared in the final products isolated by vacuum distillation.

Table 6.1. Effect of base on the alkyl 2-carboethoxyhydroxymethylacrylates formation.

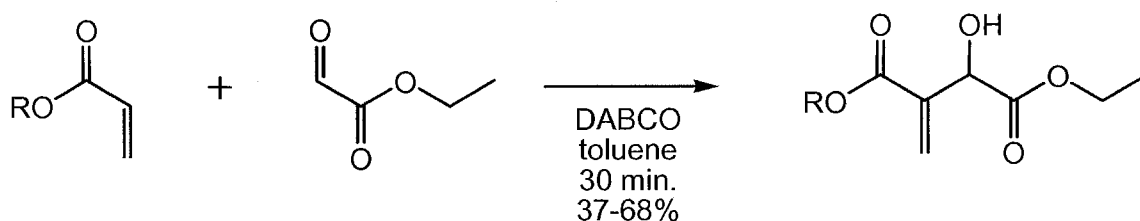
entry	base / (mol-%)	temp. (°C)	time (h)	yield (%) ^(a)
1	DMAP / (3)	25	24	31
2	Et ₃ N / (3)	25	24	17
3	DABCO / (3)	25	24 (30 min.)	68
4	DABCO / (6)	25	24 (30 min.)	65
5	DABCO / (10)	25	24 (30 min.)	62

(a) – Isolated yield after distillation.

Following this reaction scheme, a variety of alkyl 2-carboethoxyhydroxymethylacrylates were synthesized by reaction of ethyl glyoxylate with various acrylates in the presence of DABCO. The disappearance of the ^{13}C NMR

resonance peaks for the acrylate vinyl carbons and the appearance of a new peak corresponding to the new carbon substituent allowed monitoring the course of the reaction. Vacuum distillation permitted purification of the desired products. The alkyl 2-carboethoxyhydroxymethylacrylate derivatives were synthesized in yields ranging from c.a. 37 to 68% after distillation (Table 6.2).

Table 6.2. Synthesis of alkyl 2-carboethoxyhydroxymethylacrylates **1-4**.



entry	R	time (min.)	conv. (%) ^(a)	yield ^(b) (%)	compound #
1	Me	30	87	68	1
2	Et	40	92	67	2
3	t-butyl	40	81	37	3
4	n-butyl	30	91	38	4

(a) – Determined via ¹H NMR.

(b) – Isolated yield after vacuum distillation.

Considering compound **1** as a typical example, the appearance of the two peaks at 128.9 and 138.2 ppm confirmed formation of the new double bond carbons, while the appearance of the unique peak at 71.3 ppm (-CHOH carbon) confirms formation of the product. Figure 6.2 below displays the ¹³C NMR spectra of compounds **1-4**.

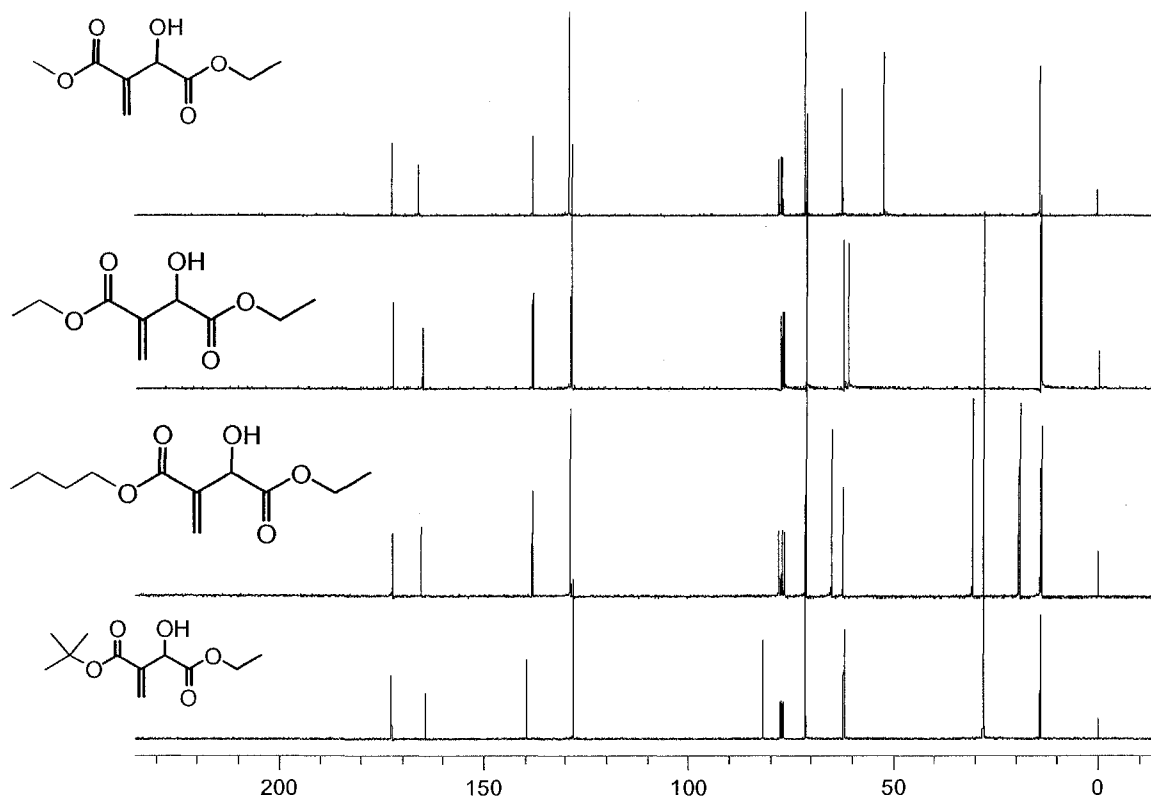


Figure 6.2. ^{13}C NMR spectra of compounds **1-4** (CDCl_3).

Kinetic study. Preliminary studies presented in Chapter V demonstrated that alkyl 2-carboethoxyhydroxymethylacrylates undergo free radical polymerization with great difficulty. We were then interested in determining their reactivity to Michael addition with primary amines. We decided to study the kinetics of the reaction between these activated alkenes and aliphatic primary amines. As a model reaction, ethyl 2-carboethoxyhydroxymethylacrylate **2** and n-hexylamine were reacted at room temperature in chloroform, under dilute conditions (5 wt-%), and monitored by real time FT-IR. The disappearance of the carbon-carbon stretching bond at 1643 cm^{-1} corresponding to the double bond of the acrylate and apparition of the carbonyl peak at 1695 cm^{-1} corresponding to the amide

formation attested of the pyrrolidinone compound formation in a very fast manner even in so dilute condition as shown in Figure 6.3.

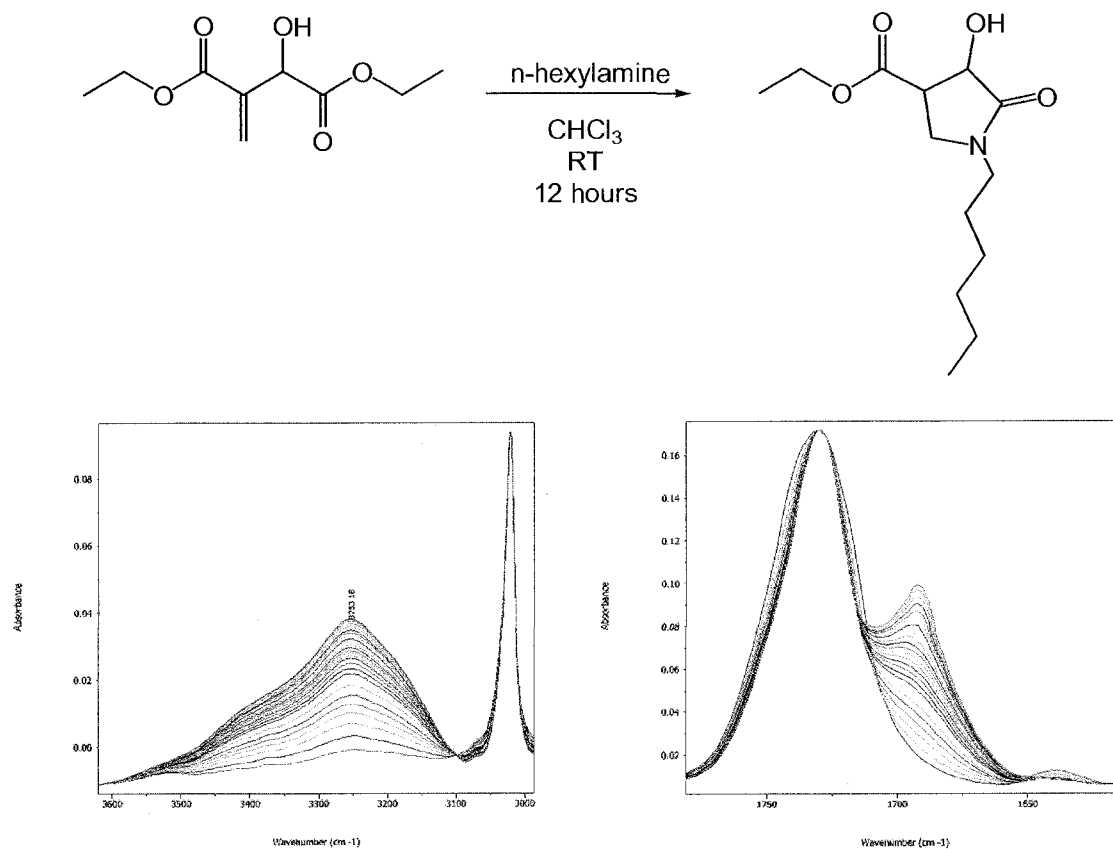


Figure 6.3. Peak evolution at 3200, 1695 and 1643 cm⁻¹.

The ¹³C NMR spectrum of the resulting crude product showed the appearance of peaks corresponding to ethanol release, which confirmed cyclization occurrence. The ethanol release was also noticed during the monitoring of the reaction by ReactIR as the increase of the peak intensity at 3200 cm⁻¹ is correlated to the production of ethanol during the course of the reaction (Figure 6.3). The conversion profile could be determined for the vinyl peak and it was noticed that 90% conversion was reached after only 2 hours with these conditions.

^1H and ^{13}C NMR were also used to confirm pyrrolidinone formation and no trace of the intermediate amine could be detected upon analysis of the product spectra. As a control, the same reaction was carried out with dimethyl itaconate, using the same conditions. It was found that alkyl 2-carboethoxyhydroxymethylacrylates reacted orders of magnitude faster than the non-alcohol substituted analog. We believe that this behavior is due to the presence of the secondary hydroxyl group attached to the α carbon which, firstly, induces hydrogen bonding that may lead to preorganization of molecules in the system, and secondly, activates both the alkene and the saturated ester carbonyl of the neighboring groups by intra- and intermolecular hydrogen bonding. This unique combination of hydrogen bonding interactions activates in multiple ways so that the reaction with primary amines leads to the extremely fast formation of multifunctional heterocycles.

To confirm this behavior, dimethyl itaconate and ethyl 2-carboethoxyhydroxymethylacrylate were mixed together in stoichiometric conditions and reacted with only one equivalent of hexylamine using the same conditions of temperature and dilution as above. The extent of the reaction was monitored by ^1H NMR. We noticed high selectivity of the reaction towards ethyl 2-carboethoxyhydroxymethylacrylate considering that, after 24 hours, 92% of the corresponding acrylate had reacted while the conversion for dimethyl itaconate reached only 8% (Figure 6.4).

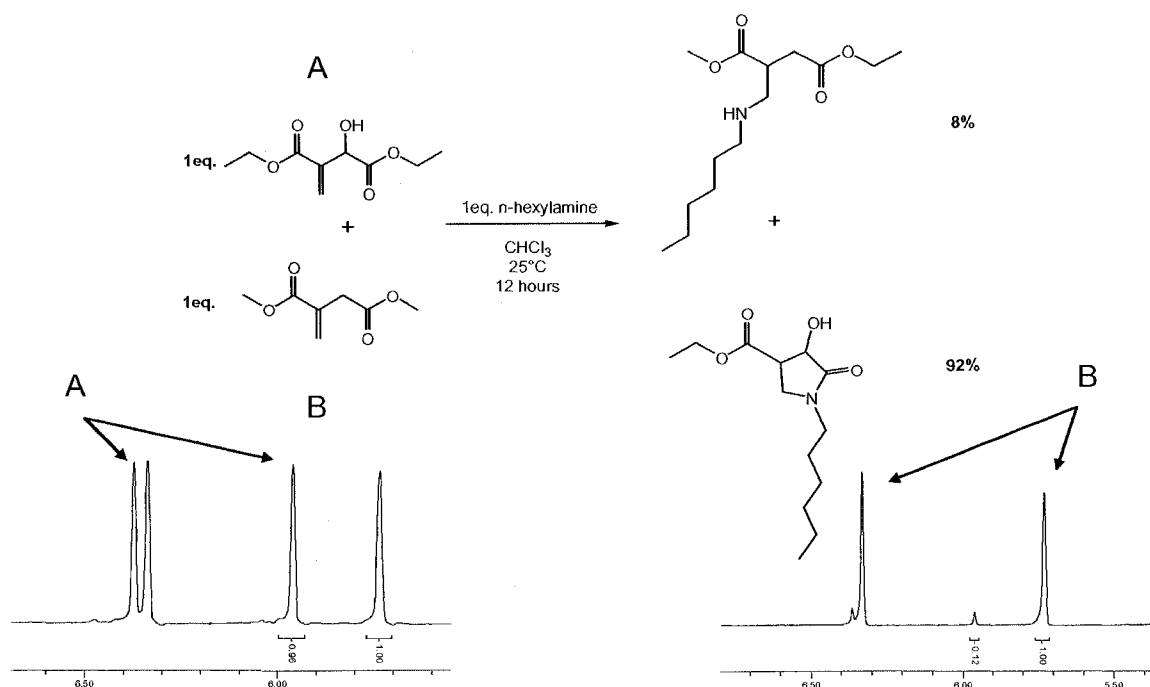


Figure 6.4. Reaction between dimethyl itaconate, ethyl 2-carboethoxyhydroxymethylacrylate and hexylamine. ^1H NMR of reaction batch before (left) and after addition of hexylamine (right) (vinyl peaks region, CDCl_3).

As shown in Figure 6.3, temperature did not have a profound effect on the overall reaction conversion and yields obtained, again confirming high reactivity of the unsaturated group to Michael addition reaction. Similar reactions were carried out with other alkyl 2-carboethoxyhydroxymethylacrylates incorporating different ester groups such as methyl, n-butyl, and t-butyl, using the same conditions described above. These compounds showed the same reactivity upon reaction with hexylamine (Figure 6.5), indicating that steric inhibition by the ester group is minimal.

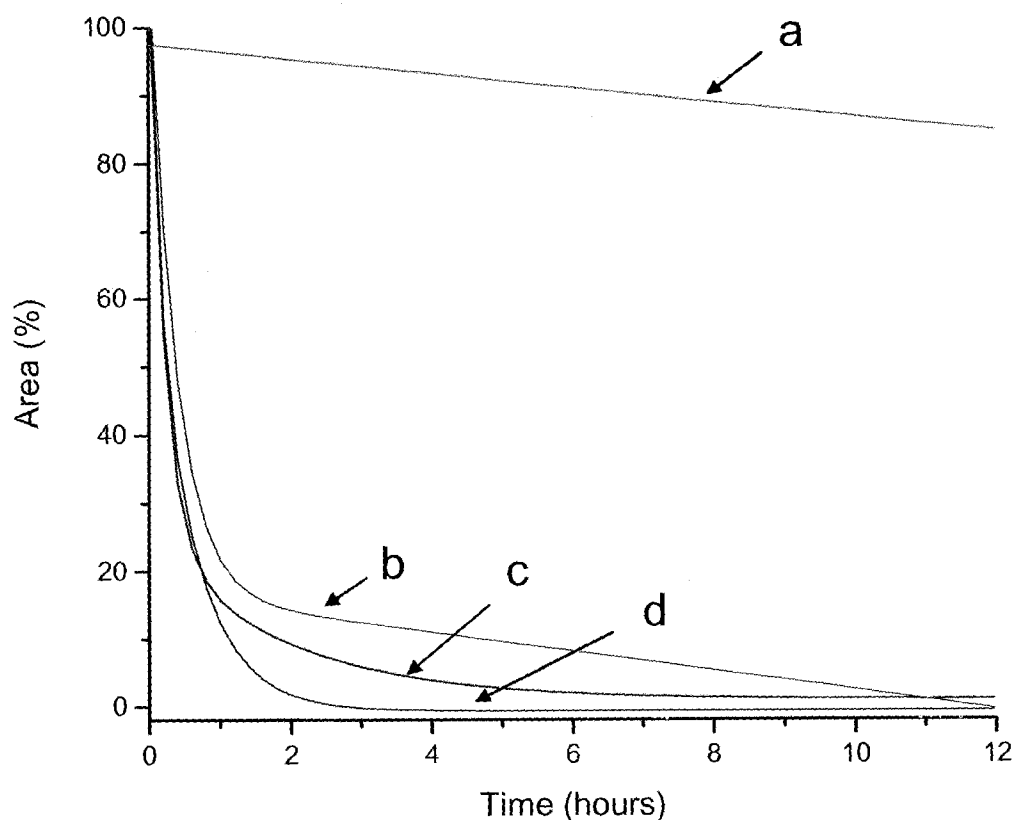
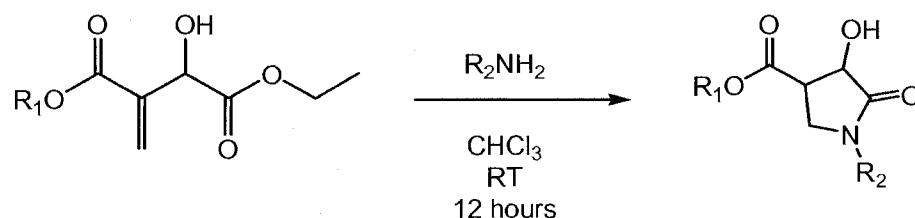


Figure 6.5. Peak area percentage at 1643 cm^{-1} (C=C stretching) as function of reaction conversion observed by real-time FT-IR for dimethylitaconate (a), ethyl 2-carboethoxyhydroxymethylacrylate (b), n-butyl 2-carboethoxyhydroxymethylacrylate (c), and methyl 2-carboethoxyhydroxymethylacrylate (d).

Synthesis of multifunctional pyrrolidinone derivatives 5-13. A variety of 2-pyrrolidinones compounds were synthesized in essentially quantitative yields (96-99%) as summarized in Table 6.4. These compounds were synthesized in a very fast manner and high purity as indicated in Table 6.4. For instance, most of the pyrrolidinone compounds were purified only by removal of amine, introduced in slight excess, under reduced pressure. NMR spectroscopy and elemental

analysis allowed confirmation each compound structure and purity, respectively. As example, ^{13}C NMR and FT-IR spectra of compound **3** are shown in Figures 6.6 and 6.7, respectively. DEPT and gHMBC experiments allowed accurate assignment of the NMR peaks for each segment of the compound. The *cis/trans* ring substitution ratio was approximately equivalent for all compounds as shown in Table 6.3.

Table 6.3. Polyfunctional 2-pyrrolidinone derivatives.



entry	R ₁	R ₂	time (h)	conv. (%)	yield (%)	% <i>cis/trans</i> ^(a)	compound #
1	Me	-(CH ₂) ₅ CH ₃	0.5	>99	99	42/58	5
2	Me	-(CH ₂) ₂ OH	0.5	>99	99	41/59	6
3	Et	-(CH ₂) ₅ CH ₃	0.5	>99	99	33/67	7
4	Et	-(CH ₂) ₂ OH	0.5	>99	99	33/67	8
5	n-butyl	-(CH ₂) ₅ CH ₃	0.5	71 (97%/24h)	97	31/69	9
6	n-butyl	-(CH ₂) ₂ OH	0.5	71 (97%/24h)	99	33/67	10
7	t-butyl	-(CH ₂) ₅ CH ₃	0.5	55 (97%/24h)	97	35/65	11
8	t-butyl	-(CH ₂) ₃ CH ₃	0.5	52 (98%/24h)	96	33/67	12
9	t-butyl	-(CH ₂) ₂ OH	0.5	55 (97%/24h)	96	35/65	13
10 ^(b)	Et	-OH	0.5	>99	98	37/63	14

(a) – Determined via ^1H NMR.

(b) – Large excess of amine was used in the preparation of this compound.

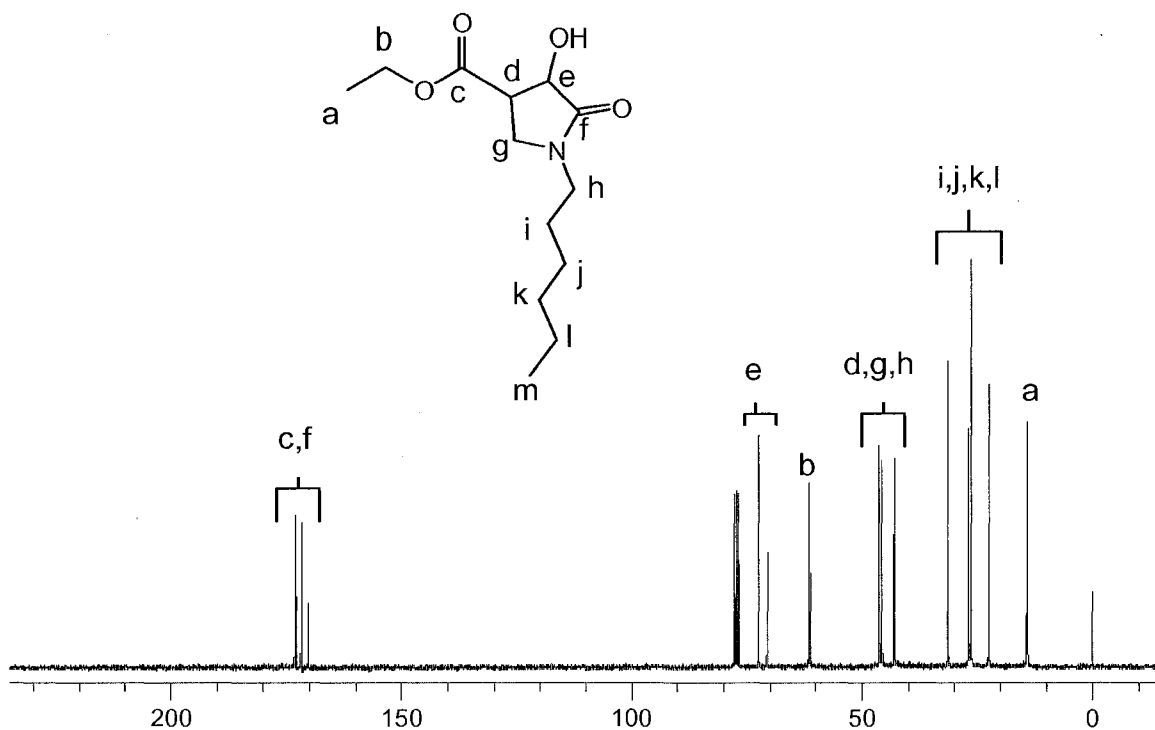


Figure 6.6. ^{13}C NMR of pyrrolidinone **6** (CDCl_3).

Pyrrolidinones **5-14** are potentially valuable for subsequent experiments aimed at the design of more complex molecules. These compounds were synthesized by reacting alkyl 2-carboethoxyhydroxymethylacrylates described above with different aliphatic primary amines such as hexylamine, butylamine or ethanolamine. All heterocycle derivatives were purified only by simple removal of solvent and excess of remaining amine under reduced pressure. No transamidation reaction was observed with the conditions described above except when hydroxylamine was used. In this case, a mixture of pyrrolidinone ester and amide derivatives was observed. Further reaction with an excess of the hydroxylamine led to the quantitative formation of the cyclic hydroxamic acid for which the ^{13}C NMR spectrum is displayed in Figure 6.8.

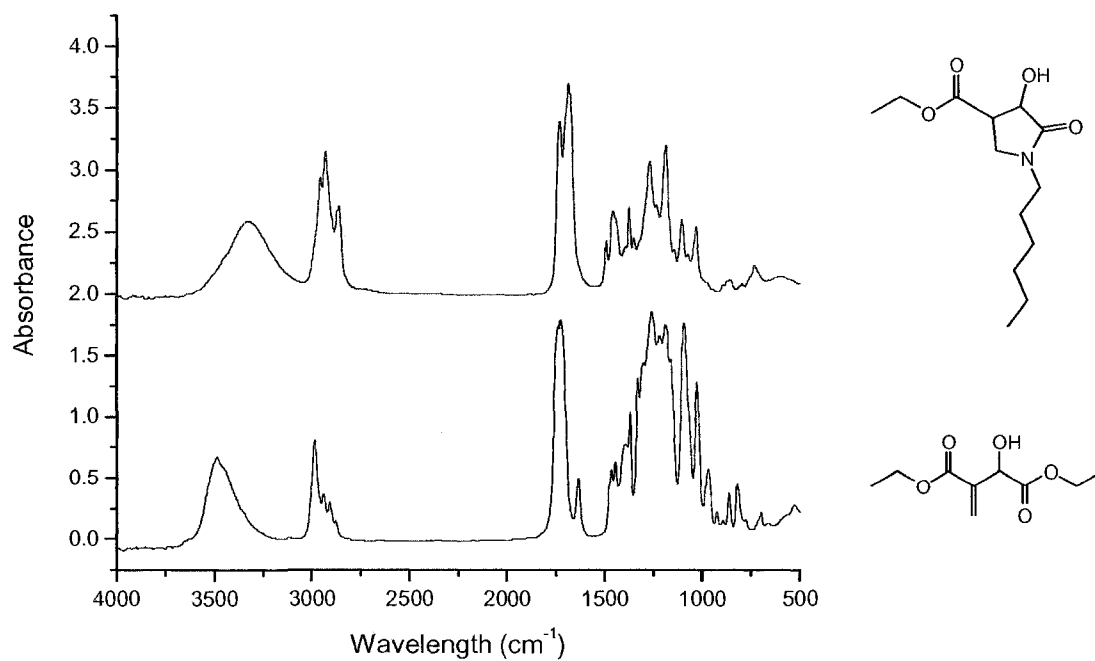


Figure 6.7. FT-IR spectra of ethyl 2-carboethoxyhydroxymethylacrylate **2** and pyrrolidinone **6**.

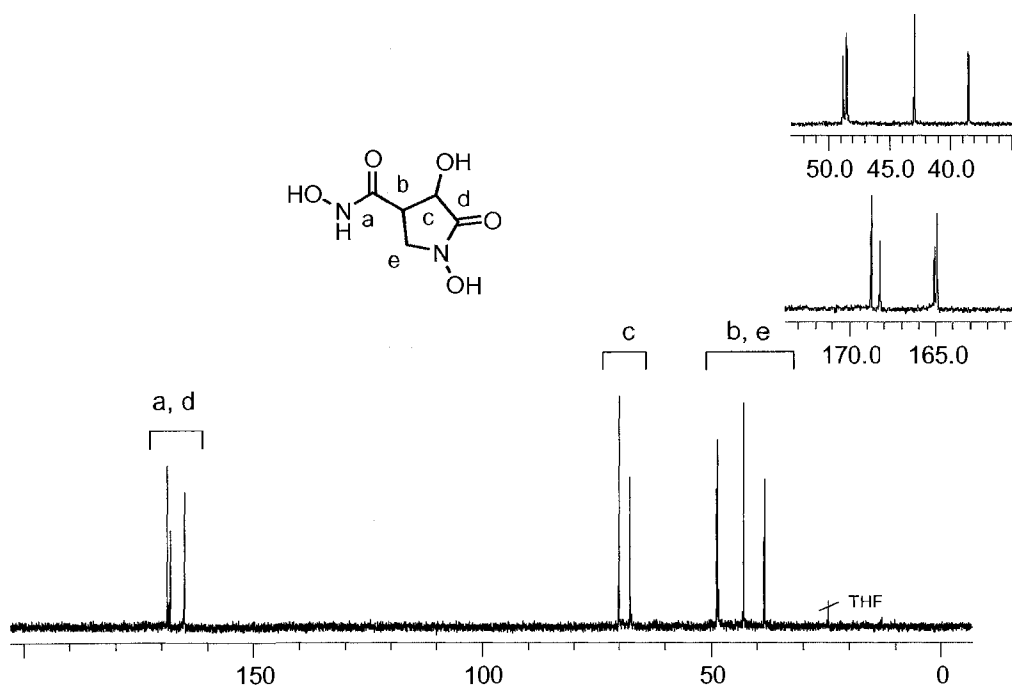


Figure 6.8. ¹³C NMR of cyclic hydroxamic acid **14** (D₂O).

The cyclic hydroxamic acid derivative **14** was obtained as a very hygroscopic white powder and exposure to air for few minutes led to its liquefaction.

Conclusions

Alkyl 2-carboethoxyhydroxymethylacrylates were synthesized successfully via the Baylis-Hillman reaction pathway. We have reported also the facile preparation in quantitative yields, of polyfunctional 2-pyrrolidinone derivatives from a highly efficient Michael addition/cyclization reaction sequence between alkyl 2-carboethoxyhydroxymethylacrylates, and aliphatic primary amines. It has been found that the addition of amines to alkyl 2-carboethoxyhydroxymethylacrylates is orders of magnitude faster than the analogous reaction involving the commercially available dimethyl itaconate. This high reactivity is believed to be due to a unique combination of intra- and intermolecular hydrogen bonding. These compounds provide a new library of polyfunctional and optically active intermediates that will certainly find application in a wide range of domains, from pharmaceutical to polymer chemistry.

This reaction attests to characteristics similar to the ones listed by Sharpless and coworkers in the early 2000s, in describing “click chemistry reactions”. Highly efficient and suffering only from release of ethanol from the 5-membered heterocycle formation, this “green” click reaction opens up potential for the design of more complex molecules and macromolecules obtained by a fast reaction and in high purity.

Experimental

Materials. Ethyl glyoxylate, 50% in toluene, was purchased from Alfa Aesar and used as received. 4-Diaza[2.2.2]bicyclooctane (DABCO), thionyl chloride, methyl acrylate, ethyl acrylate, n-butyl acrylate and t-butyl acrylate were purchased from Aldrich Chemical Company and used without further purification. Hexylamine and ethanolamine were purchased from Aldrich Chemical Company and used as received. All solvents were purchased from Acros Chemical Company, Fisher, or Aldrich Chemical Company.

Analyses. Solution ^1H and ^{13}C NMR spectra of the monomers were collected at room temperature with TMS as an internal reference on a Varian Mercury 300 MHz spectrometer operating at a frequency of 75.47 MHz for carbon. FT-IR spectra were obtained using a Mattson Galaxy series 5000 FTIR spectrometer.

General procedure for the preparation of alkyl 2-carboethoxyhydroxymethylacrylates (1-4). The various alkyl 2-carboethoxyhydroxymethylacrylate derivatives were synthesized according to previously reported literature procedure.²⁴ Ethyl glyoxylate, 50 wt-% in toluene (20.39 g, 199.7 mmol), DABCO (3.64 g, 32.4 mmol) and the corresponding acrylate (199.7 mmol) were added to a 250 ml round bottom flask. The mixture was stirred at room temperature for two hours. The crude solution was then concentrated under reduced pressure. The resulting mixture was washed with three aliquots of saturated sodium chloride solution followed by three aliquots of deionized water. The organic phase was then dried over a bed of sodium sulfate. Vacuum distillation of the residue gave the corresponding compounds **1-4**, which show the following data:

Methyl 2-carboethoxyhydroxymethylacrylate (1). Clear liquid; bp 135-137°C (20 mm Hg); c.a. 68% (isolated yield after distillation); ^1H NMR (300 MHz, CDCl_3) δ 1.26 (t, 3H, $-\text{CH}_3$), 3.68 (s, H, $-\text{OH}$), 3.78 (s, 3H, $-\text{OCH}_3$), 4.26 (q, 2H, $-\text{CH}_2\text{CH}_3$), 4.88 (s, H, $-\text{CHOH}$), 5.96 and 6.37 (s, 2H, $-\text{CH}_2=\text{C}$); ^{13}C NMR (CDCl_3) δ 14.04 ($-\text{CH}_3$), 52.12 ($-\text{OCH}_3$), 62.20 ($-\text{CH}_2\text{CH}_3$), 71.19 ($-\text{CHOH}$), 128.96 ($\text{CH}_2=\text{C}$), 138.08 ($\text{C}=\text{CH}_2$), 165.68 and 172.30 ($\text{C}=\text{O}$). FT-IR (neat, cm^{-1}) 3515, 2996, 1739, 1643, 1446, 1097, 823. Anal. Calcd for $\text{C}_8\text{H}_{15}\text{O}_5 \cdot 0.25 \cdot \text{H}_2\text{O}$: C, 50.59; H, 6.49. Found: C, 50.28; H, 6.28.

Ethyl 2-carboethoxyhydroxymethylacrylate (2). Clear liquid; bp 140-142°C (20 mm Hg); c.a. 67% (isolated yield after distillation); ^1H NMR (300 MHz, CDCl_3) δ 1.26 (t, 3H, $-\text{CH}_3$), 1.30 (t, 3H, $-\text{CH}_3$), 3.64 (s, H, $-\text{OH}$), 4.23 (t, 2H, $-\text{CH}_2\text{CH}_3$), 4.25 (t, 2H, $-\text{CH}_2\text{CH}_3$), 4.87 (s, H, $-\text{CHOH}$), 5.94 and 6.37 (s, 2H, $-\text{CH}_2=\text{C}$); ^{13}C NMR (CDCl_3) δ 14.05 ($-\text{CH}_3$), 14.11 ($-\text{CH}_3$), 61.17 ($-\text{CH}_2\text{CH}_3$), 62.19 ($-\text{CH}_2\text{CH}_3$), 71.26 ($-\text{CHOH}$), 128.77 ($\text{CH}_2=\text{C}$), 138.32 ($\text{C}=\text{CH}_2$), 165.21 and 172.39 ($\text{C}=\text{O}$). FT-IR (neat, cm^{-1}) 3516, 2998, 1737, 1643, 1446, 1098, 823. Anal. Calcd for $\text{C}_9\text{H}_{14}\text{O}_5 \cdot 0.25 \cdot \text{H}_2\text{O}$: C, 52.30; H, 7.02. Found: C, 52.01; H, 6.88.

n-Butyl 2-carboethoxyhydroxymethylacrylate (3). Clear liquid; bp 153-155°C (20 mm Hg); c.a. 37% (isolated yield after distillation); ^1H NMR (300 MHz, CDCl_3) δ 0.94 (t, 3H, $-\text{CH}_3$), 1.27 (t, 3H, $-\text{CH}_3$), 1.42 (m, 2H, $-\text{CH}_2\text{CH}_3$), 1.66 (m, 2H, $-\text{CH}_2\text{CH}_2\text{CH}_3$), 3.59 (s, H, $-\text{OH}$), 4.19 (t, 2H, $-\text{CH}_2\text{CH}_3$), 4.23 (t, 2H, $-\text{CH}_2\text{CH}_2\text{CH}_2\text{CH}_3$), 4.86 (s, H, $-\text{CHOH}$), 5.93 and 6.37 (s, 2H, $\text{CH}_2=\text{C}$); ^{13}C NMR (CDCl_3) δ 13.69 ($-\text{CH}_3$), 14.06 ($-\text{CH}_3$), 19.15 ($-\text{CH}_2\text{CH}_3$), 30.56 ($-\text{CH}_2\text{CH}_2\text{CH}_3$), 62.22 ($-\text{CH}_2\text{CH}_3$), 65.04 ($-\text{CH}_2\text{CH}_3$), 71.27 ($-\text{CHOH}$), 128.82 ($\text{CH}_2=\text{C}$), 138.28

(C=CH₂), 165.28 and 172.39 (C=O). FT-IR (neat, cm⁻¹) 3516, 2998, 1737, 1643, 1446, 1098, 823. Anal. Calcd for C₁₁H₁₈O₅·0.5*H₂O: C, 54.21; H, 8.01. Found: C, 53.84; H, 7.39.

t-Butyl 2-carboethoxyhydroxymethylacrylate (4). Clear liquid; bp 155-157°C (20 mm Hg); c.a. 38% (isolated yield after distillation); ¹H NMR (300 MHz, CDCl₃) δ 1.27 (t, 3H, -CH₃), 1.49 (s, 9H, -CH₃), 3.62 (s, H, -OH), 4.25 (t, 2H, -CH₂CH₃), 4.82 (s, H, -CHOH), 5.86 and 6.28 (s, 2H, CH₂=C); ¹³C NMR (CDCl₃) δ 14.1 (-CH₃), 27.97 (-CH₃), 62.04 (-CH₂CH₃), 71.34 (-CHOH), 81.78 (-CCH₃), 128.11 (CH₂=C), 138.55 (C=CH₂), 164.31 and 172.55 (C=O). FT-IR (neat, cm⁻¹) 3516, 2998, 1737, 1643, 1446, 1098, 823. Anal. Calcd for C₁₁H₁₈O₅·0.5*H₂O: C, 54.21; H, 8.01. Found: C, 54.31; H, 7.64.

Preparation of multifunctional pyrrolidinones derivatives (5-13). General

procedure. The corresponding alkyl 2-carboethoxyhydroxymethylacrylate (53.14 mmol) was added to a 50 ml tube equipped with an argon gas inlet. The reaction tube was then purged with argon for 30 minutes and sealed with a rubber septum. The corresponding primary amine was added dropwise in slight excess (54.21 mmol) to the previous mixture and the resulting solution was allowed to stir for 24 hours at room temperature. Upon reaction completion as monitored by ¹H NMR, the solvent was removed under reduced pressure. The concentrated product **5** was then purified by column chromatography using an ethyl acetate/hexanes mixture (2:10) as eluent. The resulting product fraction was then concentrated under reduced pressure to afford the corresponding compound **5** as a mixture of two diastereoisomers (A and B). The crude products **6-13** were

purified by distilling off the excess amine. The resulting compounds **5-13** show the following data:

Methyl 1-hexyl-4-hydroxy-5-oxopyrrolidine-3-carboxylate (5). Brown liquid; c.a. 99% yd; diastereoisomeric ratio (d.r.) 42:58; ^1H NMR (300 MHz, CDCl_3) δ 0.88 (t, 3H, $-\text{CH}_3$), 1.28 (m, 2H, $-\text{CH}_2$), 1.52 (m, 2H, $-\text{CH}_2\text{CH}_2\text{N}$), 3.74_(A) and 3.77_(B) (s, 3H, $-\text{CH}_3$), 4.59_(A) and 4.60_(B) (d, H, $-\text{CHOH}$); ^{13}C NMR (CDCl_3) δ 14.17_(A+B) ($-\text{CH}_3$), 22.52_(A+B) ($-\text{CH}_2\text{CH}_3$), 26.38 and 26.85 ($-\text{CH}_2\text{CH}_2\text{CH}_3$), 31.41 and 31.44 ($-\text{CH}_2\text{CH}_3$), 42.96 and 43.04 ($-\text{CH}_2\text{N}$), 43.07 and 45.62 ($-\text{CHCH}_2\text{N}$), 46.07 and 46.29 ($-\text{CH}_2\text{N}$), 52.16 and 52.53 ($-\text{OCH}_3$), 70.46 and 72.43 ($-\text{CHOH}$), 170.74 and 172.25 ($\text{C}=\text{O}$), 172.82 and 173.09 ($\text{NC}=\text{O}$). FT-IR (neat, cm^{-1}) 3363, 2958, 2935, 2866, 1741, 1695, 1278, 740. Anal. Calcd for $\text{C}_{12}\text{H}_{21}\text{NO}_4$: C, 59.24; H, 8.70; N, 5.76. Found: C, 59.42; H, 8.71; N, 5.84.

Methyl 4-hydroxy-1-(2-hydroxyethyl)-5-oxopyrrolidine-3-carboxylate (6). Brown liquid; c.a. 99%; d.r. 42:58; ^1H NMR (300 MHz, CDCl_3) δ 0.88 (t, 3H, $-\text{CH}_3$), 1.28 (m, 2H, $-\text{CH}_2$), 1.52 (m, 2H, $-\text{CH}_2\text{CH}_2\text{N}$), 3.74_(A) and 3.77_(B) (s, 3H, $-\text{CH}_3$), 4.59_(A) and 4.60_(B) (d, H, $-\text{CHOH}$); ^{13}C NMR (CDCl_3) δ 14.17_(A+B) ($-\text{CH}_3$), 22.52_(A+B) ($-\text{CH}_2\text{CH}_3$), 26.38 and 26.85 ($-\text{CH}_2\text{CH}_2\text{CH}_3$), 31.41 and 31.44 ($-\text{CH}_2\text{CH}_3$), 42.96 and 43.04 ($-\text{CH}_2\text{N}$), 43.07 and 45.62 ($-\text{CHCH}_2\text{N}$), 46.07 and 46.29 ($-\text{CH}_2\text{N}$), 52.16 and 52.53 ($-\text{OCH}_3$), 70.46 and 72.43 ($-\text{CHOH}$), 170.74 and 172.25 ($\text{C}=\text{O}$), 172.82 and 173.09 ($\text{NC}=\text{O}$). FT-IR (neat, cm^{-1}) 3363, 2958, 2935, 2866, 1741, 1695, 1278, 740. Anal. Calcd for $\text{C}_8\text{H}_{13}\text{NO}_5$: C, 47.29; H, 6.45; N, 6.89. Found: C, 47.39; H, 6.59; N, 7.36.

Ethyl 1-hexyl-4-hydroxy-5-oxopyrrolidine-3-carboxylate (7). Brown liquid; c.a. 99%; d.r. 33:67; ^1H NMR (300 MHz, CDCl_3) δ 0.88_(A+B) (t, 3H, $-\text{CH}_3$), 1.28_(A+B) (m, 2H, $-\text{CH}_2$), 1.52_(A+B) (m, 2H, $-\text{CH}_2\text{CH}_2\text{N}$), 4.29_(A) and 4.22_(B) (q, 2H, $-\text{CH}_3$), 4.56_(A) and 4.58_(B) (d, H, $-\text{CHOH}$); ^{13}C NMR (CDCl_3) δ 14.17_(A+B) ($-\text{CH}_3$), 22.49_(A+B) ($-\text{CH}_2\text{CH}_3$), 26.38_(A) and 26.87_(B) ($-\text{CH}_2\text{CH}_2\text{CH}_3$), 31.41_(A) and 31.44_(B) ($-\text{CH}_2\text{CH}_3$), 42.97_(A) and 43.06_(B) ($-\text{CH}_2\text{N}$), 43.06_(A) and 45.70_(B) ($-\text{CHCH}_2\text{N}$), 46.22_(A) and 46.31_(B) ($-\text{CH}_2\text{N}$), 61.53_(A+B) ($-\text{OCH}_3$), 70.53_(A) and 72.43_(B) ($-\text{CHOH}$), 170.27_(A) and 171.76_(B) ($\text{C}=\text{O}$), 172.76_(A) and 173.09_(B) ($\text{NC}=\text{O}$). FT-IR (neat, cm^{-1}) 3363, 2958, 2935, 2866, 1741, 1695, 1278, 740. Anal. Calcd for $\text{C}_{13}\text{H}_{23}\text{NO}_4$: C, 60.68; H, 9.01; N, 5.44. Found: C, 60.49; H, 8.88; N, 5.49.

Ethyl 4-hydroxy-1-(2-hydroxyethyl)-5-oxopyrrolidine-3-carboxylate (8).

Brown liquid; c.a. 99%; d.r. 33:67; ^1H NMR (300 MHz, CDCl_3) δ 1.24_(A+B) (t, 3H, $-\text{CH}_3$), 4.14_(A) and 4.18_(B) (q, 2H, $-\text{CH}_3$), 4.53_(A) and 4.57_(B) (d, H, $-\text{CHOH}$); ^{13}C NMR (CDCl_3) δ 14.14_(A+B) ($-\text{CH}_3$), 43.62_(A) and 45.91_(B) ($-\text{CH}_2\text{N}$), 45.84_(A) and 46.41_(B) ($-\text{CHCH}_2\text{N}$), 46.60_(A) and 47.18_(B) ($-\text{CH}_2\text{N}$), 59.31_(A+B) ($-\text{CH}_2\text{OH}$), 61.42_(A) ($-\text{OCH}_2$), 61.55_(B) ($-\text{OCH}_2$), 70.74_(A) and 72.46_(B) ($-\text{CHOH}$), 171.13_(A) and 171.78_(B) ($\text{C}=\text{O}$), 173.44_(A) and 173.92_(B) ($\text{NC}=\text{O}$). FT-IR (neat, cm^{-1}) 3365, 2959, 2936, 2867, 1742, 1696, 1279, 741. Anal. Calcd for $\text{C}_9\text{H}_{15}\text{NO}_5$: C, 49.76; H, 6.96; N, 6.45. Found: C, 49.36; H, 6.80; N, 6.48.

Butyl 1-hexyl-4-hydroxy-5-oxopyrrolidine-3-carboxylate (9). Brown liquid; c.a.

97%; d.r. 31:69; ^1H NMR (300 MHz, CDCl_3) δ 0.88_(A) (t, 3H, $-\text{CH}_3$), 0.94_(B) (t, 3H, $-\text{CH}_3$), 1.28_(A+B) (m, 2H, $-\text{CH}_2$), 1.40_(A+B) (m, 2H, $-\text{CH}_2\text{CH}_3$), 1.51_(A+B) (m, 2H, $-\text{CH}_2\text{CH}_2\text{CH}_3$), 1.52_(A+B) (m, 2H, $-\text{CH}_2\text{CH}_2\text{N}$), 4.17_(A+B) (q, 2H, $-\text{OCH}_2$), 4.55_(A) and

4.58_(B) (d, H, -CHOH); ¹³C NMR (CDCl₃) δ 14.16_(A+B) (-CH₃), 22.50_(A+B) (-CH₂CH₃), 26.39_(A) and 26.93_(B) (-CH₂CH₂CH₃), 31.42_(A) and 31.45_(B) (-CH₂CH₃), 42.97_(A) and 43.06_(B) (-CH₂N), 43.18_(A) and 45.72_(B) (-CHCH₂N), 46.24_(A) and 46.33_(B) (-CH₂N), 65.03_(A) and 65.37_(B) (-OCH₂), 70.52_(A) and 72.43_(B) (-CHOH), 170.34_(A) and 171.82_(B) (C=O), 172.79_(A) and 173.13_(B) (NC=O). FT-IR (neat, cm⁻¹) 3357, 2958, 2875, 1739, 1693, 746. Anal. Calcd for C₁₅H₂₇NO₄: C, 63.13; H, 9.54; N, 4.91. Found: C, 62.97; H, 9.42; N, 4.94.

Butyl 4-hydroxy-1-(2-hydroxyethyl)-5-oxopyrrolidine-3-carboxylate (10).

Brown liquid; c.a. 99%; d.r. 33:67; ¹H NMR (300 MHz, CDCl₃) δ 0.94_(A+B) (t, 3H, -CH₃), 1.37_(A+B) (m, 2H, -CH₂CH₃), 1.64_(A+B) (m, 2H, -CH₂CH₂CH₃), 4.16_(A+B) (q, 2H, -OCH₂), 4.59_(A) and 4.62_(B) (d, H, -CHOH); ¹³C NMR (CDCl₃) δ 13.68_(A) (-CH₃), 13.70_(B) (-CH₃), 19.04_(A+B) (-CH₂CH₃), 30.49_(A) and 30.52_(B) (-CH₂CH₂CH₃), 43.72_(A) and 45.97_(B) (-CH₂N), 45.91_(A) and 46.43_(B) (-CHCH₂N), 47.20_(A) and 46.65_(B) (-CH₂N), 59.38_(A) (-CH₂OH), 59.42_(B) (-CH₂OH), 65.34_(A) and 65.44_(B) (-OCH₂), 70.78_(A) and 72.48_(B) (-CHOH), 171.26_(A) and 171.80_(B) (C=O), 173.40_(A) and 173.96_(B) (NC=O). FT-IR (neat, cm⁻¹) 3360, 2955, 2935, 2866, 1740, 1697, 1278, 742. Anal. Calcd for C₁₅H₂₇NO₄: C, 53.97; H, 7.81; N, 5.71. Found: C, 53.11; H, 7.74; N, 5.96.

Tert-butyl 1-hexyl-4-hydroxy-5-oxopyrrolidine-3-carboxylate (11).

Brown liquid; c.a. 97%; d.r. 35:65; ¹H NMR (300 MHz, CDCl₃) δ 0.88_(A+B) (t, 3H, -CH₃), 1.28_(A+B) (m, 2H, -CH₂), 1.47_(A) and 1.48_(B) (m, 3H, -CH₃), 4.53_(A) and 4.54_(B) (d, H, -CHOH); ¹³C NMR (CDCl₃) δ 14.01_(A+B) (-CH₃), 22.49_(A+B) (-CH₂CH₃), 26.38_(A) and 26.93_(B) (-CH₂CH₂CH₃), 28.06_(A) and 28.11_(B) (-CCH₃), 31.41_(A) (-CH₂CH₂CH₃),

31.44_(B) (-CH₂CH₂CH₃), 42.99_(A) and 43.06_(B) (-CH₂N), 45.82_(A+B) (-CHCH₂N), 47.09_(A+B) (-CH₂N), 70.70_(A) and 72.35_(B) (-CHOH), 81.83_(A) and 81.92_(B) (-CCH₃), 169.58_(A) and 170.84_(B) (C=O), 172.73_(A) and 173.14_(B) (NC=O). FT-IR (neat, cm⁻¹) 3354, 2937, 2877, 1731, 1692, 852. Anal. Calcd for C₁₁H₁₉NO₅: C, 63.13; H, 9.54; N, 4.91. Found: C, 62.96; H, 9.39; N, 5.22.

Tert-butyl 1-butyl-4-hydroxy-5-oxopyrrolidine-3-carboxylate (12). Brown

liquid; c.a. 96% ; d.r. 33:67; ¹H NMR (300 MHz, CDCl₃) δ 0.92_(A+B) (t, 3H, -CH₃), 1.32_(A+B) (m, 2H, -CH₂), 1.47_(A) and 1.48_(B) (-CH₃), 3.89_(A+B) (-CH), 4.54_(A) and 4.57_(B) (d, H, -CHOH); ¹³C NMR (CDCl₃) δ 13.70_(A+B) (-CH₃), 19.91_(A+B) (-CH₂CH₃), 28.01_(A) and 28.05_(B) (-CCH₃), 42.62_(A) and 43.66_(B) (-CH₂N), 43.36_(A) and 45.85_(B) (-CHCH₂N), 46.41_(A) and 47.08_(B) (-CH₂N), 70.68_(A) and 72.36_(B) (-CHOH), 81.76 and 81.88 (-CCH₃), 169.55_(A) and 170.88_(B) (C=O), 172.87_(A) and 173.26_(B) (NC=O). FT-IR (neat, cm⁻¹) 3358, 2958, 2876, 1738, 1692, 846. Anal. Calcd for C₁₃H₂₃NO₄: C, 60.68; H, 9.01; N, 5.44. Found: C, 60.48; H, 8.86; N, 5.78.

Tert-butyl 4-hydroxy-1-(2-hydroxyethyl)-5-oxopyrrolidine-3-carboxylate (13).

Brown liquid; c.a. 96%; d.r. 35:65; ¹H NMR (300 MHz, CDCl₃) δ 1.37_(A) and 1.38_(B) (s, 3H, -CH₃), 3.09_(A+B) (-CH), 4.46_(A) and 4.50_(B) (d, H, -CHOH); ¹³C NMR (CDCl₃) δ 28.02_(A+B) (-CCH₃), 44.33_(A) and 45.85_(B) (-CH₂N), 45.82_(A+B) (-CHCH₂N), 47.27_(A+B) (-CH₂N), 59.24_(A+B) (-CH₂OH), 70.87_(A) and 72.36_(B) (-CHOH), 81.96_(A) and 82.08_(B) (-CCH₃), 170.37_(A) and 170.88_(B) (C=O), 173.64_(A) and 174.09_(B) (NC=O). FT-IR (neat, cm⁻¹) 3367, 2955, 2865, 1743, 1697, 1271,

740. Anal. Calcd for $C_{11}H_{19}NO_5$: C, 53.87; H, 7.81; N, 5.71. Found: C, 53.38; H, 7.98; N, 6.06.

Synthesis of cyclic hydroxamic acid 14. Methyl 2-carboethoxyhydroxymethylacrylate (53.14 mmol) was added to a 50 ml tube equipped with an argon gas inlet. The reaction tube was then purged with argon for 30 minutes and sealed with a rubber septum. Hydroxylamine was added dropwise in large excess (150.21 mmol) to the previous mixture and the resulting solution was allowed to stir for 24 hours at room temperature. Upon reaction completion, monitored by 1H NMR, the solvent was removed under reduced pressure to give compounds **14** as a white powder consisting of a mixture of two diastereoisomers (A and B, d.r. 37:63) in c.a. 98% yield.

1H NMR (300 MHz, D_2O) δ 3.09_(A+B) (-CH), 4.13_(A) and 4.22_(B) (d, H, -CHOH); ^{13}C NMR (D_2O) δ 38.49_(A) and 42.95_(B) (-CH₂N), 48.49_(A) and 48.76_(B) (-CHCH₂), 59.24_(A+B) (-CH₂OH), 70.87_(A) and 72.36_(B) (-CHOH), 164.94_(A) and 165.10_(B) (C=O), 168.25_(A) and 168.75_(B) (NC=O). FT-IR (neat, cm^{-1}) 3370, 1743, 1697, 1271, 741.

REFERENCES

- 1 Meyers, A.I.; Snyder, L. *J. Org. Chem.* **1993**, *58*, 36–42.
- 2 Bergmann, R.; Gericke, R. *J. Med. Chem.* **1990**, *33*, 492–504.
- 3 Corey, E.J.; Li, W.-D.Z. *Chem. Pharm. Bull.* **1999**, *47*, 1–10.
- 4 Nilsson, B. M.; Ringdhal, B.; Hacksell, U. A. *J. Med. Chem.* **1990**, *33*, 580–584.
- 5 (a) Hanessian, S.; Ratovelomanana, V. *Synlett* **1990**, 501–503; (b) Russ, P.L.; Caress, E.A. *J. Org. Chem.* **1976**, *41*, 149–151; (c) Kornet, M. J.; Thio, P.A.; Tan, S.I. *J. Org. Chem.* **1968**, *33*, 3637–3639; (d) Ghelfi, F.; Bellesia, F.; Forti, L.; Ghirardini, G.; Grandi, R.; Libertini, E.; Montemaggi, M. C.; Pagnoni, U. M.; Pinetti, A.; De Buyck, L.; Parsons, A. F. *Tetrahedron* **1999**, *55*, 5839–5852; (e) Cossy, J.; Cases, M.; Pardo, D. G. *Synlett* **1998**, 507–509; (f) Murakami, S.; Takemoto, T.; Shimizu, Z. *J. Pharm. Soc. Jpn.* **1953**, *73*, 1026–1028.
- 6 Currie, B.L.; Sievertsson, H.; Bogentoft, C.; Chang, J.K.; Folkers, K.; Bowers, C.Y.; Doolittle, R.F.; *Biochem. Biophys. Res. Commun.* **1971**, *42*, 1180–1184.
- 7 Dominguez, C.; Chen, G.; Xi, N.; Xu, S.; Han, N.; Liu, Q.; Huang, Q.; Siegmund, A.; Handley, M.; Liu, L.; Kiselyov, A. S. PCP Int. Appl. WO 0144230 A1 20010621, **2001**.
- 8 Ishihara, Y.; Imamura, S.; Hashiguchi, S.; Nishimura, O.; Kanzaki, N.; Baba, M. Eur. Pat. Appl. No. EP 1180513 A1 20020220, **2002**.

- 9 Fuji, S.; Kawamura, H.; Watanabe, S.; Eur. Pat. Appl. No. EP 0393607 A2 19901024, **1990**.
- 10 Bender, P.E.; Christensen IV, S.B. PCP Int. Appl. No. WO 9307141 A1 19921002, **1992**.
- 11 Kenda, B.M.; Matagne, A.C.; Talaga, P.E.; Pasau, P.M.; Differding, E.; Lallemand, B.I.; Frycia, A.M.; Moureau, F.G.; Klitgaard, H.V.; Gillard, M.R.; Fuks, B.; Michel, P. *J. Med. Chem.* **2004**, *47*, 530-549.
- 12 Beltaïef, I.; Besbes, R.; Ben Amor, F.; Amri, H.; Villiéras, M.; Villiéras, J. *Tetrahedron* **1999**, *55*, 3949–3958.
- 13 Arvanitis, E.; Motevalli, M.; Wyatt, P. B. *Tetrahedron Lett.* **1996**, *37*, 4277–4280.
- 14 (a) Maier, M.S.; González Marimon, D.I.; Stortz, C.A.; Adler, M.T. *J. Nat. Prod.* **1999**, *62*, 1565–1567; (b) Forzato, C.; Nitti, P.; Pitacco, G.; Valentin, E. *Targets in Heterocyclic Systems, Chemistry and Properties*; Attanasi, O.; Spinelli, D., Eds. **1999**, *3*, 93–115; (c) Forster, A.; Fitremann, J.; Renaud, P. *Tetrahedron Lett.* **1998**, *39*, 7097–7100.
- 15 (a) Maiti, G.; Roy, S.C. *J. Chem. Soc., Perkin Trans.* **1996**, 403–404; (b) Park, B.K.; Nakagawa, M.; Hirota, A.; Nakayama, M. *J. Antibiot.* **1988**, *41*, 751–758.
- 16 Ghatak, A.; Sarkar, S.; Ghosh, S. *Tetrahedron* **1997**, *53*, 17335–17342.
- 17 Mahato, S.B.; Siddiqui, K.A.I.; Bhattacharya, G.; Ghosal, T.; Miyahara, K.; Sholichin, M.; Kawasaki, T. *J. Nat. Prod.* **1987**, *50*, 245–247.

- 18 (a) Miltzer, J.; Kattner, L.; Strecker, A.R.; Schroeder, C.; Buschmann, J.; Lehmann, C.; Luger, P. *J. Am. Chem. Soc.* **1991**, *113*, 4218–4229; (b) Miltzer, J.; Salimi, N.; Hartl, H. *Tetrahedron: Asymmetry* **1993**, *3*, 457–471; (c) Murta, M.M.; de Azevedo, M.B.M.; Greene, A.E. *J. Org. Chem.* **1993**, *58*, 7537–7541; (d) Vaupel, A.; Knochel, P. *J. Org. Chem.* **1996**, *61*, 5743–5753; (e) Takahata, H.; Uchida, Y.; Momose, T. *J. Org. Chem.* **1995**, *60*, 5628–5633; (f) Zhu, G.; Lu, X. *Tetrahedron: Asymmetry* **1995**, *6*, 885–892; (g) Gatah, A.; Sarkar, S.; Ghosh, S. *Tetrahedron* **1997**, *53*, 17335–17342; (h) Mandal, P.K.; Roy, S.C. *Tetrahedron* **1999**, *55*, 11395–11398; (i) Bella, M.; Margarita, R.; Orlando, C.; Orsini, M.; Parlanti, L.; Piancatelli, G. *Tetrahedron Lett.* **2000**, *41*, 561–565; (j) Bohm, C.; Reiser, O. *Org. Lett.* **2001**, *3*, 1315–1318; (k) Loh, T.-P.; Lye, P.-L. *Tetrahedron Lett.* **2001**, *42*, 3511–3514; (l) Ariza, X.; Garcia, J.; López, M.; Montserrat, L. *Synlett* **2001**, 120–122.
- 19 (a) Drioli, S.; Felluga, F.; Forzato, C.; Nitti, P.; Pitacco, G. *Chem. Commun.* **1996**, 1289–1290; (b) Drioli, S.; Felluga, F.; Forzato, C.; Nitti, P.; Pitacco, G.; Valentin, E. *J. Org. Chem.* **1998**, *63*, 2385–2388.
- 20 (a) Patra, R.; Maiti, S.B.; Chatterjee, A.; Chakravarty, A.K. *Tetrahedron Lett.* **1991**, *32*, 1363–1366; (b) Dembele, Y.A.; Belaud, C.; Villieras, J. *Tetrahedron: Asymmetry* **1992**, *3*, 511–514; (c) El Alami, L.; Belaud, C.; Villieras, J. *Synthesis* **1993**, 1213–1214.
- 21 Fikentscher, R.; Hahn, E.; Kud, A.; Oftring, A. Ger. Patent DE 3444097 A1 19860605, **1986**.

- 22 Baylis, A.B.; Hillman, M.E.D. *Chem. Abstr.* **1972**, 77, 34174.
- 23 Morita, K.; Suzuki, Z.; Hirose, H. *Bull. Chem. Soc. Jpn.* **1968**, 41, 2815.
- 24 Becht, J.M.; De Lamo Marin, S.; Maruani, M.; Wagner, A.; Mioskowski, C.
Tetrahedron **2006**, 62, 4430.

CHAPTER VII

SYNTHESIS OF POLYFUNCTIONAL 2-PYRROLIDINONE ACID DERIVATIVES
FROM METHYL 2-CARBOETHOXYHYDROXYMETHYL-ACRYLATE**Abstract**

The synthesis of new polyfunctional 2-pyrrolidinone acid derivatives from methyl 2-carboethoxyhydroxymethylacrylate is described. These alkenes present an extremely high reactivity upon Michael addition with primary amines leading to a simple, mild, and efficient route to the preparation of new polyfunctional pyrrolidinones. Hydrogen bonding study via NMR on different isomeric forms of pyrrolidinone acid derivatives confirmed compound structures and also permitted determining molecular interactions, either intra- or intermolecular, that predominate in each molecular configuration.

Introduction

2-Pyrrolidinones have attracted a great amount of interest over the last decade. Many are optically active and have found applications ranging from biology to biochemistry to pharmaceuticals.¹⁻⁵ The formation of 2-pyrrolidinones from itaconic acid derivatives is a viable approach than has been widely used in the past. For example, racemic 1-benzyl-3-alkyl-4-methoxycarbonyl-2-pyrrolidinones were prepared from β -alkylated itaconates and benzylamine through a conjugate addition–lactamization sequence.⁶ (S)-(-)-4-methoxycarbonyl-2-pyrrolidinone was also synthesized by Wyatt, et al., starting from itaconic acid and (S)-(-)-1-phenylethylamine.⁷ Finally, Valentin, et al., have

reported the formation of aza analogues of paraconic acid methyl ester starting with dimethyl itaconate.⁸

Herein, we report new polyfunctional pyrrolidinone acid derivatives (Figure 7.1) obtained via Michael addition reaction of aliphatic primary amine with methyl 2-carboethoxyhydroxymethylacrylate, which in turn was obtained by the Baylis-Hillman pathway from commercial acrylate.

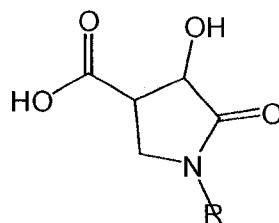


Figure 7.1. Polyfunctional 2-pyrrolidinone acid derivatives.

Results and discussion

Preparation of multifunctional pyrrolidinone acid derivatives 2 and 3. Methyl 2-carboethoxyhydroxymethylacrylate **1** was first synthesized via the Baylis-Hillman pathway following the procedure reported in chapter V.^{9,10} Methyl 1-hexyl-4-hydroxy-5-oxopyrrolidine-3-carboxylate **2** and methyl 1-methyl-4-hydroxy-5-oxopyrrolidine-3-carboxylate **3** were prepared in a fast and efficient manner by reaction of methyl 2-carboethoxyhydroxymethylacrylate with one equivalent of hexylamine and methylamine respectively, following the synthetic procedure illustrated in Chapter VI. From these compounds, we were interested in forming the corresponding carboxylic acid derivatives.

Carboxylic acid-containing 2-pyrrolidinone derivatives are interesting compounds that may exhibit interesting properties like their naturally occurring oxygen analogues, which are generally known as paraconic acids. Such

compounds possess important biological properties.¹² Among these numerous compounds (-)-methylenolactocin¹³ is isolated from the culture filtrate of *Penicillium sp.* and shows antitumor and antibiotic activity; protolichesterinic acid¹⁴ is isolated from several species of moss *Cetraria* and is an antitumor and antibacterial compound; while (-)-phaseolinic acid¹⁵ is a metabolite of a fungus, *Macrophomina phaseolina*. We decided to synthesize the carboxylic acid analog of pyrrolidinone derivatives **2** and **3** by forming first the sodium carboxylate using one equivalent of sodium hydroxide in water. Precipitation in cold acetone allowed isolation of the salt in quantitative yield. Treatment of the salt dispersion in acetone with dilute hydrochloric acid led to 1-hexyl-4-hydroxy-5-oxopyrrolidine-3-carboxylic acid **4** and 1-methyl-4-hydroxy-5-oxopyrrolidine-3-carboxylic acid **5**, each as a mixture of two diastereoisomers. Separation of the two stereoisomers was achieved by reprecipitation from acetone at -15 °C over 2 days.¹⁶

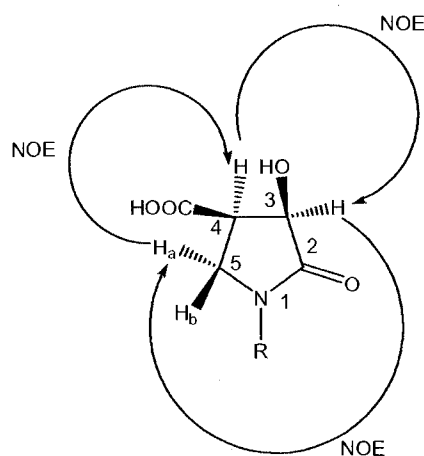


Figure 7.2. NOE correlations.

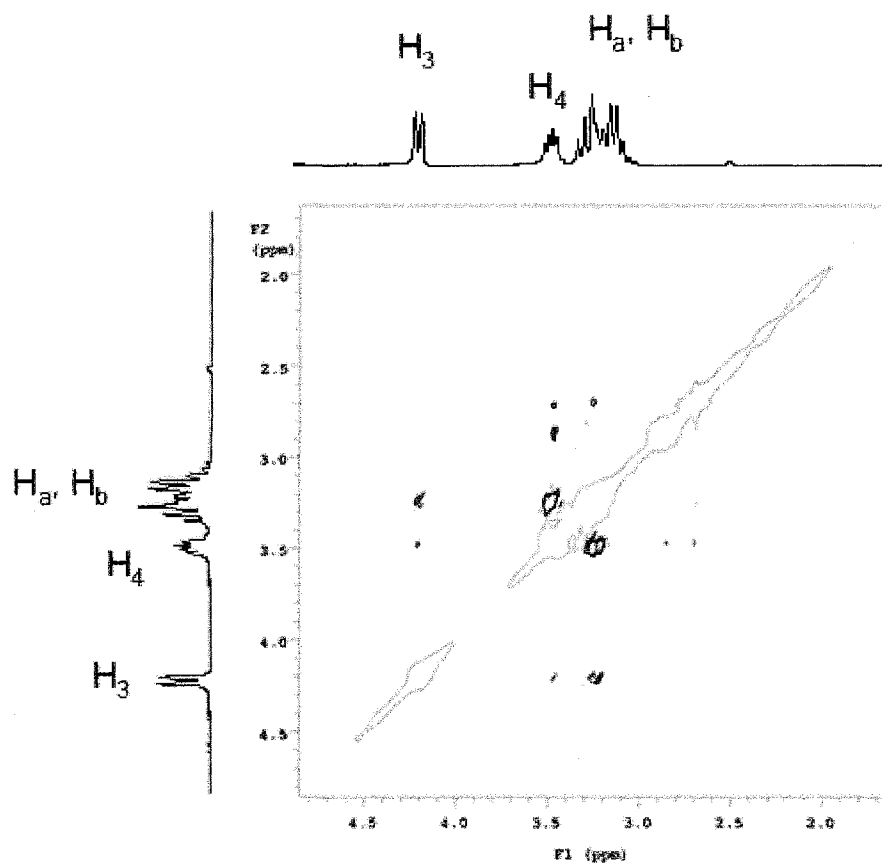
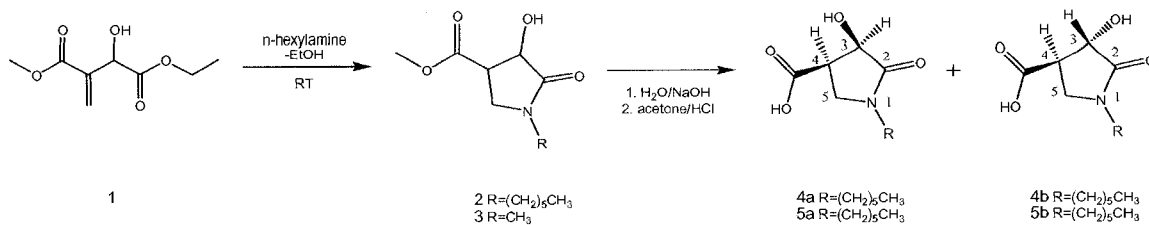


Figure 7.3. NOESY spectrum of isomer **4b** (DMSO-*d*₆).

NMR spectroscopy and elemental analysis confirmed compounds structures. DEPT and gCOSY experiments allowed accurate assignment of the NMR spectra peaks. The stereochemistry of the separated diastereoisomers was established by their NOESY spectra in which the strong NOEs between H-3, H-4, H_a-5, and H_b-5 were studied (Figure 7.2). The NOE spectra of separated diastereoisomers for compound **4** showed a lower enhancement of H-3 proton for the *trans* isomer than for the *cis* isomer (Figure 7.3). Thus, we concluded that the stereochemistry of **4a** and **4b** are of the *cis* and *trans* configurations, respectively (Scheme 7.1). ¹³C NMR spectra of both isomers are shown in Figure 7.4. The same conclusion was drawn for 2-pyrrolidinone **5** (**5a** is *cis* and **5b** is *trans*).



Scheme 7.1. Synthesis of 2-pyrrolidinone acid derivatives.

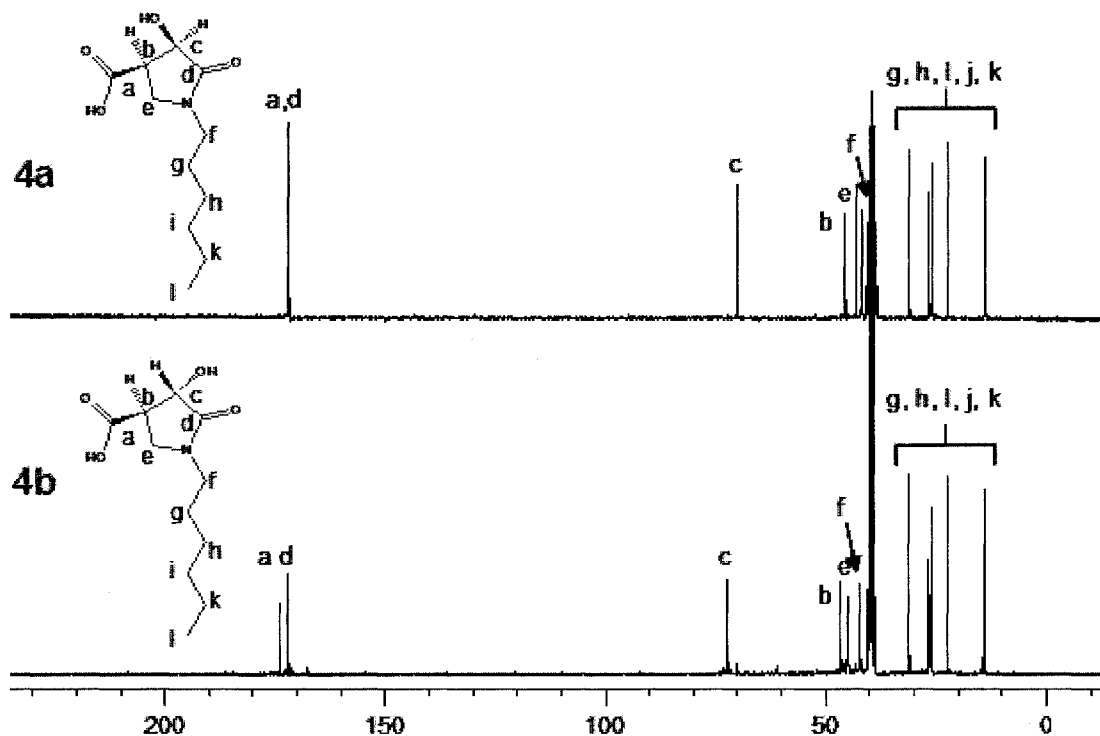
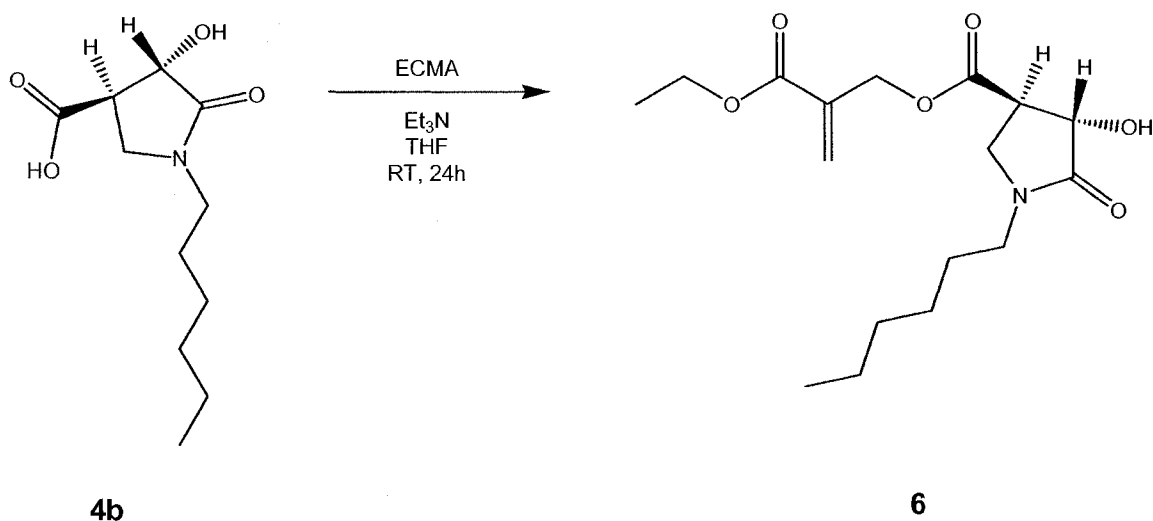


Figure 7.4. ¹³C NMR spectra of 2-pyrrolidinones 4a and 4b (DMSO-d₆).

We were interested in the subsequent preparation of a methacrylate-based monomer that incorporates a substituted 2-pyrrolidinone group. Such a monomer could be further polymerized via free radical polymerization technique and could potentially confer enhanced mechanical properties and adhesion to the resulting material. Ethyl α -chloromethylacrylate (ECMA) was reacted with both isomers individually in presence of triethylamine in tetrahydrofuran at room temperature to form the corresponding methacrylate derivative. We found that

the reaction would only proceed with **4b** leading to the formation of monomer **6** as shown in Scheme 7.2, while the same reaction, carried out with **4a** in DMSO, didn't lead to any product formation. It is believed that the molecular conformation has a strong effect on its reactivity, as demonstrated by this surprising difference in behavior. ^{13}C NMR and FT-IR spectra for monomer **6** are displayed in Figures 7.5 and 7.6.



Scheme 7.2. Synthesis of 2-pyrrolidinone-containing monomer **6**.

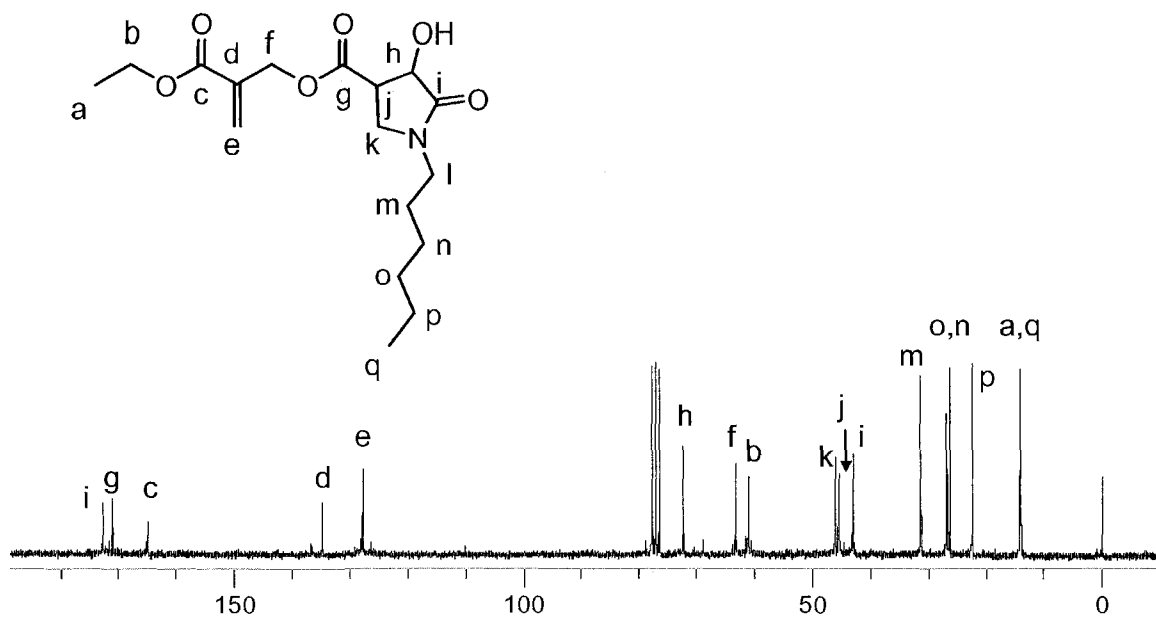


Figure 7.5. ^{13}C NMR spectrum of monomer **6** (CDCl_3).

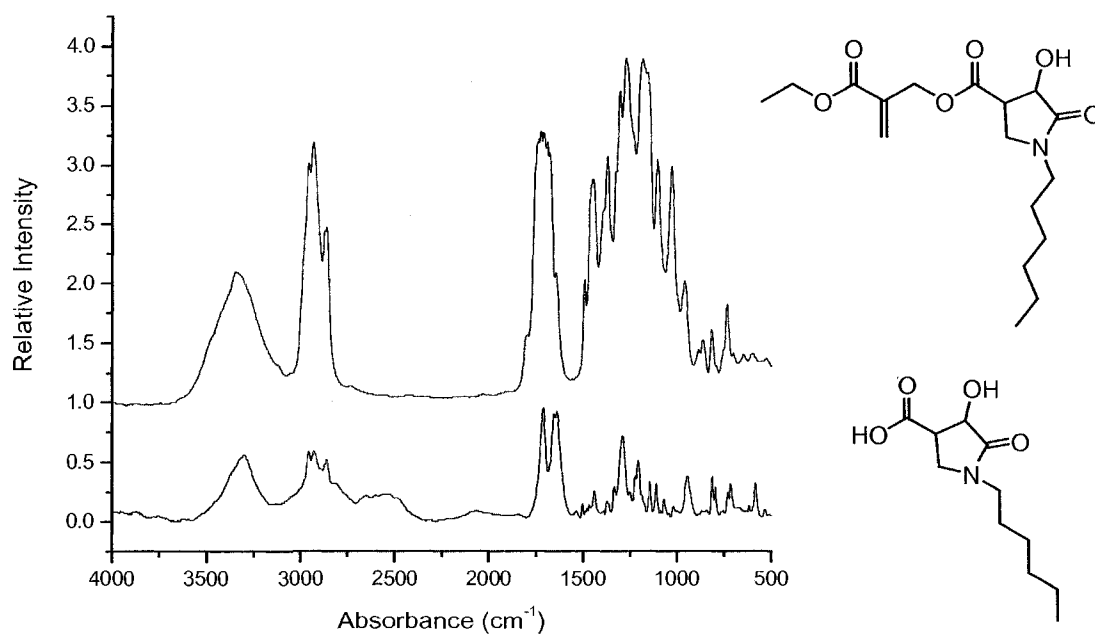


Figure 7.6. FT-IR spectra of intermediate **4** and monomer **6** (NaCl).

Crystals of isomers **5a** and **5b** were grown from methanol over a period of two days. Two different crystal shapes were observed using a polarized microscope as shown in Figure 7.7.

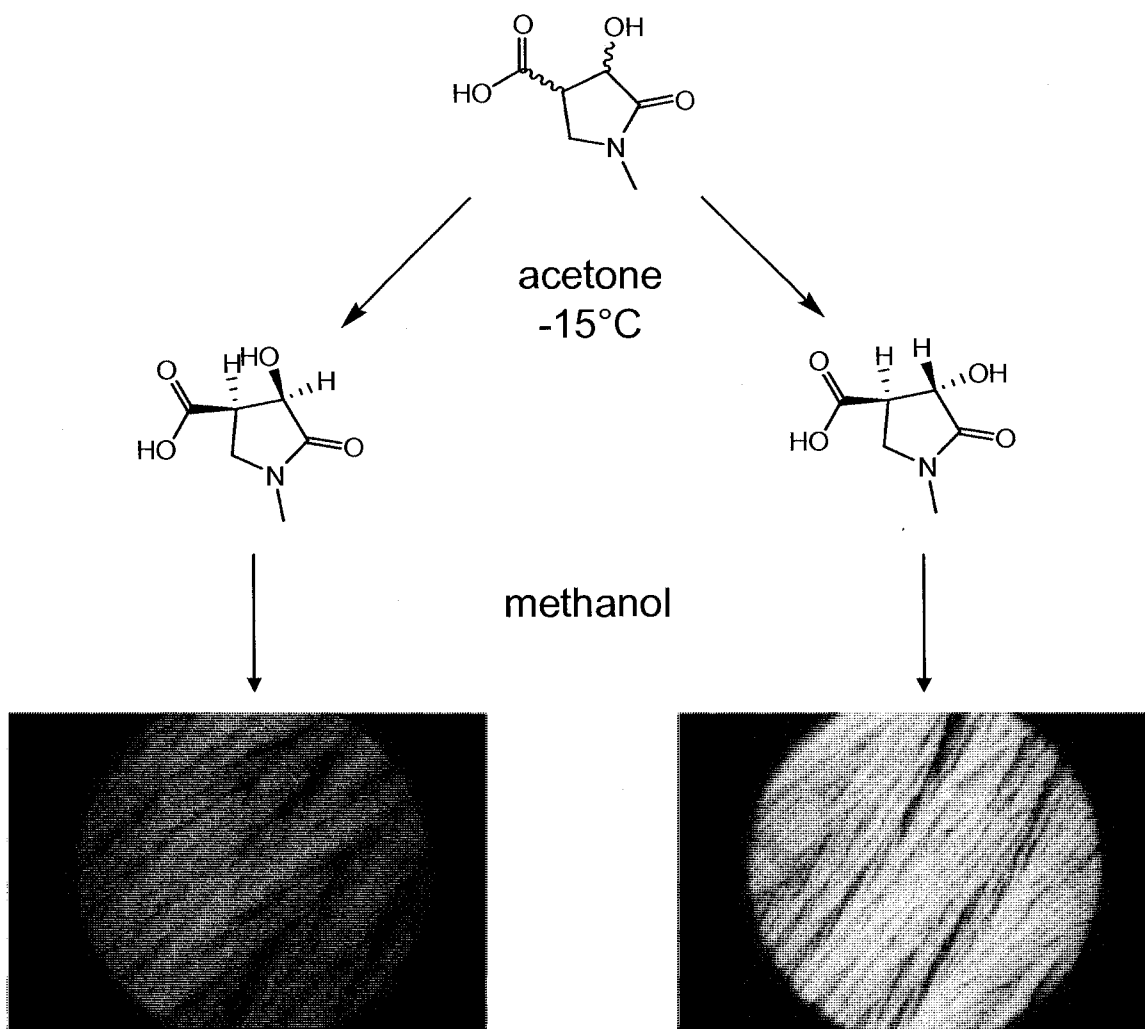


Figure 7.7. Polarized microscope photographs of crystals of **5a** and **5b**.

NMR study of hydrogen bond formation in 2-pyrrolidinone acid 5. NMR experiments involving compound **5** were carried out at different temperatures (25, 40, 65, 80 and 120 °C) in DMSO-d₆. After equilibrating at temperature, a ¹³C NMR spectrum was acquired for compound **5** composed of the isomeric mixture (**5a** and **5b**). Figure 7.8 displays the ¹³C NMR spectrum of compound **5**. Figure

7.9 displays the different spectra obtained at each temperature. First, we noticed a shift up-field with increasing temperature for all the carbon peaks corresponding to the carbonyls. This is consistent with disruption of the intermolecular hydrogen bonding causing an increase in the electronegativity of the corresponding carbonyls inducing the chemical shift variations observed.

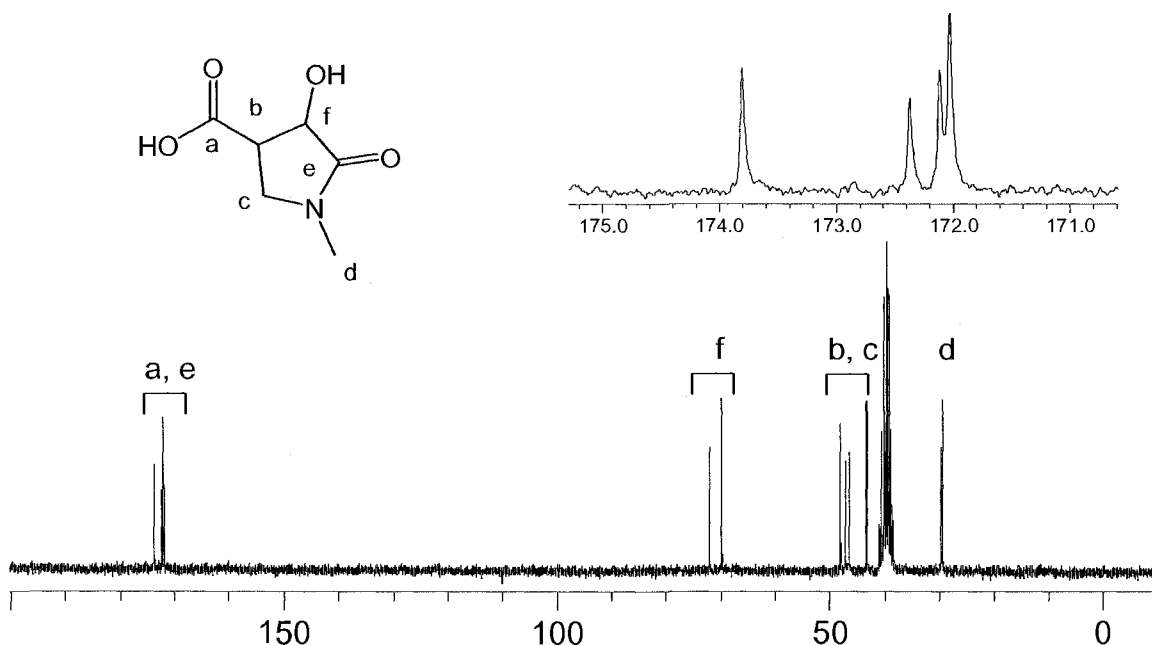


Figure 7.8. ^{13}C NMR spectrum of 4-hydroxy-1-methyl-5-oxopyrrolidine-3-carboxylic acid **5** (DMSO- d_6).

We also noticed a difference in the chemical shift variation rate between the two sets of carbonyl carbon peaks corresponding to the two different isomers in the mixture (Figure 7.9). DEPT and COSY experiments allowed the accurate assignments for those peaks. The two tallest peaks correspond to the *trans* isomer **5a** while the two smaller peaks belong to the *cis* isomer **5b**.

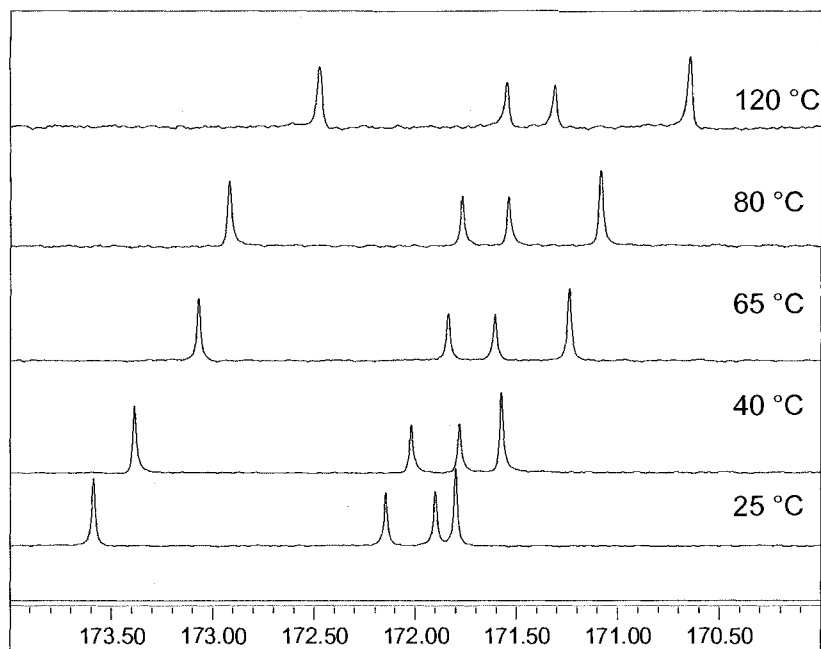


Figure 7.9. ^{13}C NMR spectra of 2-pyrrolidinone **5** at different temperatures (DMSO- d_6).

Figure 7.10 illustrates the variation profiles for the chemical shifts of the carbonyls composing the 2-pyrrolidinone derivatives. A linear correlation between the chemical shifts and the temperature was found. The difference in rate of change can be attributed to the different hydrogen bonding interactions occurring in each isomer. For instance, the *cis* form is more likely able to possess intramolecular hydrogen bonding which is more thermally stable than intermolecular interactions which the *trans* isomer possesses. By modeling and minimizing the energy for each isomer (using Chem3D Ultra v8.0) this behavior is illustrated as shown in Figure 7.11.

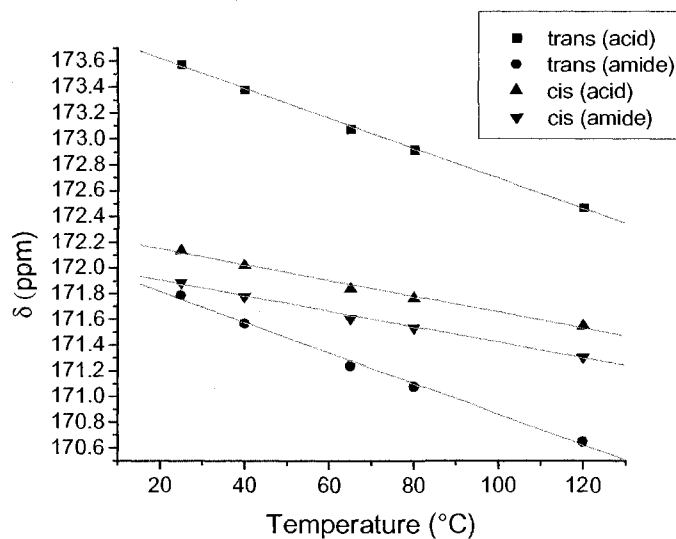


Figure 7.10. 2-Pyrrolidinone **5** carbonyl chemical shifts as function of temperature.

The pseudo 6-membered ring formed in the *cis* configuration as illustrated in Figure 7.11 (group circled), leads to a more stable form of hydrogen bonding interactions which less sensitive to temperature than the intermolecular interactions induced exclusively in the *trans* form.

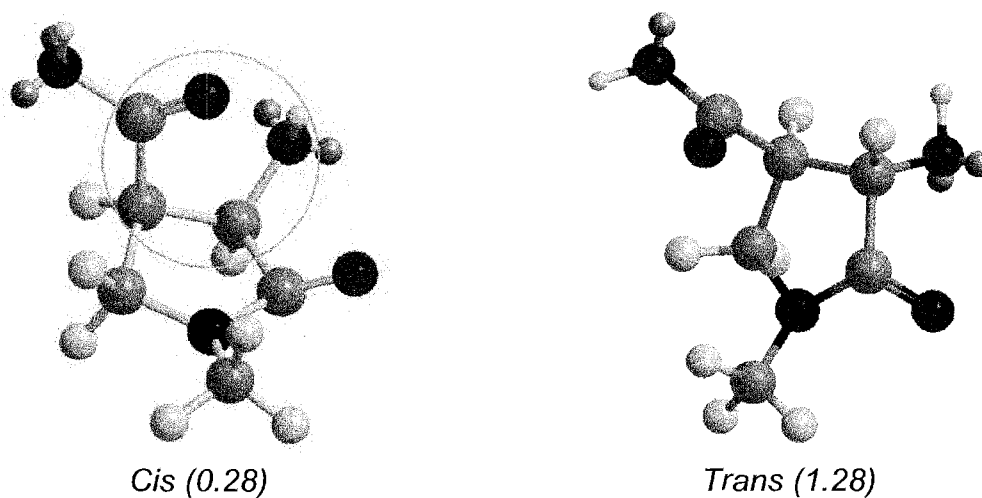


Figure 7.11. Minimized energies for *cis* and *trans* isomers **5a** and **5b**.

Conclusions

We have demonstrated that multifunctional 2-pyrrolidinone derivatives can be easily synthesized by means of a fast and efficient Michael addition/cyclization reaction involving methyl 2-(carboethoxyhydroxymethyl) acrylate and aliphatic primary amine. Subsequent separation of the two diastereoisomers was achieved by simple recrystallization from acetone, opening up potential exploration of these new heterocycles for application in the synthesis of natural product analogs and new biologically active monomers and polymers. Hydrogen bonding study via NMR confirmed product structures and also permitted determination of the molecular interactions (hydrogen bonding), either intra- or intermolecular, that predominate in each isomeric form. For instance, it is believed that the *cis* configuration leads to the formation of a pseudo 6-membered ring hydrogen bond.

Experimental

Materials. Ethyl glyoxylate, 50% in toluene, was purchased from Alfa Aesar and used as received. 4-Diaza[2.2.2]bicyclooctane (DABCO), thionyl chloride and methyl acrylate were purchased from Aldrich Chemical Company and used without further purification. Hexylamine (HA) purchased from Aldrich Chemical Company and used as received. All solvents were purchased from Acros Chemical Company, Fisher, or Aldrich Chemical Company. Ethyl α -hydromethylacrylate (ECMA) was synthesized according to previously reported procedure.¹⁴

Analyses. Solution ^1H and ^{13}C NMR spectra of the monomers were collected at room temperature with TMS as an internal reference on a Varian Mercury 300 MHz spectrometer operating at a frequency of 75.47 MHz for carbon. FT-IR spectra were obtained using a Mattson Galaxy series 5000 FTIR spectrometer. Temperature controlled experiments were carried out using an INOVA 500 MHz spectrometer.

Synthesis of methyl 2-(carboethoxyhydroxymethyl)acrylate 1. Ethyl glyoxylate, 50 wt-% in toluene (20.39 g, 199.7 mmol), DABCO (3.64 g, 32.4 mmol), and methyl acrylate (199.7 mmol) were added to a 250 ml round-bottom flask. The mixture was stirred at room temperature for two hours. The crude solution was then concentrated under reduced pressure. The resulting mixture was washed with three aliquots of saturated sodium chloride solution followed by three aliquots of deionized water. The organic phase was then dried over a bed of sodium sulfate. Vacuum distillation of the residue gave the corresponding methyl 2-carboethoxyhydroxymethylacrylate **1** as a clear liquid; b.p. 135-137°C (20 mm Hg), in c.a. 68% isolated yield.

Methyl 2-carboethoxyhydroxymethylacrylate **1**: ^1H NMR (300 MHz, CDCl_3) δ 1.26 (t, 3H, $-\text{CH}_3$), 3.68 (s, H, $-\text{OH}$), 3.78 (s, 3H, $-\text{OCH}_3$), 4.26 (q, 2H, $-\text{CH}_2\text{CH}_3$), 4.88 (s, H, $-\text{CHOH}$), 5.96 and 6.37 (s, 2H, $-\text{CH}_2=\text{C}$); ^{13}C NMR (CDCl_3) δ 14.04 ($-\text{CH}_3$), 52.12 ($-\text{OCH}_3$), 62.20 ($-\text{CH}_2\text{CH}_3$), 71.19 ($-\text{CHOH}$), 128.96 ($\text{CH}_2=\text{C}$), 138.08 ($\text{C}=\text{CH}_2$), 165.68 and 172.30 ($\text{C}=\text{O}$). FT-IR (NaCl, cm^{-1}) 3515, 2996, 1739, 1643, 1446, 1097, 823. Anal. Calcd for $\text{C}_8\text{H}_{15}\text{O}_5 \cdot 0.25^*\text{H}_2\text{O}$: C, 50.59; H, 6.49. Found: C, 50.28; H, 6.28.

Preparation of methyl 1-hexyl-4-hydroxy-5-oxopyrrolidine-3-carboxylate 2 and methyl 1-methyl-4-hydroxy-5-oxopyrrolidine-3-carboxylate 3. The 2-pyrrolidinone derivatives were synthesized by adding compound **1** (10 g, 53.14 mmol) to a 50 ml tube equipped with an argon gas inlet. The reaction tube was then purged with argon for 30 minutes and sealed with a rubber septum. The corresponding amine (54.21 mmol) was added dropwise and the resulting solution was allowed to stir at room temperature under an argon blanket. Upon reaction completion as monitored by ^1H NMR, the solvent and the excess amine were removed under reduced pressure to afford methyl 1-hexyl-4-hydroxy-5-oxopyrrolidine-3-carboxylate **2** and methyl 1-methyl-4-hydroxy-5-oxopyrrolidine-3-carboxylate **3** as mixtures of two diastereoisomers (A and B)

Methyl 1-hexyl-4-hydroxy-5-oxopyrrolidine-3-carboxylate **2**: brown liquid; yield 98%; d.r. 42:58; ^1H NMR (300 MHz, CDCl_3) δ 0.88 (t, 3H, $-\text{CH}_3$), 1.28 (m, 2H, $-\text{CH}_2$), 1.52 (m, 2H, $-\text{CH}_2\text{CH}_2\text{N}$), 3.74_(A) and 3.77_(B) (s, 3H, $-\text{CH}_3$), 4.59_(A) and 4.60_(B) (d, H, $-\text{CHOH}$); ^{13}C NMR (CDCl_3) δ 14.17_(A+B) ($-\text{CH}_3$), 22.52_(A+B) ($-\text{CH}_2\text{CH}_3$), 26.38 and 26.85 ($-\text{CH}_2\text{CH}_2\text{CH}_3$), 31.41 and 31.44 ($-\text{CH}_2\text{CH}_3$), 46.07 and 46.29 ($-\text{CH}_2\text{N}$), 43.07 and 45.62 ($-\text{CHCH}_2\text{N}$), 42.96 and 43.04 ($-\text{CH}_2\text{N}$), 52.16 and 52.53 ($-\text{OCH}_3$), 70.46 and 72.43 ($-\text{CHOH}$), 170.74 and 172.25 ($\text{C}=\text{O}$), 172.82 and 173.09 ($\text{NC}=\text{O}$). FT-IR (NaCl, cm^{-1}) 3363, 2958, 2935, 2866, 1741, 1695, 1278, 740. Anal. Calcd for $\text{C}_{12}\text{H}_{21}\text{NO}_4$: C, 59.24; H, 8.70; N, 5.76. Found: C, 59.42; H, 8.71; N, 5.84.

Methyl 1-methyl-4-hydroxy-5-oxopyrrolidine-3-carboxylate **3**: brown liquid; yield 97%; d.r. 39:71; ^1H NMR (300 MHz, CDCl_3) δ 2.88 (s, 3H, $-\text{CH}_3$), 3.77 (s, 3H, -

CH₃), 4.56_(A) and 4.60_(B) (d, H, -CHOH); ¹³C NMR (CDCl₃) δ 29.40_(A+B) (-NCH₃), 42.85_(A) and 48.52_(B) (-CH₂N), 45.88_(A) and 47.72_(B) (-CHCH₂N), 52.20_(A) and 52.54_(B) (-OCH₃), 70.11_(A) and 72.18_(B) (-CHOH), 170.66_(A) and 172.92_(B) (C=O), 172.20_(A) and 173.21_(B) (NC=O).

Synthesis of 1-hexyl-4-hydroxy-5-oxopyrrolidine-3-carboxylic acid 4 and 1-methyl-4-hydroxy-5-oxopyrrolidine-3-carboxylic acid 5. Sodium hydroxide (0.5 g, 12.4 mmol) was dissolved in 10 ml of deionized water. The corresponding 2-pyrrolidinone ester derivative (12.33 mmol) was added dropwise to this solution. The resulting mixture was allowed to stir for two hours. Upon reaction completion, the salt was precipitated in acetone, filtered off and dried under reduced pressure. The resulting white powder was then redispersed in 20 ml of acetone and further treatment with dilute hydrochloric acid led to the corresponding 2-pyrrolidinone acid derivatives **4** and **5** as mixtures of isomers (A and B). Further recrystallization from acetone led to subsequent isomers separation.

1-Hexyl-4-hydroxy-5-oxopyrrolidine-3-carboxylic acid diastereoisomer 4a. White solid (from cold acetone); yield 22%; m.p. 188°C; ¹H NMR (300 MHz, DMSO-d₆) δ 0.82 (t, 3H, -CH₃), 1.21 (m, 2H, -CH₂), 1.40 (m, 2H, -CH₂CH₂N), 4.21 (d, H, -CHOH); ¹³C NMR (DMSO-d₆) δ 14.32 (-CH₃), 22.47 (-CH₂CH₃), 26.19 (-CH₂CH₂CH₃), 31.35 (-CH₂CH₃), 43.46 (-CH₂N), 45.90 (-CHCH₂N), 40.66 (-CH₂N), 70.23 (-CHOH), 172.03 (C=O), 172.05 (NC=O). FT-IR (KBr, cm⁻¹) 3305,

2956, 2933, 2863, 1712, 1656, 1290, 948. Anal. Calcd for C₁₁H₁₉NO₄: C, 57.62; H, 8.35; N, 6.11. Found: C, 57.27; H, 8.50; N, 6.00.

1-Hexyl-4-hydroxy-5-oxopyrrolidine-3-carboxylic acid diastereoisomer 4b. Brown oil; chromatographed on silica gel with 1:1 hex-EtOAc; yield 59%; ¹H NMR (300 MHz, DMSO-d₆) δ 0.84 (t, 3H, -CH₃), 1.23 (m, 2H, -CH₂), 1.41 (m, 2H, -CH₂CH₂N), 4.20 (d, H, -CHOH); ¹³C NMR (DMSO-d₆) δ 14.31 (-CH₃), 22.44 (-CH₂CH₃), 26.23 (-CH₂CH₂CH₃), 31.29 (-CH₂CH₃), 45.19 (-CH₂N), 46.74 (-CHCH₂N), 42.25 (-CH₂N), 72.37 (-CHOH), 172.25 (C=O), 173.83 (NC=O). FT-IR (NaCl, cm⁻¹) 3353, 2904, 2902, 2869, 1727, 1711, 1654, 1273, 737. Anal. Calcd for C₁₁H₁₉NO₄: C, 57.62; H, 8.35; N, 6.11. Found: C, 57.35; H, 8.33; N, 6.03.

1-Methyl-4-hydroxy-5-oxopyrrolidine-3-carboxylic acid 5. White solid (from cold acetone); yield 34%; m.p. 190 °C; ¹H NMR (300 MHz, DMSO-d₆) δ 2.66_(A+B) (s, 3H, -CH₃), 2.87_(A+B) (m, H, -CHCH₂N), 3.22_(A+B) (t, H, -CH₂N), 3.44_(A+B) (t, H, -CH₂N), 4.18_(A+B) (d, H, -CHOH); ¹³C NMR (DMSO-d₆) δ 29.62_(A) and 29.73_(B) (-CH₃), 43.35_(A) and 48.17_(B) (-CH₂N), 46.54_(A) and 46.29_(B) (-CHCH₂N), 69.87_(A) and 72.06_(B) (-CHOH), 172.04_(A) and 172.14_(B) (C=O), 172.39_(A) and 173.77_(B) (NC=O).

Synthesis of ethyl α-(1-hexyl-4-hydroxy-5-oxopyrrolidine-3-carboxylate methyl) acrylate 6. Intermediate **4b** (2 g, 8.73 mmol) and 150 ppm of hydroquinone were added to 20 ml of dry THF in a 50 ml round bottom flask. ECMA (1.29 g, 8.73 mmol) was then added dropwise to this solution and the resulting mixture was allowed to stir overnight at room temperature. Upon reaction completion as monitored by NMR, the precipitate was filtered off and the

solvent removed under reduced pressure. Further purification via column chromatography on silica gel with 1:5 ethyl acetate:hexane gave ethyl α -(1-hexyl-4-hydroxy-5-oxopyrrolidine-3-carboxylate methyl) acrylate **6** as a brown oil in c.a. 78% yield.

^1H NMR (300 MHz, CDCl_3) δ 0.88 (t, 3H, $-\text{CH}_3$), 1.28 (m, 2H, $-\text{CH}_2$), 1.52 (m, 2H, $-\text{CH}_2\text{CH}_2\text{N}$), 4.25 (q, 2H, $-\text{CH}_2\text{CH}_3$), 4.59 (d, H, $-\text{CHOH}$), 4.91 (s, 2H, $-\text{CH}_2\text{O}$), 5.91 and 6.39 (s, 2H, $\text{CH}_2=\text{C}$); ^{13}C NMR (CDCl_3) δ 14.01 ($-\text{CH}_3$), 14.17 ($-\text{CH}_3$), 22.49 ($-\text{CH}_2\text{CH}_3$), 31.40 ($-\text{CH}_2\text{CH}_2\text{CH}_3$), 26.38 ($-\text{CH}_2\text{CH}_2\text{CH}_2\text{N}$), 26.93 ($-\text{CH}_2\text{CH}_2\text{N}$), 46.17 ($-\text{CH}_2\text{N}$), 43.07 ($-\text{CHCH}_2\text{N}$), 45.46 ($-\text{CH}_2\text{N}$), 61.12 ($-\text{CH}_2\text{CH}_3$), 63.34 ($-\text{CH}_2\text{O}$), 72.40 ($-\text{CHOH}$), 127.84 ($-\text{CH}_2=\text{C}$), 134.86 ($-\text{CCH}_2$), 165.04 and 171.11 ($-\text{C}=\text{O}$), 172.72 ($-\text{NC}=\text{O}$). FT-IR (NaCl, cm^{-1}) 3351, 2960, 2935, 2870, 1741, 1729, 1685, 1654, 1277, 819.

REFERENCES

- 1 Meyers, A.I.; Snyder, L.J. *Org. Chem.* **1993**, *58*, 36–42.
- 2 Bergmann, R.; Gericke, R.J. *Med. Chem.* **1990**, *33*, 492–504.
- 3 Corey, E.J.; Li, W.-D.Z. *Chem. Pharm. Bull.* **1999**, *47*, 1–10.
- 4 Nilsson, B.M.; Ringdhal, B.; Hacksell, U.A. *J. Med. Chem.* **1990**, *33*, 580–584.
- 5 (a) Hanessian, S.; Ratovelomanana, V. *Synlett* **1990**, 501–503; (b) Russ, P.L.; Caress, E.A. *J. Org. Chem.* **1976**, *41*, 149–151; (c) Kornet, M.J.; Thio, P.A.; Tan, S.I. *J. Org. Chem.* **1968**, *33*, 3637–3639; (d) Ghelfi, F.; Bellesia, F.; Forti, L.; Ghirardini, G.; Grandi, R.; Libertini, E.; Montemaggi, M.C.; Pagnoni, U.M.; Pinetti, A.; De Buyck, L.; Parsons, A.F. *Tetrahedron* **1999**, *55*, 5839–5852; (e) Cossy, J.; Cases, M.; Pardo, D.G. *Synlett* **1998**, 507–509; (f) Murakami, S.; Takemoto, T.; Shimizu, Z. *J. Pharm. Soc. Jpn.* **1953**, *73*, 1026–1028.
- 6 Beltaïef, I.; Besbes, R.; Ben Amor, F.; Amri, H.; Villieras, M.; Villieras, J. *Tetrahedron* **1999**, *55*, 3949–3958.
- 7 Arvanitis, E.; Motevalli, M.; Wyatt, P.B. *Tetrahedron Lett.* **1996**, *37*, 4277–4280.
- 8 Felluga, F.; Pitacco, G.; Prodan, M.; Pricl, S.; Visintin, M.; Valentin, E. *Tetrahedron: Asymmetry* **1999**, *12*, 3241–3249.
- 9 Fikentscher, R.; Hahn, E.; Kud, A.; Oftring, A. Ger. Patent DE 3444097 A1 19860605, **1986**.

- 10 Forster, A.; Fitremann, J.; Renaud, P. *Tetrahedron Lett.* **1998**, *39*, 7097–7100.
- 11 Maiti, G.; Roy, S.C. *J. Chem. Soc., Perkin Trans.* **1996**, *1*, 403–404.
- 12 Ghatak, A.; Sarkar, S.; Ghosh, S. *Tetrahedron* **1997**, *53*, 17335–17342.
- 13 Mahato, S.B.; Siddiqui, K.A.I.; Bhattacharya, G.; Ghosal, T.; Miyahara, K.; Sholichin, M.; Kawasaki, T. *J. Nat. Prod.* **1987**, *50*, 245–247.
- 14 Smith, T.J.; Mathias, L.J. *Biomacromolecules* **2002**, *3*, 1392–1399.

CHAPTER VIII
SYNTHESIS AND POLYMERIZATION OF NEW MULTIFUNCTIONAL
PYRROLIDINONE METHACRYLATE MONOMERS

Abstract

Methacrylates containing multifunctional 2-pyrrolidinone were synthesized in good yields. These monomers give very fast photopolymerization rates both in homopolymerizations and with hydroxyethyl methacrylate (HEMA) leading to crosslinked polymers. Soluble homopolymers were obtained via solution-free radical polymerization. Thermal analysis allowed illustrating both a beta and a glass transition for the polymer prepared.

Introduction

Copolymers containing *N*-vinylpyrrolidone (NVP) or hydroxyethyl methacrylate (HEMA) are used in many applications in the biomedical field, especially in contact lenses and biocoatings.¹⁻⁶ It was shown that NVP copolymers adhered to porcine intestine and created a hydrophilic surface for cell adhesion and cell growth.⁷ Copolymers of NVP and poly(ethylene glycol) diacrylate gave hydrogels capable of drug delivery.⁸ Copolymerizing hydrophobic monomers with NVP, HEMA, acrylic acid, and acrylamide greatly expands their applicability in biomaterials. For example, copolymer coatings of 70% MMA with HEMA gave good adhesion to vascular stents and resulted in significantly reduced vessel wall response.⁹ NVP possesses some drawbacks, however, such as a poor reactivity in copolymerization reactions due to compositional drift during the course of polymerisation leading to leaching of unpolymerizable

monomer.¹⁰⁻¹² One alternative approach to addressing these problems is to modify the pyrrolidinone monomer itself, with the aim of improving the monomer reactivity, to minimize compositional drift during the reaction, and to enhance hydrophilicity in order to allow some control over the equilibrium swelling of hydrogels based on the monomers.¹³

Methacrylate monomers have also found great uses in medical and dental applications such as bone cements, dental fillings, bioadhesives, and hydrogels. One major problem attached to many of these methacrylate derivatives resides in their low rates of polymerization leading to the same leaching problems encountered NVP and causing irritation of the surrounding tissues and even cell death. Incorporation of pendent groups that do not alter the fast polymerization rates or inherent adhesion properties of methyl methacrylate-based systems is required in most applications.

Bowmann, et al., have recently demonstrated that both intermolecular interactions, such as hydrogen bonding and aromatic heterocyclic ring stacking effects, plus intramolecular effects have a significant impact on the monomer reactivity of methacrylates in particular.¹⁴ They also showed that the presence of a secondary functionality greatly affects the rate of polymerization.¹⁵ Hoyle, et al., also illustrated the effect of hydrogen bonding on the overall rate of polymerization of methacrylate monomers.¹⁶ Decker et al. suggested that the reactivity is a result of an efficient chain transfer reaction that involves labile hydrogens from the newly introduced functional group.^{17,18} It has also been shown that the rate of polymerization is increased when pendent heterocyclic

groups are incorporated in the monomer; groups which have been shown to reduce termination.¹⁶ High rates of polymerization lead to less leachable monomer from these systems while larger pendant groups can also increase glass transition temperatures (T_g s) and reduce shrinkage of the copolymer systems usually used in biomaterial applications.

Alkyl α -hydroxymethylacrylate (RHMA) chemistry allows tailoring of both polymerizability and final polymer properties.¹⁹⁻²¹ For example, conversion of the hydroxymethyl group to esters was found to dramatically increase rates of polymerization.²² More recently, we have discovered the extreme reactivity of alkyl 2-carboethoxyhydroxymethyl-acrylates upon reaction with primary amines leading to a simple, mild, and efficient route to the preparation of new polyfunctional pyrrolidinones and pyrrolidinone methacrylate monomers.²³

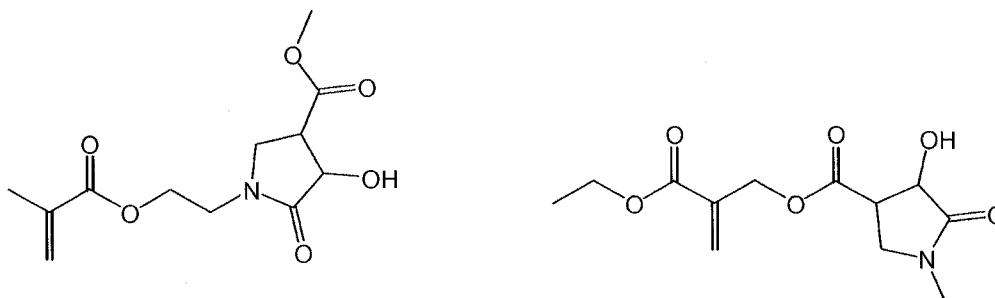


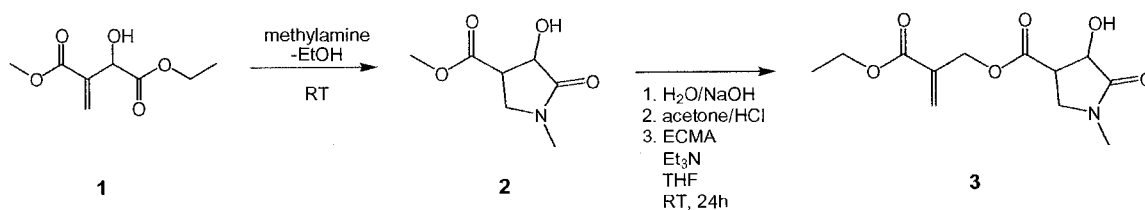
Figure 8.1. Structures of 2-pyrrolidinone containing monomers.

In this work, we are investigating new methacrylate monomers incorporating pyrrolidinone pendant groups capable of strong hydrogen-bonding interactions (Figure 8.1). Optically active, 2-pyrrolidinone compounds have found applications in areas ranging from biology to biochemistry and pharmaceuticals. Two different systems are studied one incorporates a pyrrolidinone unit as a

second functionality, the other incorporates a pyrrolidinone unit into a hydroxymethacrylate monomer through an ester linkage.

Results and Discussion

Monomer preparation. Methyl 2-carboethoxyhydroxymethylacrylate **1** was synthesized following the procedure reported in Chapter V. Monomer **3** was synthesized in two steps from pyrrolidinone **2** and ECMA with an overall yield of 76% and in 98% purity as determined by NMR analysis (Scheme 8.1). The monomer was soluble in water, chloroform, methanol, ethyl acetate, methylene chloride and tetrahydrofuran.



Scheme 8.1. Synthesis of 2-pyrrolidinone monomer **3**.

The ¹³C NMR spectrum of monomer **3** is shown in Figure 8.2. An APT experiment allowed the accurate assignments of each peak (Figure 8.3), confirming monomer structure.

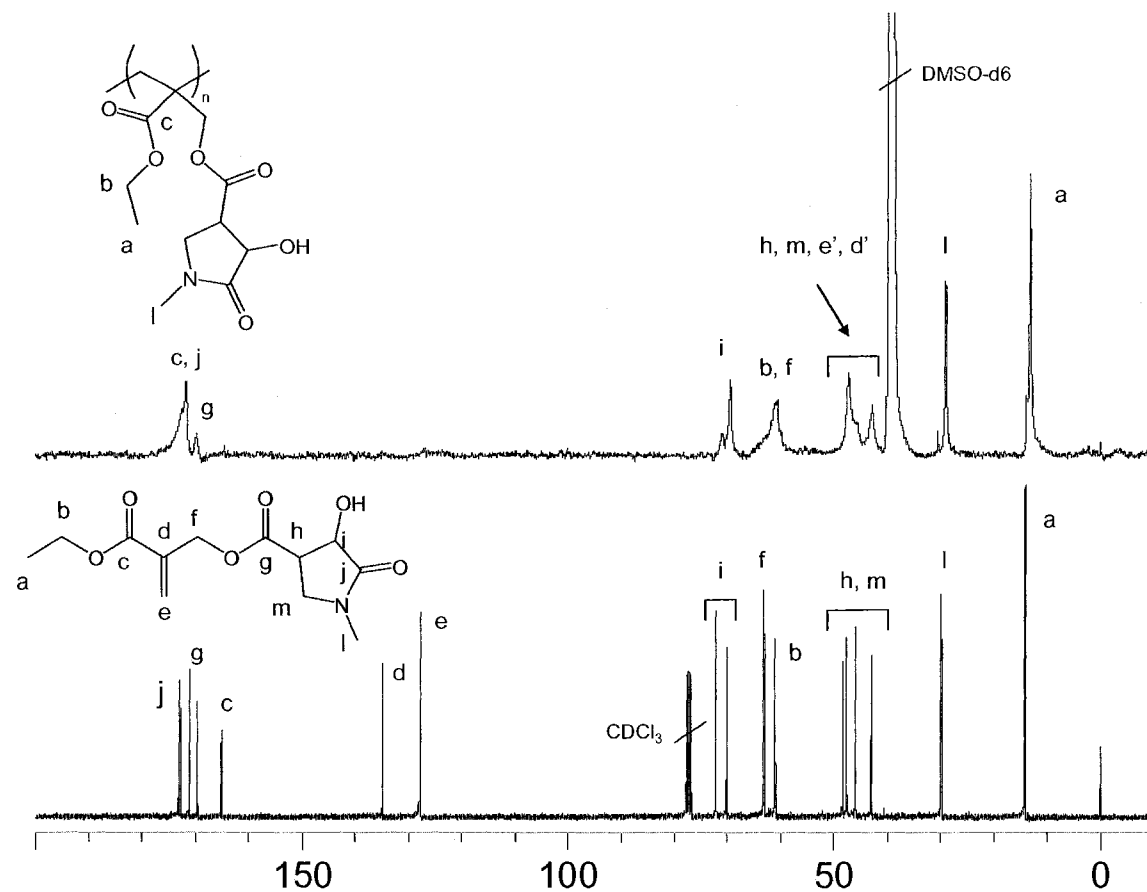


Figure 8.2. ^{13}C NMR spectra of 2-pyrrolidinone monomer **3** (CDCl_3) and the corresponding homopolymer PyP1 (DMSO-d_6).

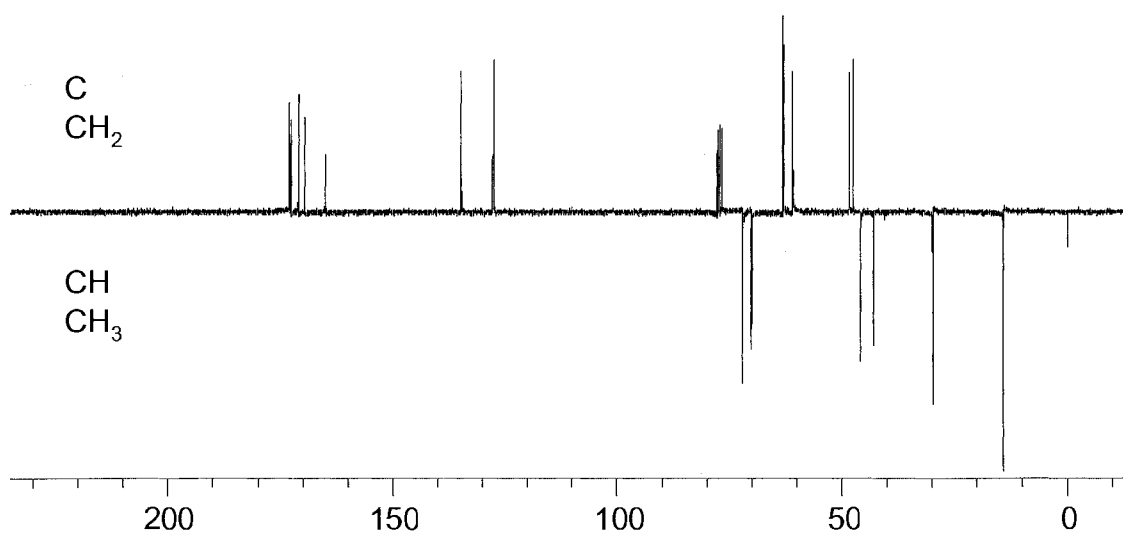


Figure 8.3. APT spectrum of 2-pyrrolidinone monomer **3** (CDCl_3).

Monomer **4** was synthesized in one step from methyl 2-carboethoxyhydroxymethylacrylate **1** and 2-aminoethyl methacrylate hydrochloride in the presence of triethylamine (Scheme 8.2) with an overall yield of 82% and in 95% purity as determined by ^1H NMR analysis. 2-Aminoethyl methacrylate hydrochloride suffers from intramolecular rearrangements upon deprotonation. In the present reaction, the high yield obtained testifies of a highly efficient Michael addition to methyl 2-carboethoxyhydroxymethylacrylate at room temperature. The unusual reactivity of these latter allows minimizing any side reaction and rearrangement that could happen in other conditions. As reported in the previous chapter, a unique combination of intra- and intermolecular hydrogen bonding interactions leads to an extremely fast formation of pyrrolidinone compounds such as monomer **4**. The resulting monomer was soluble in the same solvents listed for monomer **3**. The ^{13}C NMR spectrum is shown in Figure 8.4, confirming its structure; the spectrum of its polymer (to be discussed later) is included for comparison.

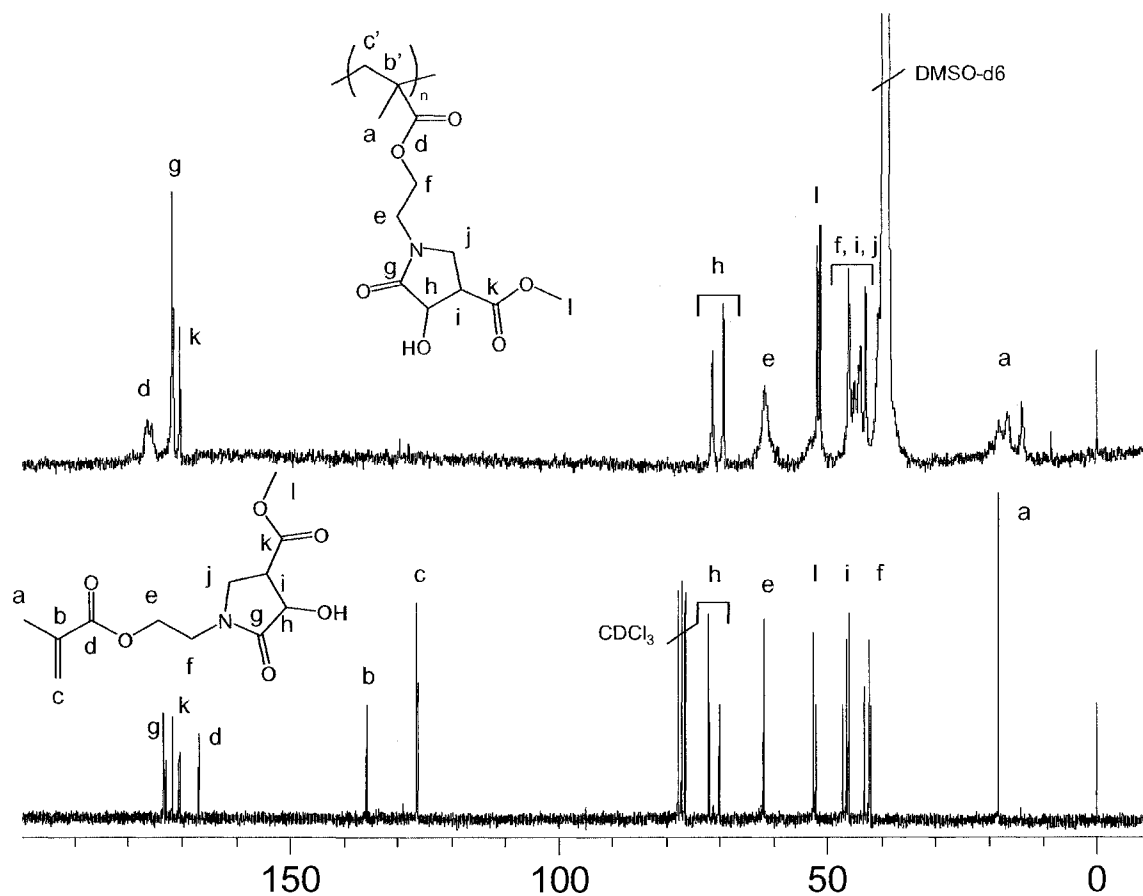


Figure 8.4. ^{13}C NMR spectra of 2-pyrrolidinone monomer **4** (CDCl_3) and the corresponding homopolymer PyP2 (DMSO-d_6).

Photopolymerizations. The steady-state polymerization kinetics of the monomers designed above was investigated and their comparison to standard mono- and divinyl polymerization systems are presented in Figure 8.5. The monomers structures and a quantification of their polymerization characteristics are presented in Table 8.1. The reactivity of these model systems was examined from several perspectives. Rate information at different conversions is used to evaluate aspects of the polymerization that have the greatest impact on the overall cure behavior. Thus, trends in polymerization rate at low conversion, e.g.,

less than 10%, have been compared with those at later stages using the maximum polymerization rate. Additionally, an effective combination of these two rates, a measure of cure time, was evaluated using quantification of the time necessary to achieve 60% conversion.

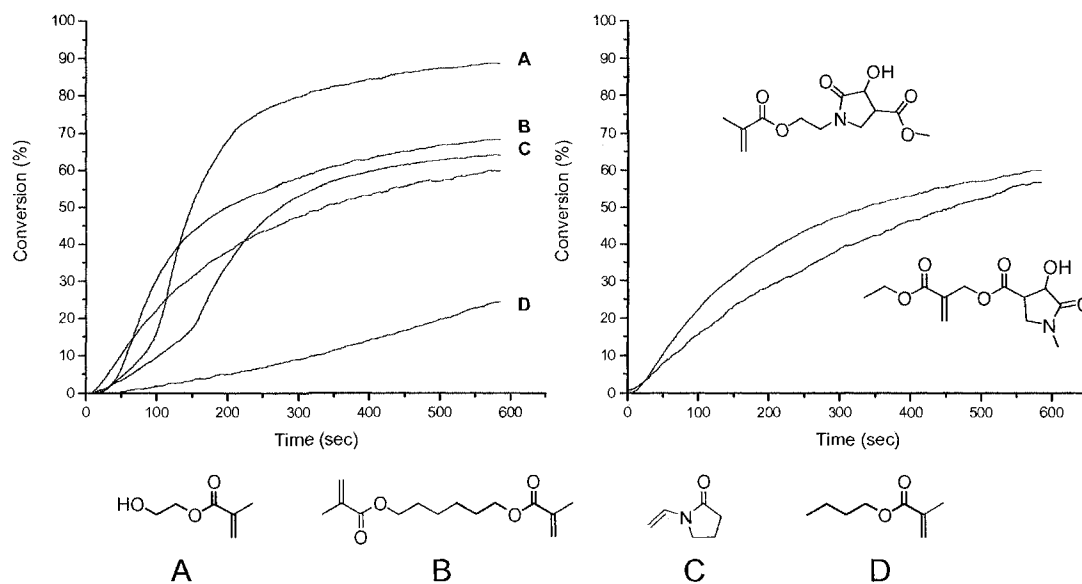
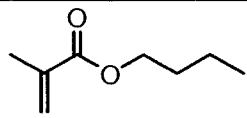
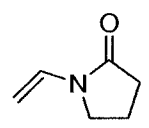
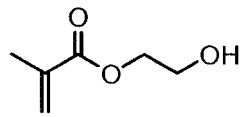
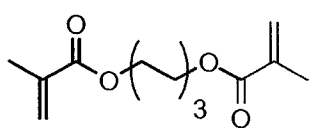
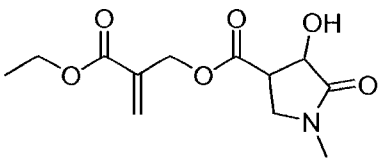
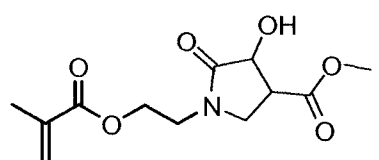


Figure 8.5. Photopolymerization conversion values for a series of methacrylate monomers.

Table 8.1. Performance analysis of methacrylate monomers at 25°C.

monomer	$[DB]_0$ ^(a)	T_m (°C)	$R_{P,10\%conv.}$ ^(b)	$R_{P,Max.}$ ^(c)	Conv. at $R_{P,Max.}$ (%)	Conv. _{Max.} (%) ^(d)	time to Conv. =50%
 BMA	6.3	<25	0.0002	0.0006	-	24	N/A
 NVP	9.4	<25	0.0014	0.0036	30	64	273
 HEMA	8.2	<25	0.0022	0.0091	32	88	147
 HDDMA	7.8	<25	0.006	0.008	20	68	198
 Monomer 3	4.6	60	0.0012	0.0014	15	56	452
 Monomer 4	4.4	<25	0.002	0.0024	12	60	332

(a) - Initial double bond concentration.

(b) - Normalized measure of "initial" polymerization rate: R_p /double bond concentration at 10% conversion.

(c) - Normalized measure of the maximum polymerization rate, $R_{p,max}$ /double bond concentration at $R_{p,max}$.

(d) - Maximum conversion reached after 600 s of irradiation at ambient conditions.

From Figure 8.5 and Table 8.1, we can observe that monomers **3** and **4** reach conversion values comparable to NVP and HDDMA. Also, all monomers, except monomers **3** and **4**, present an induction period and an autoacceleration period caused either by an increase in viscosity due to hydrogen bonding interactions, crosslinking, or molecular weight increase. The absence of induction period for the pyrrolidinone monomers is attributed to the intrinsic high compound viscosity caused by high intermolecular interactions.

It has already been shown that hydrogen bonding is an important parameter that can affect system mobility and organization during polymerization resulting in enhanced rates due to formation of dimer-like species. Hydrogen bonding generally leads to a viscosity increase that results in reduced termination and enhanced polymerization kinetics.¹⁸ Monomers **3** and **4** conversion profiles were shown to be very close to the HDDMA conversion profile suggesting that these monomers behave similarly to multifunctional monomers via intermolecular association as illustrated in Figure 8.6.

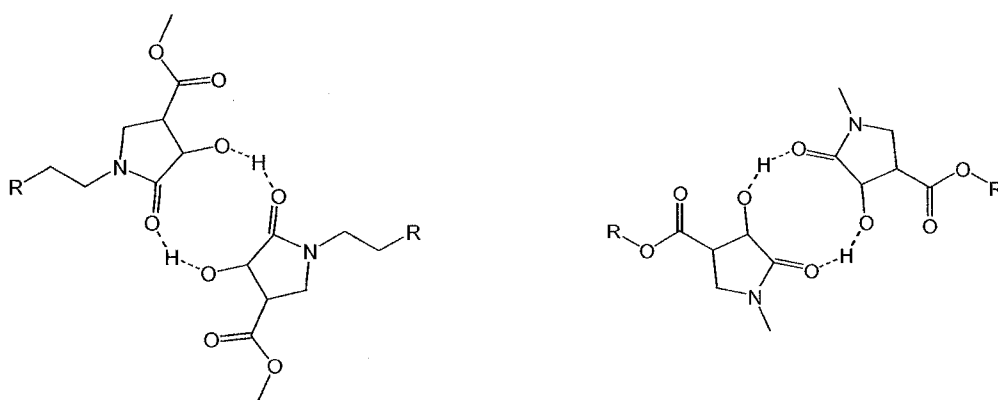


Figure 8.6. Hydrogen bonding interactions for the pyrrolidinone methacrylates investigated.

We were also intrigued by the low conversion values observed after 600 seconds. One explanation for these results may reside in the fact that these monomers can induce chemical crosslinking during photopolymerization leading then to exclusion of the polymer from its own monomer. For instance, we observed that the polymers recovered from photopolymerization of monomers **3** and **4** were all insoluble in organic solvent such as THF, DMSO, DMF and NMP, suggesting gel formation due to chemical crosslinking. It has been postulated in the past, in similar systems incorporating pyrrolutamic acid, that methine hydrogen loss, for example, would generate a captodative radical capable of cross-linking by radical-radical coupling. Here, radical abstraction could involve two adjacent groups.

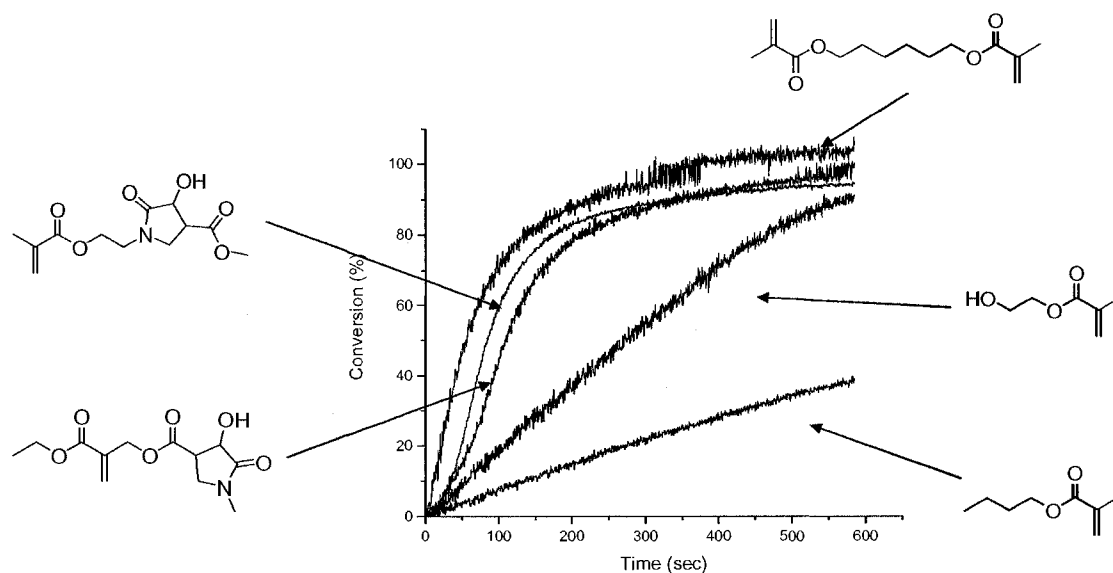


Figure 8.7. Conversion profiles for methacrylates in NMP (50/50).

A complex combination of intermolecular hydrogen bonding and chemical crosslinking may alter our ability to interpret the data summarize in Table 8.1. We decided then to carry out photopolymerization reactions of the pyrrolidinone

monomers, HEMA, HDDMA and BMA in NMP in order to eliminate any effect of hydrogen bonding and crosslinking. As shown in Figure 8.7, a significant increase in the rate of polymerization was observed for monomer **3** and **4** which argues that solubility plays a major role in the polymerization. For instance, dilution in a polar solvent like NMP or DMSO did not lead to crosslinked material. With the same conditions, a decrease in the rate of polymerization of HEMA was observed. We conclude that in these conditions, monomers **3** and **4** show higher reactivity than HEMA.

Photocopolymerization results of the pyrrolidinone monomers with HEMA are displayed in Figure 8.8 below. It can be observed that conversions reach high values which suggests that the new comonomers copolymerize well with HEMA. The relative increase of the rates in polymerization when the concentration of pyrrolidinone-containing methacrylate increases is attributed to a viscosity increase of the monomer mixture.

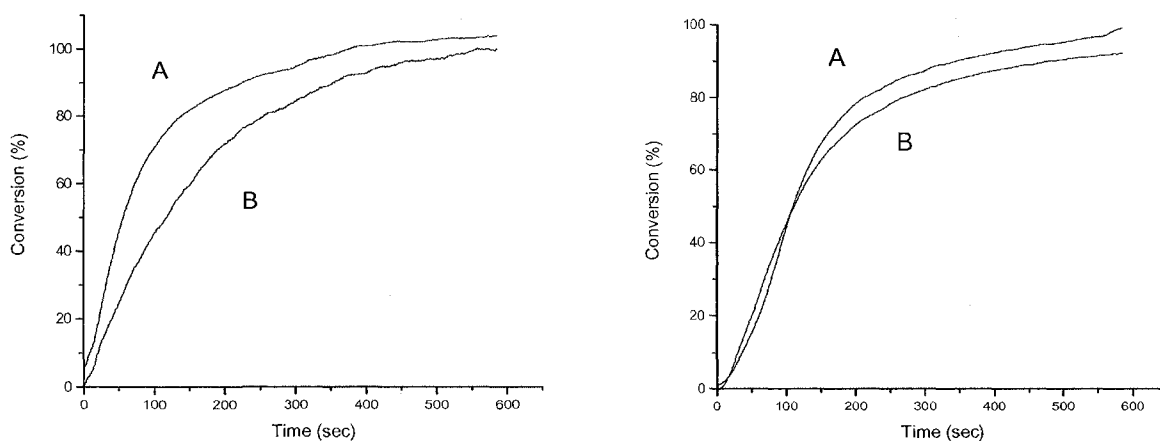


Figure 8.8. Photocopolymerization conversion values for HEMA/Monomer 1, 4:1 mixture (A) and 1:1 mixture (B).

Solution free radical polymerizations and polymer characterization. The pyrrolidinone-containing monomers were polymerized in DMSO under argon atmosphere using azobisisobutyronitrile (AIBN) as the initiator (0.1 mol-%) at 65 °C. Polymers were precipitated in acetone and dried under reduced pressure before characterization. The homopolymers **PyP1** and **PyP2** correspond to the polymerization of monomer **3** and monomer **4**, respectively. ^{13}C NMR spectra of the monomers along with that of the polymers obtained by solution polymerization in DMSO are displayed in Figures 8.2 and 8.4. Both polymers were highly soluble in DMSO while initial attempts to polymerize these monomers in methanol and THF gave insoluble polymers and low yields. It is believed that crosslinking may arise via chain transfer involving the pyrrolidinone ring hydrogens in the latter.

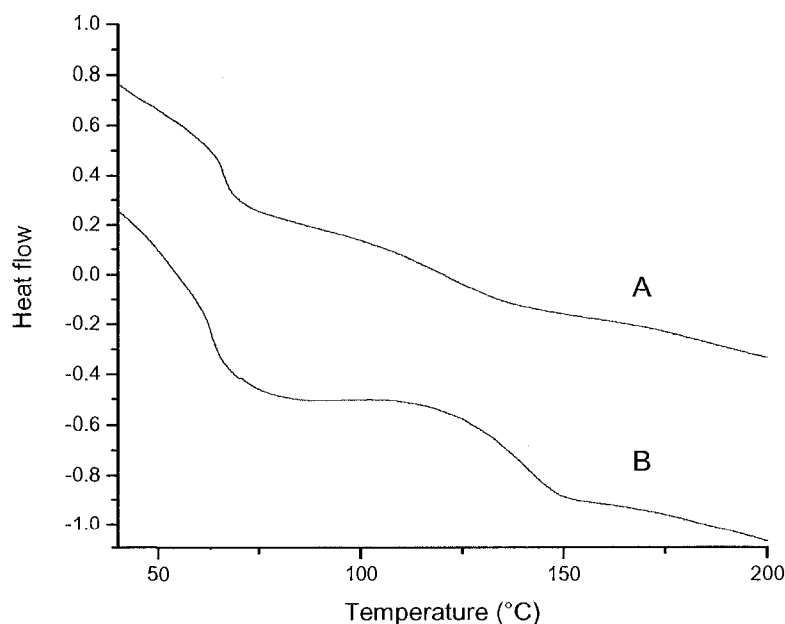


Figure 8.9. DSC traces of polymers **PyP2** (A) and **PyP1** (B) (second scans).

Dynamic scanning calorimetry experiments were carried out and allowed determining T_gs of both homopolymers. **PyP1** showed a T_g at 145 °C while **PyP2** showed a T_g at 122 °C (Figure 8.9). We can explain this difference in glass transition by the closest proximity from the backbone of the heterocycle pendant group in **PyP1** compared to **PyP2**. This has the effect of reducing local mobility of the pendant groups. This behavior explains also the extensive broadening of the peaks in the ¹³C NMR spectrum of **PyP1**. Indeed, by comparing the spectra of the two homopolymers, we can clearly see the effect of reduced mobility on the heterocycle carbon peaks. The close proximity of the pendant groups in **PyP1** may also result in intramolecular hydrogen bonding interactions which would influence greatly segmental motion. DSC traces of homopolymers revealed also a sharp transition at 65 °C. This transition is attributed to the breaking of intermolecular hydrogen bonding interactions between the heterocycle pendant groups. Both polymers display the same transition, suggesting similar interactions in both systems. This correlates with the fact that the main association between pendant groups may be the one proposed previously in Figure 8.6.

Conclusions

New multifunctional pyrrolidinone-containing methacrylate monomers were synthesized successfully. These monomers display rates of polymerization comparable to difunctional methacrylates such as hexanediol dimethacrylate. Hydrogen bonding interactions induced by the pyrrolidinone unit may lead these monomers to behave as difunctional compounds. These monomers

copolymerize very well with HEMA. Thermal properties of the homopolymers obtained by solution free radical polymerization revealed two distinctive transitions. One can be attributed to the glass transition, the other to a pseudo-beta transition induced by disruption of the hydrogen bonding interactions promoted by the heterocycle pendant groups. These monomers open up a new window on pyrrolidinone compounds that can be efficiently incorporated into polymers that may find applications in the biomedical field.

Experimental

Materials. The commercially available monomers used for the experimental studies are n-butyl methacrylate (BMA), 1,6-hexanediol dimethacrylate (HDDMA), N-vinyl pyrrolidone (NVP) and 2-hydroxyethyl methacrylate (HEMA). Ethyl α -hydroxymethylacrylate (EHMA) was donated by Nippon Shokubai Co., Tokyo, Japan. Ethyl α -chloromethylacrylate (ECMA) was synthesized from MHMA according to previously reported literature.²⁵ Ethyl glyoxylate, 50% in toluene, was purchased from Alfa Aesar and used as received. 4-Diaza[2.2.2]-bicyclooctane (DABCO) and methyl acrylate were purchased from Aldrich Chemical Company and used without further purification. Methylamine (40 wt-% in water) was purchased from Aldrich Chemical Company and used as received. 2,2'-Azobis(2-methylpropionitrile) (AIBN) was purchased from Aldrich and recrystallized from methanol before use. All solvents were purchased from Acros Chemical Company, Fisher, or Aldrich Chemical Company. Photopolymerizations were performed using the ultraviolet initiator 2-hydroxy-2-methyl-1-phenyl-1-propanone (Darocur 1173, Ciba Geigy, Hawthorne, NY).

Preparation of methyl 2-(carboethoxyhydroxymethyl)acrylate 1. Ethyl

glyoxylate, 50 wt-% in toluene (20.39 g, 199.7 mmol), DABCO (3.64 g, 32.4 mmol) and the methyl acrylate (17.19 g, 199.7 mmol) were added to a 250 ml round-bottom flask. The reaction was slightly exothermic. The mixture was stirred at room temperature for 2 hours. The crude solution was then concentrated under reduced pressure. The resulting mixture was washed with 3 aliquots of saturated sodium chloride solution followed by 3 aliquots of deionized water. The organic phase was then dried over a bed of sodium sulfate and vacuum distillation of the residue gave methyl 2-carboethoxyhydroxymethylacrylate **1** as a clear liquid in c.a. 68% yield (bp 135-137°C (20 mm Hg)).

^1H NMR (300 MHz, CDCl_3) δ 1.26 (t, 3H, $-\text{CH}_3$), 3.68 (s, H, $-\text{OH}$), 3.78 (s, 3H, $-\text{OCH}_3$), 4.26 (q, 2H, $-\text{CH}_2\text{CH}_3$), 4.88 (s, H, $-\text{CHOH}$), 5.96 and 6.37 (s, 2H, $-\text{CH}_2=\text{C}$); ^{13}C NMR (CDCl_3) δ 14.04 ($-\text{CH}_3$), 52.12 ($-\text{OCH}_3$), 62.20 ($-\text{CH}_2\text{CH}_3$), 71.19 ($-\text{CHOH}$), 128.96 ($\text{CH}_2=\text{C}$), 138.08 ($\text{C}=\text{CH}_2$), 165.68 and 172.30 ($\text{C}=\text{O}$). FT-IR (neat, cm^{-1}) 3515, 2996, 1739, 1643, 1446, 1097, 823. Anal. Calcd for $\text{C}_8\text{H}_{15}\text{O}_5 \cdot 0.25 \cdot \text{H}_2\text{O}$: C, 50.59; H, 6.49. Found: C, 50.28; H, 6.28.

Preparation of methyl 1-methyl-4-hydroxy-5-oxopyrrolidine-3-carboxylate 2.

Compound **1** (10 g, 53.14 mmol) was added to a 50 ml tube equipped with an argon gas inlet. The reaction tube was then purged with argon for 30 minutes and sealed with a rubber septum. Methylamine (40 wt-% in water) was added dropwise in slight excess (5.48 g, 54.21 mmol) to the mixture and the resulting solution was allowed to stir for 24 hours at room temperature. Upon reaction completion as monitored by ^1H NMR, the solvent was removed under reduced

pressure. Once concentrated, the crude product was purified distilling off the excess of amine to give methyl 1-methyl-4-hydroxy-5-oxopyrrolidine-3-carboxylate **2** as a brown oil in c.a. 96% and as a mixture of two stereoisomers (A and B; d.r. 42:58).

^1H NMR (300 MHz, CDCl_3) δ 0.88 (t, 3H, $-\text{CH}_3$), 1.28 (m, 2H, $-\text{CH}_2$), 1.52 (m, 2H, $-\text{CH}_2\text{CH}_2\text{N}$), 3.74_(A) and 3.77_(B) (s, 3H, $-\text{CH}_3$), 4.59_(A) and 4.60_(B) (d, H, $-\text{CHOH}$); ^{13}C NMR (CDCl_3) δ 14.17_(A+B) ($-\text{CH}_3$), 22.52_(A+B) ($-\text{CH}_2\text{CH}_3$), 26.38 and 26.85 ($-\text{CH}_2\text{CH}_2\text{CH}_3$), 31.41 and 31.44 ($-\text{CH}_2\text{CH}_3$), 42.96 and 43.04 ($-\text{CH}_2\text{N}$), 43.07 and 45.62 ($-\text{CHCH}_2\text{N}$), 46.07 and 46.29 ($-\text{CH}_2\text{N}$), 52.16 and 52.53 ($-\text{OCH}_3$), 70.46 and 72.43 ($-\text{CHOH}$), 170.74 and 172.25 ($\text{C}=\text{O}$), 172.82 and 173.09 ($\text{NC}=\text{O}$). FT-IR (neat, cm^{-1}) 3363, 2958, 2935, 2866, 1741, 1695, 1278, 740. Anal. Calcd for $\text{C}_{12}\text{H}_{21}\text{NO}_4$: C, 59.24; H, 8.70; N, 5.76. Found: C, 59.42; H, 8.71; N, 5.84.

Preparation of 4-hydroxy-1-methyl-5-oxopyrrolidine-3-carboxylic acid 2'.

Methyl 1-methyl-4-hydroxy-5-oxopyrrolidine-3-carboxylate **2** was first treated with 1 equivalent of sodium hydroxide in 10 ml of deionized water. The resulting mixture was allowed to stir for 1 hour before precipitating it in 80 ml of acetone. The white salt formed was then filtered off, re-dispersed in 50 ml of acetone and treated with dilute hydrochloric acid. The precipitate was filtered off and dried under reduced pressure to afford 4-hydroxy-1-methyl-5-oxopyrrolidine-3-carboxylic acid **2'** as a white powder in c.a. 96% and as a mixture of two stereoisomers (A and B; d.r. 42:58).

Synthesis of monomer 3. ECMA (2 g, 13.45 mmol), 4-hydroxy-1-methyl-5-oxopyrrolidine-3-carboxylic acid **3** (2.86 g, 13.45 mmol) and triethylamine (1.36 g,

13.45 mmol) were added to 15 ml of dry THF. The resulting mixture was allowed to stir for 24 hours at room temperature. The white precipitate was filtered off and the crude solution concentrated under reduced pressure to give monomer **4** as a brown oil and in c.a. 76% yield.

^1H NMR (300 MHz, CDCl_3) δ 0.88 (t, 3H, $-\text{CH}_3$), 1.28 (m, 2H, $-\text{CH}_2$), 1.52 (m, 2H, $-\text{CH}_2\text{CH}_2\text{N}$), 4.25–4.30 (q, 2H, $-\text{CH}_2\text{CH}_3$), 4.59 (d, H, $-\text{CHOH}$), 4.91 (s, 2H, $-\text{CH}_2\text{O}$), 5.91 and 6.39 (s, 2H, $\text{CH}_2=\text{C}$); ^{13}C NMR (CDCl_3) δ 14.01 ($-\text{CH}_3$), 14.17 ($-\text{CH}_3$), 22.49 ($-\text{CH}_2\text{CH}_3$), 31.40 ($-\text{CH}_2\text{CH}_2\text{CH}_3$), 26.38 ($-\text{CH}_2\text{CH}_2\text{CH}_2\text{N}$), 26.93 ($-\text{CH}_2\text{CH}_2\text{N}$), 46.17 ($-\text{CH}_2\text{N}$), 43.07 ($-\text{CHCH}_2\text{N}$), 45.46 ($-\text{CH}_2\text{N}$), 61.12 ($-\text{CH}_2\text{CH}_3$), 63.34 ($-\text{CH}_2\text{O}$), 72.40 ($-\text{CHOH}$), 127.84 ($-\text{CH}_2=\text{C}$), 134.86 ($-\text{CCH}_2$), 165.04 and 171.11 ($-\text{C}=\text{O}$), 172.72 ($-\text{NCO}$). FT-IR (NaCl, cm^{-1}) 3351, 2960, 2935, 2870, 1741, 1729, 1685, 1654, 1277, 819.

Synthesis of pyrrolidinone monomer 4. 2-Aminoethyl methacrylate

hydrochloride (5 g, 30.18 mmol) and **1** (5.67 g, 30.18 mmol) were added to 50 ml of dry THF in a 250 ml round bottom flask placed in a ice/acetone bath.

Triethylamine (3.54 g, 35 mmol) was then added dropwise to the stirring mixture.

The resulting solution was allowed to stir until the temperature reached room temperature. The mixture was stirred for 12 more hours. The crude solution was then precipitated in cold diethyl ether. The white precipitate was filtered off and the crude solution concentrated under reduced pressure. The resulting brown oil was washed 3 times with n-hexane and dried under reduced pressure to afford monomer **4** as a brown oil and as a mixture of two stereoisomers (A and B; d.r. 50:50) in c.a. 82% yield.

^1H NMR (300 MHz, CDCl_3) δ 1.94 (s, 3H, $-\text{CH}_3$), 3.74_(A) and 3.78_(B) (s, 3H, $-\text{CH}_3$), 5.60_(A) and 5.61_(B) (s, 1H, $-\text{CH}_2=\text{C}$), 6.10_(A) and 6.11_(B) (s, 1H, $-\text{CH}_2=\text{C}$); ^{13}C NMR (CDCl_3) δ 18.31_(A+B) ($-\text{CH}_3$), 42.15_(A) and 43.23_(B) ($-\text{CH}_2\text{N}$), 42.24_(A) and 4.17_(B) ($-\text{CHCH}_2\text{N}$), 46.51_(A) and 47.28_(B) ($-\text{CH}_2\text{N}$), 52.27_(A) and 52.62_(B) ($-\text{OCH}_3$), 70.16_(A) and 72.08 ($-\text{CHOH}$), 126.36_(A) and 126.41_(B) ($-\text{CH}_2\text{C}$), 135.70_(A) and 135.76_(A) ($-\text{CCH}_2$), 166.98_(A) and 167.05_(B) ($\text{C}=\text{O}$), 170.57_(A) and 173.07_(B) ($\text{C}=\text{O}$), 171.91_(A) and 173.41_(B) ($\text{NC}=\text{O}$).

Analyses. Solution ^1H and ^{13}C NMR spectra of the intermediates and monomers were collected on a Varian Mercury 300 MHz spectrometer operating at a frequency of 75.47 MHz for carbon. NMR spectra were recorded at room temperature using CDCl_3 with TMS as an internal reference. Solution ^{13}C NMR spectra of the polymers were collected on an INOVA 500 MHz spectrometer. NMR spectra were recorded at room temperature using $\text{DMSO}-d_6$ with TMS as an internal reference. FT-IR spectra were obtained using a Mattson Galaxy series 5000 FTIR spectrometer. ReactIR experiments were conducted on a ReactIRTM (ASI Applied Systems Inc., Mettler Toledo). Dynamic scanning calorimetry (DSC) experiments were performed on a TA Instrument 2920, controlled by a Thermal Analyst 2100. All scans were taken at a heating rate of 10 °C/min under nitrogen atmosphere, to a maximum of 250 °C than cooled to room temperature and re-scanned at the same heating rate. The Tg values were recorded from the second scan data for the samples.

Fourier transform infrared spectroscopy (FT-IR). FT-IR studies were conducted with a modified Bruker IFS 88 FT-IR spectrometer with a horizontal

sample accessory. UV light from an Oriel lamp system equipped with a 200 Watt, high-pressure mercury-xenon bulb was channeled to the sample chamber through a fiber-optic cable. Photoinitiated polymerization was performed by exposing a thin sample (ca. 25 μm) between two sodium chloride salt plates to continuous UV light filtered and centered at 365 nm for duration of 10 min. Irradiation intensity was evaluated at 11.4 mW/cm^2 . The process was monitored by the FT-IR operating at a scanning rate of 5 scans/sec. with the series 9811 radiometer (Vernon Hills, IL). The initiator used was 3 wt-% of Darocur 1173 for all samples. Acrylate conversion was monitored with the C=C stretching vibration at 1630 cm^{-1} or the C=C twisting vibration at 812 cm^{-1} . The kinetics of the polymerizations were obtained at an ambient temperature of 25 $^{\circ}\text{C}$. Results of the DPC experiments were evaluated using Origin 7 SR2 from OriginLab.

Solution polymerizations. Solution polymerizations were carried out in different solvents such as THF, methanol and DMSO with AIBN as an initiator, freshly recrystallized from methanol. During the reactions done in THF and methanol, polymer precipitation occurred and the obtained products were insoluble after drying. Soluble polymers of Monomers **3** and **4** were obtained using DMSO as a solvent and AIBN as an initiator. Monomers and 0.1 mol-% of initiator were dissolved in DMSO and degassed by bubbling nitrogen through the solutions for 30 min. The resulting mixture was then placed in an oil bath that was preheated to 65 $^{\circ}\text{C}$ and the polymerization was allowed to proceed for 24 hours to ensure high monomer conversion. The solution remained homogeneous during the

reaction. Upon completion of reaction as monitored by ^1H NMR the polymer was precipitated into acetone and dried under reduced pressure at room temperature.

REFERENCES

- 1 Wichterle, O. *Encyclopedia of Polymer Science and Technology* **1971**, *15*, 273-91.
- 2 Gregonis, D.E.; Chen, C.M.; Andrade, J.D. *ACS Symp. Ser.* **1976**, *31*, 88-104.
- 3 Peppas, N.A.; Mikos, A.G. *Hydrogels in Medicine and Pharmacy*, Peppas. CRC Press **1986**, *1*, 1-24.
- 4 Tighe, B.J.; Kishi, M. *Optician* **1988**, *21*, 196.
- 5 Perera, D.I.; Shanks, R.A. *Polymer Int.* **1995**, *36*, 303.
- 6 Perera, D.I.; Shanks, R.A. *Polymer Int.* **1995**, *37*, 133.
- 7 Kao, F.; Manivannan, G.; Sawan, S.P. *J. Biomed. Mater. Res. (Appl. Biomater.)* **1997**, *38*, 191-196.
- 8 Yamini, C.; Shantha, K.L.; Rao, P.J. *Macromol. Sci., Pure Appl. Chem.* **1997**, *12*, 2461-2470.
- 9 Bair, F.W.; van der Veen, F.H.; Benzina, A.; Habets, J.; Koole, L.H. *J. Biomed. Mater. Res.* **2000**, *52*, 193-198.
- 10 Davis, T.P.; Hugh, M.B. *Polymer* **1990**, *31*, 513.
- 11 Bork, J.F.; Coleman, L.E. *J. Polym. Sci.* **1960**, *43*, 413.
- 12 Davis, T.P.; Hugh, M.B. *Macromolecules* **1989**, *22*, 2824.
- 13 Iskander, G.M.; Baker, L.E.; Wiley, D.E.; Davis, T.P. *Polymer* **1998**, *39*, 4165-4169.
- 14 Kilambi, H.; Stansbury, J.W.; Bowman, C.N. *Macromolecules* **2007**, *40*, 47-54

- 15 Berchtold, K.A.; Nie, J.; Stansbury, J.W.; Hacıoglu, B.; Beckel, E.R.; Bowman, C.N. *Macromolecules* **2004**, *37*, 3165-3179
- 16 Zhou, H.; Li, Q.; Lee, T.Y.; Guymon, C.A.; Jonsson E.S.; Hoyle, C.E. *Macromolecules* **2006**, *39*, 8269-8273
- 17 Decker, C. *Nucl. Instrum. Methods Phys. Res. B* **1999**, *151*, 22-28.
- 18 Moussa, K.; Decker, C.J. *Polym. Sci., Polym. Chem.* **1993**, *31*, 2197-2203.
- 19 Mathias, L.J.; Kusefoglu, S.H.; Kress, A.O.; Lee, S.; Dickerson, C.W.; Thames, S.F. *Polym. News* **1992**, *17*, 36-42.
- 20 Avci, D.; Mathias, L.J. *J. Polym. Sci., Part A: Polym. Chem.* **1999**, *37*, 901-907.
- 21 Jariwala, C.P.; Mathias, L.J. *Macromolecules* **1993**, *26*, 5129-5136.
- 22 Avci, D.; Kusefoglu, S.H.; Thompson, R.D.; Mathias, L.J. *Macromolecules* **1994**, *27*, 1981-1982.
- 23 Morizur, J-F.; Mathias, L.J. *Tetrahedron Letters* **2007**, *48*, 5555-5559.
- 24 Smith, T.J.; Mathias, L.J. *Biomacromolecules* **2002**, *3*, 1392-1399.
- 25 Mathias, L.J.; Warren, M.R.; Huang, S. *Macromolecules* **1991**, *24*, 2036-2042.

CHAPTER IX
SUPRAMOLECULAR MATERIALS FROM NEW POLYFUNCTIONAL
PYRROLIDINONE ACID DERIVATIVES

Abstract

Multifunctional bis-2-pyrrolidinone derivatives synthesized from alkyl 2-carboethoxyhydroxymethylacrylates via a very efficient Michael addition/cyclization reaction sequence were found to form supramolecular associations that give rise to polymer-like behavior. The compounds examined displayed glass transition temperatures and were highly soluble in water.

Introduction

Recently, 'smart materials' or stimuli-responsive polymers (i.e. those that change their properties in response to temperature, solvent, light or chemical additives) have received attention with a view to expanding their range of applications. Central to the properties of such materials are non-covalent interactions which permit a rapid response to a change in environment while their strength and selectivity can be controlled easily by synthetic variation. One example is the assembly and disassembly of structural motifs such as DNA¹, fundamental to translation and transcription in biology. Synthesis of polymers by linking monomers via non-covalent interactions, or generating polymer networks by using non-covalent interactions of functionalized side chains, would therefore represent an attractive approach to the construction of stimuli-responsive soft materials.^{2,3} Hydrogen-bonds are attractive because they are highly directional, and when several are used in concert, strong binding results. When built into an

array, the placement of donor and acceptor functionalities creates the selectivity. Thus, there has been much interest invested in the study of arrays of hydrogen-bonds because the strength and selectivity of interaction are important in determining the properties of the resulting polymers.

Linear arrays of hydrogen-bonds offer the advantage of constraining the hydrogen-bonding 'glue' with which monomers are linked together into one well-defined unit with limited possibilities for interaction with other functional motifs. The first use of arrays of hydrogen-bonds in the assembly of supramolecular polymers was reported by Lehn and co-workers in 1993, who described the assembly of polymeric, liquid crystalline and lyotropic mesophases using 2,6-diamidopyridine- and thymine-functionalized building blocks.^{4,5} Previous report in the literature indicates that pyroglutamic acid may be useful in forming molecular associations.⁶

We have recently been interested in a highly efficient Michael addition/cyclization reaction sequence involving alkyl 2-carboethoxyhydroxymethylacrylates and primary amines that lead to the design of new polyfunctional pyrrolidinone compounds in a fast and high purity manner.⁷ Here we present the synthesis of new polyfunctional bis-pyrrolidinone acid derivatives and some characterizations suggesting that these compounds form supramolecular associations.

Results and Discussion

We have demonstrated in the previous chapters that multifunctional 2-pyrrolidinone derivatives can easily be synthesized by means of a extremely fast

and efficient Michael addition/cyclization reaction sequence involving methyl 2-carboethoxyhydroxymethylacrylate and aliphatic primary amines. No evidence of the Michael adduct amine intermediate was detected upon analysis of the final product ^{13}C NMR spectra attesting to a quantitative cyclization step. In this work, we were interested in synthesizing bi-2-pyrrolidinone by reacting n-butyl 2-carboethoxyhydroxymethylacrylate with different diamines such as diethylenetriamine, ethylene diamine, and hexamethylene diamine.

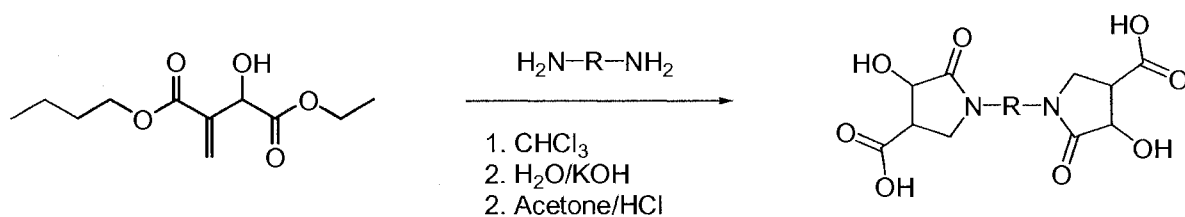


Table 9.1. Bis-pyrrolidinone acid derivatives characteristics.

entry	diamine	R	yield (%)	Tg (°C)
BP1	ethylenediamine	(CH ₂) ₂	95	82
BP2	1,6-hexanediamine	(CH ₂) ₆	89	67
BP3	diethylenetriamine	(CH ₂) ₂ NH(CH ₂) ₂	94	68

Slight excess of the alkene was added in order to ensure the formation bis-2-pyrrolidinone exclusively. Upon reaction completion as monitored by ^1H NMR, the excess of amine and the solvent were removed under reduced pressure to afford bis-pyrrolidinone diester derivatives in high yield and purity. The structures of the different compounds were investigated by NMR spectroscopy but elemental analysis remained the most reliable technique to confirm structures. No accurate assignment of the compounds NMR peaks could be obtained due to the extreme spectral complexity. For instance, Figure 9.1 below displays the ^{13}C NMR spectrum of the bis-pyrrolidinone diester intermediate to the synthesis of **BP1**.

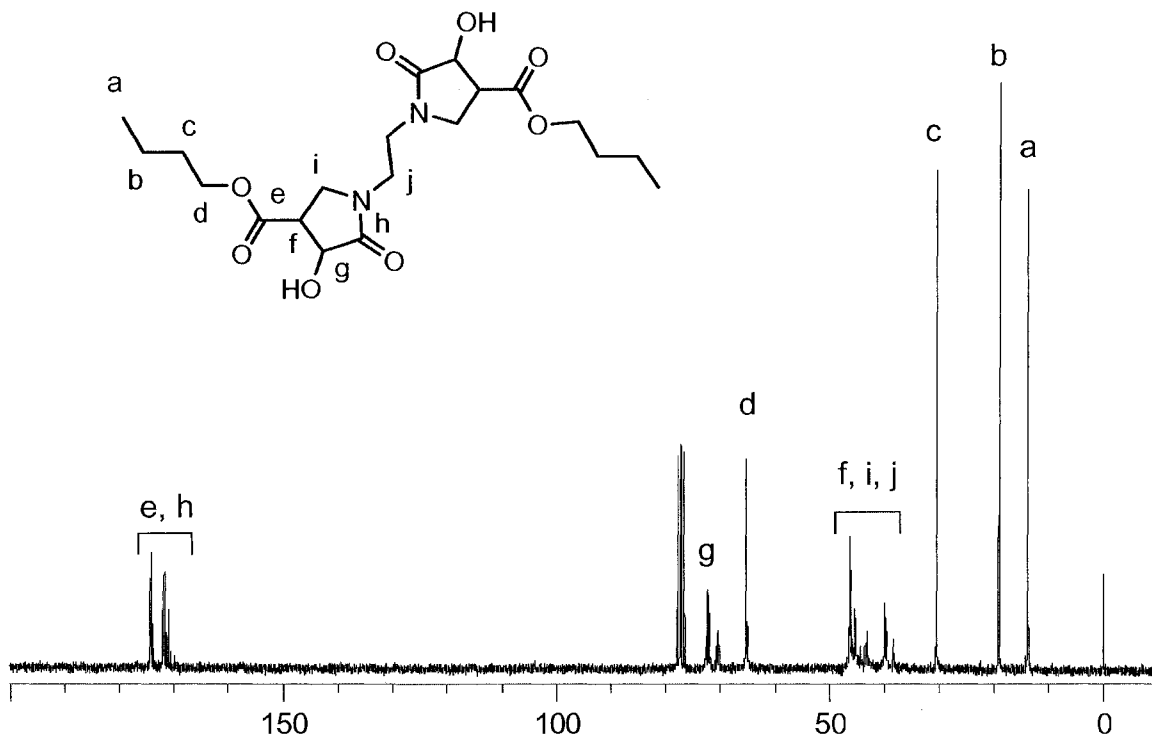


Figure 9.1. ^{13}C NMR spectrum of bis-pyrrolidinone intermediate (CDCl_3).

The peak multiplicity observed in the ^{13}C NMR of the intermediate displayed above can be explained by the fact that this compound is a mixture of three different isomers. Indeed, the bispyrrolidinone compounds are statistically constituted of a combination of different heterocycle configurations: *cis-cis*, *trans-trans* and *trans-cis/cis-trans*. In a *cis-trans* configuration, both groups will influence each other differently than in a *cis-cis* configuration so that the chemical shifts associated with the *cis* group in the first configuration are different than those in the *cis-cis* configuration. It was noticed that this multiplicity decreases as the spacer length between the two pyrrolidinone groups increases as illustrated in Figure 9.2 that displays the ^{13}C NMR carbonyl regions of each diester intermediate. This can be explained by the fact that the reciprocal influence of the heterocycles decreases as the distance that separates these groups increases.

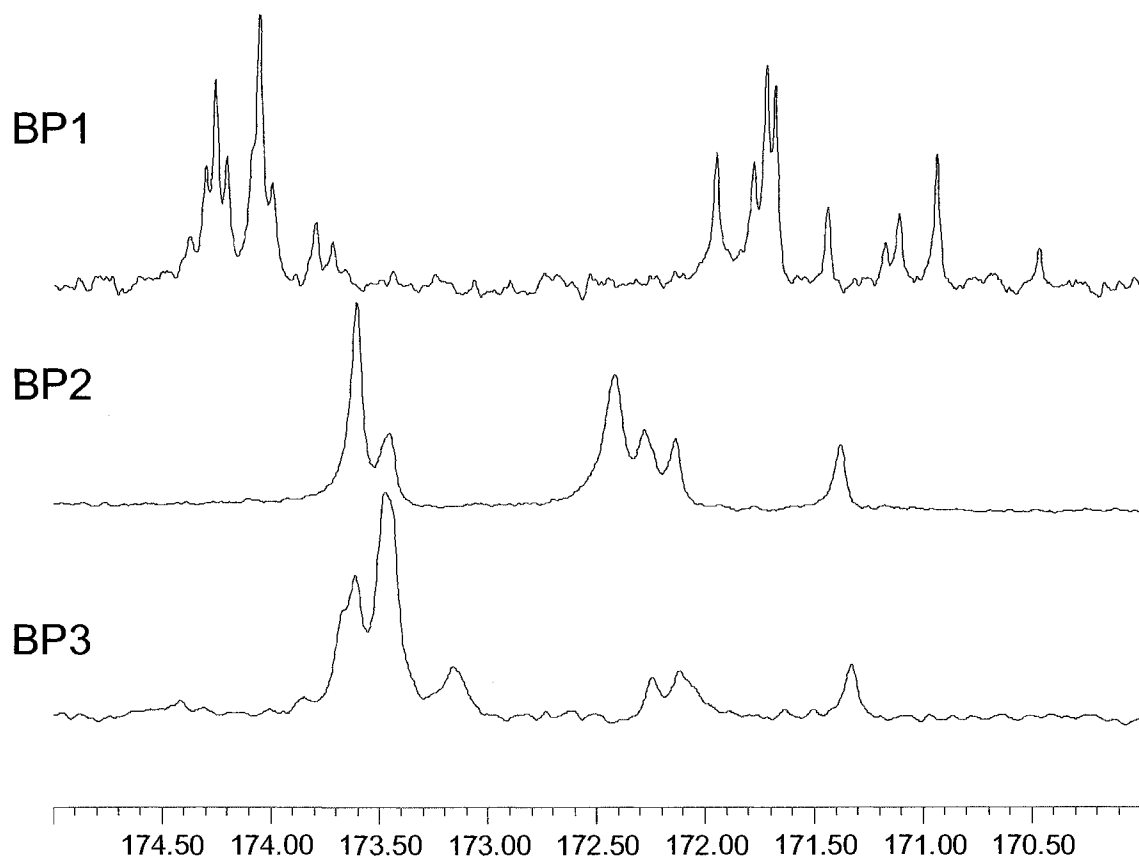


Figure 9.2. ¹³C NMR carbonyl regions of diester intermediates (CDCl₃).

Treatment of the diester intermediates with sodium hydroxide and hydrochloric acid led to the formation of the bis-pyrrolidinone acid derivatives **BP1**, **BP2** and **BP3** (Table 9.1). Similar peak multiplicity was observed in the ¹³C NMR spectra of the di-acid derivatives (Figure 9.3).

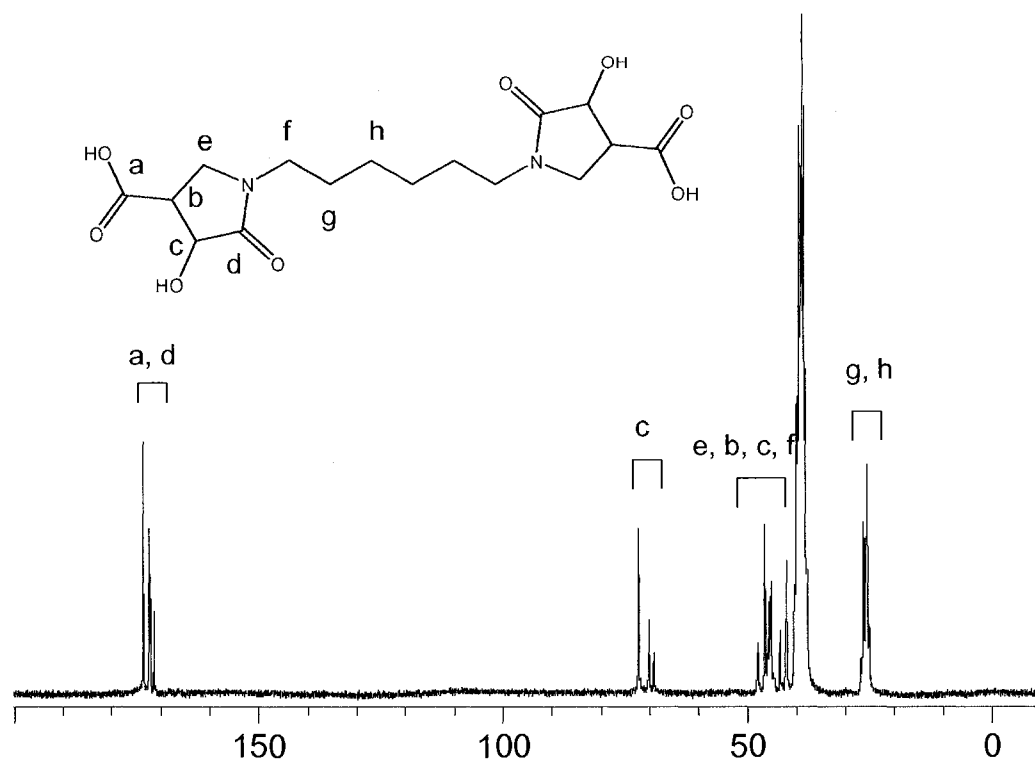


Figure 9.3. ^{13}C NMR spectrum of **BP2** (DMSO- d_6).

The melting points of **BP1**, **BP2** and **BP3** were estimated to range between 180 °C and 220 °C depending on sample. All the samples were found to be highly hygroscopic and exposure of the material to atmospheric moisture for a short period resulted in “melted gel” material as illustrated in Figure 9.4 below.

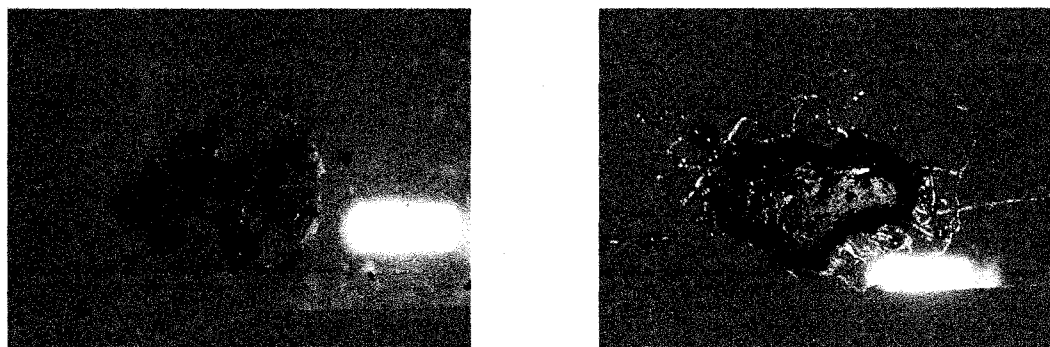


Figure 9.4. Bis-2-pyrrolidinone acids (**BP2**) before exposure (left) and after exposure (right) to air.

Water absorption would be expected to break up the hydrogen bonding interactions between pyrrolidinone units. Compounds stored under nitrogen, in sealed test tubes, retained their integrity, confirming this hypothesis. The all series of bis-pyrrolidinone was found to be soluble in water. **BP1**, **BP2**, and **BP3** were then analyzed using differential scanning calorimetry (Figure 9.5). Thermal transitions at 82, 67, and 68 °C, respectively, were observed but no melting point could be detected in the temperature range evaluated.

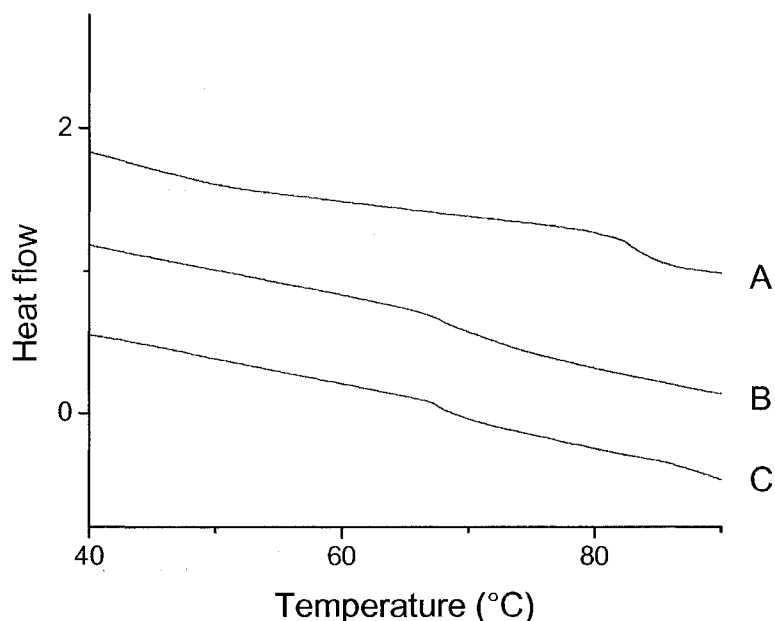


Figure 9.5. DCS traces for **BP1** (A), **BP2** (B) and **BP3** (C) (second scans).

Thermogravimetric analysis (TGA) showed that the compounds were stable up to 280 °C before decomposition. The observations of thermal transitions resembling glass transition temperatures, solvent precipitation and the change in mechanical properties when exposed to water seem to indicate that

these bis-2-pyrrolidinones form hydrogen bonded supramolecular associations as illustrated in Figure 9.6.

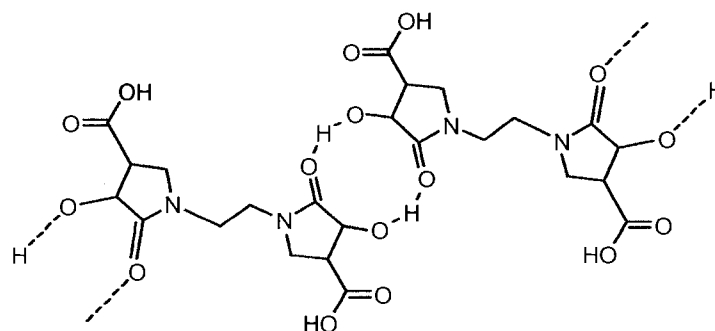


Figure 9.6. Proposed supramolecular association (**BP1**).

Experimental

Materials. Ethyl glyoxylate, 50% in toluene, was purchased from Alfa Aesar and used as received. 4-Diaza[2.2.2]bicyclooctane (DABCO), methyl acrylate, hexamethylene diamine, ethylene diamine and diethylene triamine were purchased from Aldrich Chemical Company and used as received. All solvents were purchased from Acros Chemical Company, Fisher, or Aldrich Chemical Company.

Characterization. ^1H and ^{13}C NMR analyses were performed on samples dissolved in DMSO- d_6 containing 0.1% TMS or CDCl_3 containing 0.1% TMS as internal reference using a Varian Mercury 300 MHz spectrometer operating at a frequency of 75.47 MHz for carbon. Thermal gravimetry analysis (TGA) experiments were performed on a TA 2960, controlled by a Thermal Analyst 2100. The temperature was ramped at a heating rate of 10 $^\circ\text{C}/\text{min}$, under inert atmosphere, to a temperature well above the degradation temperature (600 $^\circ\text{C}$).

Dynamic scanning calorimetry (DSC) experiments were performed on a TA Instrument 2920, controlled by a Thermal Analyst 2100. All scans were taken at a heating rate of 10 °C/min under nitrogen atmosphere, to a maximum of 220 °C than cooled to room temperature and re-scanned at the same heating rate.

Preparation of methyl 2-carboethoxyhydroxymethylacrylate 1. This alkyl 2-carboethoxyhydroxymethylacrylate derivative was synthesized according to previously reported literature procedure.¹⁷ Ethyl glyoxylate, 50 wt-% in toluene (20.39 g, 199.7 mmol), DABCO (3.64 g, 32.4 mmol) and methyl acrylate (199.7 mmol) were added to a 250 ml round-bottom flask. The mixture was stirred at room temperature for two hours. The crude solution was then concentrated under reduced pressure. The resulting mixture was washed with three aliquots of saturated sodium chloride solution followed by three aliquots of deionized water. The organic phase was then dried over a bed of sodium sulfate and vacuum distillation of the residue gave the corresponding compounds which show the following data:

Clear liquid; bp 135-137°C (20 mm Hg); c.a. 68% isolated yield after distillation; ¹H NMR (300 MHz, CDCl₃) δ 1.26 (t, 3H, -CH₃), 3.68 (s, H, -OH), 3.78 (s, 3H, -OCH₃), 4.26 (q, 2H, -CH₂CH₃), 4.88 (s, H, -CHOH), 5.96 and 6.37 (s, 2H, -CH₂=C); ¹³C NMR (CDCl₃) δ 14.04 (-CH₃), 52.12 (-OCH₃), 62.20 (-CH₂CH₃), 71.19 (-CHOH), 128.96 (CH₂=C), 138.08 (C=CH₂), 165.68 and 172.30 (C=O). FT-IR (neat, cm⁻¹) 3515, 2996, 1739, 1643, 1446, 1097, 823. Anal. Calcd for C₈H₁₅O₅·0.25·H₂O: C, 50.59; H, 6.49. Found: C, 50.28; H, 6.28.

Preparation of multifunctional bis-pyrrolidinone acid derivatives. General procedure. Methyl 2-carboethoxyhydroxymethylacrylate (53.14 mmol) was added to a 50 ml tube equipped with an argon gas inlet. The reaction tube was then purged with argon for 30 minutes and sealed with a rubber septum. The corresponding diamine (54.21 mmol) was added dropwise to this mixture and the resulting solution was allowed to stir for 24 hours at room temperature. Upon reaction completion as monitored by ^1H NMR, the solvent was removed under reduced pressure. Once concentrated, the crude product was purified by precipitation into hexanes. The resulting product was then dried under reduced pressure to afford the corresponding compounds **BP1**, **BP2**, and **BP3** as mixtures of diastereoisomers combinations (*cis/cis*, *cis/trans* and *trans/trans*).

REFERENCES

- 1 Philp, D.; Stoddart, J.F. *Angew. Chem. Int. Ed.* **1996**, *35*, 1155–1196.
- 2 Ciferri, A. *Supramolecular Polymers, 2nd edn, Taylor and Francis, Boca Raton, Florida* **2005**.
- 3 Brunsveld, L.; Folmer, B.J.B.; Meijer, E.W.; Sijbesma, R.P. *Chem. Rev.* **2001**, *101*, 4071–4097.
- 4 Gulick-Krymicki, T.; Fouquey, A.M.; Lehn, J.M. *Proc. Natl. Acad. Sci. U.S.A.* **1993**, *90*, 163–167.
- 5 Kotera, M.; Lehn, J.M.; Vigneron, J.P. *J. Chem. Soc., Chem. Commun.* **1994**, 197–199.
- 6 Tsiourvas, D.; Paleos, C. M.; Skoulios, A. *Liq. Cryst.* **1999**, *26*, 953-957.
- 7 Morizur, J-F.; Mathias, L.J. *Tetrahedron Letters* **2007**, *48*, 5555-5559.

CHAPTER X

NEW BIODEGRADABLE POLY(ESTER AMIDE)S FROM ALKYL 2-CARBO-
ETHOXYHYDROXYMETHYLACRYLATES**Abstract**

The synthesis of alkyl 2-carboethoxyhydroxymethylacrylates via the Bayllis-Hillmann reaction pathway is described. These compounds are found to be poor monomers when involved in free radical polymerizations but present an extremely high reactivity upon Michael addition with primary amines leading to a simple, mild and efficient route to the preparation of new multifunctional heterocycles and polymers with potential applications in biodegradable coatings. Real-time NMR spectroscopy permitted monitoring the extent of the reaction sequence and determining the conversion profile of reactants and Michael adduct intermediate. Poly(ester amide)s derived from diamines and hexane bis-2-carboethoxyhydroxymethylacrylate were synthesized at room temperature by means of a very efficient Michael addition/cyclization polymerization. These polymers display excellent adhesion to metal, glass and paper substrates and interesting hydrolytic susceptibility.

Introduction

Biodegradable polymers have attracted great attention over the past decade, especially those that are moisture sensitive due to their degradability in water. Poly(ester amide)s obtained by polycondensation are susceptible to hydrolytic and biological degradation but retain good mechanical properties and processing behavior.¹⁻⁴ Carothers in 1932 was the first to synthesize poly(ester

amide)s from diacids, diols, and diamines.⁵ Since then, a wide variety of such polymers have been formed.⁶ Among them, special interest presently exists for poly(ester amide)s made from naturally occurring compounds based on their potential as biomedical materials. For instance, poly(ester amide)s made from amino acid⁷ derivatives and from carbohydrate-based monomers⁸ constitute two main families under investigation. Biodegradable polymers are currently being investigated for use in wound closure (sutures); orthopedic fixation devices; dental, cardiovascular and intestinal applications; and drug delivery systems.⁹⁻¹¹ Current biodegradable devices are made of polyesters are either homopolymers and copolymers of glycolide.¹²⁻¹⁴ However, poly(ester amide)s that incorporate glycolic acid units have recently been investigated for use as biodegradable sutures.^{15,16}

We have been exploring an interesting Michael addition/cyclization reaction sequence involving alkyl 2-carboethoxyhydroxymethylacrylates (Figure 10.1) and primary amines. As described earlier in this dissertation, such alkenes present an extremely high reactivity to Michael addition with primary amines providing a simple, mild and efficient route for the preparation of new polyfunctional 2-pyrrolidinone derivatives (Chapter V).¹⁷ It is believed that this behavior is due to the presence of the secondary hydroxyl group attached to the α carbon which induces hydrogen bonding that may lead to preorganization of molecules in the system and activates both the alkene and the saturated ester carbonyl of the neighboring molecules. This unique combination of intra- and intermolecular hydrogen bonding activates the alkene for reaction with primary

amines and leads to the extremely fast cyclization multifunctional heterocycles. The presence of this hydroxyl group also activates adjacent ester carbonyl groups, increasing the hydrolytic susceptibility of the ester. These unique characteristics make alkyl 2-carboethoxyhydroxymethylacrylates interesting compounds for the design of biodegradable materials obtained by a fast, high conversion reaction sequence. The presence of the pyrrolidinone unit within the backbone promotes moisture sensitivity of the final polymer as well as its adhesion to a wide range of substrates.

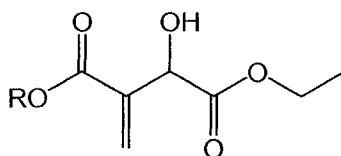


Figure 10.1. Alkyl 2-carboethoxyhydroxymethylacrylates.

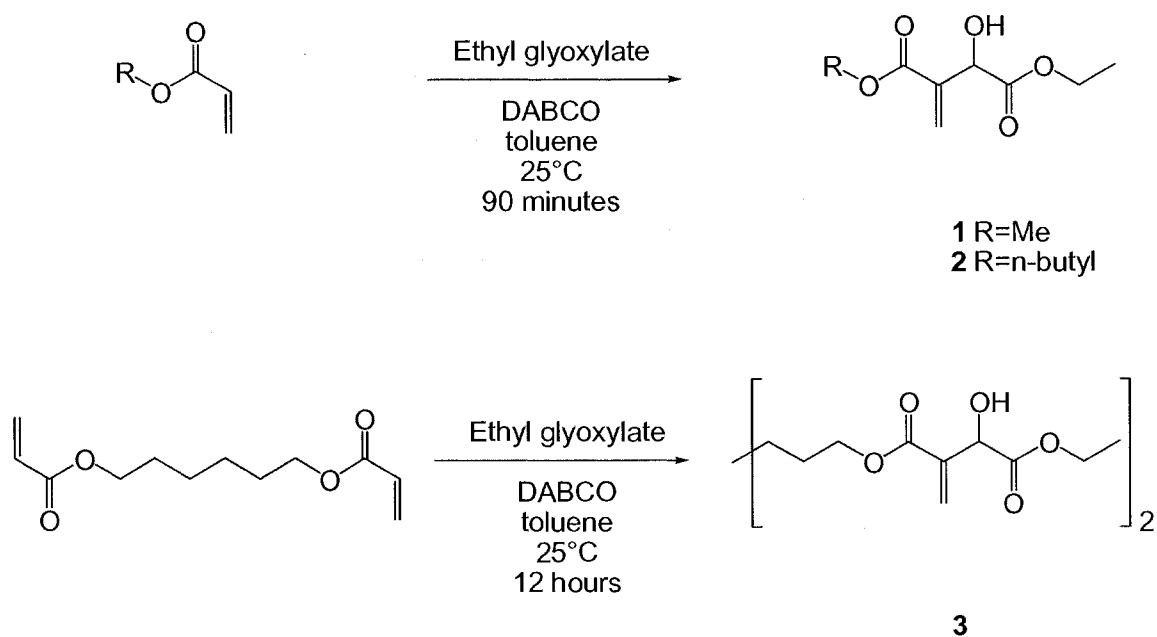
Herein, we report the synthesis of new poly(ester amide)s from hexane bis-2-carboethoxyhydroxymethylacrylate monomer. Also described is Michael addition/cyclization polymerization kinetics investigated via real-time NMR spectroscopy. The final polymer physical properties are also discussed.

Results and Discussion

Synthesis of alkyl 2-carboethoxyhydroxymethylacrylates **1**, **2** and **3**.

Following the synthetic procedures describes in previous chapters, alkyl 2-carboethoxyhydroxymethylacrylates were synthesized via the Baylis-Hillmann pathway from ethyl acrylate and *n*-butyl acrylate, respectively, as shown in Scheme 10.1. The difunctional monomer **3** was synthesized following the same reaction pathway. 1,6-Hexanediol diacrylate was reacted with ethylene glyoxylate in toluene in the presence of DABCO. Upon reaction completion, the crude product

was purified by column chromatography to give slightly yellow oil in 65% yield with 96% purity as determined by NMR spectroscopy (Figure 10.2). The main impurity is attributed to monosubstituted diacrylate that could not be separated by column chromatography. The appearance of the two peaks at 128.9 and 138.2 ppm correspond to the carbons of the newly formed double bond, while the appearance of the unique peak at 71.3 ppm (-CHOH carbon) confirms formation of the expected product.



Scheme 10.1. Synthesis of alkyl 2-carboethoxyhydroxymethylacrylates **1**, **2** and

3.

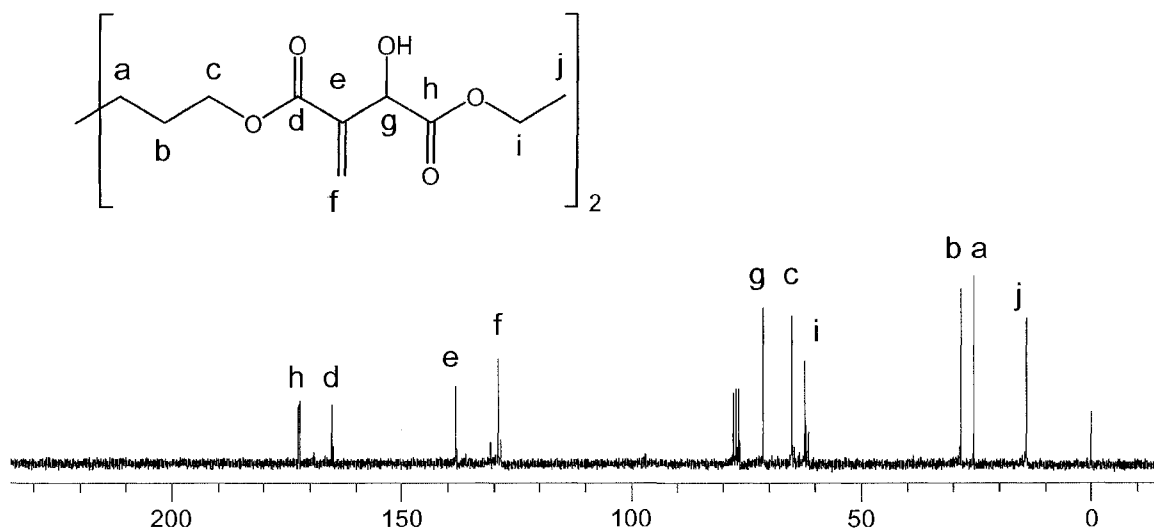


Figure 10.2. ^{13}C NMR spectrum of hexane bis-2-carboethoxyhydroxymethylacrylate **3** (CDCl_3).

Michael addition reaction and polymerization kinetics study. While these monomers do not undergo free radical copolymerization easily, giving only low polymer yields and molecular weights, we have demonstrated in previous work that multifunctional 2-pyrrolidinone derivatives can easily be synthesized by means of an extremely fast and efficient Michael addition/cyclization reaction sequence. For example, methyl 2-carboethoxyhydroxymethylacrylate and aliphatic primary amines react quickly and cleanly attesting to the utility of such alkenes.¹⁷ No evidence of the Michael adduct intermediate could be detected upon analysis of the final product by NMR spectroscopy, confirming efficient cyclization to the pyrrolidinone.

We were interested in investigating the kinetics of this Michael addition/cyclization reaction sequence involving two alkyl 2-carboethoxyhydroxymethylacrylates, methyl and butyl derivatives (**1** and **2**), and hexylamine by means of real-time NMR spectroscopy in CDCl_3 . These alkenes show such high

reactivity upon addition of primary amines that dilution at 10 wt-% of the starting materials in chloroform-d1 was necessary to obtain ^{13}C NMR spectra of intermediates. Figure 10.3 shows spectral changes observed for reaction of the diethyl ester **1** and hexylamine. On the basis of changes in the characteristic peaks during Michael reaction, especially those of the protonated carbon of the acrylate double bond at 128.2 ppm (C_1), α -carbon of the adduct at 71.7 ppm (C_2), and ethanol methylene carbon at 58.2 ppm (C_3), the kinetics of formation of the Michael adduct intermediate and then the heterocycle could be investigated (Figure 10.3). The normalized peak evolution profiles for the reaction between compound **1** and hexylamine are presented in Figure 10.4. It was found that the Michael addition step is much faster than the formation of the corresponding heterocycle, allowing evolution profiles for the Michael adduct intermediate formation and disappearance to be determined.

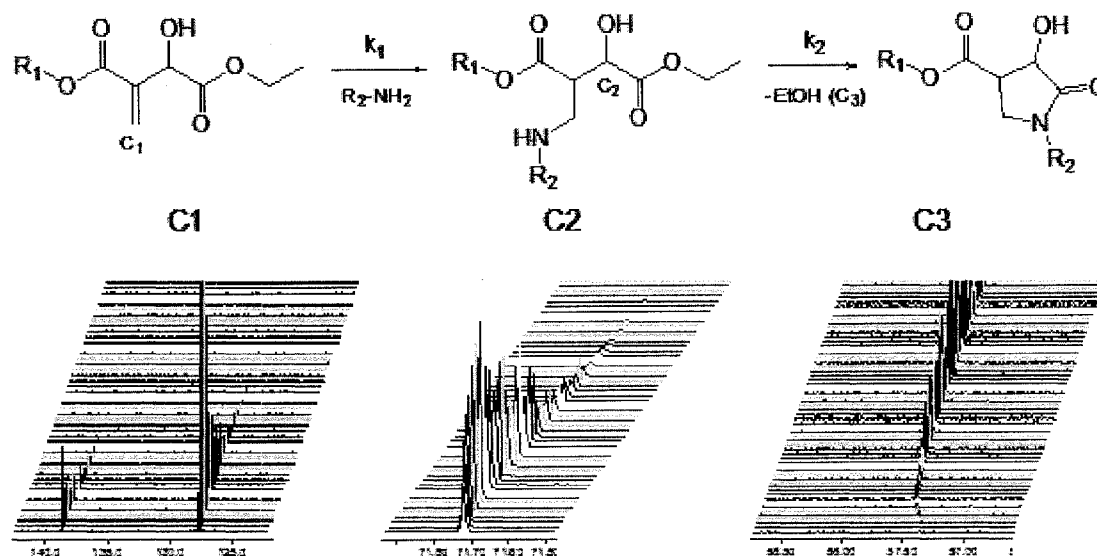


Figure 10.3. Real-time ^{13}C NMR monitoring of the Michael addition/cyclization reaction ($\text{R}_1=\text{CH}_2\text{CH}_3$, $\text{R}_2=(\text{CH}_2)_5\text{CH}_3$, in CDCl_3).

The heterocycles **1'** and **2'** formed from ethyl α -carboethoxyhydroxymethylacrylates **1** and **2**, respectively, were isolated by evaporation of the solvent under reduced pressure. The resulting compounds were found to be a mixture of two diastereoisomers (A and B) based on data presented in the experimental section. Two distinct sets of peaks were observed in the ratio 33:67 and 31:69 for **1'** and **2'**, respectively.

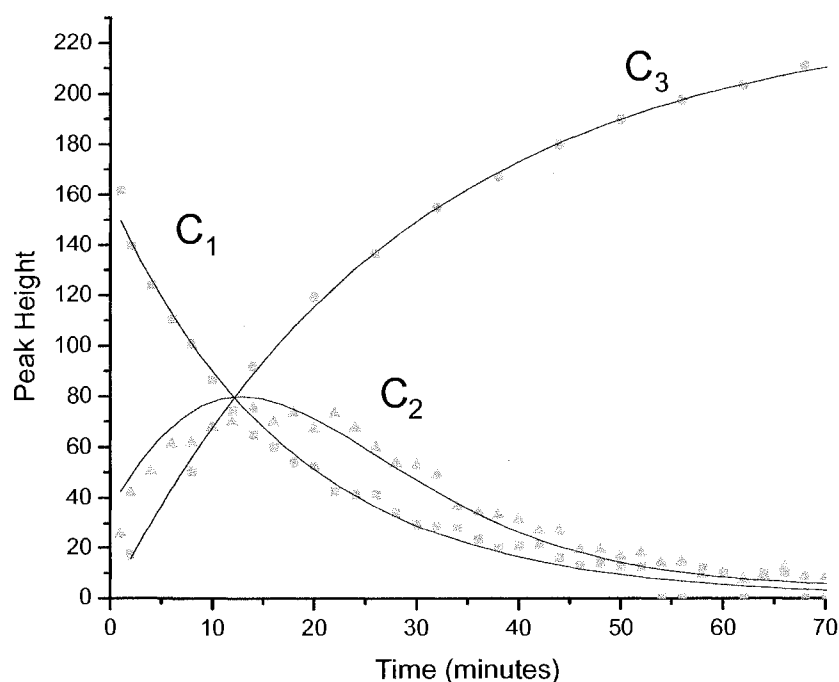
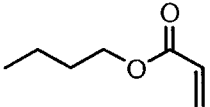
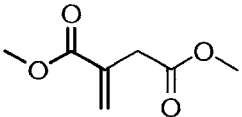
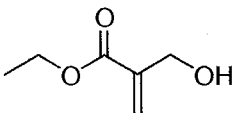
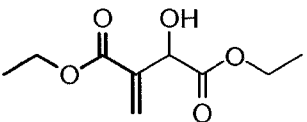
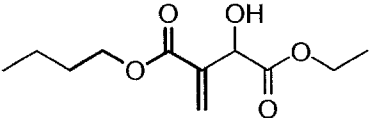
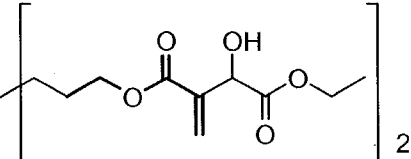


Figure 10.4. Real-time ^{13}C NMR profiles of carbon C_1 , C_2 and C_3 for the reaction between ethyl 2-carboethoxyhydroxymethylacrylate **1** and hexylamine.

The same reactions were carried out with other alkenes such as butyl acrylate, dimethyl itaconate and ethyl α -hydromethylacrylate. Michael addition reaction and heterocycle formation conversion are reported in Table 10.1. Both ethyl and butyl α -(carboethoxyhydroxymethyl)acrylate derivatives displayed

Table 10.1. Michael addition/cyclization reaction characteristics.

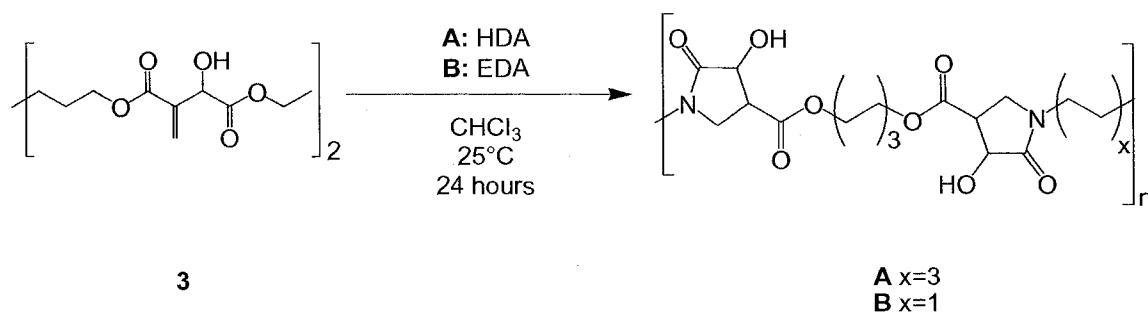
entry	alkene	amine	Michael addition conversion after 2 hours (%) ^(a)	cyclization conversion after 2 hours (%) ^(a)
1		hexylamine	8	-
2		hexylamine	12	(b)
3		hexylamine	54	-
4		hexylamine	100	98
5		hexylamine	100	97
6		hexamethylene Diamine	100	98

(a) – Determined from analysis of ¹H NMR spectrum after 2 hours.

(b) – No heterocycle formation could be noticed.

Polymer characterization. Poly(ester amide)s were formed following the synthetic route presented in Scheme 10.2 using two diamines, HMDA and EDA. Polymerizations were carried out in chloroform at room temperature for 24 hours to ensure high monomer conversion. Upon removal of the solvent under reduced

pressure, the resulting polymers were collected. Dissolution in organic solvent was attempted, but the materials remained insoluble in all organic solvents tried. It is believed that some degree of crosslinking arises perhaps due to competing intermolecular transamidation. Dynamic scanning calorimetry experiments did not reveal any transition which confirms the fact that these materials possess some degree of crosslinking (Table 10.2). Thermal gravimetry analysis experiments allowed determining the onset of thermal degradation for the two polymers synthesized and both polymers degrading at approximately 280 °C. The polymers collected were highly hygroscopic and swelled in water and methanol but did not dissolved. Figures 10.6 and 10.7 show CP/MAS spectra for the resulting polymers **A** and **B** obtained by Michael addition/cyclization polymerization. In Figure 10.7, the ^{13}C NMR spectra of polymer **A** and butyl 1-hexyl-4-hydroxy-5-oxopyrrolidine-3-carboxylate **2'** are superposed to show peaks similarities between the two materials. This comparison allowed assigning the polymer carbon peaks.



Scheme 10.2. Synthesis of poly(ester amide)s **A** and **B**.

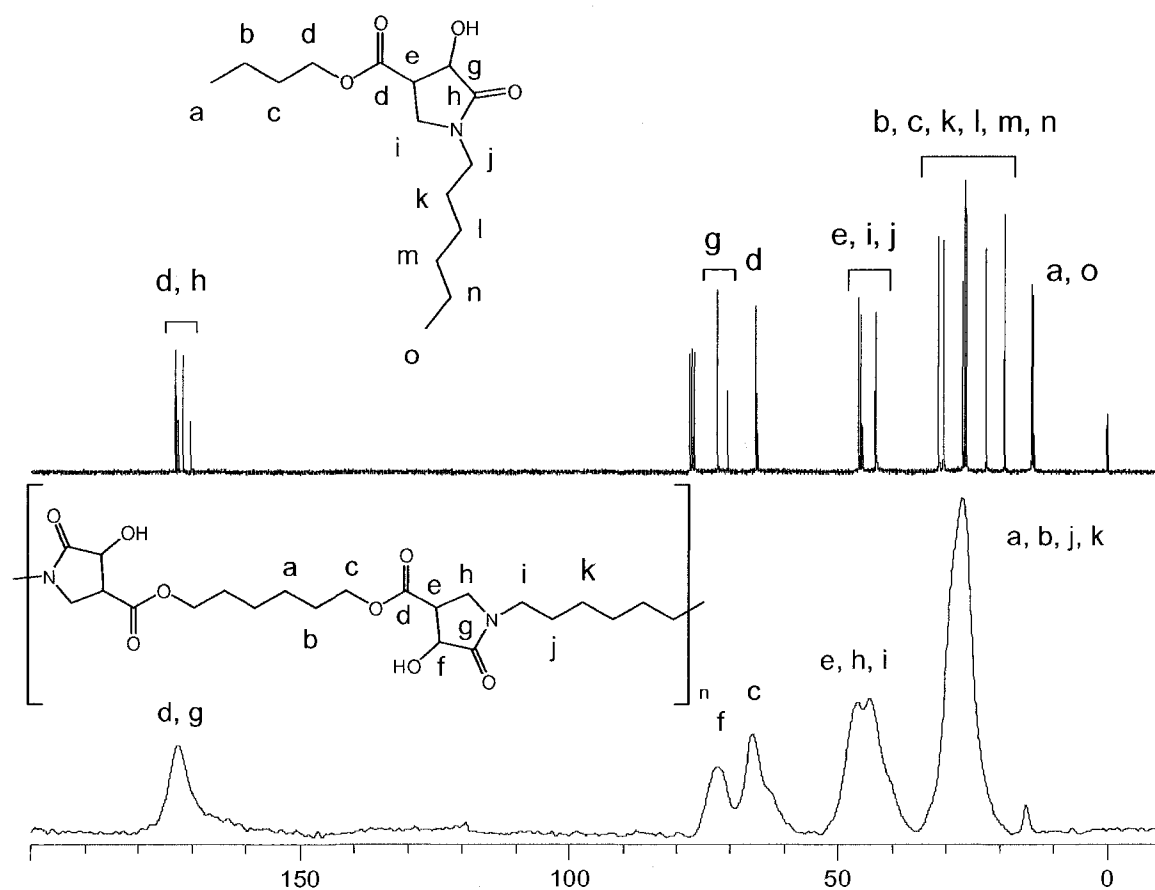


Figure 10.6. ^{13}C NMR spectra of butyl 1-hexyl-4-hydroxy-5-oxopyrrolidine-3-carboxylate **2'** (top, CDCl_3) and poly(ester amide) **A** (bottom, solid state CP/MAS).

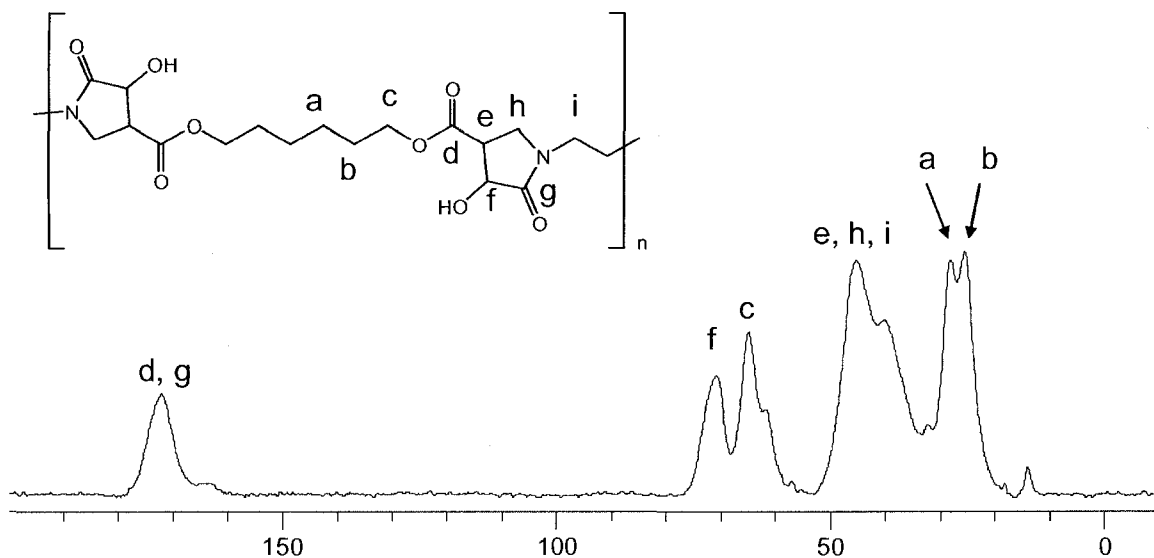


Figure 10.7. ^{13}C NMR spectrum of poly(ester amide) **B** (solid state CP/MAS).

Coatings were formed by deposition of polymer synthesized in chloroform on different substrates (glass, steel and paper) using slow evaporation of the solvent overnight. The resulting films displayed excellent adhesion to all substrates as indicated by attempts to physically remove the corresponding films from their substrates. Quantitative characterization of the adhesion is current being investigated. This remarkable adhesion may be attributed to the combination of pendant alcohol and backbone pyrrolidinone that together can promote specific interactions with such substrates. For example, hydrogen bonding with glass and paper can involve OH groups on polymer and substrate interactions, or surface hydroxyls bonding to ester and pyrrolidinone carbonyls. On metal, a similar combination of interactions may involve metal-carbonyl bonding and metal oxide hydrogen bonding with polymer alcohol groups.

Preliminary study showed that these materials are highly susceptible to hydrolysis in mild conditions (pH=8). This behavior is currently under

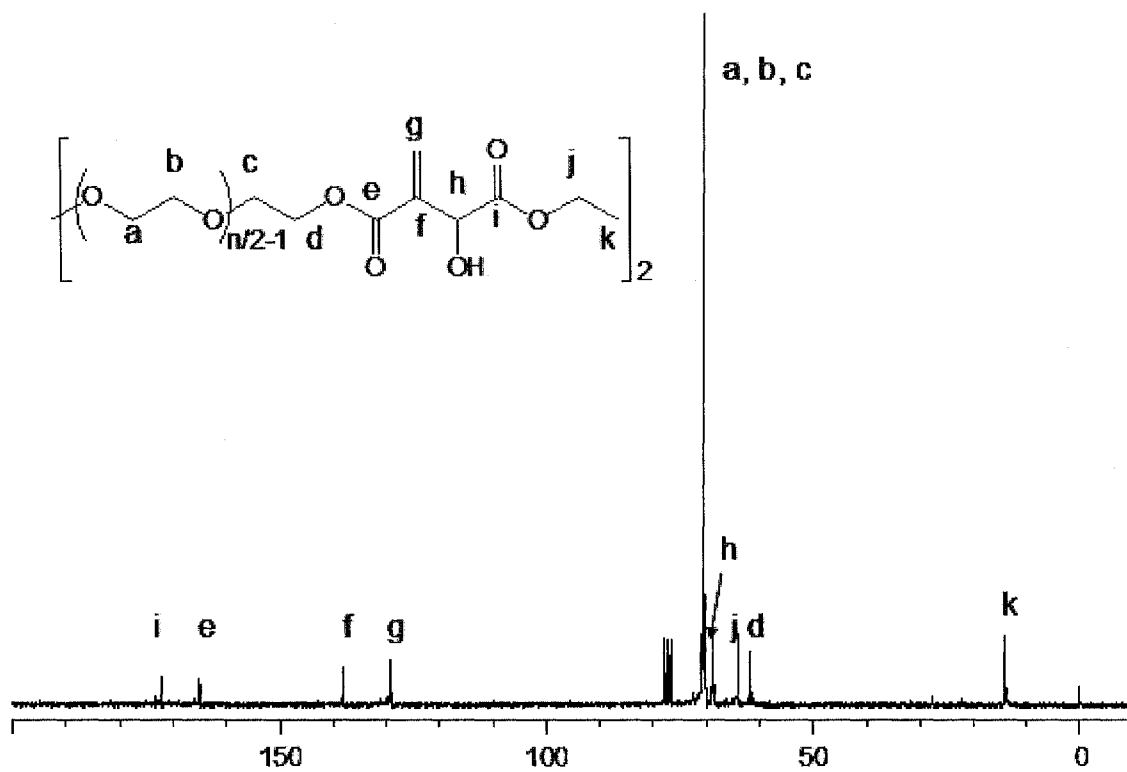
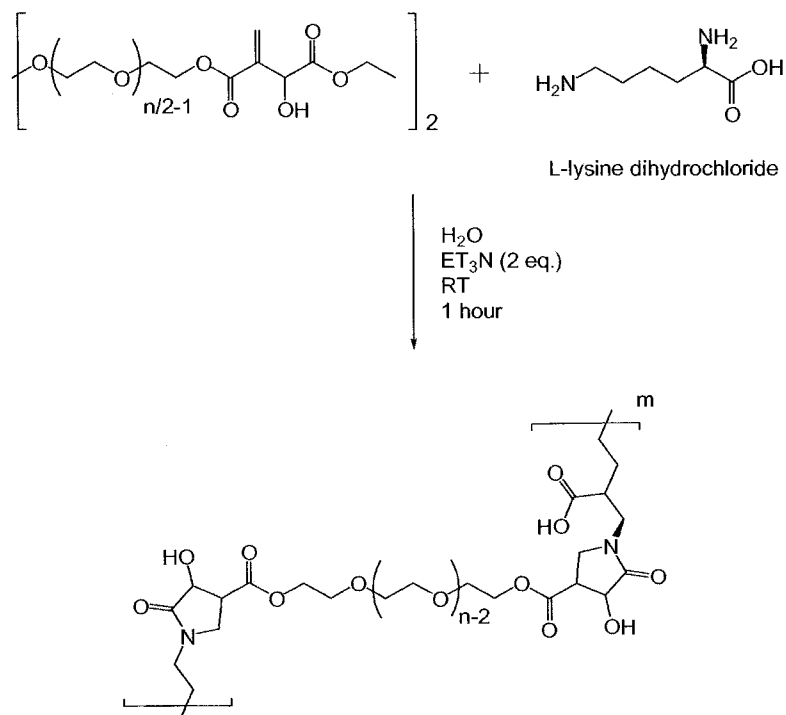


Figure 10.8. ^{13}C NMR spectrum of monomer **4** (CDCl_3).



Scheme 10.3. Synthesis of poly(ester amide) **C**.

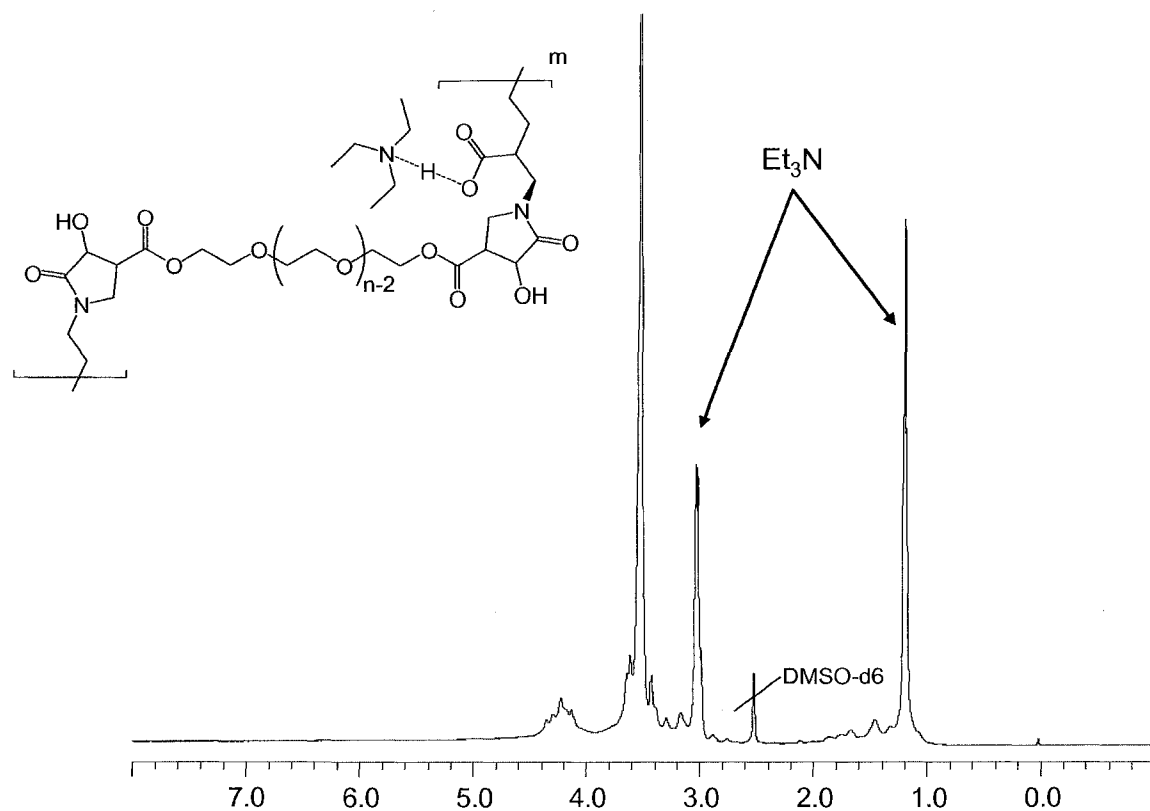


Figure 10.9. ^1H NMR spectrum of poly(ester amide) **C** (CHCl_3).

No peak was detected in the vinyl region, suggesting high monomer conversion and high efficiency of the polymerization process in such mild conditions. Such hydrophilic polymer presents high potential in a wide range of bio-medical applications such as bio-adhesives, bio-coatings and biodegradable polymers.

Conclusions

Kinetics studies were carried out of the Michael addition/cyclization reaction sequence involving known and new alkyl 2-carboethoxyhydroxymethyl-acrylates and primary amines using real-time NMR spectroscopy. This allowed determination the conversion profiles of the Michael adduct intermediate. It was

shown that these alkenes are rapidly consumed at a much higher rate than the formation of the corresponding heterocycles in the second step. Alkyl 2-carboethoxyhydroxymethylacrylates were shown to be orders of magnitude more reactive than commercially available dimethyl itaconate and butyl acrylate. We hypothesize that hydrogen bonding involving the allylic alcohol promotes both the initial amine attack and the subsequent cyclization to pyrrolidinone.

Based on this sequence of reactions, new biodegradable poly(ester amide)s that incorporate 2-pyrrolidinone in their backbone were synthesized efficiently via an ultra-fast, clean and mild Michael addition/cyclization polymerization route. The intra- and intermolecular interactions responsible for the high reactivity of the starting alkene monomers may also be responsible for the high hydrolytic susceptibility of the final polymer. The multifunctionality of the pyrrolidinone groups confers excellent adhesion of the polymer to glass, paper and metal substrates. This new polymerization route opens up new perspectives in the formation of biodegradable polymers with enhanced hydrolytic susceptibility and adhesion to specific substrates such as glass, paper, metals and biological tissue.

Experimental

Materials. Ethyl glyoxylate, 50% in toluene, was purchased from Alfa Aesar and used as received. 4-Diaza[2.2.2]bicyclooctane (DABCO), 1,6-hexanediol diacrylate (HDDA), poly(ethylene glycol) diacrylate (PEGDA), n-butyl acrylate, ethyl acrylate and dimethyl itaconate were purchased from Aldrich Chemical Company and used without further purification. Hexylamine (HA), hexamethylene

diamine (HMDA), ethylene diamine (EDA), and L-lysine dihydrochloride were purchased from Aldrich Chemical Company and used as received. All solvents were purchased from Acros Chemical Company, Fisher, or Aldrich Chemical Company. Ethyl α -hydromethylacrylate was synthesized according to previously reported procedure.¹⁸

Analyses. *Monomer characterization.* Solution ^1H and ^{13}C NMR spectra of the monomers were collected at room temperature with TMS as an internal reference on a Varian 300 MHz spectrometer at a ^{13}C frequency of 75.47 MHz. FT-IR spectra were obtained using a Mattson Galaxy series 5000 FTIR spectrometer.

Polymer characterization. Solid state NMR experiments were performed on a Varian 400 MHz spectrometer operating at a ^{13}C frequency of 100.62 MHz and equipped with a double-resonance H/X CP-MAS 4-mm probe for CP/MAS experiments. The MAS rate was fixed at 10 kHz, and each experiment was recorded at ambient temperature (294 ± 1 K). Thermal gravimetry analysis (TGA) experiments were performed on a TA 2960, controlled by a Thermal Analyst 2100. The temperature was ramped at a heating rate of 10 °C/min, under nitrogen atmosphere, to a temperature well above the degradation temperature (600 °C). Dynamic scanning calorimetry (DSC) experiments were performed on a TA Instrument 2920, controlled by a Thermal Analyst 2100. All scans were taken at a heating rate of 10 °C/min under nitrogen atmosphere, to a maximum of 220 °C then cooled to room temperature and rescanned at the same heating rate.

In Situ Monitoring of Michael Addition Reaction and Polymerization. Michael addition reactions involving alkyl 2-carboethoxyhydroxymethylacrylates **1** and **2**,

and an equimolar amount of hexylamine were monitored via real-time NMR spectroscopy in deuteriochloroform using a Varian Inova 500 MHz spectrometer. The monomer concentration was approximately 10 wt-% and the reaction was carried out at room temperature. ^{13}C NMR spectra were recorded every 2 minutes (32 scans/spectrum). Similar conditions and equipment were used in monitoring Michael addition polymerization involving diacrylate **3** and hexamethylene diamine.

Preparation of alkyl 2-carboethoxyhydroxymethylacrylates 1 and 2. The corresponding alkyl 2-carboethoxyhydroxymethylacrylate derivatives were synthesized according to previously reported literature procedure.¹⁷ Ethyl glyoxylate, 50 wt-% in toluene (20.39 g, 199.7 mmol), DABCO (3.64 g, 32.4 mmol) and the corresponding acrylate (199.7 mmol) were added to a 250 ml round-bottom flask. The mixture was stirred at room temperature for 2 hours. The crude solution was then concentrated under reduced pressure. The resulting mixture was washed with 3 aliquots of saturated sodium chloride solution followed by 3 aliquots of deionized water. The organic phase was then dried over a bed of sodium sulfate and vacuum distillation of the residue gave the corresponding compounds **1-4** which showed the following data:

Ethyl 2-carboethoxyhydroxymethylacrylate 1. Clear liquid; bp 140-142°C (20 mm Hg); 67% yield (isolated yield after distillation); ^1H NMR (300 MHz, CDCl_3) δ 1.26 (t, 3H, $-\text{CH}_3$), 1.30 (t, 3H, $-\text{CH}_3$), 3.64 (s, H, $-\text{OH}$), 4.23 (t, 2H, $-\text{CH}_2\text{CH}_3$), 4.25 (t, 2H, $-\text{CH}_2\text{CH}_3$), 4.87 (s, H, $-\text{CHOH}$), 5.94 and 6.37 (s, 2H, $-\text{CH}_2=\text{C}$); ^{13}C NMR (CDCl_3) δ 14.05 ($-\text{CH}_3$), 14.11 ($-\text{CH}_3$), 61.17 ($-\text{CH}_2\text{CH}_3$), 62.19 ($-\text{CH}_2\text{CH}_3$), 71.26

(-CHOH), 128.77 (CH₂=C), 138.32 (C=CH₂), 165.21 and 172.39 (C=O). FT-IR (neat, cm⁻¹) 3516, 2998, 1737, 1643, 1446, 1098, 823. Anal. Calcd for C₉H₁₄O₅·0.25*H₂O: C, 52.30; H, 7.02. Found: C, 52.01; H, 6.88.

n-Butyl 2-carboethoxyhydroxymethylacrylate **2**. Clear liquid; bp 153-155°C (20 mm Hg); 37% yield (isolated yield after distillation); ¹H NMR (300 MHz, CDCl₃) δ 0.94 (t, 3H, -CH₃), 1.27 (t, 3H, -CH₃), 1.42 (m, 2H, -CH₂CH₃), 1.66 (m, 2H, -CH₂CH₂CH₃), 3.59 (s, H, -OH), 4.19 (t, 2H, -CH₂CH₃), 4.23 ((t, 2H, -CH₂CH₂CH₂CH₃), 4.86 (s, H, -CHOH), 5.93 and 6.37 (s, 2H, CH₂=C); ¹³C NMR (CDCl₃) δ 13.69 (-CH₃), 14.06 (-CH₃), 19.15 (-CH₂CH₃), 30.56 (-CH₂CH₂CH₃), 62.22 (-CH₂CH₃), 65.04 (-CH₂CH₃), 71.27 (-CHOH), 128.82 (CH₂=C), 138.28 (C=CH₂), 165.28 and 172.39 (C=O). FT-IR (neat, cm⁻¹) 3516, 2998, 1737, 1643, 1446, 1098, 823. Anal. Calcd for C₁₁H₁₈O₅·0.5*H₂O: C, 54.21; H, 8.01. Found: C, 53.84; H, 7.39.

Preparation of multifunctional pyrrolidinones derivatives 1' and 2'. General Procedure. The corresponding alkyl 2-carboethoxyhydroxymethylacrylate (53.14 mmol) was added to a 50 ml tube equipped with an argon gas inlet. The reaction tube was then purged with argon for 30 minutes and sealed with a rubber septum. Hexylamine was then added dropwise and in slight excess (5.48 g, 54.21 mmol) and the resulting solution was allowed stirring for 24 hours at room temperature. Upon reaction completion as monitored by ¹H NMR, the solvent was removed under reduced pressure. The crude products were purified by distilling off the excess of amine. The resulting compounds **1'** and **2'** show the following data:

Ethyl 1-hexyl-4-hydroxy-5-oxopyrrolidine-3-carboxylate (1'). Brown oil; c.a. 99%; d.r. 33:67; ^1H NMR (300 MHz, CDCl_3) δ 0.88_(A+B) (t, 3H, $-\text{CH}_3$), 1.28_(A+B) (m, 2H, $-\text{CH}_2$), 1.52_(A+B) (m, 2H, $-\text{CH}_2\text{CH}_2\text{N}$), 4.29_(A) and 4.22_(B) (q, 2H, $-\text{CH}_3$), 4.56_(A) and 4.58_(B) (d, H, $-\text{CHOH}$); ^{13}C NMR (CDCl_3) δ 14.17_(A+B) ($-\text{CH}_3$), 22.49_(A+B) ($-\text{CH}_2\text{CH}_3$), 26.38_(A) and 26.87_(B) ($-\text{CH}_2\text{CH}_2\text{CH}_3$), 31.41_(A) and 31.44_(B) ($-\text{CH}_2\text{CH}_3$), 42.97_(A) and 43.06_(B) ($-\text{CH}_2\text{N}$), 43.06_(A) and 45.70_(B) ($-\text{CHCH}_2\text{N}$), 46.22_(A) and 46.31_(B) ($-\text{CH}_2\text{N}$), 61.53_(A+B) ($-\text{OCH}_3$), 70.53_(A) and 72.43_(B) ($-\text{CHOH}$), 170.27_(A) and 171.76_(B) ($\text{C}=\text{O}$), 172.76_(A) and 173.09_(B) ($\text{NC}=\text{O}$). FT-IR (neat, cm^{-1}) 3363, 2958, 2935, 2866, 1741, 1695, 1278, 740. Anal. Calcd for $\text{C}_{13}\text{H}_{23}\text{NO}_4$: C, 60.68; H, 9.01; N, 5.44. Found: C, 60.49; H, 8.88; N, 5.49.

Butyl 1-hexyl-4-hydroxy-5-oxopyrrolidine-3-carboxylate (2'). Brown oil; c.a. 97%; d.r. 31:69; ^1H NMR (300 MHz, CDCl_3) δ 0.88_(A) (t, 3H, $-\text{CH}_3$), 0.94_(B) (t, 3H, $-\text{CH}_3$), 1.28_(A+B) (m, 2H, $-\text{CH}_2$), 1.40_(A+B) (m, 2H, $-\text{CH}_2\text{CH}_3$), 1.51_(A+B) (m, 2H, $-\text{CH}_2\text{CH}_2\text{CH}_3$), 1.52_(A+B) (m, 2H, $-\text{CH}_2\text{CH}_2\text{N}$), 4.17_(A+B) (q, 2H, $-\text{OCH}_2$), 4.55_(A) and 4.58_(B) (d, H, $-\text{CHOH}$); ^{13}C NMR (CDCl_3) δ 14.16_(A+B) ($-\text{CH}_3$), 22.50_(A+B) ($-\text{CH}_2\text{CH}_3$), 26.39_(A) and 26.93_(B) ($-\text{CH}_2\text{CH}_2\text{CH}_3$), 31.42_(A) and 31.45_(B) ($-\text{CH}_2\text{CH}_3$), 42.97_(A) and 43.06_(B) ($-\text{CH}_2\text{N}$), 43.18_(A) and 45.72_(B) ($-\text{CHCH}_2\text{N}$), 46.24_(A) and 46.33_(B) ($-\text{CH}_2\text{N}$), 65.03_(A) and 65.37_(B) ($-\text{OCH}_2$), 70.52_(A) and 72.43_(B) ($-\text{CHOH}$), 170.34_(A) and 171.82_(B) ($\text{C}=\text{O}$), 172.79_(A) and 173.13_(B) ($\text{NC}=\text{O}$). FT-IR (neat, cm^{-1}) 3357, 2958, 2875, 1739, 1693, 746. Anal. Calcd for $\text{C}_{15}\text{H}_{27}\text{NO}_4$: C, 63.13; H, 9.54; N, 4.91. Found: C, 62.97; H, 9.42; N, 4.94.

Preparation of hexane bis-2-carboethoxyhydroxymethylacrylate 3. Ethyl glyoxylate, 50 wt-% in toluene (20.39 g, 199.7 mmol), DABCO (3.64 g, 32.4

mmol) and 1,6-hexanediol diacrylate (technical grade, 80%, 28.24 g, 199.7 mmol) were added to a 250 ml round-bottom flask. The mixture was stirred at room temperature for two hours. The crude solution was then concentrated under reduced pressure. The resulting mixture was washed with three aliquots of brine solution followed by three aliquots of deionized water. The organic phase was then dried over a bed of sodium sulfate and column chromatography (10:1 hexane/ethyl acetate) gave the corresponding product as clear oil in c.a. 47% isolated yield.

^1H NMR (300 MHz, CDCl_3) δ 1.26 (t, 3H, $-\text{CH}_3$), 1.30 (t, 3H, $-\text{CH}_3$), 3.64 (s, H, $-\text{OH}$), 4.23 (t, 2H, $-\text{CH}_2\text{CH}_3$), 4.25 (t, 2H, $-\text{CH}_2\text{CH}_3$), 4.87 (s, H, $-\text{CHOH}$), 5.94 and 6.37 (s, 2H, $-\text{CH}_2=\text{C}$); ^{13}C NMR (CDCl_3) δ 14.05 ($-\text{CH}_3$), 61.17 ($-\text{CH}_2\text{CH}_3$), 62.19 ($-\text{CH}_2\text{CH}_3$), 71.26 ($-\text{CHOH}$), 128.77 ($\text{CH}_2=\text{C}$), 138.32 ($\text{C}=\text{CH}_2$), 165.21 and 172.39 ($\text{C}=\text{O}$). FT-IR (cm^{-1} , NaCl) 3516, 2998, 1737, 1643, 1446, 1098, 823.

Preparation of PEG bis-2-carboethoxyhydroxymethylacrylate 4. Ethyl glyoxylate, 50 wt-% in toluene (2 g, 19.6 mmol), DABCO (3.64 g, 32.4 mmol) and PEGDA (11.2 g, 19.6 mmol) were added to a 50 ml round-bottom flask. The mixture was stirred at room temperature for three days. The crude solution was then treated with hydrochloric acid to remove the catalyst. The white precipitate was then filtered off. The solvent was removed under reduced pressure to give the corresponding product as yellow oil in c.a. 87%.

^1H NMR (300 MHz, CDCl_3) δ 1.26 (t, 3H, $-\text{CH}_3$), 1.30 (t, 3H, $-\text{CH}_3$), 3.65 (s, 44H, $-\text{CH}_2\text{O}$), 4.23 (t, 2H, $-\text{CH}_2\text{CH}_3$), 4.25 (t, 2H, $-\text{CH}_2\text{CH}_3$), 4.87 (s, H, $-\text{CHOH}$), 5.94 and 6.37 (s, 2H, $-\text{CH}_2=\text{C}$); ^{13}C NMR (CDCl_3) δ 14.11 ($-\text{CH}_3$), 61.17 ($-\text{CH}_2\text{CH}_3$),

62.19 (-CH₂CH₃), 69.62 (-CH₂O), 71.28 (-CHOH), 128.77 (CH₂=C), 138.36 (C=CH₂), 165.23 and 172.40 (C=O).

Preparation of Michael adduct polymers A and B. In a typical polymerization procedure, the corresponding diamine (11.61 mmol) was added to hexane bis-2-carboethoxyhydroxymethylacrylate **3** (0.5 g, 11.61 mmol) in 5 ml of chloroform. The polymerization was carried out at room temperature and monitored by ¹H NMR. Upon reaction completion, the solution was precipitated in diethyl ether under vigorous stirring. The polymer was collected and dried under reduced pressure for two days.

REFERENCES

- 1 Villuendas, I.; Molina, I.; Regaño, C.; Bueno, M.; Martínez de Ilarduya, A.; Galbis, J.; Muñoz-Guerra, S. *Macromolecules* **1999**, *32*, 8033.
- 2 Paredes, N.; Rodríguez-Galán, A.; Puiggali, J. *J. Polym. Sci. Part A: Polym. Chem.* **1998**, *37*, 2521.
- 3 Int-Veld, J.P.A.; Shen, Z.R.; Takens, G.A.J.; Dijkstra, P.; Feijen, J. *J Polym Sci Part A: Polym. Chem.* **1994**, *32*, 1063.
- 4 Goodman, I.; Seahan, R. *J. Eur. Polym. J.* **1991**, *26*, 1081.
- 5 Stapert, H.R.; Bouwens, A.M.; Dijkstra, P.J.; Feijen, J. *Macromol. Chem. Phys.* **1999**, *200*, 1921.
- 6 Carothers, W.H.; Hill, J.V. *J. Am. Chem. Soc.* **1932**, *54*, 1566.
- 7 Timmermann, R.; Doi, Y.; Steinbuechel, A. Wiley-VCH: New York **2003**, *4*, 315.
- 8 Paredes, N.; Rodríguez-Galán, A.; Puiggali, J.; Peraire, C. *J. Appl. Polym. Sci.* **1998**, *69*, 1537.
- 9 Molina, I.; Bueno, M.; Galbis, J.A. *Macromolecules* **1995**, *28*, 3766.
- 10 Langer, R. *Nature* **1998**, *392*, 5.
- 11 Pentti, U.; Rokkanen, P.; Böstman, O.; Hirvensalo, E.; Mäkelä, E.A.; Partio, E.K.; Päätiälä, H.; Vainionpää, S.; Vihtonen, K.; Törmälä, P. *Biomaterials* **2000**, *21*, 2607.
- 12 Marler, J.J.; Upton, J.; Langer, R.; Vacanti, J.P. *Adv. Drug Deliver. Rev.* **1998**, *3*, 165.
- 13 Chu, C.C. CRC Handbook: Boca Raton, FL **1997**, 65.

- 14 Schmitt, E. E.; Polistina, R. A. *US Patent* 3,297,033, **1967**.
- 15 Bezwada, R.S.; Jamiolkowski, D.D.; Lee, I.; Agarwal, V.; Persivale, J.;
Trenka-Benthin, S.; Ermeta, M.; Suryaderwara, J.; Yang, A.; Liu, S.
Biomaterials **1995**, *16*, 1141.
- 16 Barrows, T. H. *US Patent* 4,529,792, **1985**.
- 17 Morizur, J-F.; Mathias, L.J. *Tetrahedron Letters* **2007**, *48*, 5555-5559.
- 18 Mathias, L.J.; Warren, R.M.; Huang, S. *Macromolecules* **1991**, *24*, 2036.
- 19 Baylis, A.B.; Hillman, M.E.D. *Chem. Abstr.* **1972**, *77*, 34174.
- 20 Morita, K.; Suzuki, Z.; Hirose, H. *Bull. Chem. Soc. Jpn.* **1968**, *41*, 2815.